The effect of particle size and density on pressure gradients in horizontal pipelines in lean phase pneumatic conveying

by

Linda Margaret Hyder

Thesis submitted in partial fulfillment of the requirements
for the award of the degree of
Doctor of Philosophy
under the conditions of the award
of higher degrees of
The University of Greenwich

The University of Greenwich
Greenwich, London, UK

March 2000

The effect of particle size and density on pressure gradients in horizontal pipelines in lean phase pneumatic conveying

by

Linda Margaret Hyder

Synopsis

This project was brought about by the need to improve the accuracy of predicting the pressure losses along pneumatic conveying systems, and in particular, an investigation into the reasons why materials behave differently to each other when conveyed pneumatically along pipelines. It was intended that the information obtained from the project, would improve the accuracy of predicting the pressure losses along pneumatic conveying systems used in industry. A study has shown that no other researcher has investigated the differences between several materials in a systematic approach.

This thesis outlines the procedures followed that led to the development of a graph that can be used as an aid for predicting the pressure losses along straight sections of pipeline. Groups of materials that were similar to each other except for the individual particle properties of median particle size or density, were used to find a connection between the properties and the pressure losses. From these comparisons, a fundamental appreciation was obtained, regarding the effect of these particle properties on the characteristic relationships of pressure drop to conveying conditions, and hence an optimum approach to modelling was developed.

To obtain test data, the materials were conveyed around a test pipeline at the smaller end of the industrial scale. The pressures were measured along the pipeline to determine the pressure gradients in straight sections, and the pressure drop caused by the bends. Data storage and retrieval systems were used to transfer the data to additional software for analysis. The data was analysed for each material, and then collectively for all the materials, to determine a relationship between the pressure losses and the particle properties. The development of the test rig to meet the objectives of the project, the analysis of the results, and the development of the graph, are explained in detail.

Acknowledgements

I would like to thank a number of people who have supported and encouraged me throughout the duration of this project, and helped me bring it to fruition.

I would like to thank Professor Alan Reed and Dr. Mike Bradley of The Wolfson Centre for Bulk Solids Handling Technology at the University of Greenwich, for initiating the project and for fulfilling the roles of supervisors and mentors. Dr. Mike Bradley deserves special recognition having laid the foundations for this project in his research, and for always finding time to discuss work in progress and helping with the direction of the project during difficult periods. Also by having faith in my abilities when self doubt arose, and for thorough proof reading of the final document.

The assistance of the technical staff at of The Wolfson Centre for Bulk Solids Handling Technology at the University of Greenwich, was greatly appreciated. In particular John O'Connor, Mike Holman and Tony Kelly.

Financial support from the Engineering and Physical Sciences Research Council, and The Wolfson Centre for Bulk Solids Handling Technology at the University of Greenwich, is gratefully acknowledged. Further thanks to Tioxide of Grimsby, who very kindly donated some of the test materials.

I would like to thank my family and friends for their support, patience and understanding, throughout the time it took to complete this project. In particular my husband Bob, my sons, Michael and Robert, and my mother Jean McCarthy. I would also like to thank my husband Bob and my friend Lynn Whaley who encouraged me through the many ups and downs that led to the completion of this project.

Finally, I would like to dedicate this project to my close friend Patricia Gilbert, who had she still been with us, would have been so delighted that I had completed it.

Author's Note

All of the work in this thesis is the sole and original work of the author, except where stated otherwise by acknowledgement or reference.

Table of Contents

Detailed breakdown of the table of contents

The Chapters

The Appendices

Chapter 1

Introduction

1.1 Introduction

The pneumatic conveying of materials along pipelines is widely used in many industry sectors as a means of transporting raw materials, intermediates and finished products from one location to another. The types of materials pneumatically conveyed include industrial chemicals, food products, and minerals, over a range of particle sizes from 1 micron to 12mm (or larger). The distances between the beginning and the end of a pipeline can range from as little as a few metres to several hundred metres. The advantages of using such systems are that pipelines can be directed around the walls and ceilings in a plant to avoid obstructions, which leaves floor space free; material is fully enclosed within the pipeline thereby hazardous substances can be contained; conversely, containment means minimal risk of contamination of conveyed material, and as with all types of solids conveyed in this way, the possibility of a spillage is much reduced compared to mechanical conveying.

Despite the benefits of this method of handling, the design of pneumatic conveying systems has been problematic since they were originally used over a century ago. This is because designers of pneumatic conveying systems need to know an estimated total pressure loss across the proposed system, in order to provide a sufficient, but economical system that will cause as little degradation to the product conveyed as possible, minimize the power consumption, and reduce the amount of wear to the system. Due to the complexity of the relationship between solids and air during pneumatic conveying, each material behaves differently when transported in this way. Even products that are presumed to be alike can react differently if they have been processed in a dissimilar way, or mined from different parts of the country.

When two distinct materials are conveyed separately along the same conveying system, the pressure losses will be different. This is known because workers in industry who have conveyed a product along a system efficiently, and decided to change the product, have often had problems conveying the new material. As the system will not have changed, the differences can only be attributed to the change in the particles conveyed. This difference in the conveying characteristics from one material to another, makes it difficult to predict the pressure drop along a new system without undertaking conveying characteristic tests with the material.

At present, system pressure losses are estimated using a number of methods, which are predominately the testing and scaling approach, the analytical approach, and those systems designed from a knowledge of using the same or similar materials. The systems designed on a knowledge based on previous experience of the same material or a very similar material, often work very well without problems. However, there are those that do not work as well because the particle sizes may be different, or the product has come from a different source and behaves differently when conveyed. The analytical approach is where analytical models are used to predict the pressure losses along straight pipe sections, and through bends, but the models often consist of complicated equations and are not workable due to inaccuracies from results, as noted by Wypych[W3]. The testing and scaling method, consists of performing pilot-scale test work using material that will be conveyed in the proposed system, to obtain its conveying characteristics. The results are then scaled to predict the pressure losses for the designed system. These procedures are workable, but expensive, so less complicated and/or more accurate methods are always sought after.

Research on pressure losses along straight pipelines in a horizontal, vertical and inclined position, and across bends of varying orientation, angles and radii, is continuously required. This is because the amount of research that has been carried out into pneumatic conveying, has not yet covered every aspect of all the various orientations of pipeline and bends to a level that would give confidence to a designer of pneumatic conveying systems. However, if a pattern could be found that predicts the pressure losses between various materials tested under the same pipeline orientation and conveying conditions, a model may be developed that would be beneficial both to industry and for other researchers to build on. It was these ideas that influenced the direction of this project.

As a result, the objective for the project became the desire to examine products during pneumatic conveying, and see if a link between the products could be identified. It was intended that this would make the prediction of estimating the pressure losses along a conveying system easier. As the testing and scaling method was known to work, the test work could be carried out using a pilot scale test rig with assurance.

Specifically, the aim was to test a number of materials under the same pneumatic conveying conditions, in order to determine if a pattern emerged that could be used in a derived model or method to predict pressure losses. Alternatively, it was anticipated that the results could be used to simplify the existing prediction method, or at least reduce the amount of test work presently required to determine the conveying characteristics of a range of materials.

Each material has several characteristics that distinguish it from any other product, and with so many variables involved, it was considered important to determine the properties that were thought to have a dominant effect on the pressure losses along a pipeline. Each product to be conveyed has bulk properties as well as individual particle properties. Hence, research by other authors into the properties of both bulk and individual particle that were thought to have an effect on the pressure losses, was an important consideration in the direction of the project.

1.2 Overview of project

A brief overview of the project is given below.

All the particle characteristics were considered and analysised for their overall effect on the pressure losses. The outcome established that there were three main particle characteristics that were likely to have a major effect on pressure losses during pneumatic conveying. These were the particle size, shape and density.

The particle shape criterion for all the selected materials, was that their particles should be as spherical as possible, thereby reducing the measurable characteristics to be that of particle size and density.

Six materials were initially selected for the test program, each product having either particle size or particle density in common with one or more materials within the selected group, and all having a fairly rounded shape. Conveying trials on all the materials yielded large quantities of data that was processed and analysed. From the results, a graph was derived that gives an indication of the pressure losses along straight sections of pipeline during pneumatic conveying, using the particle density and particle size properties of a material. In addition, a relationship between the effect of the particle size and density on the pressure losses, was identified.

Having derived the graph, it followed that other materials should be tested to ascertain the usefulness of the graph. An additional four materials were obtained from other projects and not necessarily for their connection with the initial test materials, and were subsequently tested under the same conditions as the original six products.

The results were processed and analysed to obtain specific data from each material. The data acquired was referred to the graph for comparison. The results did not compare favorably for two of the products, and consequently the limitation of the value of the graph was obvious. This meant

that the graph would only be beneficial if the material under investigation fell into certain categories. From the additional materials that were tested and compared well with the graph, the categories that were similar to the original materials used to develop the graph, gave some indication of the classification of materials that could be used with the graph. They were all non-food products, free flowing, reasonably rounded in shape, hard, fairly robust, and did not absorb moisture.

Chapter 2

Establishing the direction of the project

2.1 Review of objectives

The main objective of this project was to quantify the effect of the particle properties having the most influence on the pressure losses, during the pneumatic conveying of solids along horizontal pipelines. The decision to investigate individual particle properties, resulted from the fact that a vast range of materials are pneumatically conveyed along pipelines in industry, but no widely applicable correlation between the particle properties and the pressure losses had previously been identified. The direction of the project was led by the idea that a connection may be identified in the analysis of behaviour of the materials that had been carefully chosen and pneumatically conveyed under identical conveying conditions. If a relationship was found, then a model could be developed that may be used to predict the pressure losses for other materials.

2.2 Research to date

The requirements to achieve the main objective, involved the concept of pressure change along a pipeline consisting of straight sections and bends, during the pneumatic conveying of solids. Pressure change (and it's relationship to pipe size, and flow rates of air and solids), is the key to conveying system design since it dictates the type and size of equipment needed to deliver air and solids to the pipeline, as well as the power requirement and flow conditions.

To develop a project methodology, it was necessary to first explore the means by which pressure loss predictions could be made and used by system designers. An investigation into the current methods that were used to make these predictions, revealed that there were two main approaches to date. The first was the process where analytical models are used to predict the pressure losses along straight pipe sections, and through bends. The second, is where a laboratory test rig is used to measure the pressure losses by conveying the actual material that the system will be designed for, and scaling the results to those predicted for the final system.

The outcome of the studies for the first approach, showed most mathematical models included variables in complicated equations that were difficult to obtain values for [E1], or needed experimental test results to obtain certain values [T2]. In addition, the comparison between the

results from one author to another rarely correlated well; each was usually derived from only a narrow range of flow conditions.

The second approach takes the material the system will be conveying, and by carrying out a number of conveying trials around a test rig for a wide range of conveying conditions, results are obtained for the pressure losses along the pipelines [A2,W3,P5,B1]. To estimate the pressure losses caused by the effect of the bends, some workers have used an equivalent mean length of straight pipe [M8], but this was believed not to be satisfactory. The most reliable method was thought to be to measure the losses separately for the straights and bends, as shown by Bradley [B1]. The pipeline is usually of a smaller bore diameter, (between 50 to 100mm diameter) than the proposed plant system (often 75 to 300mm), so the results are scaled up accordingly; research had shown scaling for diameter to compare well in practice[B1].

Following the initial investigation, an essentially empirical approach to this project was thought to be the appropriate method by which to achieve the objectives.

A review of the state of the art revealed that the most relevant research to date had concentrated on measuring the pressure profile caused by a bend and in adjacent straight sections, to determine the pressure gradient along straight sections and bend loss. This was usually achieved by fitting pressure transducers along two straight lengths of a conveying line with a bend in between [B1, M3, P3]. An existing test rig was available that could be modified for use with this project. The test rig was also fitted with pressure transducers along two straight sections, with a test bend in-between. It was decided that to best fulfil the objectives of the project, part of the modifications would include the installation of supplementary pressure transducers along two extra straight sections of the test rig. This would give measured pressure gradients along four consecutive straight sections for each test run, and by fitting three identical test bends in-between the straights, the data for determining the pressure losses caused by the effect of three bends.

No other author had measured the pressure losses in this way, and the benefits would include the reduction of the number of test runs necessary to obtain the conveying characteristics of each material. This is because the conveying conditions of air velocity and suspension density are different for each straight section, when the pressure decreases as the solids and air travel along the pipeline. Other benefits were that a clearer picture could be observed of the pressure changes along a pipeline with several bends, and it would give an opportunity to interchange the test bends. This exercise would ascertain whether the nominally identical bends would give indistinguishable pressure losses when operating under the same conveying conditions.

Some work had been carried out by authors who used several materials to compare the pressure losses between them, but they were mainly limited to granular products [V1, C2, M2, R1]. Of those authors and others who used several materials to compare the results for the effect of particle sizes, several found the increase in particle size did have an effect on increasing the pressures losses [V1, M1, M2, S1,R1], but for very lean phase flow conditions. However, the results were often obtained from straight sections that did not allow for the acceleration length after a bend, and therefore not long enough for the results to be considered reliable [R3]. This confirmed that any pressure measurements taken along straight sections of pipeline, should be for as wide a range of flow rates as high as possible within the constraints of the rig, and obtained from pressure tappings fitted along a sufficiently long length of pipeline [M2,M3,T2]. It would ensure that the solids following a bend were in a steady state of flow before pipeline pressures were recorded. For these reasons, the pressure tappings along the two extra straight sections, were fitted at a suitable distance of 5m downstream of each test bend.

The literature reviewed also identified that comparisons between both powdered and granular materials had often been used to classify the minimum conveying velocity, or for research concerning dense phase flow only, but not pressure loss differences [W5,J1,B2,H2,C1]. In addition, when comparisons were measured between materials, it was either the particle size or terminal settling velocity that was compared [S1, C1], indicating that the particle size and density were considered as particle properties having a large influence on pressure losses. The particle shape was also an important factor with regards to the pressure losses, as stated in several papers [M2, S1, T1, B2]. The conclusions from these papers were taken into consideration with deciding on the most relevant characteristics to investigate when comparing the effect of particle properties on the pressure losses. Hence, the particle properties thought to have the most influence on the pressure losses, were the particle size, density and shape. A more detailed analysis can be found in chapter 4.

2.3 Program to achieve objectives

Having decided on the particle properties that were to be investigated for their effect on the pressure losses during pneumatic conveying, to achieve the project objective, required the selection of several materials to be used in the test programme. Therefore, the initial test program aimed to examine a minimum of six materials. It was envisaged that subsequently, additional materials would be tested to validate any correlations established. The test work on each material required the full range of conveying conditions to be determined, so that comparisons between results of similar values of air velocity and suspension density could be made. In addition, the test programme included repeated test runs periodically, to observe if any degradation of the material

affected the pressure losses. As part of the monitoring of the materials, samples would also be taken regularly to detect any deterioration of the particles.

It was conceivable that the pipe walls would wear through during the pneumatic conveying test programme, as some of the test materials were known to be abrasive. It was this expectation that led to the order of the test programme. The order for which the materials were tested, depended on the characteristics of each material. For example, the material that would not noticeably degrade, or erode the pipeline, would be used during the commissioning period and as the first test material for analysis. The remaining materials would also be selected in order of availability, rate of degradation and abrasive wear on the pipe walls, so that data accumulated from completed test work could be analysed whilst a new pipeline was installed or repaired.

In the light of the above considerations, the project methodology was established as:-

- to identify the particle properties that have the greatest influence on the pressure losses during pneumatic conveying.

- to identify and obtain a group of materials which could be sourced readily and reasonably cheaply, which would give a matrix of progressive changes in one particle property at a time.

- to build or modify a test rig to enable reliable and reproducible test results to be achieved.

- to identify the conveying conditions that all the test materials should cover, and ensure these were fully covered.

- to analyse the results from all the test materials with the aim of finding a connection between the particle properties and the pressure losses.

- if a relationship could be found, to develop a model that may be used to predict the pressure losses along a pipeline based on particle characteristics.

- to compare any prediction model results (if one was developed) to those of additional measured data, in order to determine if the prediction model could be used to design systems.

Having determined the objectives, and listed the necessary steps to achieve them, the order of the work programme was defined, as follows:-

1. Identify modifications required to the existing test rig. How they could be achieved, the cost of the modifications, and the time scale involved to carry them out.

2. Implement necessary modifications.

3. Selection of materials for the project. Identify suitable materials available in the laboratory. Ascertain where the remaining materials could be obtained and their costs, and decide at what stage of the test programme they should be purchased.

4. The commissioning of the modified test rig.

5. Analysis of test results on the first test material.

6. Change over the test materials, and proceed with the test programme.

7. Continue analysis as the test work results on each material was completed, to find a correlation between pressure gradient and particle properties, that can be used in a pressure loss prediction model.

8. Undertake further tests runs with additional materials, to test the correlations.

Ultimately, it transpired that due to constraints of time, only the effect of particle properties on pressure gradients in straight pipes were examined, and flow conditions were limited to lean phase (suspension) flow. However, within these limitations, the above work and project objectives would be fully achieved.

Chapter 3

Brief description of the test rig and commissioning stage

3.1 Introduction

The initial aim of the project was to convey pneumatically, several materials under the same conveying conditions, and compare the differences between the measured pressure losses. In order to compare any differences, the materials would have to be similar to each other, except for one property, so that any pressures changes would be attributed to the differences in particle characteristics.

The proposed test programme for the project included test work on several materials, and initially six products were selected. The test work on each product involved conveying the material around a test rig, and measuring the pressure gradient along straight sections of pipeline. By varying the mass flow rate of solids and air into the pipeline, a wide range of conveying conditions could be measured, within the limitations of the test rig.

In order for comparisons to be made between the different materials, the accuracy of the test data was an important aspect. If for example, two test runs were carried out using the same conveying conditions, the results should be the same theoretically, or within a small tolerance. The accuracy of repeated test run data was also a method of evaluating the reliability of the system. Furthermore, in order to limit the amount of test work, it was considered necessary to obtain as many reliable data points as possible from each test run. With some materials it would be necessary to restrict the number of times that they were conveyed around the test rig, as they were liable to degrade quicker than others. This was another way of ensuring that the data obtained from the test runs was dependable, and as wide ranging as possible in terms of the number of conditions tested.

3.2 Test rig requirements

The object of using a test rig, was to ensure that the test materials could be pneumatically conveyed around a pipeline consisting of straight sections and bends, to measure the conveying characteristics of each test material. The pressure measurements were to be determined separately for straight sections and bends, by measuring the pressure profiles in the vicinity of bends, as detailed in appendix 2. It was intended that the conveying characteristics would be determined by

changing the inlet air supply and solids feed rate into the conveying line for each test, and measuring pressures at regular intervals along the pipeline.

The test rig should be comprised of mainly long, straight horizontal sections, and the bends in a horizontal to horizontal configuration. Horizontal test sections were preferred, because most pipelines used in industry are in a horizontal configuration.

It was considered important that any straight test section should be of a sufficient length to ensure that any pressure readings taken to determine straight pipe pressure gradients, was from a satisfactory distance downstream of a bend. Long straight sections were essential because the solids slow down on impact with a bend, and require a minimum length of at least 5 metres (and often 8 metres), to be reaccelerated to the velocity of the conveying air [R3]. In addition to the distance recommended for the solids to be reaccelerated, a suitable length of pipe was required to enable the pressure gradient along the straight section to be determined. This was achieved by measuring the pressure at regular intervals along the pipe. Hence, the straight length of pipe should be as long as could be accommodated within the space available, but the minimum length should include the re-acceleration length, and be of a sufficient length to ensure several pressure readings are taken along the pipe, while the material was in a steady state of flow.

It was necessary to select the pipe for use as part of the test rig, of a suitable nominal bore diameter. The particle sizes of the test materials, ranged from a median particle size of 30μm to 4mm. This restricted the choice of pipe. It was essential not to use pipe with too small a bore, as it was felt that the ratio of the pipe diameter to the particle diameter may influence the pressure losses if that ratio was not sufficiently large (i.e. in the range of industrial practice). From the pipe sizes available within the laboratory, a 50mm nominal bore sized pipe (53mm in bore) was selected. This would satisfy the requirements mentioned, but ensure that the minimum quantity of bulk solids would be needed to complete each test.

To measure the pressure gradient along the pipeline, and the pressure losses caused by the effect of a bend, pressure tappings placed at regular intervals along a straight section of pipe, seemed a suitable method for obtaining the data, as used by Bradley [B1].

3.3 The test rig

The test rig for the project was capable of conveying a variety of materials along a pipeline system, consisting of a number of bends and separated by sufficiently long straight sections. The medium weight steel pipeline, 53mm bore diameter, 80m in length, was made up of mainly horizontal straight lengths of pipe, with two short vertical sections of pipe at the inlet and outlet of the conveying line.

The test section of the pipeline was in a horizontal orientation, with the test bends also in horizontal to horizontal alignment. It consisted of four consecutive 17m straight sections, separated by three identical test bends. To obtain data points, pressure transducers were placed at regular intervals along the straights in the test section, taking into account the acceleration zone after a bend. In some parts of the system new pressure tappings were fitted, and the first transducer was positioned 5m downstream of the apex of each bend.

Pressure transducers enabled the pressure losses to be monitored along a total of four consecutive straight sections, and it was also possible to study the effects caused by three bends (see figure 3.1). By designing the test section in this way, it was possible to reduce the number of test runs required. This is because the air velocity and suspension density changes from one section to the next as the solids and air move along the pipeline. Therefore, from each test run there were four different values of the pressure gradient, midpoint air velocity, midpoint suspension density and midpoint air density. Also, three different values were determined for the pressure losses caused by the bends. Suitable data retrieval and processing equipment was required to accommodate the large amount of data that would be generated from the pressure transducers, and the number of materials included in the test programme.

A high pressure blow tank of $1.5m^3$ capacity, and pressure rating of 6 bar, was used to feed solids into the pipeline. The air feed to the blow tank was generated from reciprocating compressors, via receivers, filter/water trap, regulator and choked flow nozzles. The choked flow nozzles controlled the air flow rates to the blow tank, enabling fixed flow rates to be set up.

A volumetric screw feeder was used in conjunction with a blow tank to control the amount of material being fed into the conveying line. The screw feeder was used to enable repeatable and consistent data to be obtained from test runs carried out under similar conveying conditions. An instrumentation and control system was used to drive and monitor the screw rotation under load, which comprised a thyristor drive unit to control the speed of a D.C. motor.

The speed of screw feeder was monitored using a tachometer placed on the screw shaft. The tachometer was connected to a potentiometer and counter on a remote mimic panel in the control room, to regulate the mass flow rate of solids into the conveying line.

The flow rate of solids was monitored by measuring the amount of material falling into a receiving hopper mounted on load cells, at the end of the conveying line. Two valves between the receiving hopper and blow tank completed the test loop, so that material could be dropped through into the blow tank from the receiving hopper after a test run, in readiness for the next test. Full details regarding the test rig are found in appendix 3.

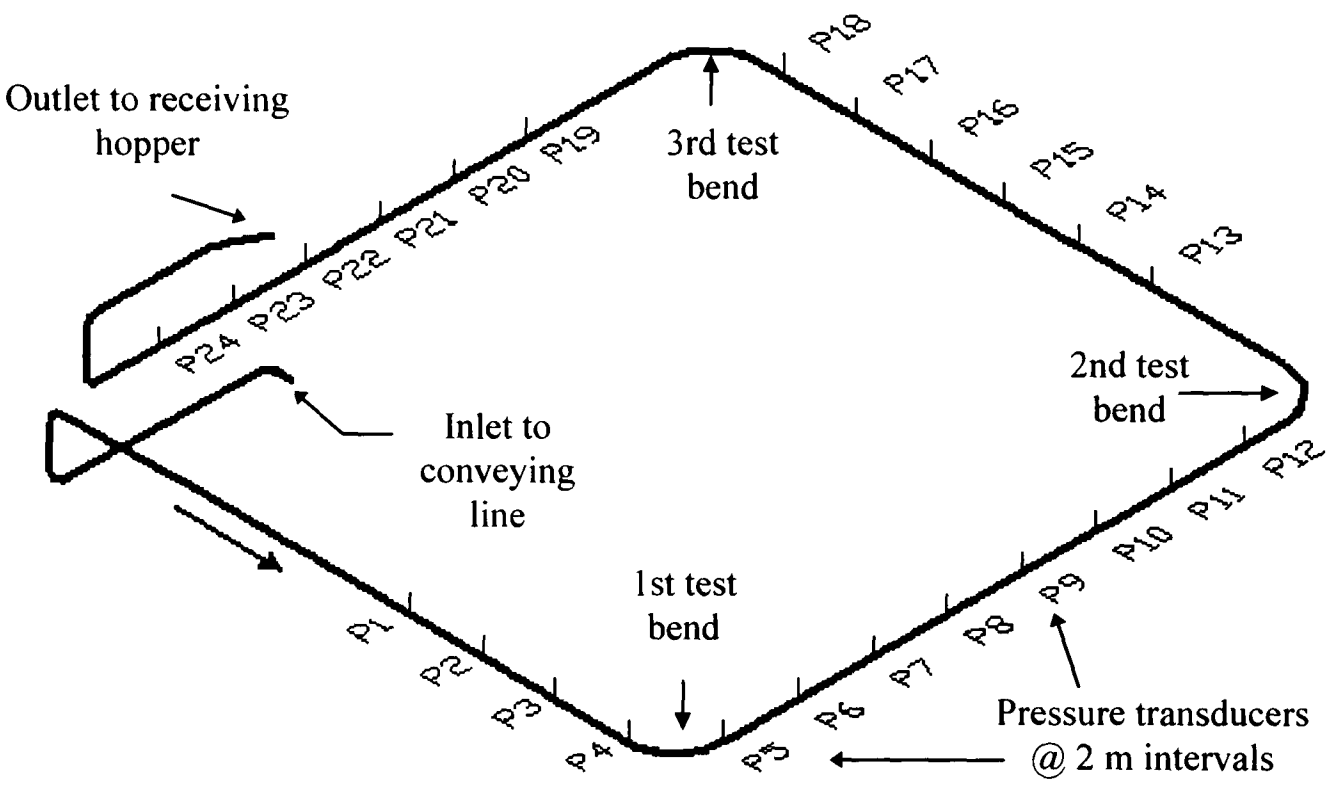

Figure 3.1: Layout of the test rig pipeline showing the positions of the pressure transducers and test bends.

3.4 Commissioning stage

Once the modifications to the test rig had been completed, the pressure transducers were calibrated using air only and a test pressure gauge. The first test material was used to commission the rig, to ensure everything was working as required before the test programme commenced. Polyethylene pellets were selected from the test materials, because they are robust and therefore could withstand numerous conveying runs around the test loop without noticeably degrading.

The commissioning of the test rig, determined that all the equipment and instrumentation on the rig was working correctly in order to achieve the project objectives. This included the mechanical, electrical, computer and software components of the rig. The most important task was to convey the product under stable controlled conditions, produce results that were reliable and consistent, and to process the data.

To cover the full range of conveying conditions, the minimum air velocity at which the material could be conveyed without blocking the pipeline, was established. This was achieved by initially conveying at a high air velocity and low suspension density where the material was certain to convey. Subsequent tests at reduced air velocities, were performed until the line blocked with material, and the minimum air velocity was determined.

For the main test runs, the pressure transducers and load cell output were scanned every 1 second, for 150 readings. Full details are found in appendix 4 as to how these values were determined.

During the commissioning period, the conveying line was blocking at a much higher inlet air velocity than previously recorded (based on previous work using the pellets) and would not convey in dense phase. Alterations to the conveying line were tried, but did not change the results, which were found to be a consequence of using the screw feeder. Therefore, the decision was taken that the comparisons between all the test material results, would be confined to lean phase conveying.

Chapter 4

Test materials

4.1 Introduction

The initial test program aimed to examine six materials. They were carefully selected to be as far as possible, fairly free flowing, rounded in shape, and would not degrade too quickly during pneumatic conveying. Other requirements of the materials were that they should be similar to at least one other material in the programme, so that going from one material to another would give rise to a change in the value of only one characteristic at a time.

This was to examine whether the effects of individual particle characteristics on pneumatic conveying could be identified, so that more consistent models for conveying characteristics could be established.

4.2 Material properties

The main object of the research was to compare the differences between several different materials conveyed pneumatically, in the expectation that a pattern may be found that would predict the pressure losses for other materials. This would then reduce the number of trials that system designers would have to carry out to measure actual pressure losses in specific systems.

4.2.1 Deciding upon the key particle properties

In order to compare differences between products, a list of all the variables of a bulk material or individual particle was drawn up in order to identify what would be likely to affect the pressure drop. From the list, the measurable properties were considered. The availability of methods of measuring the characteristics of a material were considered as this would have an effect on deciding what properties to compare in conveying tests. For example, some material characteristics such as the particle density and size distribution are easily measured with specifically manufactured equipment. Other characteristics such as the coefficient of restitution and surface roughness are not so easily measured.

It was apparent that many different measurable characteristics could be identified, but not all would have an effect on the pressure drop. For example, toxicity would affect the system design, but would not have a relevance on the pressure drop.

A list of characteristics, properties and behavioral attributes of a material or individual particle was drawn up, shown below.

List of characteristics

Abrasiveness	Hydroscopicity	Thermoplasticity
Aeration properties	Wall friction	Chemical composition
Coefficient of restitution	Colour	Combustibility
Corrosiveness	Degradability	Density
Ease of communition	Elasticity	Explosiveness
Fibrousness	Width of size distribution	Hardness
Melting point	Toxicity	Size
pH	Production method	Plasticity
Porosity	Surface roughness	Reactivity

From the list above, the major characteristics that were thought likely to have an effect on the pressure gradient during pneumatic conveying were considered and the following "working" particle characteristics list produced.

Particle Characteristics

Median size	Melting point	Elasticity
Coefficient of restitution	Shape (roundness/angularity)	Hydroscopicity
Density	Hardness	Thermoplasticity
Plasticity	Porosity	

Examining the particle characteristics that would be likely to have a major effect of the pneumatic conveying of solids, the thought processes led to an examination of what is likely to happen to a particle as it is entrained in air and travels along a pipeline. The weight of a particle is considered because the heavier the particle, the more energy it will take to lift it from the bottom of the pipe. Therefore the density and mass of the particle would both be important. Once a particle is entrained in air, how much energy is needed to keep it moving could well depend on the shape of the particle because this affects the pressure drag.

4.2.2 Previous work

The work of others was investigated to determine what particle characteristics had been identified as influencing the pressure drop during pneumatic conveying, and the conclusions of their work. Williams [W4] equations are based on the established equation used to predict the pressure losses in single phase flow for air only. He represented the pressure drop during the conveying of solids by means of an equivalent length of pipe which would give the same pressure drop when handling air only. The equations for relating total equivalent length to mass flow rate of solids for any given pressure drop for dilute phase only, have a factor that varies for each type of material, according to the material shape. However, the factor is the same for most powdered and granular material, because tests showed that materials with a good percentage of fines or powders in relation to spheres most often will act as powered or granular materials. There is no guide as to how this factor may vary or how its value may be determined for any particular material, nor any indication as to how many materials were tested.

Previous work on the modelling of pressure drop across bends and along straight sections for two phase gas-solids flow, highlighted the fact that there was little research into the measured pressure drop differences between materials of similar particle size, shape or density. Mendies et al [M2] carried out an investigation using three plastic materials of similar particle shape and density, but with different particle sizes. They evaluated the solids velocity by the cross-correlation method of velocity measurement, whereby two probes spaced axially along the pipe detect the electrostatic flow noise. Pairs of electrodes were inserted at various points along the pipe, while pressure tappings were connected to U-tube water manometers to measure the pressure distribution along the pipe, in a pilot test plant. There were a total of 5 lengths of horizontal pipe measuring 11 metres, using maximum solids loading ratios (SLR) of 9. From a graph representing their results, the smaller the particle, the higher the solids velocity. Their results indicated that the particle size has an effect on the solids velocity. They also found that the air velocity and SLR did not influence the acceleration length of the material, which took 4 to 5 metres, in agreement with Rose and Duckworth [R3].

Raherman and Jindal [R1] carried out experiments in vertical and horizontal conveying of rough rice, milled rice and soybean for solids loading ratio of 0.7 to 3.5 in 54, 68 and 82mm inside dia. pipes. The pressure drops were measured using 'U' tube manometers. The particle sizes ranged from 3 - 7 mm. However, due to the low solids loading ratio, a large proportion of the pressure drop was due to air only. The total pressure drop was modelled as the pressure drop of the air plus the solids pressure drop. The Fanning equation (also known as the Darcy equation) was used to estimate the

air contribution to pressure drop in both the horizontal and vertical pipelines. An equation analogous to Fanning's equation but involving a solids friction factor, dispersed solids density and solids velocity was used to represent the solids contribution. Their findings were in good agreement with the experimental and estimated values, but for use with particles ranging from 3 to 7 mm at very low solids loadings. Comparison between the particles sizes were not included in the paper.

The work by Geldart [G2] dealing with fluidization characteristics of different types of particulate bulk solids, showed that the median particle size and differences in the densities of the solids and the fluidizing medium, are important properties in that process. From a knowledge of the mean particle size and particle density, it is possible to make a reasonably reliable estimate of the minimum fluidizing velocity. He does say that although these particle properties generally have the major influence on the fluidization characteristics of the material, there are other variables which may also have a significant effect., i.e. materials that have a very wide size distribution, very fine particle sizes or are cohesive.

Clark et al [C2] measured the pressure drop for 5 granular materials in a 1 inch (25mm) diameter pipe. The test rig consisted of four straight lengths of pipe, up to 13.7m, joined by bends and instrumented with pressure tappings at suitable intervals. There were insufficient experiments carried out for a complete correlation of the pressure drop for all materials. They had hoped that an index could be used to relate the pressure drop to the physical properties of the material.

Michaelides and Lai [M7] conveyed 5 materials in a test rig with 9m horizontal straights, and a 180 degree bend in between. The straights were not long enough for re-acceleration of the material to terminal velocity after the bend. The bend pressure drop was measured from the inlet of the bend, to the outlet of the bend, thereby not allowing for the downstream effect of the bend which was shown by Bradley [B1], and Rose and Duckworth [R3] to be the major part of the bend pressure losses.

4.2.3 Final choice of particle properties

From the work of those authors examined above, it was apparent that examination of the differences between materials, and their effect on the pressure drop during pneumatic conveying, was an area that required further research. The effect of particle size and shape as having an influence on the pressure drops is identified in several works, indicating the importance of those particle properties on pneumatic conveying, and the need for further investigation.

The particle characteristics which were chosen as most likely to affect the pressure drop caused by solids during pneumatic conveying, were particle size, shape and density. The decision to choose these properties were based on initial thought processes stated previously, and work by other authors such as Mendies et al [M2] and Clark et al [C2] who also came to the same conclusions as to what particle characteristics would affect the pressure gradients during pneumatic conveying. Choosing the right materials for the test work would enable a systematic investigation of the effects of these particle properties on pressure drop. It would be necessary to choose the materials with great care to ensure individual properties could be varied across a range without others varying, and this would need to be done across a broad matrix of values of the properties chosen.

4.3 Selection of initial test materials

To enable comparisons between the test results from the different materials to be the goal in the analysis of the test work, it was necessary to ensure as much as possible that the particle properties of each material were as similar as practicable to at least one (and preferably more) other materials, with the exception of one of the variables. An example of this is shown by the choice of using both sandy and ground ilmenite in the test program; these came from the same source, the ground ilmenite having been reduced in particle size by processing; the particle shape was also slightly different in this case, an inevitable result of the size reduction process, illustrating the difficulty in changing just one variable.

The final choice of the initial test materials is shown below, along with the relationships between them.

4.3.1 Initial selection of six materials

Silica flour

Particle size range 0-40μm

Particle density 2700 kg/m^3

Ground ilmenite

Particle size range 5-40 μm

Particle density 4600 kg/m^3

Olivine sand

Particle size range 200-300 μm

Particle density 3280 kg/m^3

Sandy ilmenite

Particle size range 125-180 μm

Particle density 4600 kg/m^3

Golden pea gravel	Polyethylene pellets
Particle size range 1-3mm	Particle range 3 mm
Particle density 2700 kg/m³	Particle density 914 kg/m³

The principal points of comparison between the test materials were:-

Ground ilmenite and sandy ilmenite	Same material and density, different sizes and shape
Polyethylene pellets and golden pea gravel Sandy ilmenite and olivine sand Silica flour and ground ilmenite	Similar size and shape, different density and material
Silica flour, olivine sand and golden pea gravel	Similar shape and density, similar material, different sizes

As all the trials possible were completed for each test material, within the constraints of the test rig and conveying characteristics of the product, the results were processed and analysed. After the first three test materials, the analysis produced some interesting results (found in the analysis of test results, chapter 6) that showed a trend in the data which could be used when correlating and predicting the pressure gradient along straight sections of pipeline. Further work on the remaining three test materials enabled a graph to be produced using the processed and analysed data points from all six test materials. The particle size versus particle density were plotted on the graph and curves were drawn on the graph for the derived coefficient relating to each test material. This graph (graph 4.1) showed promising results which called for further test work to validate the findings.

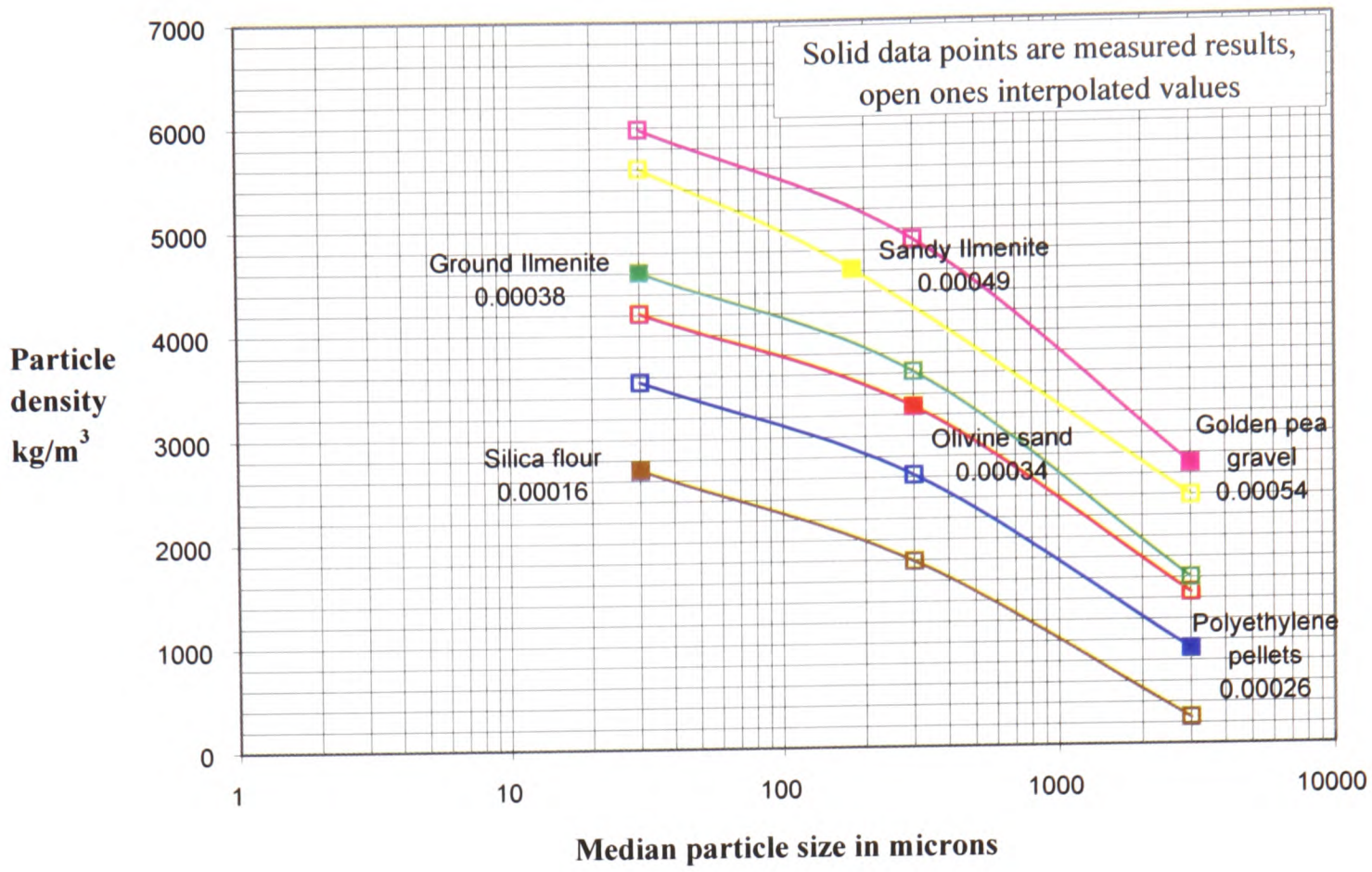

Graph 4.1: The six materials and their coefficients

4.4 Additional four test materials

From the first six test materials, graph 4.1 was produced showing the pressure drop coefficient for each material. The coefficient for each product was determined from the analysed test data from all the test work on that material. Each material has its specific particle density, median particle size, and coefficient. Once this graph was produced, it was clear that further materials should be tested to substantiate the worth of the graph.

There were materials at the laboratory which were available for use because they had either been used once or twice without degrading, or they were superfluous to requirements. Granulated sugar was one of the materials that would be of use for limited test work initially because it degrades easily, but would also be useable when it had been degraded to the size of icing sugar. The sugar in its two states would be another material where the density would remain the same, while the size and shape would be different. Boral lytag was available, which would be of a similar particle size range and material to that of the golden pea gravel, but a different particle density. Finally, glass beads were available, which were similar to the silica flour, olivine sand and golden pea gravel, in particle density and chemical composition, while also having the same particle size as granulated sugar.

The aim of the additional test materials was to verify the graph, consequently, it was not crucial if they matched any of the previously tested materials in density or size exactly.

The particle properties are listed below for the additional test materials. The relationship between them and the previous six materials are also listed below. In total, there were ten materials that were conveyed along the test pipeline, the data processed and analysed, then the resulting coefficients used in the prediction method to determine the pressure losses along straight sections of pipeline.

Granulated sugar
Particle size range 500-800μm
Particle density 1600 kg/m³

Icing sugar
Particle size range 100-400μm
Particle density 1600 kg/m³

Boral lytag
Particle size range 2800-4700μm
Particle density 1560 kg/m³

Glass beads
Particle size range 400-800μm
Particle density 2500 kg/m³

The principal points of comparison between the additional test materials were:-

Granulated sugar and icing sugar.	Same material and density, different sizes and shape.
Granulated sugar and glass beads.	Similar size, different density and material.

The principal points of comparison between the additional test materials and the original test materials were:-

Boral lytag and golden pea gravel.	Similar size and material, different density.
Boral lytag, golden pea gravel and polyethylene pellets.	Similar size, different density and material.

Glass beads, silica flour, olivine sand and golden pea gravel.	Similar material and density, different sizes and shape.

To recap, the principal points of comparison between the original test materials had been:-

Ground ilmenite and sandy ilmenite.	Same material and density, different sizes and shape.
Polyethylene pellets and golden pea gravel.	Similar size and shape, different density and material.
Sandy ilmenite and olivine sand.	Similar size and shape, different density and material.
Silica flour and ground ilmenite.	Similar size and shape, different density and material.
Silica flour, olivine sand and golden pea gravel.	Similar shape and density, similar material, different sizes.

4.5 Particle shape

At the beginning of the project, the particle shape was considered to be an important characteristic with regard to its influence on the pressure losses during pneumatic conveying of solids. However, although the materials chosen for the initial test programme were intended to be rounded in shape, so that shape could not be attributed to any differences in the pressure losses between materials of similar size or density, in reality, it proved more difficult to find materials that keep their shape after being processed. For example, sandy ilmenite is rounded in shape, but to obtain ilmenite in a noticeably different size range, ground ilmenite was selected. Sandy ilmenite is ground to reach its reduced particle size, and as a consequence, the particle shape is altered.

For these reasons, comparisons between materials that only have particle shape in common were not investigated, but all the materials in the test programme are rounded or angular shaped, as shown in the photographs below.

4.6 Photographs of the test materials before conveying tests with particle data

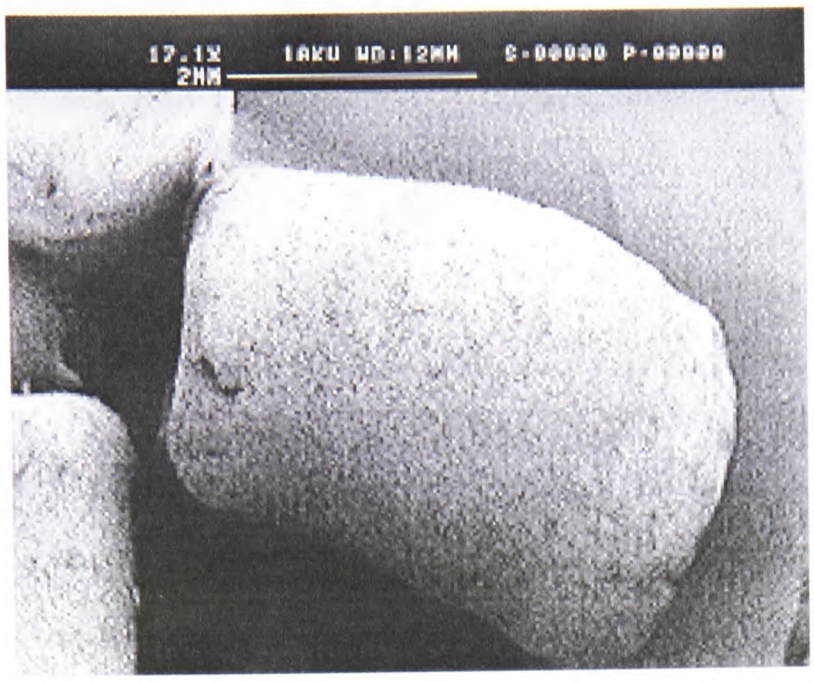

Polyethylene pellets

Polyethylene pellets

Particle range 3 mm

Particle density 914 kg/m³

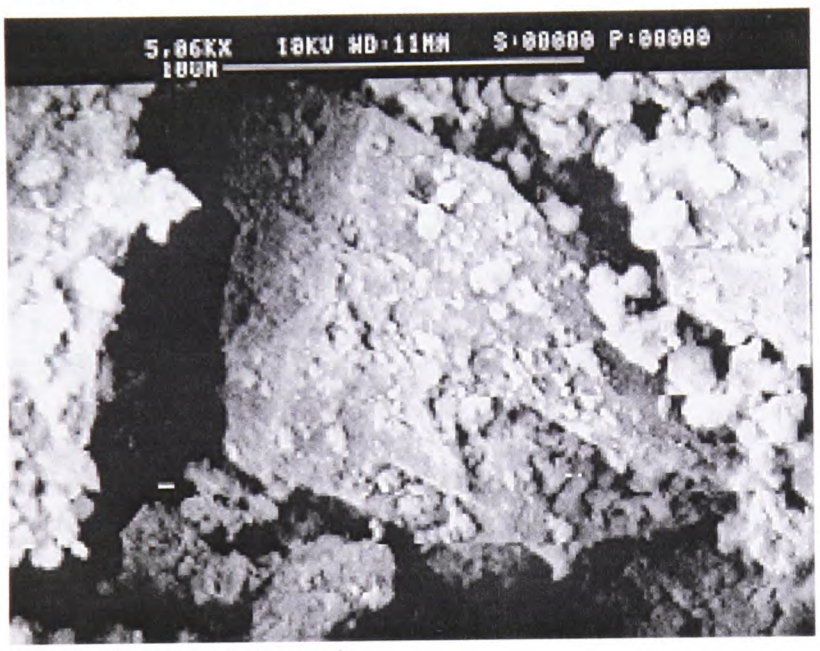

Unused ground ilmenite

Ground ilmenite

Particle size range 5-40 µm

Particle density 4600 kg/m³

Unused sandy ilmenite

Sandy ilmenite

Particle size range 125-180 µm

Particle density 4600 kg/m³

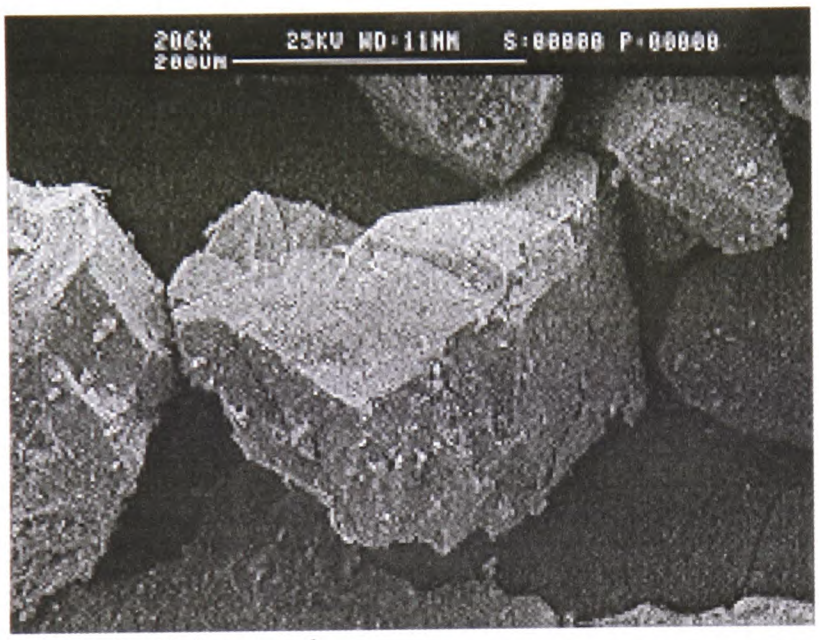

Unused olivine sand

Olivine sand

Particle size range 200-300 µm

Particle density 3280 kg/m³

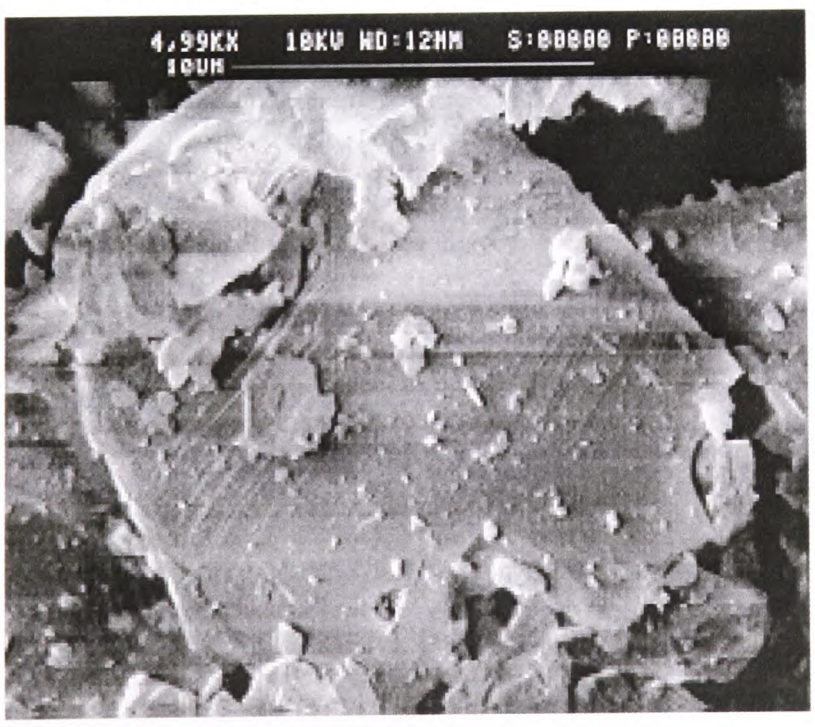

Unused silica flour

Silica flour

Particle size range 0-40µm

Particle density 2700 kg/m³

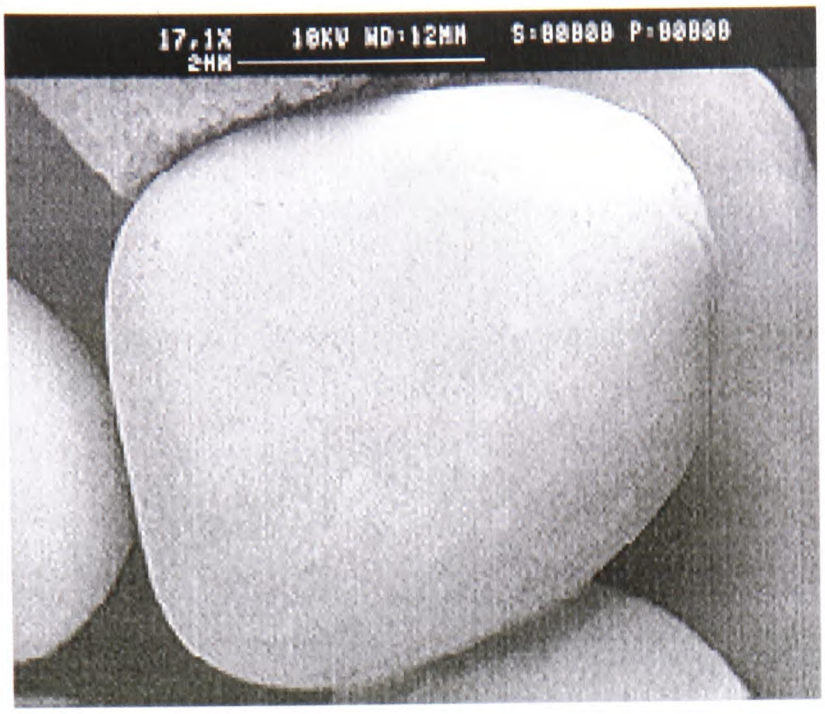

Unused golden pea gravel

Golden pea gravel

Particle size range 1-3mm

Particle density 2700 kg/m³

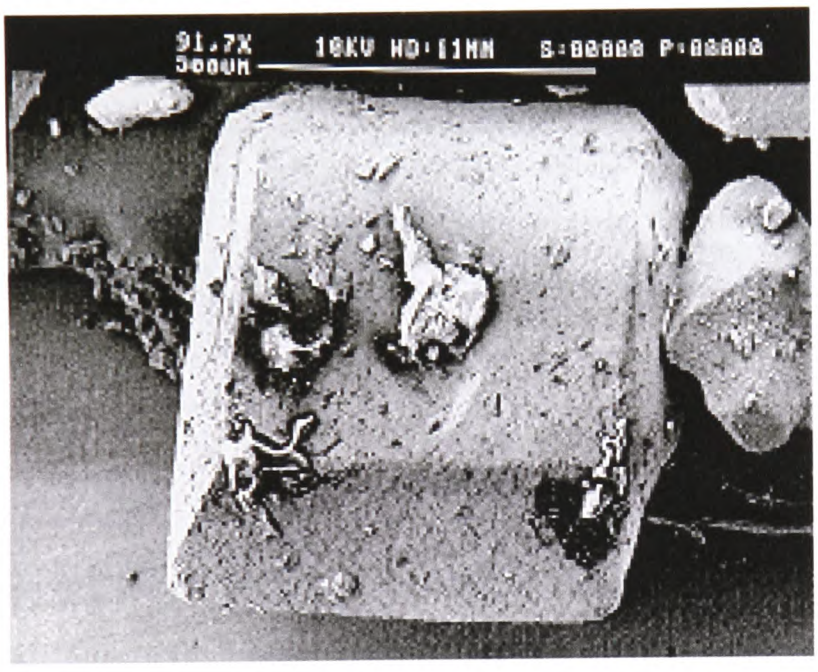

Unused granulated sugar

Granulated sugar

Particle size range 500-800µm

Particle density 1600 kg/m³

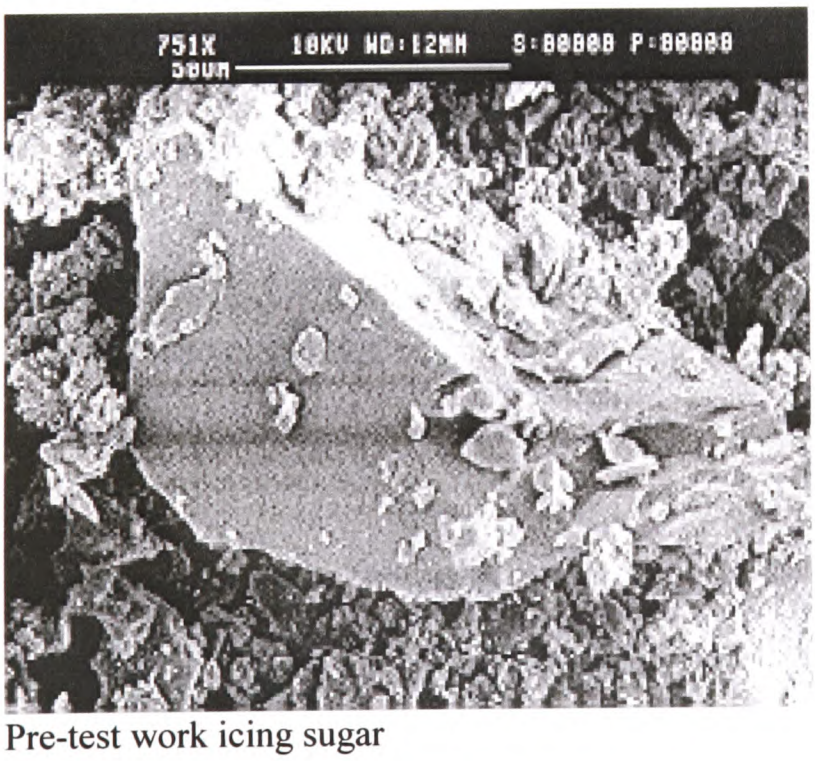

Pre-test work icing sugar

Icing sugar

Particle size range 100-500µm

Particle density 1600 kg/m³

Pre-test work boral lytag

Boral lytag

Particle size range 2800-4700 µm

Particle density 1560 kg/m³

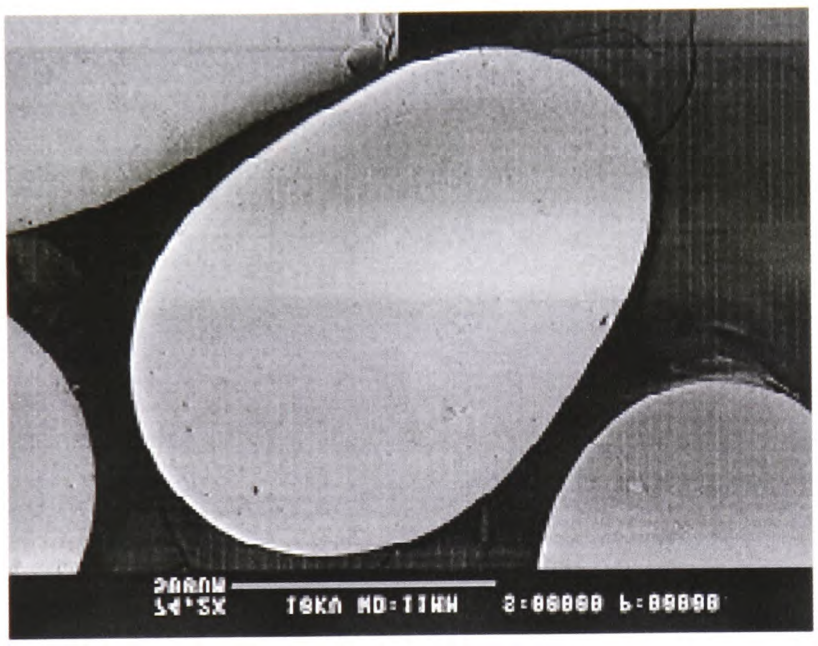

Unused glass beads

Glass beads

Particle size range 400 - 800 µm

Particle density 2500 kg/m³

Chapter 5

Main test programme

5.1 Introduction

The initial test programme was devised while the test rig modifications were carried out. During that period, the options and number of test materials in the programme, the range of conveying conditions, and the approximate number and order of test runs were considered. Having carefully selected six materials for the programme, the amount of data that could be produced by so many products confirmed the need for a systematic programme.

The aim of the test programme was to cover as wide a range of conveying conditions as possible within the limitations of the test rig. Test runs using the same conveying conditions of mass flow rate of air and solids, would have to be repeated periodically for each material, to compare repeatability of the test results to ensure particle degradation was not affecting the results. Materials that were abrasive and therefore expected to erode the pipeline bends, would be closely monitored in repeated tests for comparative purposes. Another reason for the repeated tests for identical conveying conditions, was to determine if the screw feeder was capable of producing the same conditions for both tests.

Some materials were expected to convey in both dense and lean phase, whilst lean phase conveying only would be possible with others due the nature of the material. Materials that degraded quickly would have to start with low air velocities and higher suspension densities, because the higher the air velocity, the faster the particles would break or wear down, which in turn would alter the median particle size and size distribution of the product. It was important to obtain data while the particles were relatively unchanged. Those materials would cover the basic range of conditions within the first 15 test runs. Material samples were taken every 5 test runs to check on the particle degradation.

5.2 Selecting the initial test material

The initial test material used for the commissioning of the test rig was polyethylene pellets. The details of the commissioning trials, difficulties and solutions are presented in appendix 4. This material was included in the test programme for several reasons; previous work had been undertaken using the same pellets by another researcher, so data on the conveying characteristics

was available for comparison purposes if required; they were useful as a product that could be compared in particle size to another of the test materials; they were a robust product that could withstand the repeated test runs necessary for commissioning the modified test rig, and they were conveniently loaded in the test rig ready for conveying.

The pellets were expected to be conveyed in both lean and dense phase because they do so when using an ordinary blow tank. During the commissioning it was found that the feeder could not support dense phase flow with this material. With this knowledge, and the fact that there were many more materials to test, the decision was taken that the test programme would solely concentrate on lean phase conveying at this stage.

In addition, the screw feeder had a maximum speed of rotation, which determined the maximum suspension density the pellets were capable of reaching. Due to the low particle density value of the pellets, the range of conveying characteristics obtained for the pellets were confined (in terms of mass flow rate of solids) when compared to the results from the other test materials. The full range of test results can be found on compact disc (CD) with this thesis.

5.3 Use of ilmenite

Following the polyethylene pellets test runs, the choice for the next material to be tested was between the materials already obtained and stored in the laboratory in preparation for the test work. These materials were sandy ilmenite, ground ilmenite and olivine sand. The ground ilmenite was processed from the same batch as the sandy ilmenite by the company that supplied the material, Tioxide, of Grimsby. This meant that these two materials had identical densities, but different sizes and shapes. The decision to test the ground ilmenite next was taken because it was expected to cause least damage to the internal surfaces of the pipeline out of all three materials available.

From all the test materials selected as part of this research project, the two ilmenites were the materials of most interest. No other pair of products were as similar to each other as these because they originated from the same batch of sandy ilmenite, with only a size reduction process applied to produce the ground ilmenite. They were also not expected to degrade significantly during the conveying test runs. These two materials could not be compared to the polyethylene pellets, as they had no property quantitatively in common with the pellets, so any comparisons between all the test materials so far would have to wait until more materials had been tested.

5.3.1 Test programme using ground ilmenite

The first few tests using the ground ilmenite were carried out using the same process as used for the initial test material, polyethylene pellets, in that low solids loading ratios were used initially in order to get the work started. Once the mass flow rate of solids was increased, the pressure losses across the test bends were far greater than any displayed using the pellets, as were the pressure gradients along the straight test sections. This was thought to be due to the high particle density of the ilmenite. In addition, the pressure drop across all three test bends appeared to be of a similar value for all three bends in each test run, again unlike those determined from the pellets data which was changing from bend to bend and test run to test run.

Further tests on the ground ilmenite showed that for most of the range of tests, the pressure gradient along the pipe increased as air velocity increased and suspension density decreased, as expected. However, for a few tests, the pressure gradients decreased as the air velocity increased and the suspension density decreased along the pipe.

5.3.2 Linear fit applied to pressure gradients along the straights

During the period when the conveying tests using the ground ilmenite were carried out, the large extent of the amount of raw and subsequently processed data generated by all the test work became apparent. For that reason, other ways of representing the data from the pellets were investigated because the task would be far greater as more materials produced results from their own test runs. The main objective was to find a method that would detect a trend through the pressure gradients along the straight test sections. That would enable the data to be analysed further and modelled with the aim of reaching the project objectives, which was to compare the pressure differences between several materials with at least one common variable between each. At this stage, the pressure losses across the test bends were also of interest, as it was only later when the extent of the data and the amount of analysis involved caused the decision to be taken, that the analysis of bend effects would be abandoned in favour of a more concentrated examination of straight pipe pressure gradients. As the modelling of the pressure gradients along the straight sections were part of the process of calculating pressure losses caused by the bends, this was another reason to resolve any problems early on.

In the graph plotting section of the software used to analyse the processed data, an option was available to take any available points, and fit a straight line regression through them. For the test sections of pipeline, the averaged pressure values from each pressure transducer during the steady

state portion of one test run, were plotted on a graph against the distance of the tappings from the start of the test section, as shown on graph 5.1.

For each straight test section, the averaged data points had a least squares best fit line applied to them to identify the pressure gradient for each straight section. Taking all four values for the pressure gradients of the sections, as determined from the least square equations, a linear fit was applied so that the gradients progressed from the first to the last straight section in order. In this way, a sensible (linear) progression of gradients, fitted to the straight pipe pressure data, was ensured for every test run. The linear progression is shown on graph 5.2.

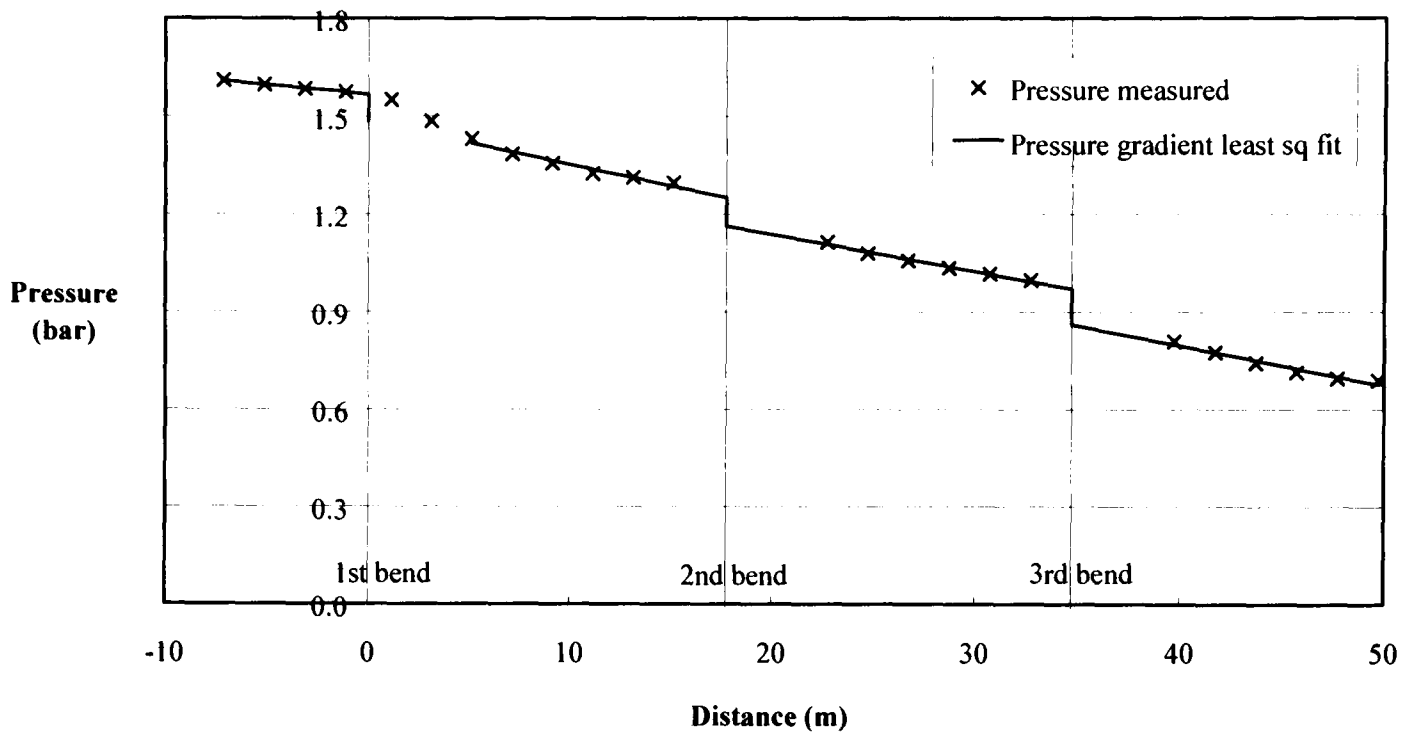

Graph 5.1: Pressure transducers versus distance along pipeline, with least squares and linear progression of gradients fitted through data points. The first two data points after the first test bends are ignored in the least square best fit line through the data points. The reasons for this is to take account of the acceleration length following a bend, and is explained in more detail in appendix 5.

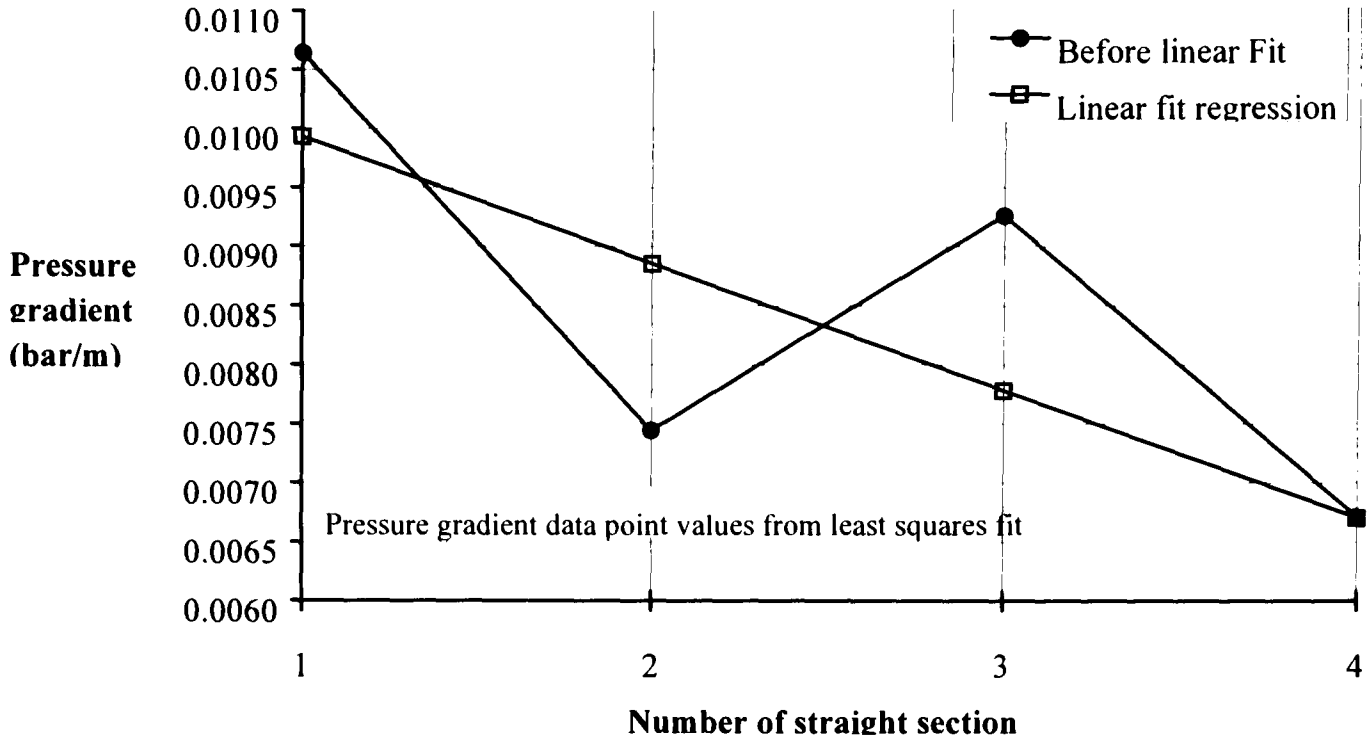

Graph 5.2: This graphs data points represent the pressure gradient for each straight test section. They show the values calculated using the least squares best fit line through the pressure values along the straights, and the linear fit regression through the same data points to give a progressive order to the gradients. The results shown are from test run 10234.

The values for the pressure gradients from the least squares best fit line through the pressure transducers averaged values, for test run 10234, are shown on table 5.1, together with the gradient values for re-fitting to the data points.

Table 5.1: Pressure gradient data points for each straight section of pipe. The values used were taken from test run number 10234, using ground ilmenite.

Number of straight section	Least squares best fit	Linear fit regression
	(mbar/m)	(mbar/m)
1	0.010640405	0.0099322
2	0.007445302	0.0088570
3	0.009263938	0.0077818
4	0.006711261	0.0067067

The linear fit through the gradients, was considered as the best way to compensate for the tendency of the pressure gradient in the third straight test section not to fit in order between the others. The investigation described in appendix 4 had not revealed the cause, so the only way of

dealing with it was in the analysis. This method was applied to all the polyethylene pellets data, and to that from the ground ilmenite. The method was subsequently used for processing and analysing all the test results in the project.

5.3.3 Analysis of straight test sections pressure gradients

From the processed results of each test run, there were four revised solids pressure gradients representing the four straight test sections. From the known mass flow rate of air and measured pressure, the air velocity at the midpoint of each straight test section was determined, together with the midpoint suspension density for each straight test section. These were the variables used to plot various graphs in the pursuit of a way to represent the data that would summarize the conveying characteristics of each material in a concise way.

When a graph of the solids contribution to pressure gradient versus suspension density was plotted (see chapter 6), it was difficult to determine any correlations due to the amount of scatter apparent in the data. The data was plotted on various graphs until a method of analysing the data was found, and is also explained in detail in chapter 6. To summarise, a coefficient was determined from the test work, which (for each material) could be used in a pressure loss prediction method to predict the pressure gradient along straight sections of pipeline.

5.3.4 Test programme using sandy ilmenite

Having completed all the tests using the ground ilmenite, it was unloaded and replaced with the sandy ilmenite. This was chosen as the next material so that comparisons with the ground ilmenite could commence immediately.

Starting with the same conveying conditions as the ground ilmenite, the test work began by finding the minimum conveying velocity for the sandy ilmenite test material. As the ground ilmenite was processed from the same batch of sandy ilmenite, it was assumed that the minimum conveying velocities would be similar to each other. However, the conveying line blocked several times when trying to convey the sandy ilmenite at the same air velocity and suspension density as the ground ilmenite, indicating that the minimum conveying air velocity for the sandy ilmenite was higher at 13.8 m/s than for the ground ilmenite at 11.9 m/s. As the only difference between the two materials was the particle size and shape, the conclusion was that these variables have a definite effect on the minimum conveying velocity during pneumatic transport. The difference in median particle size was 10:1 between the sandy and the ground ilmenite, the shape of the sandy ilmenite was fairly rounded

and smooth, while the ground ilmenite consisted of various fragmented shapes and microscopic bits of dust. Photographs of all the material particles can be found in appendix 7.

Another difference in behaviour between the two materials was that the sandy ilmenite caused greater pressure losses across the conveying system. This made it difficult to repeat the higher range of conveying rates obtained using the ground ilmenite, because the pressure required for these tests exceeded the limitations of the test rig. This behaviour gave an immediate indication that the increased particle size produced greater pressure losses for the same conveying conditions as those measured from a similar material of smaller particle size.

5.3.5 Results from previous test work using sandy ilmenite

A consultancy report in 1986 written for a client assessing the suitability of sandy ilmenite for conveying, noted the author's acknowledgment that a high density product requires a high conveying line pressure drop when compared to less dense products.

The report did not recommend dense phase conveying, but concluded that due to the high air velocities that are necessary to convey in dilute phase (together with the particle hardness of the material) sandy ilmenite should be conveyed as close to the minimum conveying velocity as possible. However, test work results showed an unstable region near the minimum conveying air velocity of 18 m/s, and recommended a minimum conveying velocity of around 21 - 22 m/s.

Those conclusions appeared to concur with the results of the test work using sandy ilmenite in the current programme.

5.4 Interchanging test bends

During the test work on each test material, as batches of test runs were completed, the raw data was processed and analysed, and examined to identify whether there were any problems. The type of problems anticipated were associated with the pressure transducer readings, which experience had suggested could arise from blocked tappings along the pipeline.

Leaving the analysis until all the test runs had been completed could have meant repeating tests unnecessarily. This approach also gave an indication of the magnitude of pressure losses across the test bends, in addition to those along the straight test sections.

5.4.1 Objective

During the analysis of several test runs using the sandy ilmenite, it appeared that for these test runs, the pressure losses across the first test bend were relatively higher than the two succeeding test bends. Therefore, the decision was taken to interchange two of the test bends to see what effect it would have on the subsequent test results .

Test bends 1 and 3 were interchanged in order to compare results and determine whether the large pressure drop from the first test bend was due to the conveying nature of sandy ilmenite, or differential wear on the test bends. Table 5.2 displays the results.

Table 5.2. Comparative test results following interchange of bends

Test Number	$\dot{m}_{air}$	$\dot{m}_{solids}$	Comments on the pressure drop along straights, and the pressure losses caused by the bends	
	kg/sec	t/hr	Straights	Bends
10300 Before changes	0.09399	3.11	almost the same for all straights	inconsistent across all bends
10321 After changes	0.09399	3.11	gradients successively increase.	pressure drop decrease consistently along pipeline.
10311 Before changes	0.12053	5.6	gradients slightly increase	before changes inconsistent
10322 After changes	0.12053	5.6	gradients increase greater	first bend about the same, but bends 2 & 3 reduced drop.
10314 Before changes	0.14638	4.67	steeper gradients before	first bend larger than second and third
10323 After changes	0.14638	4.67	gradients increase still, but not as much.	all similar to each other.
10316 Before changes	0.16399	4.7	steeper gradients before	first bend larger than second and third
10324 After changes	0.16399	4.7	gradients increase still, but not as much.	all similar to each other.

5.4.2 Conclusions on interchanged bends

Interchanging test bends 1 and 3 had an effect on the pressure losses across the test section. At the lower air velocities, the pressure gradients along the straights increased after the changes, while the pressure losses across the bends were more consistent.

At the higher air velocities after the interchanges, the pressure gradients reduced along the straight sections, while the bend pressure losses became similar to each other, as opposed to the first bend having a much larger pressure drop, as was the case before the changes.

The difference to the pressure readings seemed to be directly related to the interchanging of the first and third bends. The third test bend would have been affected more by wear due to its position towards the end of the conveying line, where the air velocity is higher and the pressures lower. Interchanging that bend with a less worn bend near the beginning of the pipeline would be thought to reduce the pressure losses across the third bend which affects the pressure losses along subsequent straight sections. If the pressure drop caused by the bend is less, then the pressure is higher at the beginning of the straight section the bend leads into, which will then affect the pressure drop along the rest of the pipeline.

The reduced pressure losses across the first test bend at the higher air velocities, could not be accounted for. The only explanation could be that the bend was fitted more accurately between the two straight sections, than the previous bend had been. No other reason could be found as the bend dimensions were identical and the bend direction of flow the same.

After the bends were interchanged, the analysis on the test results was revised to take account of the test run results before the interchanged bends. In addition when bends were removed and replaced for any reason, the best fit possible was achieved to avoid any problems of increased pressure losses caused by badly fitting bends such as misalignments.

5.5 Olivine sand test programme

After the sandy ilmenite was unloaded, a new batch of olivine sand was purchased for the test work. Although some olivine sand was already stored for this research project, it had been used previously and degraded to an extent. Olivine sand is slightly angular in shape, and test work using this product would inevitably produce fines by rounding off the particles during conveying along the pipeline. For

this reason, the number of tests carried out on this material were the minimum number in order to cover the range of conveying characteristics possible within the limitations of the test rig.

5.6 Wear on test bends

It was during the test runs using the olivine sand, that the first problems occurred with bends wearing out through erosion. It started with the bends close to the receiving hopper, where the air velocity was highest during pneumatic conveying. Within completing nine test runs, five bends needed repairing because holes had occurred where they had been worn though. Four of these were short radius bends ranging from 30 to 40 cms radius, whilst the fifth was the long sweeping bend leading into the receiving hopper. As there were only nine bends in the complete conveying system, it was inevitable that the test bends would be next to wear through. It was predicted that the last test bend would be the first to puncture, because of the air velocity increase along the system. For these reasons, three new bends were fabricated to the same specifications as the original bends in readiness, and were inserted after the third test bend wore through.

5.6.1 Comparisons between test results before and after bend replacements

Selected tests were repeated after the new test bends were installed, using the same conveying conditions as those previously used. This was to compare the data and determine whether the worn bends made a difference on the pressure gradients along the straight, and the pressure losses caused by the bends.

The results are displayed on table 5.3, and graphically displayed on graph 5.3, 5.4 and 5.5. They show that for three out of the four tests carried out after the new bends were installed, the pressure losses caused by the bends had reduced, while the straight pipe pressure gradients had increased marginally. For the remaining comparison test (10408 and I0431) the pressure drop across the first test bend increased after the changes, while the other test bends only differed slightly. The pressure gradients were also reduced. Both test runs had the highest solids loading ratio out of all the comparison tests, for the lowest air mass flow rate. An interesting finding from all the tests was that the overall pressure drop between the transducers 1 and 24, did not seem to have changed after the new bends were installed, because the rise in pressure gradients and the fall in bend losses cancelled out the differences.

Table 5.3. Results of tests to identify whether the new test bends have an affect on the measured pressure losses.

Test No.	**mass solids** kg/s	**mass air** kg/s	**SLR**	**P1-P24** bar	**Bend losses** mbar			**Gradient of straight** mbar/m			
					1	2	3	1	2	3	4
10415 old bends	2.217	0.1145	19.36	0.8713	174	111	96	4.3	7	9.7	12.3
10418 new bends	2.10	0.1145	18.34	0.8678	116	68	38	6.7	9.6	12.5	15.4
Conclusion - after new bends, bend losses reduce while straight gradients increase											
10417 old bends	0.689	0.1209	5.7	0.4682	54	58	56	3.7	4.6	5.6	6.6
10419 new bends	0.767	0.1209	6.34	0.4743	41	26	12	4.5	6.1	7.6	9.2
Conclusion - after new bends, bend losses reduce while straight gradients increase											
10408 old bends	2.353	0.0967	24.3	0.942	111	61	39	9.2	11.8	14.4	17
10431 new bends	2.172	0.0967	22.4	0.858	133	69	33	6.7	9.5	12.3	15.1
Conclusion - after new bends, bend losses increase in first bend, while straight gradients reduce											
10414 old bends	1.411	0.1145	12.32	0.655	84	75	81	6.5	7.1	7.7	8.3
10440 new bends	1.376	0.1145	12.0	0.6257	79	59	55	5	6.6	8.2	9.8
Conclusion - after new bends, bend losses reduce while straight gradients increase											

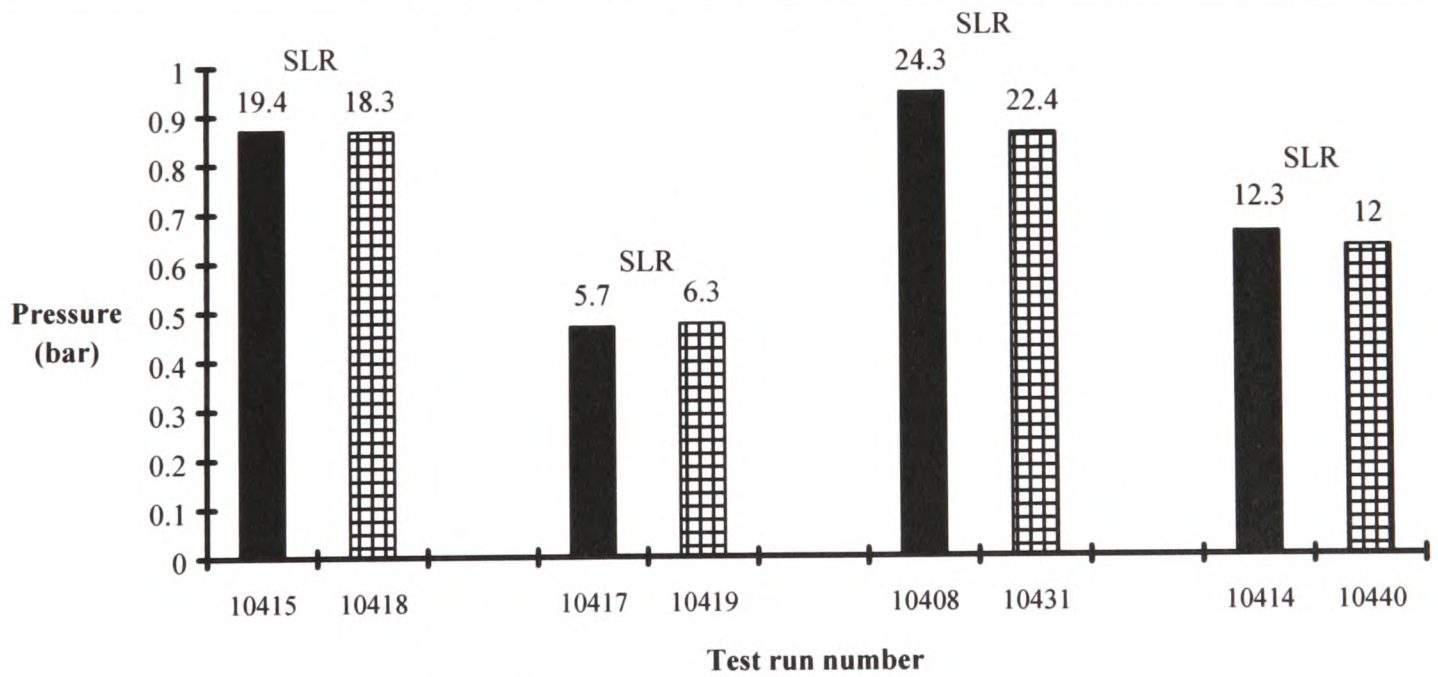

Graph 5.3: The results show the pressure loss across the test section, from pressure transducer 1 to 24, for the old test bends and with the new test bends. The solids loading ratio is also shown for each test run.

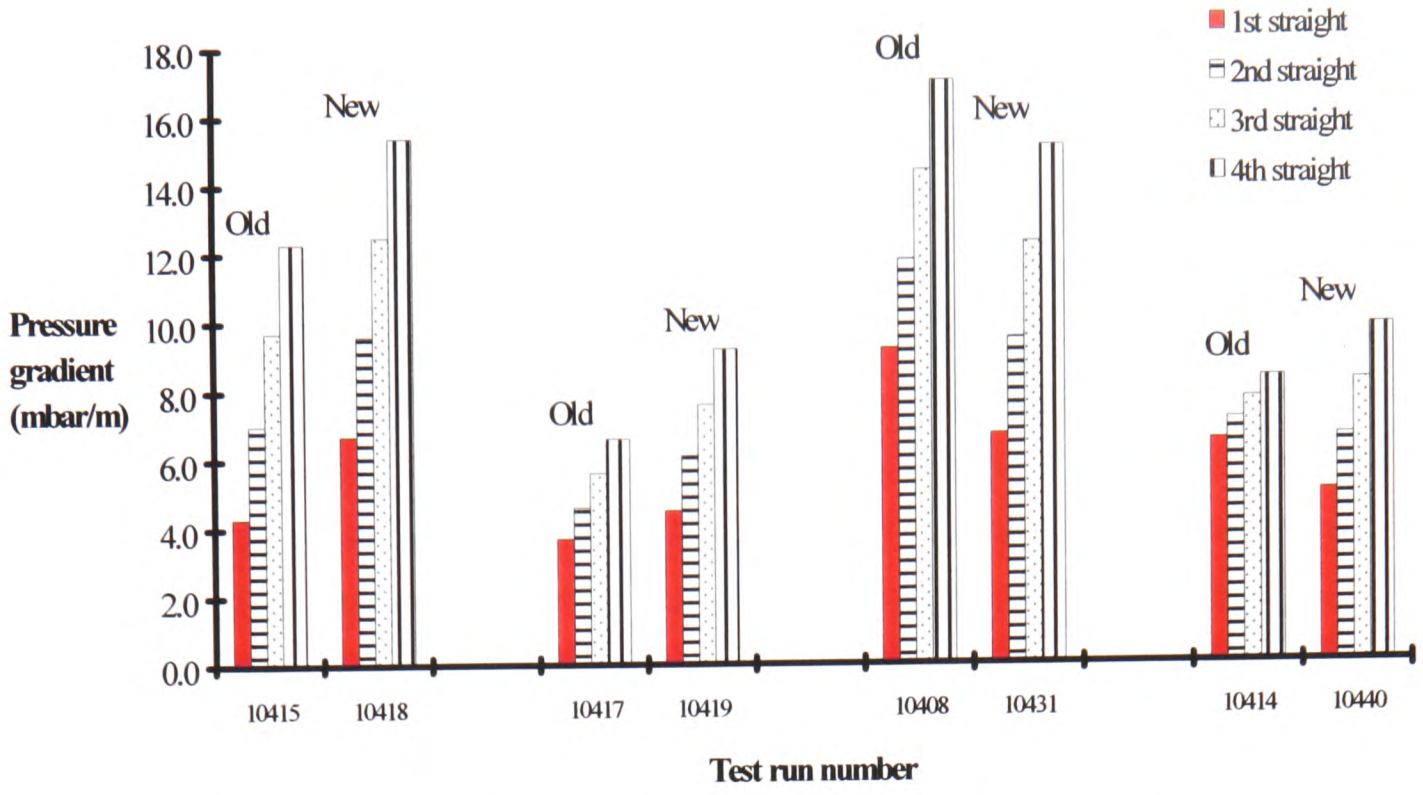

Graph 5.4: The pressure gradients along the straights with the old and then the new test bends along the test section.

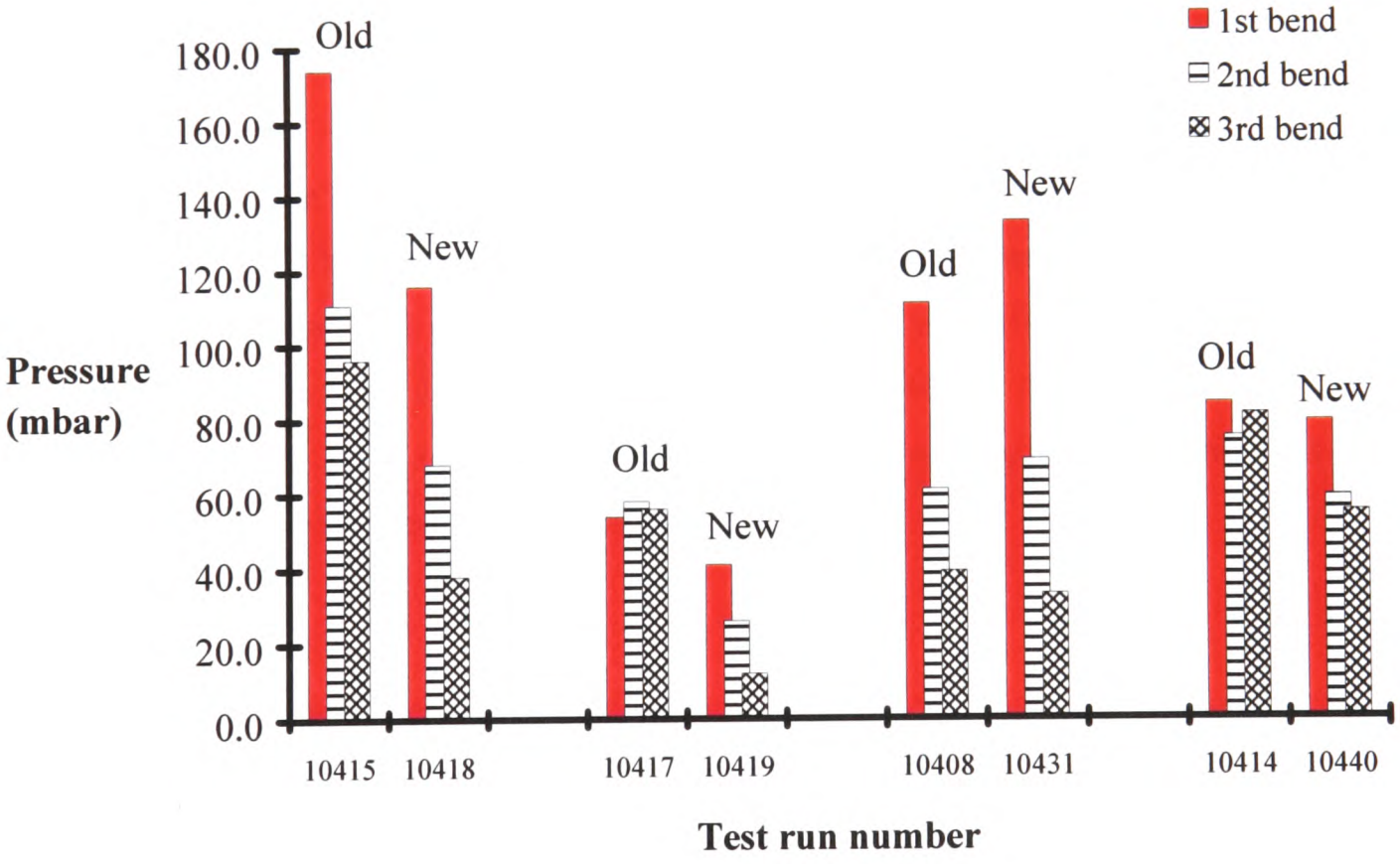

Graph 5.5: The pressure losses caused by the bends, with the old and then the new test bends fitted along the test section.

The table of results and graphs 5.3, 5.4 and 5.5 above, show that the pressure losses across a bend and along straight sections of pipeline, depend on the condition of the bend regarding how much

wear has taken place. However, graph 5.3 also shows that the overall pressure drop along the test section did not depend on the condition of the bends, as the pressure losses were similar across the test section for all cases before and after the bends were replaced.

From graph 5.3, the overall pressure drop across the test section does reduce slightly with the new test bends, as the solids loading ratio decreases, but probably only due to the reduced feed rate of solids. However, it is not practicable in industry to continually change the bends in a pipeline when pneumatically conveying, unless the bends wear through. Therefore, any slight reduction in the pressure losses are limited in time until the bends begin to wear and the pressures losses increase slightly, so the differences with the old and new bends were regarded as insignificant to the overall results.

5.6.2 Effects of new bends

The differences between the total pressure losses caused by the bends as displayed on graph 5.5, are displayed as a ratio versus the number of tests that were carried out using the new test bends. The test bends were replaced after test number 10417, so the difference between tests 10417 and 10419 (which was a repeat of 10417) was that only two test runs had been performed using the new bends.

The ratio between the bend pressures are almost half for those two tests, as is the case with tests 10415 and 10418. In both tests 10415 and 10417, the pressure losses caused by the bends were obtained from tests that were performed towards the very end of the bends useful life, just before it punctured, while the repeated tests (10418 and 10419) were carried out immediately after the new bends were installed. Graph 5.6 shows that as the new bends wear in, the ratio between the pressure losses caused by the bends gets closer to unity.

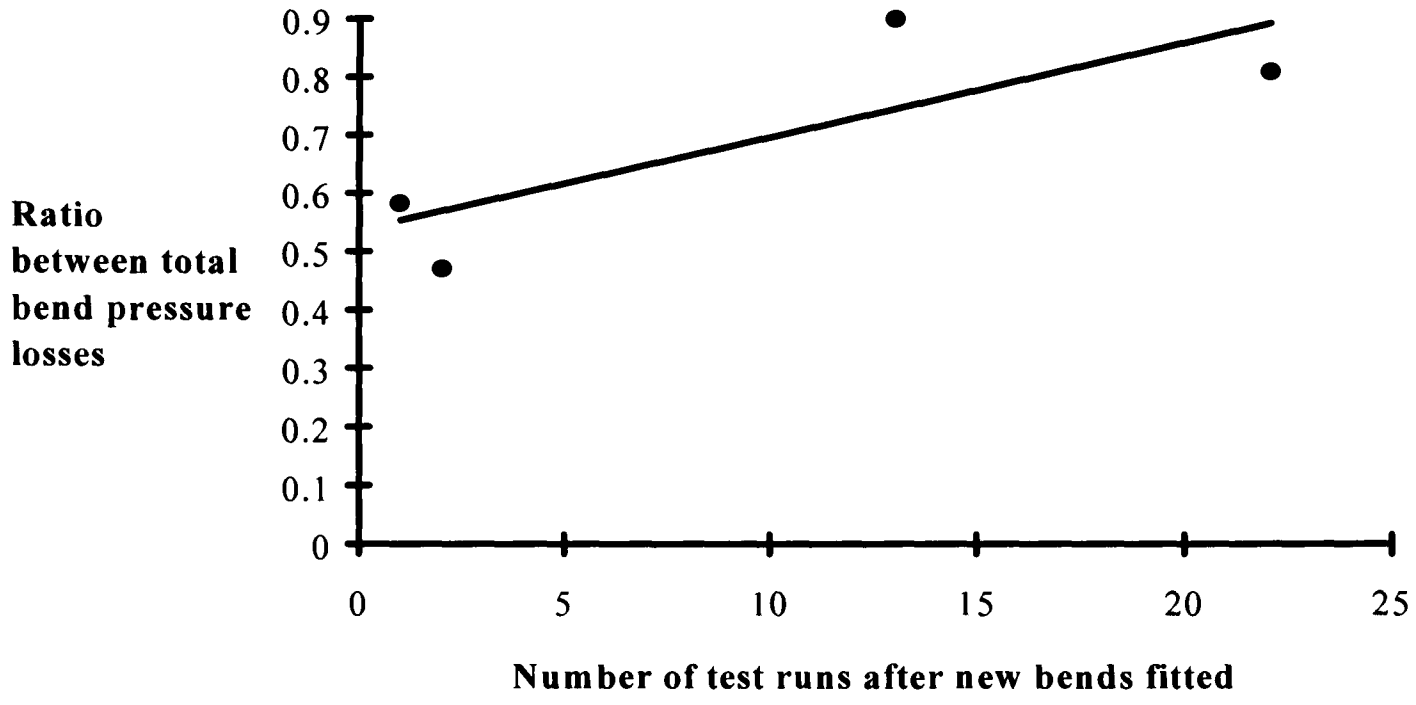

Graph 5.6. The differences in the total pressure losses caused by the bends, measured from data obtained from tests before and after the new bends were installed, are plotted against the number of test runs that were carried out using the olivine sand.

The reason why the total pressure losses across the test section appear to be almost unchanged, despite the large reduction in the pressure losses across the bends for two sets of the comparison test runs, is due to the slight increase in the pressure gradients along the straight sections. This also appears predominately in the tests carried out just after the new bends were installed, and settled down as the bends wore in. The results are shown on graph 5.7 below.

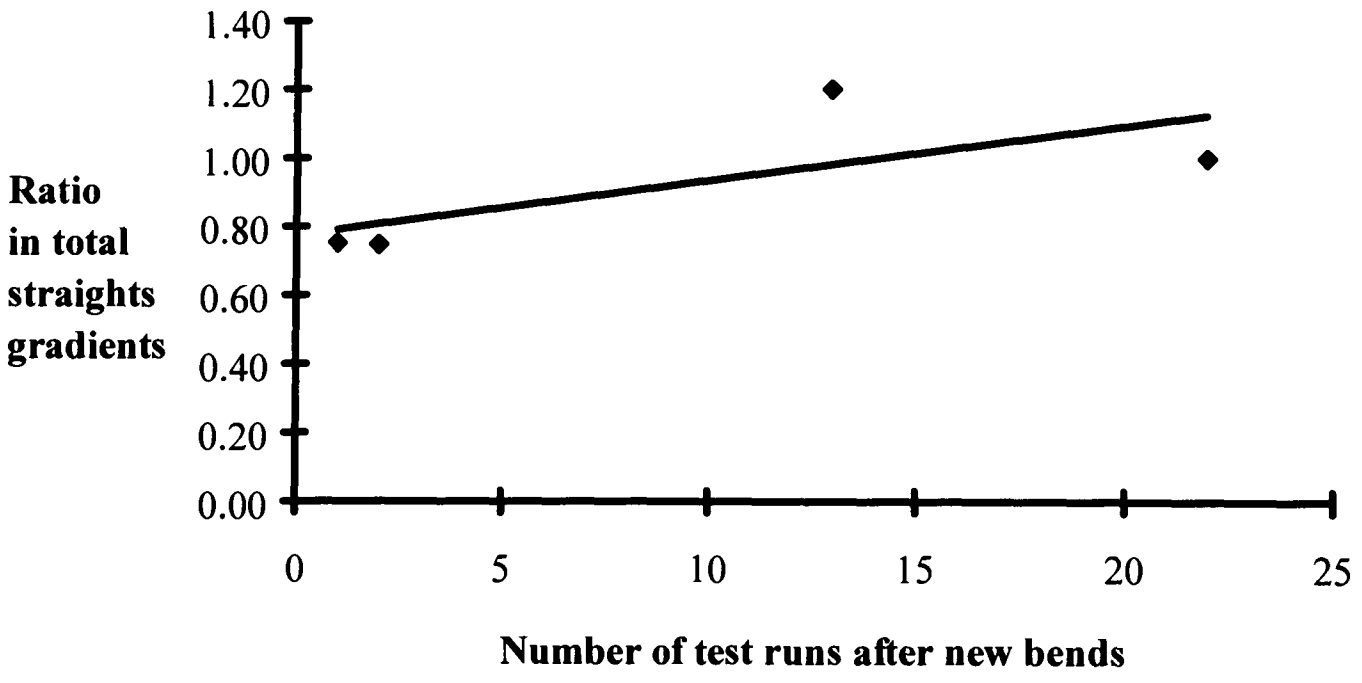

Graph 5.7: The ratio in the averaged pressure gradient along the straights after the new bends were installed, versus the number of test runs carried out.

It must be noted from graphs 5.3 to 5.7 that the pressure losses caused by the bends change substantially (i.e. the ratio is as high as 0.5:1 for the new:old bends) whereas the straight pipe gradients change only a little in comparison.

5.7 Analysis of results on test materials to date

During the processing of the data from the all the test runs, it was apparent that the pressure losses measured using the olivine sand for the same conveying conditions, were considerably lower than those for both the ilmenites. This was expected because the olivine sand had a lower particle density than the ilmenite.

5.8 Samples taken to monitor particle degradation

In order to monitor the degradation of the olivine sand during the conveying test runs, samples of the material were taken at set intervals. This process enabled the samples to be examined and the results observed so that the median particle size and shape could be determined. As the particle size and shape were two of the variables that were considered most likely to affect the pressure losses along a pneumatic conveying pipeline, the particle sizes in particular were closely monitored.

The three test materials preceding the olivine sand, had samples taken before and after the test work so that their particle size and shapes could be recorded. As these materials were not considered likely to degrade at a sufficient rate that would affect the pressure gradient results, samples were not taken at regular intervals during the test work as was the case for the olivine sand.

The particle size analysis on the olivine sand was carried out using the Malvern laser particle sizing equipment[R6]. It was found that by the end of the test work using the olivine sand, the median particle size had reduced from just over 300 microns when new, to 250 microns. The material had been conveyed 23 times around the test rig, but over 42 tests had been completed. That was possible because at low air velocities, or for tests requiring low mass flow rates of solids, several test runs could be completed using a small proportion of the material stored in the receiving hopper. When the test run was finished, the screw feeder was stopped and the air to the blow tank turned off. It must be noted that 42 tests gives 42 x 3 = 126 conditions of suspension density and air velocity for recording the pressure losses caused by the bends, and 42 x 4 = 168 pressure gradients along straight sections of pipe.

5.9 Silica flour test runs

Out of the two remaining test materials to be conveyed in the initial test programme, the product selected for the next set of tests was silica flour. This material has a similar particle density to that of the olivine sand, and is of a similar chemical composition. It also had the same mean particle size as that of ground ilmenite. However, the small particle size of 30 microns (median particle size) meant that this product being silica based, was hazardous to the lungs if inhaled. As with all the materials used in the project, COSHH health and safety standards were complied with. This is because inhalation of the respirable size particles of crystalline silica can give rise to fibrosis of the lungs (commonly referred to as silicosis [H3]).

The hazardous nature of the silica flour, and the problem with bends wearing through along the conveying pipeline, resulted in added precautions being implemented to minimise any spillages that may occur if a bend wore through. This is because high pressure in the pipeline during a conveying cycle will force material through a small hole in the pipeline, even if the inlet air to the conveying pipeline is turned off very quickly.

For the reasons stated above, the test work using the silica flour took longer to complete, as the pipeline was visually monitored during and after each test run to identify any possible leaks as soon as possible after they occurred.

5.9.1 Silica flour full test data and problems with identifying "solids contribution" to pressure gradient

When all the test work had been completed using the silica flour, all the processed and analysed results were plotted on graphs by the same method used for all the previously tested materials. On the graph that displays the solids contribution to pressure gradient values, against the midpoint suspension density, (graph 5.8), there appeared to be several data points that fell below the origin. The values below the origin on the y axis for the pressure gradient for the solids contribution to the pressure losses, indicated that instead of a pressure loss, the total pressure gradient when conveying solids was less than for air only, to the extent that the 'solids contribution' was negative.

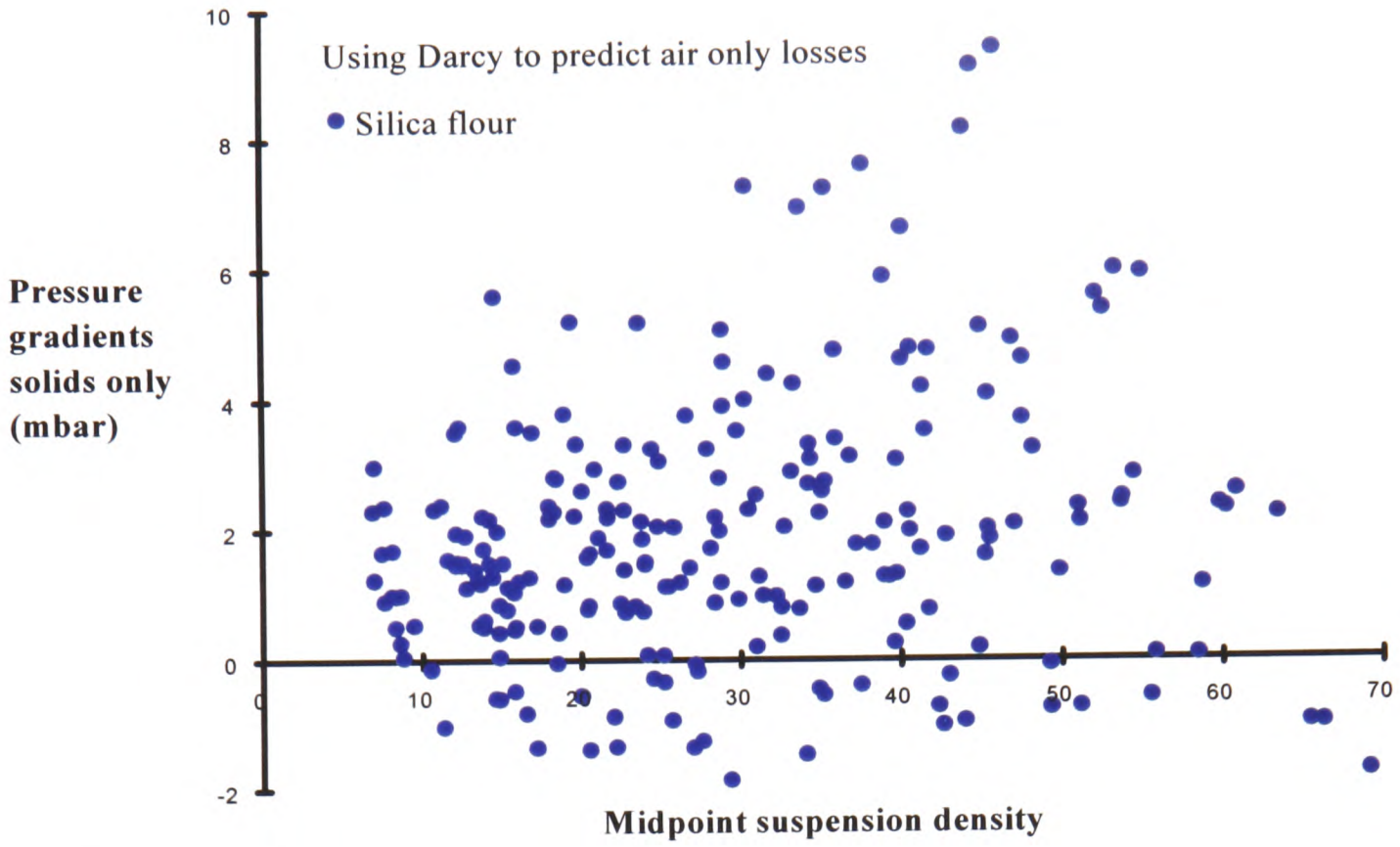

Graph 5.8. Pressure gradients along straight test sections for the solids contribution only to the total pressure drop, versus the midpoint suspension density, using silica flour.

This result gave cause for concern because it is unusual to observe a reduced pressure gradient when solids are conveyed in air, because frictional losses occur when the particles collide with each other or the pipe walls. Energy losses occur as the particles 'catch up' with the conveying air[L2]. This had also occurred when the polyethylene pellets data was plotted, but because the polyethylene pellets have a low particle density and together with the problems associated with the pressure gradients along the straights, it was assumed that the negative values resulted from problematic conveying runs so those test results were not included in the analysis. It was also thought that for very low suspension densities, the solids contribution did not have much effect on the conveying line pressure losses and by deducting the air only values from the total pressure losses, the results would not show any pressure losses.

The data was examined in several ways in search of a reason why the results appeared to show a negative solids contribution. The individual test runs were re-examined and analysed to see whether mistakes were made in the initial analysis.

It is normally expected that when solids are introduced into a pneumatic conveying line, an increase in the pressure drop along the pipe is measured. However, under certain circumstances, the opposite can happen whereby a reduction in the overall pressure drop is experienced. This is a

phenomenon known as 'drag reducing flow'. This was not thought to be the reason causing the pressure gradient increase for certain conveying conditions, because work by Ashenden [A1] concludes that the phenomena is restricted to fine powders in small bore pipelines (25mm) and the test rig pipeline was twice the diameter, i.e. 50 mm nominal bore. In addition, the same effect had been noticed with the polyethylene pellets (as mentioned earlier), and the median particle size for the polyethylene pellets was 3 mm, far exceeding the 'fine powder' specification as quoted by Ashenden [A1].

The solids contribution to the total pressure loss was derived by deducting the 'air only' pressure loss contribution from the measured pressure loss data along the pipeline. This 'air only' contribution had been calculated using the Darcy equation. Thinking logically about the problem, concluded that the air only contribution could be inaccurate. Therefore it was decided that this aspect should be tested for accuracy and if found to be inadequate then another method should be used instead.

5.9.2 Air only test results to determine new equation

It seemed the best solution to obtain an accurate measurement of the pressure losses due to the air, was that the 'air only' contribution should be measured using the test rig. To achieve this, the silica flour was unloaded and the blow tank cleaned leaving the test rig empty of material. Several tests were completed to obtain results for analysis. The mass flow rate of air was increased for each test to cover the range of air velocities used to convey the test materials. The results from all four straight test sections, were plotted and a curve fitted to the data. Graph 5.9 displays the results and the equation of the curve.

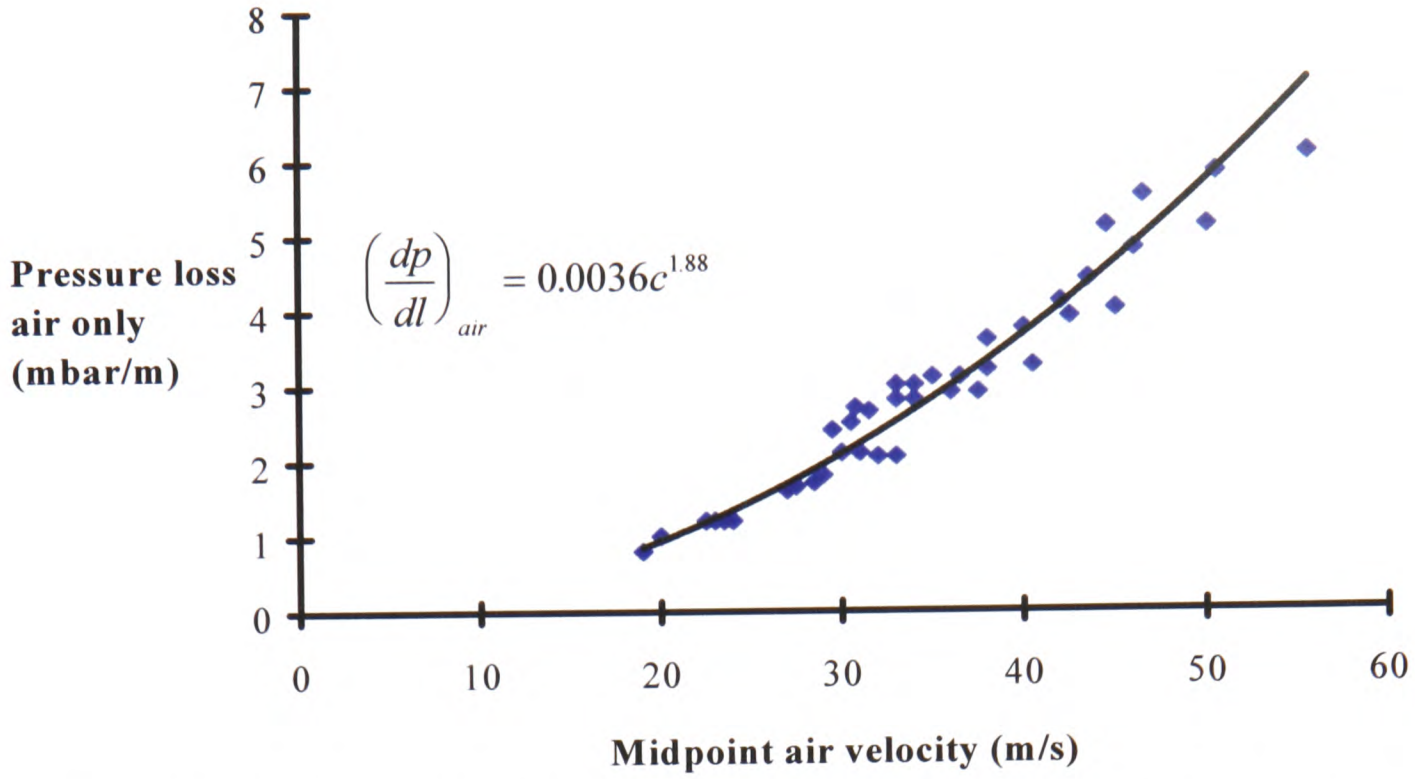

Graph 5.9: Graph plotted from air only conveying tests to determine power law equation.

The equation defining the curve fitted through the data points and shown on graph 5.9 is repeated below:-

$$\left(\frac{dp}{dl}\right)_{air} = 0.0036c^{1.88}$$

where c = midpoint air velocity in metres per second.

The equation of the curve from the 'air only' graph, was used to re-calculate the air only contribution to the total pressure losses of the silica flour test results. The revised values were used to determine the solids contributions to the pressure gradients, which were re-plotted on graph 5.10. Compared to graph 5.8, the differences are apparent and closer to what would have been expected in real terms. That is, introducing solids in a pipeline, would always produce an increase in the pressure gradient along the system over the range of suspension density used in this project.

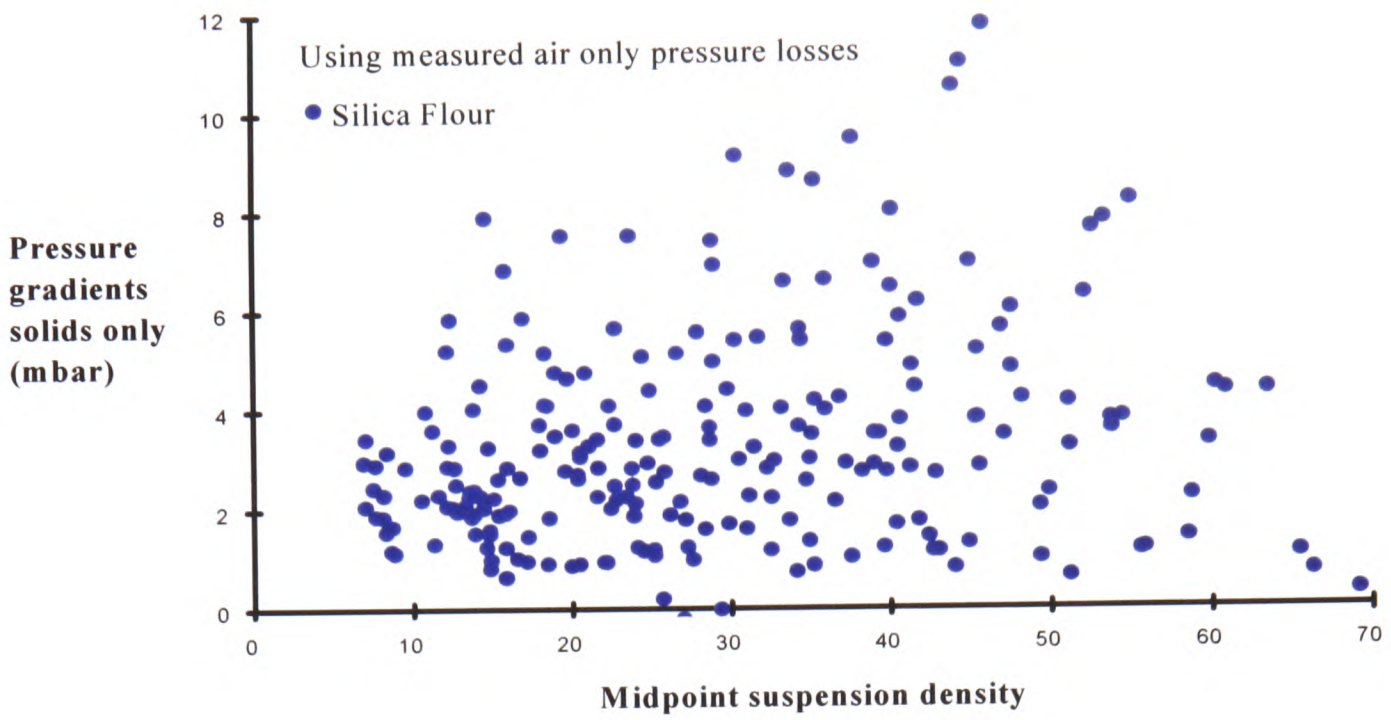

Graph 5.10: Solids contribution to pressure gradients along straight test sections using the modified values for the air contribution.

The new means for evaluating the solids contribution to the total pressure gradients along the straight test sections, meant that the data from all the four test materials previously tested also required reprocessing. The graphs plotted showing the pressure gradients for solids only, against the midpoint suspension density values for selected midpoint air velocity ranges, showed a marked improvement in that the data on these graphs were less scattered than before. An example of graphs using the solids contribution to the total pressure gradient, with the Darcy method of calculating the air, and after with the new air contribution values, are shown on graphs 5.11 and 5.12.

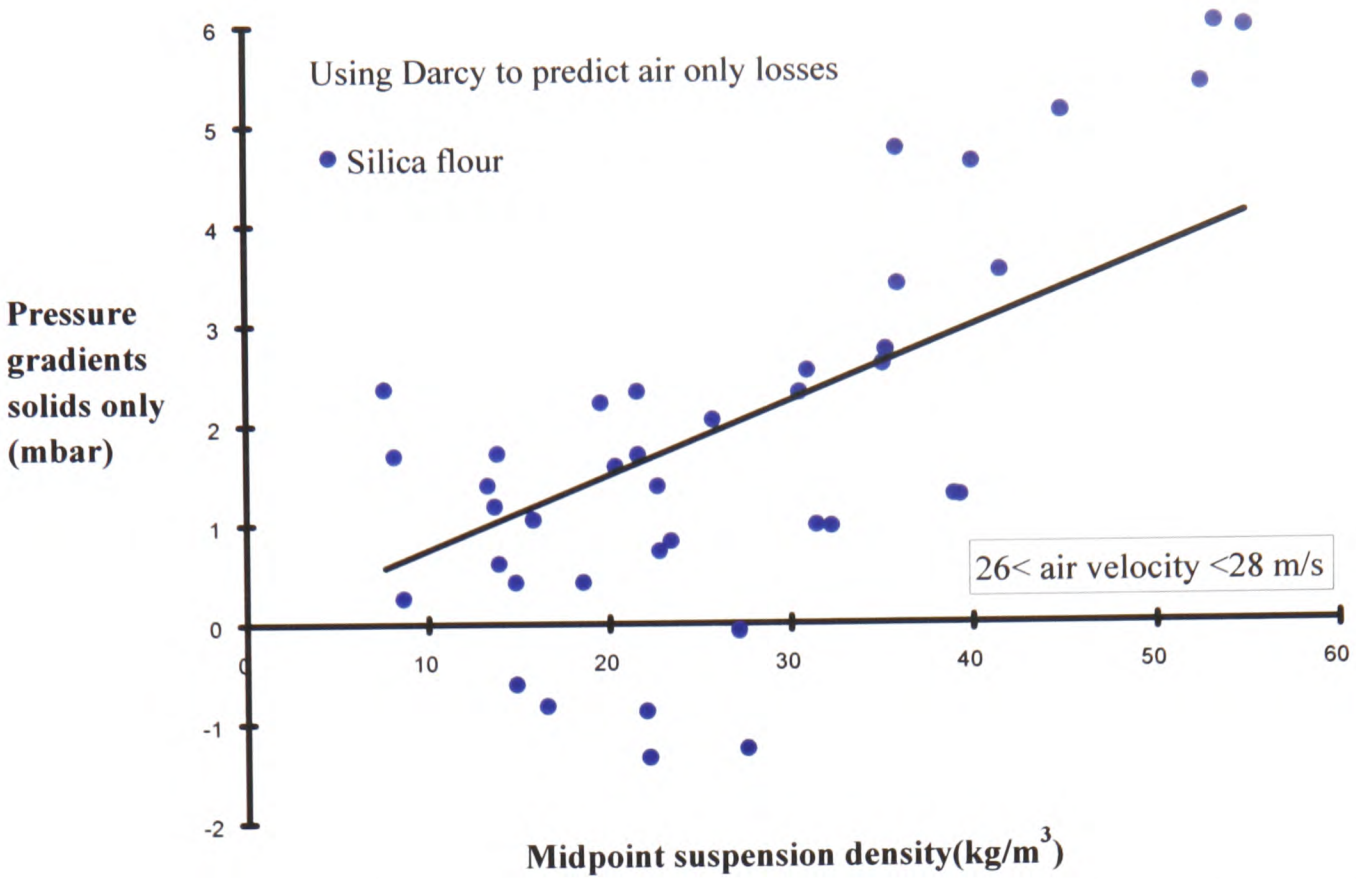

Graph 5.11: Example of solids contribution to pressure gradients along straight test sections, using Darcy to predict the air only pressure losses.

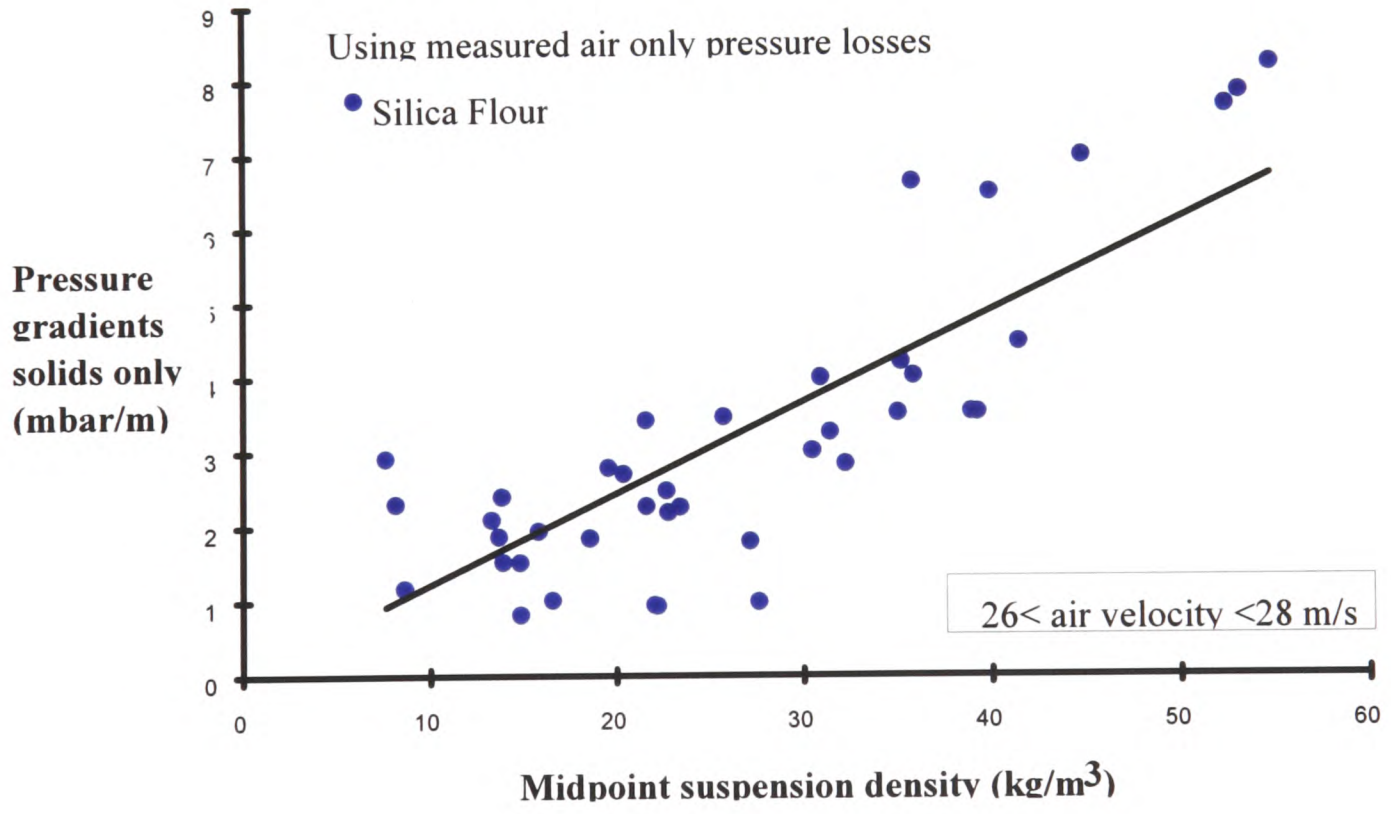

Graphs 5.12: Solids contribution to pressure gradients along straight test sections, using air contribution values calculated from the correlations.

The results displayed on the graphs above, show that the negative y axis pressure gradients are no longer exhibited. The revised method of calculating the air only contribution to the pressure losses was then applied to all the test material results.

5.10 Golden pea gravel test programme

The last material in the initial test programme could now be purchased and loaded into the test rig. The final material previously selected, was golden pea gravel. It was chosen because it could be compared with the olivine sand and silica flour having a similar particle density, and also the polyethylene pellets having a similar particle size and shape.

5.10.1 Particle size

The golden pea gravel was only available for purchase in a particle size range of 2 - 5 mm. As the polyethylene pellets had a mean particle size of 3.2 mm, the oversized and undersized particles would need to be sieved out. This meant that more material would have to be bought than required. According to the supplier, over half the particles should have been within the size range requested. Therefore, one and a half tonnes of golden pea gravel was ordered as three quarters of a tonne of this material was thought necessary to cover the conveying characteristics that should be practicable to measure.

A considerable time was taken to sieve the material. First a 4mm aperture sized sieve was used to screen out the oversized particles. Secondly, a 2.8 mm aperture sized sieve was used to screen out the undersized particles. Over half the gravel was over sized, with half of the remaining gravel undersized. This left one quarter of the total one and a half tonnes, weighing only 370 kg. As the quantity of useable material within the required particle size range was only half of the anticipated amount, there were three options available.

1. Order the same amount of material again, and spend another 7 working days repeating the sieving process.

2. Re-sieve the oversized material with a bigger aperture sized sieve, so that there would be more material for each test run.

3. Work with the 370 kg of correct sized gravel, and see if enough results could be obtained.

The problem with option 3, was that it would take several test runs to determine if there was enough material to cover the full range of conveying limits for this material. By that time, the material would have started to degrade and would need the undersized particles sieved out if fresh material was to be added. On the other hand, it did not seem worth pursuing options 1 or 2 when there may have been enough for conveying trials in the first place. Thus the decision was taken to work with what was available in the desirable size range.

In the event, by using a carefully selected order of test conditions i.e. low mass flow rates of air and higher mass flow rates of solids in the early tests so as to prevent the material degrading too quickly, enough data was taken to give a reasonably wide range of conveying conditions.

5.10.2 Test work using the golden pea gravel

Several problems arose whilst conveying this material. The butterfly valve releasing material from the receiving hopper into the blow tank needed manual assistance for every test run. On two occasions, the screw conveyor jammed, and no amount of hand turning the motor could release it. It was only leaving the rig over night that it somehow managed to free itself. There was one large and one small blow out when bends wore out. Unfortunately, silica flour dust was still in the pipeline which resulted in a large area being covered in dust.

Lastly, and more importantly, there was not really enough material to get sufficient data at the higher air velocities and larger mass flow rates of solids. This was because initially, there would be a pressure transient when the material was introduced into the conveying line, and by the time the pressure settled down to a steady state at these high velocity and flow rate conditions, the material had almost run out, or pressure had not steadied out at all.

Samples of the gravel were taken after every five cycles around the test rig, even if the test results were not suitable. This was to enable the degradation of the test material to be monitored with respect to particle size. Table 5.4 and graph 5.13 show the results from the samples taken.

Table 5.4. Results from samples taken periodically of golden pea gravel

Golden pea gravel particle size analysis				
Number of times material has been conveyed around test rig	Weight of material in grams		Percentage of total weight	
	> 2.8 mm	< 2.8 mm	> 2.8 mm	< 2.8 mm
New	857.4	0.6	99.9	1
5	342.7	36.3	90.4	9.6
10	312.6	47.6	86.8	13.2
15	303.9	56.4	84.4	15.6
21	424.5	49.4	89.5	10.5
26	444.7	107.9	80.5	19.5
31	120.5	96.3	55.5	44.5

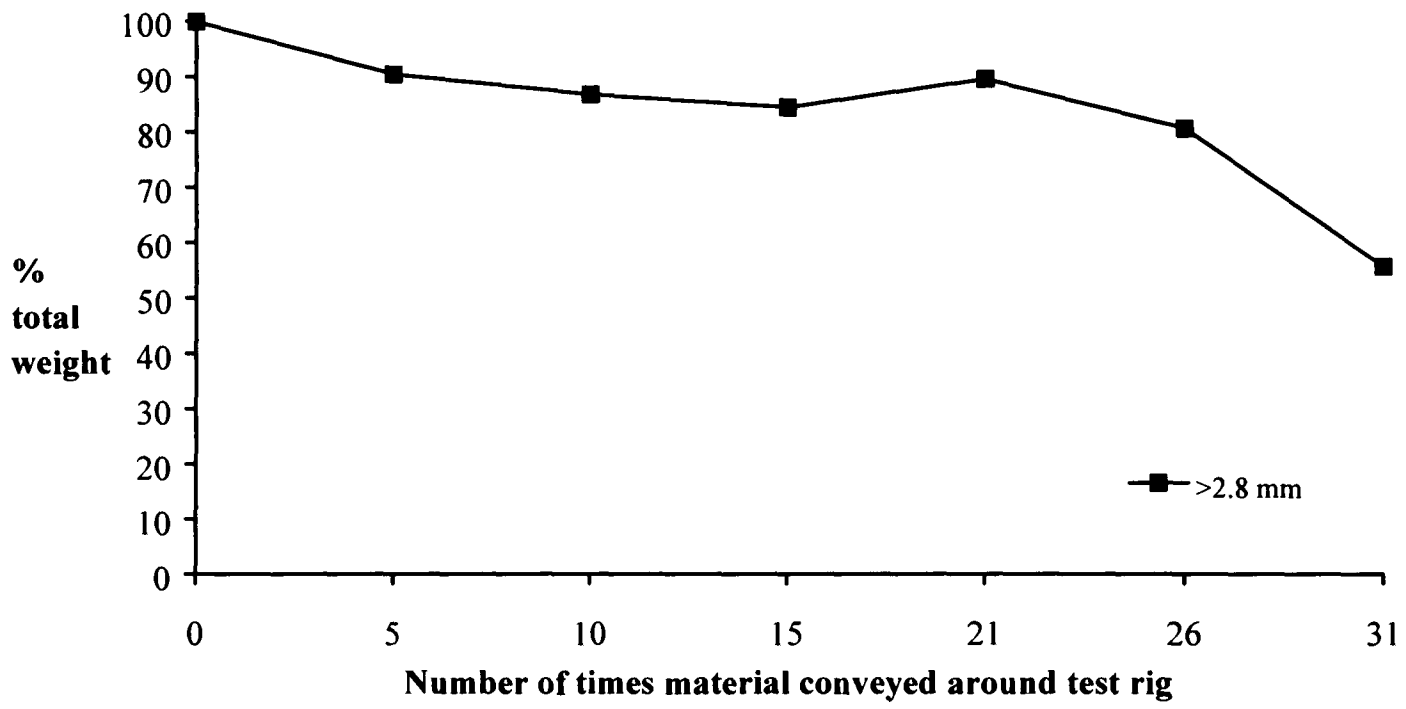

Graph 5.13: The results from the sieved samples of golden pea gravel

During the test work for all the materials, several test runs were repeated for the same conveying condition, so that the results could be compared to determine whether the particle degradation made a difference to the results. The results of such tests using the gravel, did not show a significant difference, probably due to the limited number of test runs and the fact that most of the work in the air velocity range of interest, that is between 20 and 30 m/s, was carried out when there was little change in the particle sizes. From table 5.4, the particles did not degrade substantially from test runs 5 to 21, when most of the mid range of conveying tests were completed. The first 5 runs would be for the lowest air velocity ranges, and the last tests were for the highest air velocity ranges, together with some repeated tests.

5.11 Size analysis on all the new and used test materials

The Malvern laser particle sizing equipment [R6] was used to measure samples of the smaller sized particle test materials, taken before and after the test work. The larger particles such as the gravel and polyethylene pellets, were too large for the Malvern equipment, so their particle size distribution was determined using a selection of sieves. The conclusions for all the test materials under 400 microns, on the size analysis based on the results using the Malvern, were that the changes were too small to have any significant effect on the results (see chapter 7). For the larger sized particles, tests on the polyethylene pellets concluded that the median particle sizes had not noticeably changed. Whereas the golden pea gravel had a growing percentage of broken particles as the number of conveying cycles increased, which was taken into account during the data analysis on the gravel.

5.12 Analysis of all the initial test materials

Having completed the test work on all six materials that were originally selected, the analysis of the relationships between the test materials was continued. A detailed analysis of the test results is included in the following chapter, and thus shows the discovery of the apparently consistent relationship between the particle density, particle median diameter and the incremental pressure loss caused by the addition of solids to the air flow.

Chapter 6

Detailed analysis of test results

6.1 Introduction

This chapter presents in detail the development of the technique which was used for the in-depth analysis of the test data and the search for correlations.

6.1.1 Materials

The initial test programme was conceived to incorporate six materials, with the aim of measuring and comparing the pressure losses along a pipeline, and searching for correlations between pressure drop and particle properties such as size distribution and density. The six materials were carefully selected for their relationship to at least one other of the test materials, in that they shared either the particle size or density in common. The reasons for the selection are detailed in chapter 4.

The first material used in the test programme was polyethylene pellets. The pellets were also used in the commissioning of the test rig, and were chosen because they are robust and would not degrade significantly during repeated conveying. The development of the technique for processing the raw data, and its subsequent analysis, proved to be a continuous process throughout the duration of the test work and beyond. In fact, the final method of analysing the data into the definitive form, did not occur until after the first stage of the test programme had been completed, when all six materials had been investigated. It was only after the first set of six test materials had been analysed, that a second stage in the test programme was needed to verify the findings from the first part of the test programme. The second stage of the test programme comprised of four additional test materials, hence totaling ten test materials in all.

6.1.2 Initial data gathering

Each test run produced raw data scanned from 26 pressure transducers along the test rig, including two which monitored the upstream and blow tank air pressures. In addition, readings were taken from three load cell outputs that were positioned beneath a receiving hopper. Taking differences in the readings from the load cells enabled the mass flow rate of material entering the receiving hopper to be determined. During each test run the transducers and load cells were

scanned for data every second, over a 150 or 200 second time period. The longer time period became necessary when testing relatively degradable products, such as the sugar (see chapter 7). The raw data was stored in a data logger and transferred to a computer after each test run was completed. Once stored in the computer, the raw data was then processed and analysed, and transferred to a database. Each material had its own database, so that at the end of both stages of the test programme, there were ten databases, each representing one test material.

6.1.3 Initial analysis of raw data

When all the raw data from each test run carried out on the polyethylene pellets (the first material) had been processed, the analysis of the completed results was initiated. A detailed description of the development from raw data to a graph representing all the results from a test run is found in appendix 5. In summary, a graph is plotted showing the averaged pressure results from the 150 raw data values for each transducer against the time period of the test run. From the graph, a steady state period was selected from which all subsequent results are calculated. At the same time, for each straight test section, a least squares best fit line is plotted through the data points, in order to determine the pressure gradient along each straight section of instrumented pipeline. A linear progression in gradients was applied to all four straight sections, so that a methodical pattern was given to all the pressure gradients, see chapter 5. It was at this point that the more detailed analysis of the data, to which this chapter relates, began.

6.2 Analysis of processed data - Stage 1

6.2.1 The concept of solids and air contributions to total pressure gradient

The pressure gradient observed by the transducers along the straight sections of pipeline, monitors the pressure losses for the solids and the air conveyed as a mixture. The complex interaction involving the two phases along a pipeline are usually represented as a model displayed below.

$$\left(\frac{dp}{dl}\right)_{total} = \left(\frac{dp}{dl}\right)_{aironly} + \left(\frac{dp}{dl}\right)_{solids}$$

where $\left(\frac{dp}{dl}\right)_{total}$ = pressure gradient observed in pipe, in bar per metre

$\left(\frac{dp}{dl}\right)_{aironly}$ = pressure gradient when solids are absent, predicted using conventional means e.g. an equation similar to the Darcy or Fanning equation produced by tests using air only along the pipeline, in bar per metre.

$\left(\frac{dp}{dl}\right)_{solids}$ = Additional pressure gradient, in principle caused by the addition of the solid particles to the air, in bar per metre.

The model is purely a concept used as a convenient means of thinking about why the pressure drop increases when solids are introduced, and storing the data.

The pressure losses along straight pipelines due to the 'solids contribution' are commonly used in data analysis because it is considered that the 'air only' pressure contribution to the total pressure losses are small in comparison. Under certain conditions, i.e. very low suspension densities and low air velocities, and in pipes of small size, the air only contribution can increase and become more significant. During the analysis of the data in this project, the air only contribution was shown to make a notable contribution for some materials conveyed at low solids flow rates, see chapter 5.

6.2.2 Analysis of the pressure gradient for the 'solids only' contribution

Applying the linear progression of gradients, the "air only" contribution to the pressure gradients was deducted from the total pressure gradient results, leaving the pressure gradients for the solids contribution to the pressure drop per unit length. Using these results, a final graph was plotted of the pressure gradient for each straight section against the midpoint suspension density determined for each straight section. An example using the polyethylene pellets is shown on graph 1. The 'air only' contribution was determined using the Darcy equation at this stage, but was subsequently re-assessed using the 'air only' contribution equation determined from test work. See chapter 5.

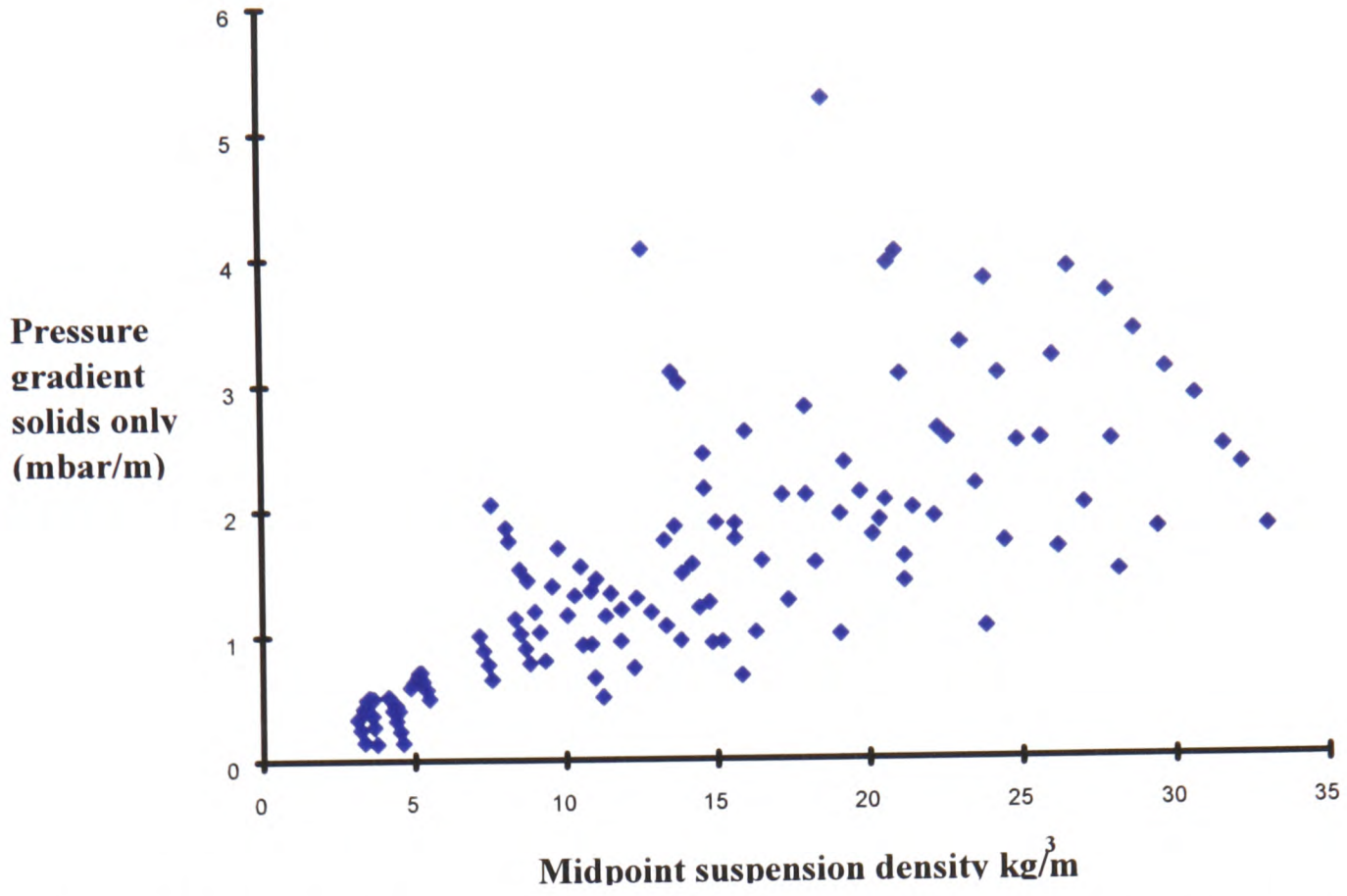

Graph 6.1: 'Solids only' pressure gradients along straight test section versus the midpoint suspension density, for polyethylene pellets. The 'air only' contribution using the Darcy equation was deducted from the total pressure gradients.

Graph 6.1 shows all the processed results, but there is a wide scatter of data which showed that a direct correlation between the pressure gradients for the solids and suspension density alone was not sufficient. Therefore, an investigation into more applicable ways in which the data could be presented and utilized was carried out. It was decided to separate the data shown in graph 6.1, still using the same variables, but only plotting the data from individual air velocity ranges.

6.2.3 Separation of the air velocity data to correlate the pressure gradient against the suspension density

As stated earlier, several steps were taken to eventually reach the data analysis method that was used to present the data obtained from the test programme. From graph 6.1 which represented all the test data, the results were separated into individual air velocity ranges. This was one of a number of steps taken to find a trend in the data so that it could be used to determine how the material behaves during pneumatic conveying. Graph 6.2 shows the results from a 4 m/s air velocity range, with 4 mathematical models drawn through the data points.

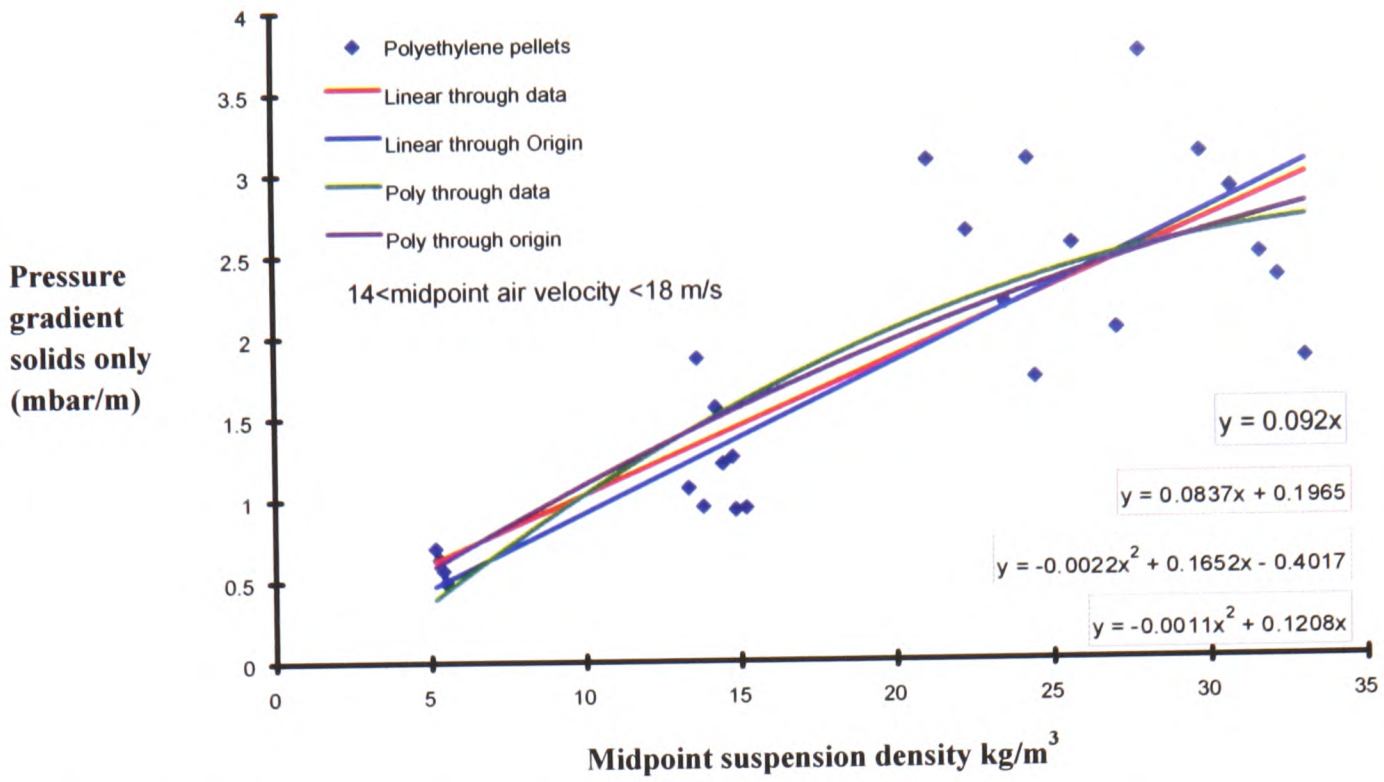

Graph 6.2: Pressure gradients along straight test sections for the air velocity range, 14 to 18 m/s, versus the midpoint suspension density.

Initially, each air velocity range covered up to 4 m/s e.g. from 14 to 18 m/s. For each range, all the data points had several mathematical models fitted to them, and equations representing each line were calculated. The four mathematical models used were,

- a linear line through all the data
- a linear line through all the data, but going through the origin
- a polynomial curve through all the data
- a polynomial curve through all the data, but going through the origin

As displayed on graph 6.2, none of the four curves or lines showed a reasonable correlation with the data. The exception was the higher air velocity ranges i.e. over 30 m/s, which had fewer data points to plot. The reason for the reduced number of data points for higher air velocities, is that the majority of the midpoint air velocity data fell between 20 and 30 m/s. The results of this analysis led to the air velocity ranges being further divided for the individual graph plotting, of the pressure gradient versus the midpoint suspension density.

6.2.4 Air velocity ranges for individual graph plotting

After some experimentation, it was discovered that the optimum air velocity range should cover a 2 m/s spread of air velocities. For example, for the air velocity range of 16 m/s and 18 m/s, the midpoint air velocity values ranged from 16.00 m/s to 17.99 m/s as shown on graph 6.3.

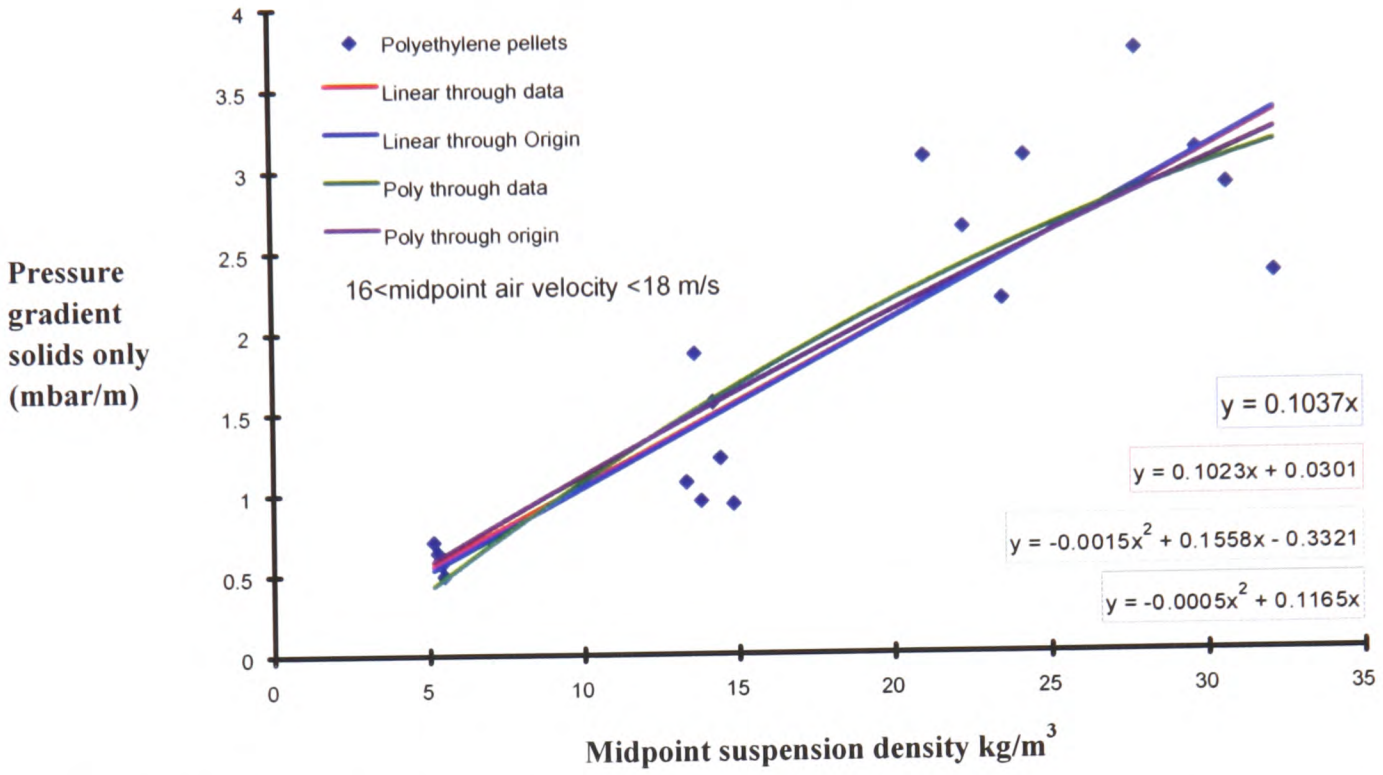

Graph 6.3:, as graph 6.2 but with the reduced air velocity range from 4 to 2 m/s.

There was still some scatter of the data points on each individual air velocity range graph, as shown from graph 6.3, but now the scatter was more obvious when there were fewer data points from which to plot a straight line. That was once more for the very high values over 30 m/s, and very low air velocity ranges of less than 18 m/s. This problem was put to one side to be addressed at a later date, when a prediction method was developed.

Once the air velocity ranges were reduced to 2 m/s, the correlations between the pressure gradients for the solids contribution and suspension density were much clearer with less scatter of the data either side of the mathematical models. The results of analysing the four mathematical models through the data for all the graphs covering the air velocity ranges, showed that the linear fit through the data points starting at the origin was as good as the others, so this was chosen because it was the simplest. Plotting the mathematical model through the origin was logical because there can be no solids contribution if no solids are flowing.

Each straight mathematical model had the equation,

$$\frac{dp}{dl}_{solids} = m\rho_s$$

where $\frac{dp}{dl}_{solids}$ = pressure gradient for the solids contribution to the total pressure gradient along the straight section of pipeline.

m = the slope of the line.

ρ_s = suspension density - kg of solid transported per cubic metre of conveying air flowing (using true volume flow rate of air at the pressure in the pipe, as opposed to "free air" conditions).

The suspension density is not the true density of the mixture in the pipe in terms of the actual mass of solids present in each unit volume of air inside the pipe, it is the mass of solids conveyed by every actual cubic metre of air passing a point in the pipeline. That is because in practice, the average density of the mixture (kg of solids in every actual cubic metre of air) will be higher, because the solids travel more slowly than the air, the difference being due to the slip velocity [L2].

For practical purposes the value for the true suspension density is not easily obtained, so the value determined by the mass of solids conveyed by every actual cubic metre of air passing a point is used as the suspension density, to enable the variable to be used easily in the models.

The number of individual graphs were limited to the extent of air velocities measured along the test sections for conveying test runs on that material. For example, polyethylene pellets recorded midpoint air velocity values from 11 to 37 m/s, whereas the range for ground ilmenite went from 15 to 42 m/s.

The values for each straight mathematical model fitted to individual graphs for the 2 m/s midpoint air velocity range, were plotted on graph 6.4 together with the values from the 4 m/s ranges. Two polynomial mathematical models were drawn through each set of data points, to illustrate the effect subdividing the air velocity ranges has on the equation formed from those results.

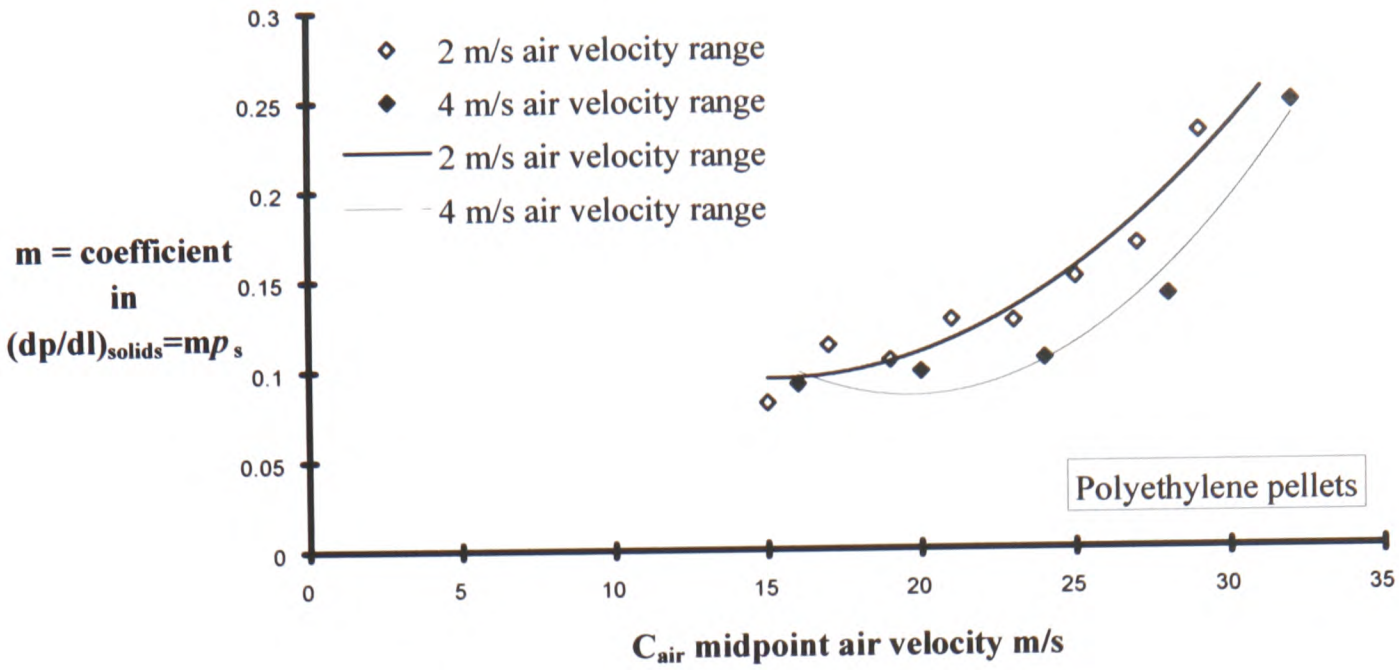

Graph 6.4: showing the two sets of data points of the slope values from selected air velocity ranges, versus the midpoint air velocity. Polynomial curves have been fitted to each set of data points.

It can be seen that using too wide an air velocity range changes the slope of the line through the data because the differences between a 4 m/s air velocity range, obviously have an effect on the pressure gradient and suspension density values, whereas narrowing the range from which the data is obtained gives a more accurate picture of the averaged data values. In particular, for the pellets, the higher air velocity ranges had fewer data points than most of the other materials in the test programme. It was not possible to convey the pellets at high velocity ranges with high solids loading ratios because of the low particle density of the product, when using the screw conveyor. The speed of the motor of the screw conveyor was limited by the gear unit (see appendix 3) which could not physically rotate any faster to put more material into the conveying line to obtain higher suspension densities. Therefore, the 4 m/s air velocity range would not have many data points from which to draw the slope from, as shown in graph 6.2.

6.2.5 Correlation for the pressure gradient against air velocity

Graph 6.4 was repeated using the 2 m/s air velocity intervals only. This was so that mathematical lines could be drawn through the data points, in the search for a model that could be used in a pressure loss prediction method. The mathematical model lines in graph 6.5 consisted of:-

- a linear line through all the data
- a polynomial curve through all the data

- an exponential curve through all the data
- a power law curve through all the data

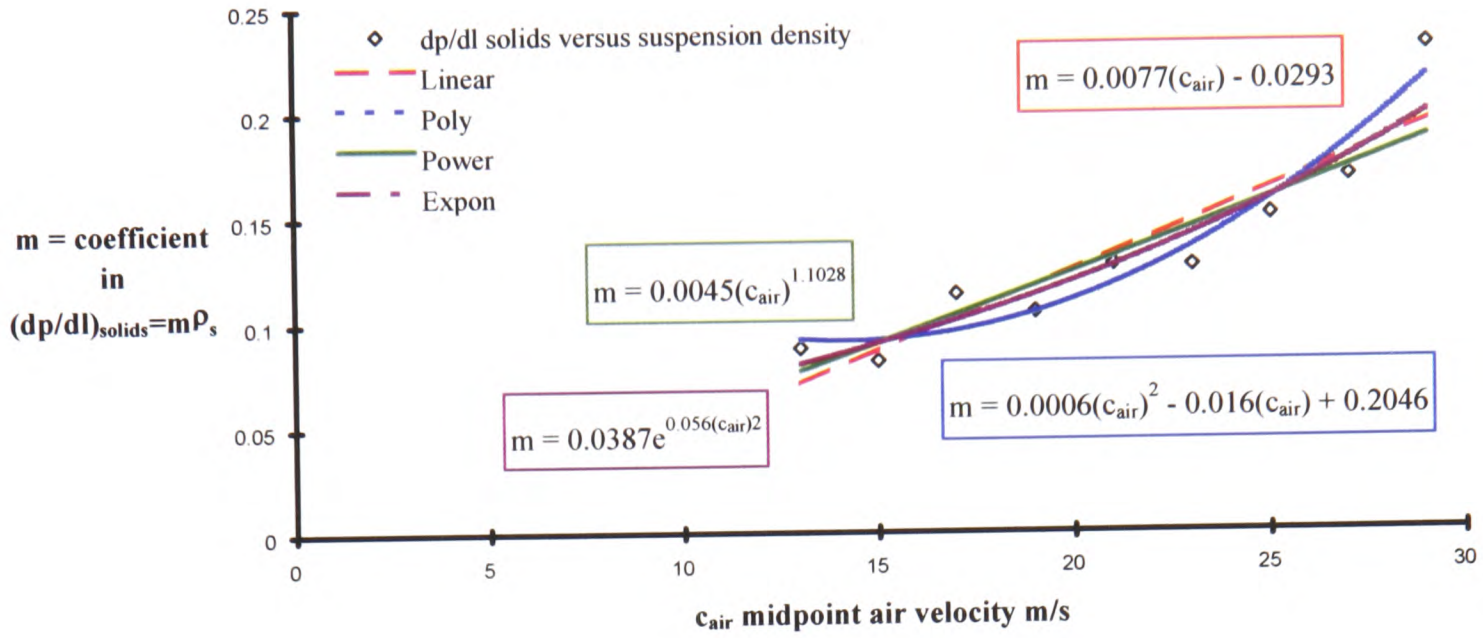

Graph 6.5: Results of slopes versus midpoint air velocity range, with four mathematical models fitted through the data. The equations for each model are displayed on the graph.

Graph 6.5 showed four different mathematical models fitted to the data points. All the constants from the various mathematical models were used in the model to predict the pressure gradient along straight sections. When all the results were compared, there was little difference between them.

Of the four different mathematical models used, all fitted the data about equally well. Consequently, the choice of which to adopt was made partly on the results of attempts to use these different models for predicting pipeline pressure loss (which were equivocal in terms of which model would be best, see section 6.2.4) but also partly based on a consideration of other factors. First it seemed reasonable to choose a correlation which went through the origin since it could be argued that the solids would make no contribution to the pressure gradient at zero velocity.

This tended to suggest the rejection of the linear model with offset since it gave a negative solids contribution at zero velocity. Without such an offset, a linear model gave a poor fit to the data. The polynomial model, in addition to not passing through the origin, would clearly be difficult to conceptualise in terms of physical modelling and at the same time would give great difficulty in reconciling the irregular dimensionality arising from incorporating more than one power of the primary variable (i.e. c_{air}^2 as well as c_{air}).

This left the two favourites as the exponential and power law models. Of the two, the exponential would clearly also give rise to difficult challenges in achieving dimensional homogeneity whereas the power law would be a little easier to deal with in this respect. Also, many common natural processes have behaviour patterns which can be approximated by a power law, so it was believed to be a more likely candidate to be able to reconcile with physical models, should these prove possible to construct.

In order to make the model as simple as possible to reconcile with physical models, it would clearly be desirable to use an integer exponent in the power law model, so consideration was given to the possibility of "forcing" the exponent value accordingly. An exponent of 1 on air velocity would not be acceptable as the resulting linear model would give a poor fit. However, it was considered an exponent of 2 on air velocity would be most convenient as this would give rise to dimensional homogeneity in the equation (akin to the velocity squared term in the Darcy or Fanning equation) and may well give a better fit to the data. Accordingly, it was decided to attempt to use a square law to represent the data.

To see how the equation would fit to the data points on graph 6.5, the square law was plotted on the graph using several constants until the best curve that fitted the data points was found. This was found to be with a constant of 0.00026, and although it did not fit the data points too closely at the lower air velocity ranges where there was less data available, the range from 20 to 30 m/s, showed a reasonably good fit. Graph 6.6 is a duplicate of graph 6.5, but displays the additional curve using the square law equation.

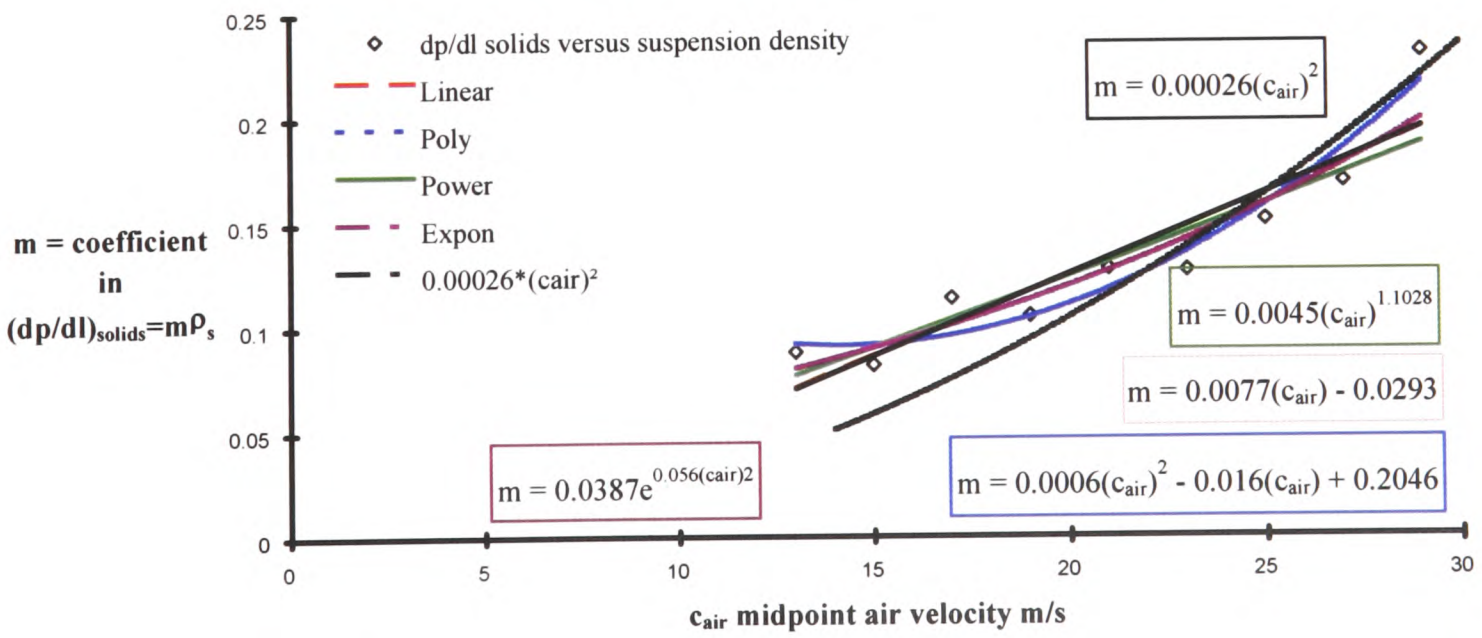

Graph 6.6: Repeat of graph 6.4, but with the square law equation curve added.

The constant used in the square law equation, now became the only number required to model the entire set of data, so this was then referred to as the coefficient for the polyethylene pellets. Each subsequent material tested, if modelled in this way, would have its individual coefficient determined from the test work.

6.3 Prediction method development

Once the model described above, and the coefficient values for each material had been established, it was clearly necessary to test these by using a pressure loss prediction method to predict the overall pipeline pressure drop, and compare the results to measured pressure losses taken from test runs.

The coefficient was used in a spreadsheet designed to calculate the predicted pressure gradients along the straight sections of horizontal pipelines. A detailed description of the spreadsheet can be found in appendix 5.

6.3.1 Initial comparison across the test rig system

The preliminary equation used in the prediction method consisted of the polynomial curve on graph 6.5, because at this stage the final selection of a square-law had not been made. The method used the equation to predict the pressure gradients along the straight sections of pipelines, while the pressure losses caused by the bends were actual values taken from the test work results. The actual values were only used initially as a temporary measure to test the prediction method, as it was at this stage hoped that the pressure losses caused by the bends would be modelled later on in the project.

When the results were compared, they did not show a very close correlation, so the remaining three mathematical models from graph 6.5 were used so that there were four sets of predictions to be compared to the measured results. As shown on graph 6.7, all the models used shown in graph 6.5, under predicted the pressure drop across the system.

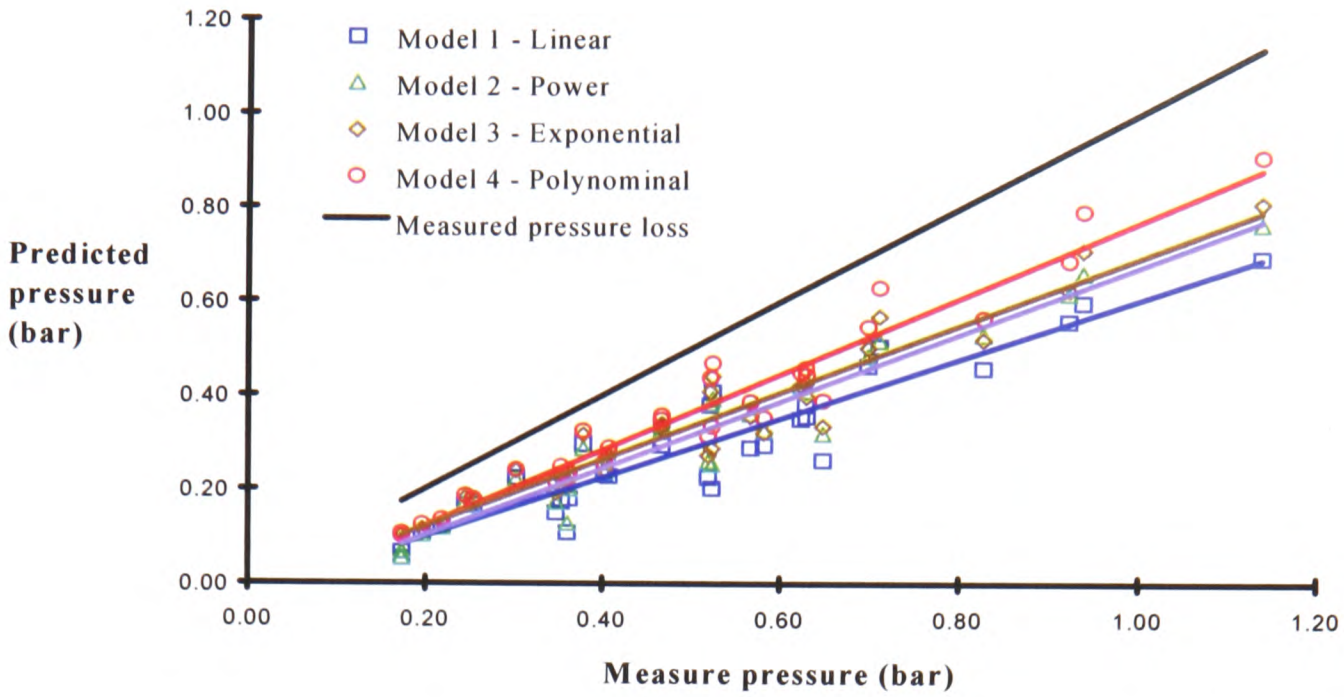

Graph 6.7: Differences between measured and predicted pressure losses. The data determined using the four models show a linear fit equation line drawn through the data points.

It was thought that it might be possible to obtain a closer prediction by using a more sophisticated model in the prediction method, so that the difference between the predicted pressure gradients and the measured pressure gradients obtained from the test work, would be closer. Therefore a closer fitting mathematical model through the m values in $\left(\frac{dp}{dl}\right)_{solids} = m\rho_s$ (from selected air velocity ranges in graph 6.5) was used which was a 4th order polynomial curve. The prediction method was used once more in the spreadsheet developed to predict the conveying line pressure gradients, in the hope that the predictions would be closer to the measured results. However, they were not noticeably any different to the 3rd order polynomial results, and not shown for that reason. The results of the comparisons discussed above, concluded that either the data analysis method or the way in which the model was used, was not appropriate.

It was felt that the method used to predict the pressure gradients along the straight sections was worth using, because of the fundamental way in which the raw data was obtained, and the development of the analysis on that data.

This was partly because most of the test rig was fitted with pressure transducers, which meant that most of what was actually happening during a test run was recorded, leaving just the beginning and the end sections of the rig without pressure transducers fitted at regular intervals. Although the sections before and after the test section were not long in length (14 and 7 metres) they each had

bends and vertical sections of pipeline which made it difficult to predict what the pressure losses in those sections would be. Based on these circumstances, an investigation into whether the comparison areas were fairly defined so that the prediction method could be validated, was initiated.

6.3.2 Pressure drop prediction from pressure transducer number 24

Any prediction method using models of straight pipe pressure gradients and bend losses calculates the pressure loss for the overall pipeline system in a piece by piece approach. It operates by determining the pressure losses for each straight section, starting at the outlet of the pipeline where values of pressure were known and the air velocity could be found. Starting at the end of the conveying line is usual when trying to predict the pressure losses along a positive pressure conveying system, because the pressures are unknown at the inlet to the conveying line, and known at the outlet (atmospheric). Working backwards along the system the pressure losses for each section and bend can be determined and added up to get the total pressure drop, for any number of pipeline configurations.

At the end of each straight section, the pressure loss caused by a bend is added to the pressure loss accumulated up to and including the preceding straight section. For the purposes of comparison, the values for the bend pressure losses were taken from the test results of the three test bends from the test run being simulated, averaged, and then multiplied by the number of bends in the system, regardless of their orientation. The method would then start the prediction for the next straight section using the new set of values, until it reached the inlet to the conveying line. An equivalent length of horizontal straight pipeline was used to estimate the losses in the vertical sections of pipeline, by simply doubling the length of the vertical section of pipeline [M8].

The comparisons between the measured and predicted pressure loss were for the entire pipeline, and as shown in graph 6.7 they showed a poor agreement. The method was under predicting the pressure losses. The differences may have been due to the unknown pressures losses in the vertical straight sections and a number of horizontal to vertical bends near the inlet and outlet ends of the pipeline. There was also a long sweeping bend into the receiving hopper and a ball valve near the outlet, neither of which were accurately modelled by the analysis. Therefore, another approach was needed to compare the prediction method results with the measured results, which would eliminate some of the unknown factors in the system. It was decided to predict the pressure losses across the system starting from the blow tank at the inlet, to the last pressure transducer near the outlet of the pipeline (number 24). See diagram 6.1 for the test rig layout and positioning of pressure transducers.

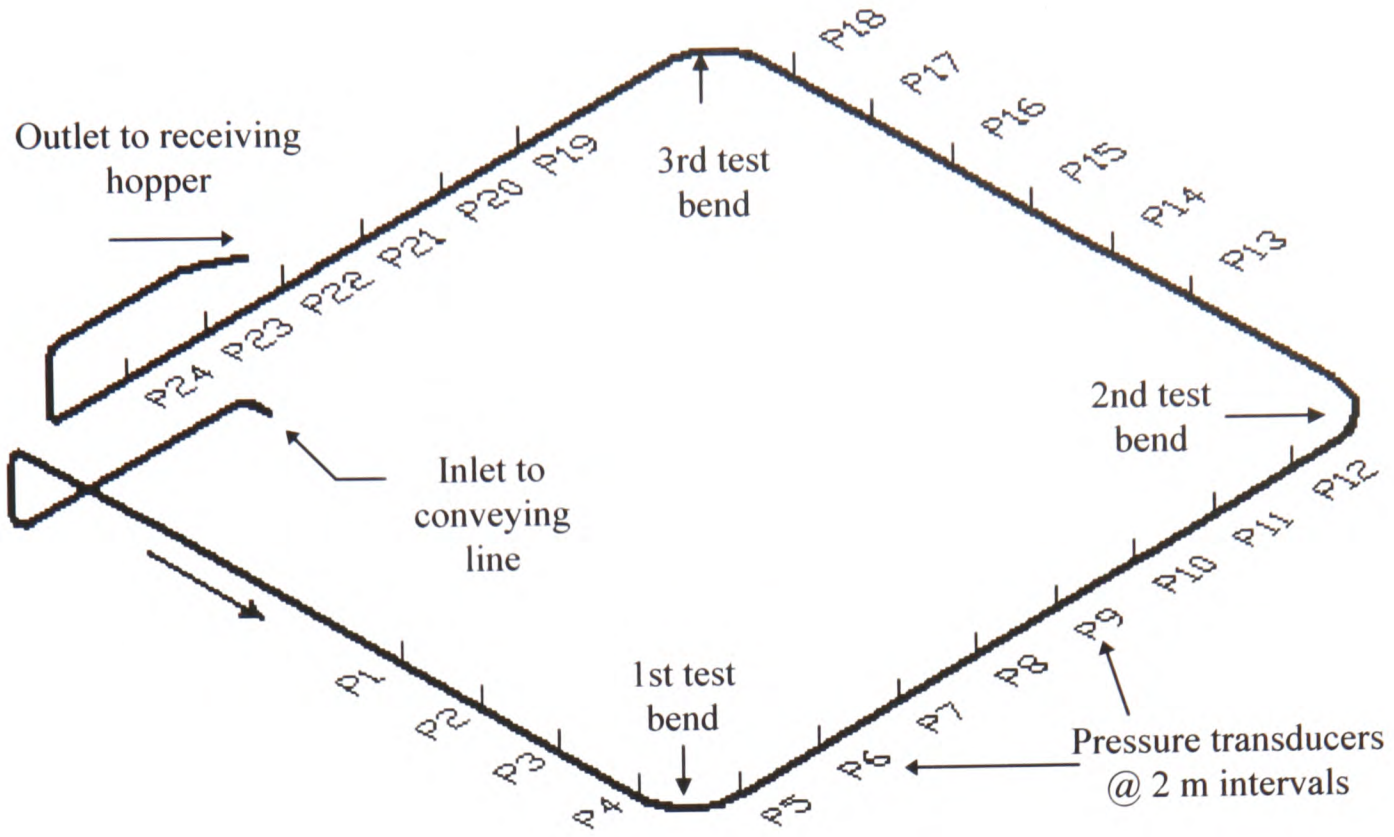

Diagram 6.1: Test rig layout.

The measured pressure losses were calculated from pressure transducer 24, to the inlet to the conveying line, and compared with the predicted pressure losses covering the same section of pipeline. Graph 6.8 shows the results of the investigation, and although the predicted results are closer to the measured results than for the previous method, there is still a significant difference.

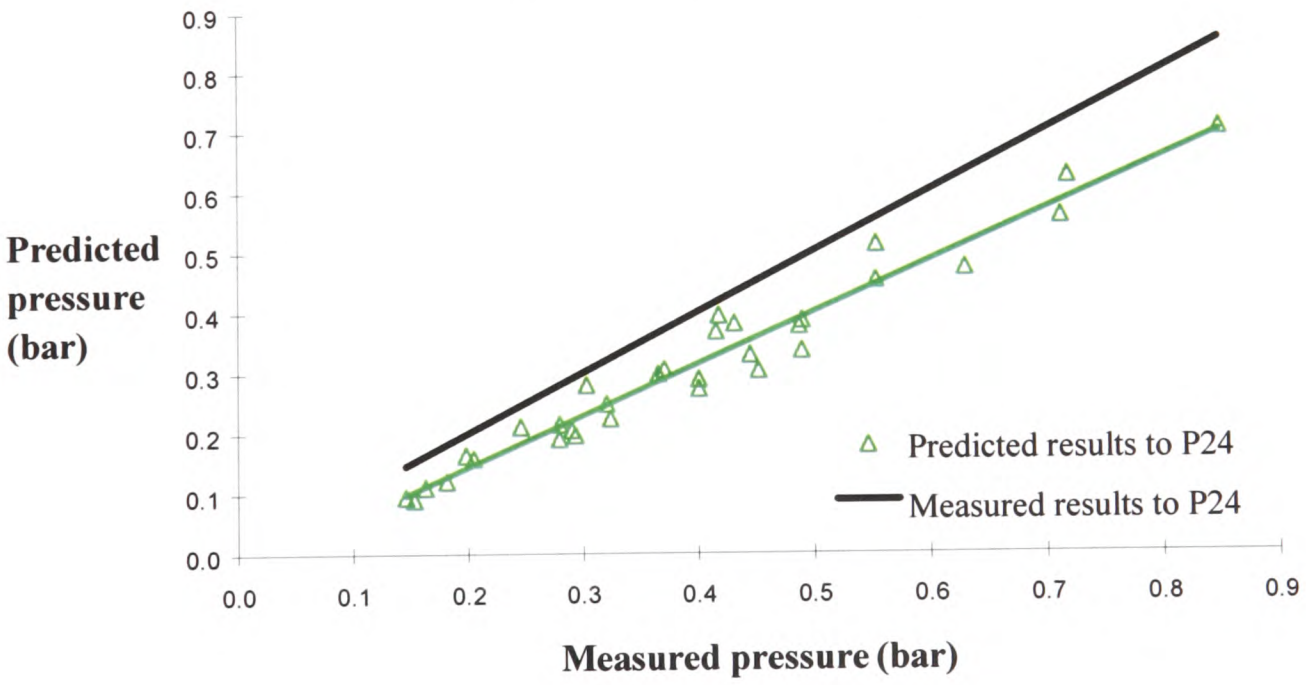

Graph 6.8: Differences between measured and predicted pressure drop across system to pressure transducer 24. The predicted results are determined using the square law equation, shown on graph 6.6.

From the results of both prediction exercises up to this point, it was evident that an improvement was made by eliminating some of the less well understood elements from the system. This gave some cause for optimism on the value of the models.

6.3.3 Pressure drop prediction between pressure transducers 1 and 24

The pressure loss prediction results using the last pressure transducer (number 24) to the inlet pressure of the conveying line, indicated that pressure losses outside the test section were not so easy to estimate. For that reason, following the above mentioned investigation from the blow tank to pressure transducer number 24, a similar exercise was performed, but this time just using the readings from transducers 1 and 24. The unknown pressure losses eliminated using this method, were the pressure losses resulting from the material entering the conveying line from the drop-out box at the end of the screw (see appendix 3) almost directly into a bend, and a vertical length of pipe leading into another bend before entering the first instrumented straight section of pipeline.

That would mean predicting the pressure losses across a purely horizontal section of four straight pipelines, separated by three test bends. The pressure drop between the two transducers mentioned, covered a distance of 57 metres. There would not be any parts of the test section where pressure losses were unknown, as transducers were fitted all along the pipeline at regular intervals.

As the prediction method covers just the test section, it should be the most effective method of comparing the model with the measured losses, as the actual values for the bends were added to the predicted pressure drop for the straight sections. It also eliminated elements of the rig that did not have models to predict the pressure losses for them, i.e. vertical pipes and the initial acceleration.

Graph 6.9 displays the measured and predicted losses covering the test section. It can be seen that the model has over predicted most of the results. This is believed to be acceptable, as it is considered prudent to over predict the pressure losses by a small amount, whereas under predicting them would not be acceptable. When designing a system, it is important to use equipment capable of reaching pressures high enough to convey the material to the end of the pipeline. Under-predicting the pressure losses may result in the conveying line blocking as either the air mover or feeder does not have sufficient capability to deal with the pressure, or the material falls out of suspension as a result of the air velocity being too low when the air is compressed further by the unexpected high pressure.

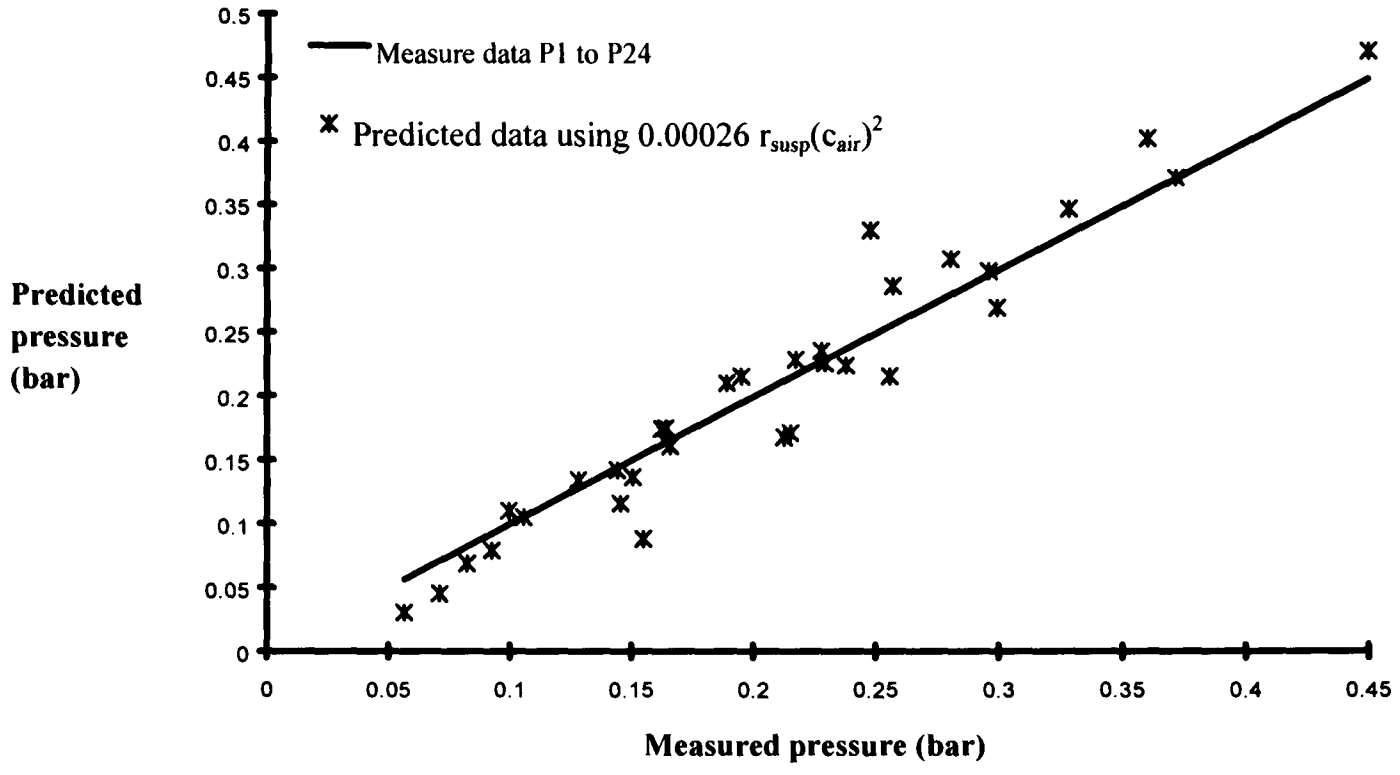

Graph 6.9: Results of predicted and measured losses from pressure transducer 1 to 24. The predicted results are determined using the square law equation, shown on graph 6.6.

6.4 Collation of test materials coefficients

As the data for each test material was processed, analysed, and its database completed, the data points from which the coefficient (k) for each material was determined, was plotted on a graph together with data from the other test materials. Graph 6.10 shows the differences between the first three materials in terms of the values of k in $\frac{dp}{dl}_{solids} = k\rho_s(c_{air})^2$.

After the sandy ilmenite and ground ilmenite results were displayed on the graph, it was apparent that from materials similar in particle density, but of two particle size ranges, the pressure losses and consequently value of 'm', were consistently higher with larger particle size.

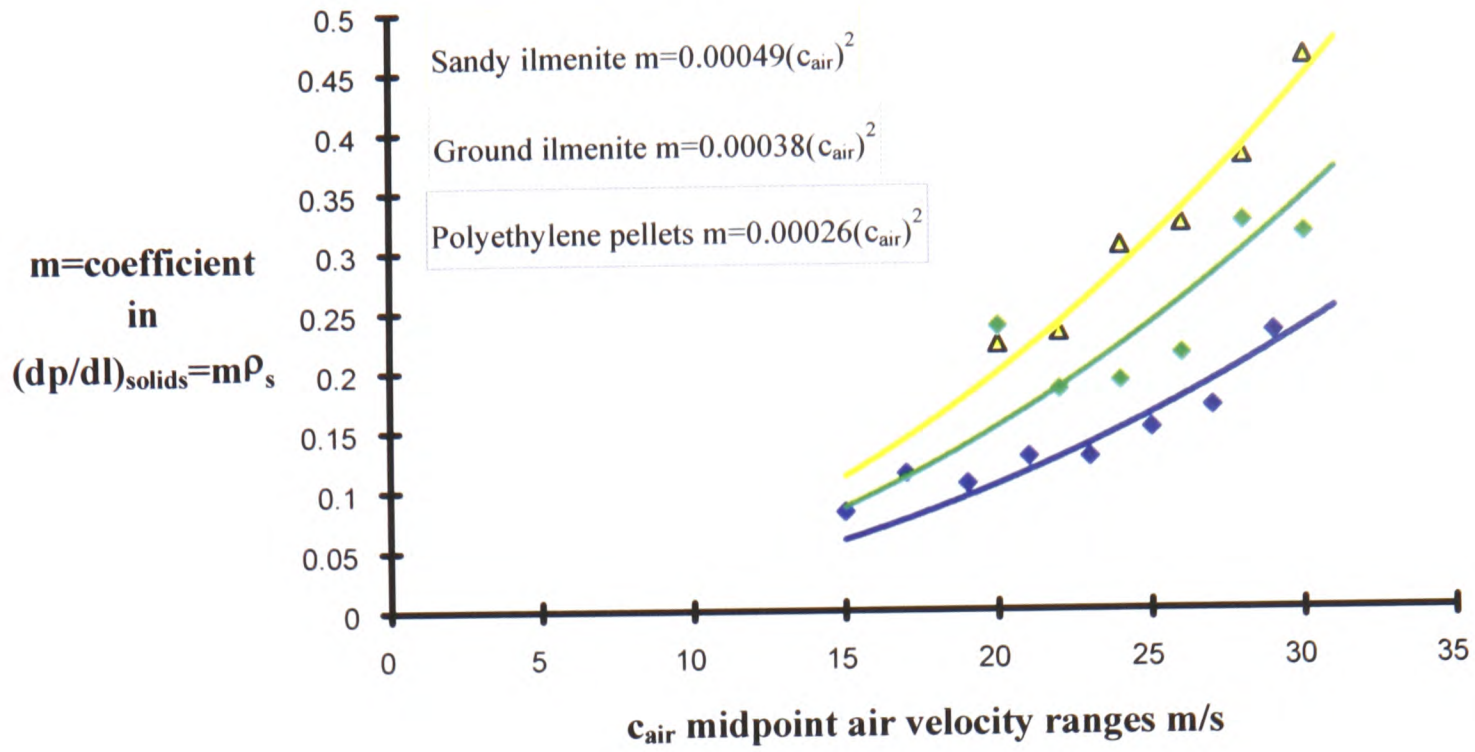

Graph 6.10: The first three materials and their coefficients are shown on a graph plotting their slopes values versus the midpoint air velocity.

As all the test work and the database was completed for each material, the new data points that determined the coefficient were added to graph 6.10. The completed set of coefficients from the original six test materials are displayed on graph 6.11.

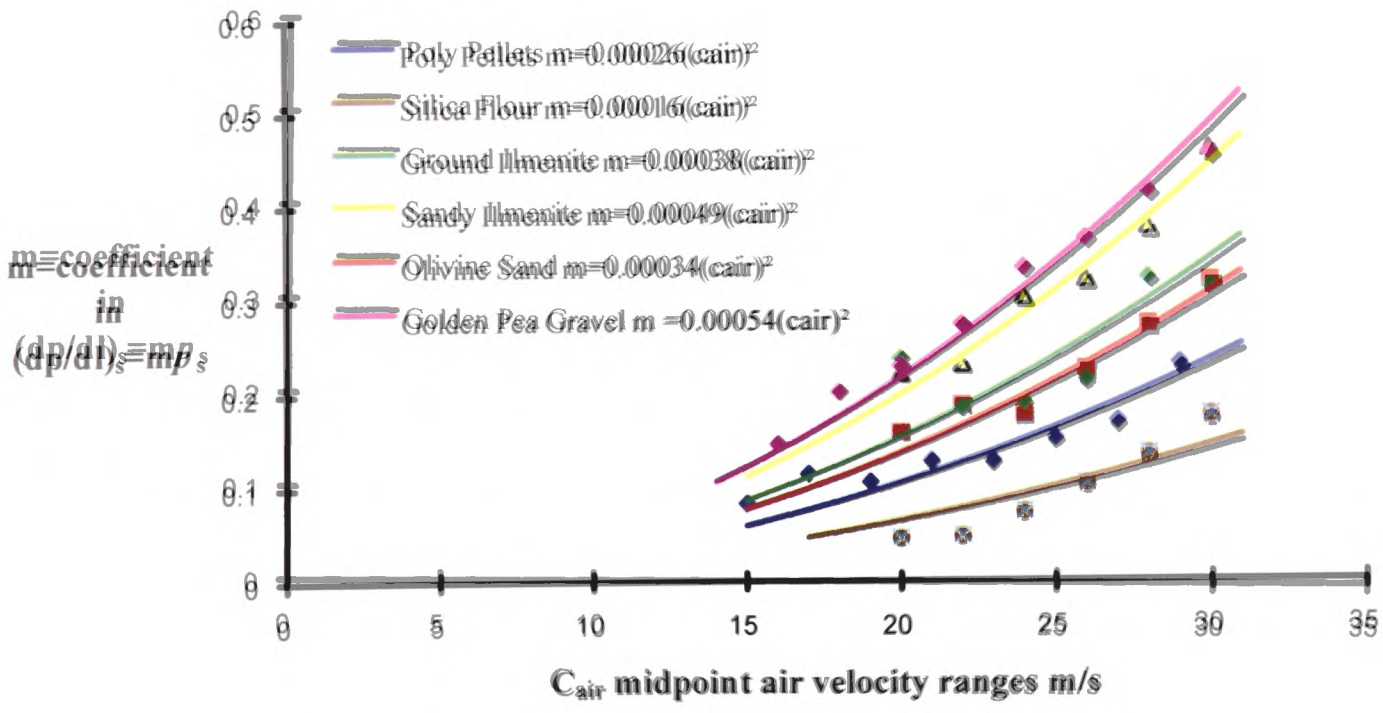

Graph 6.11: showing all six coefficients versus air velocity ranges.

Various ways of displaying the relevant variables including the 'k' values, for all the test materials was considered. The creation of a graph that would utilize both the measured variables of the particle size and particle density of a material, together with the 'k' values determined from test work, was the objective. Several graphs were plotted by alternating the variables and coefficients

(k) on each axis, in order to find a way of displaying the data for each material in a manageable form.

Each graph that was produced had only six data points, each one representing the culmination of the test work on each of the initial six test materials. A way of developing each graph was explored in the search for a graph that could be used to predict the pressure gradient along straight sections of pipeline, for materials that had not been subject to any test work.

As there were sets of materials with common variables, the connection between results from those series were the main focus of any plotted graphs. Any links that could be identified between the sets of materials enabled curves to be drawn and hence equations calculated to model them. The correlations between similar materials with all but one variable of particle size or particle density in common, would demonstrate the effect that variable has on the pressure losses along straight sections of pipeline. The materials with particle properties in common were plotted together on graphs 6.12 to 6.14.

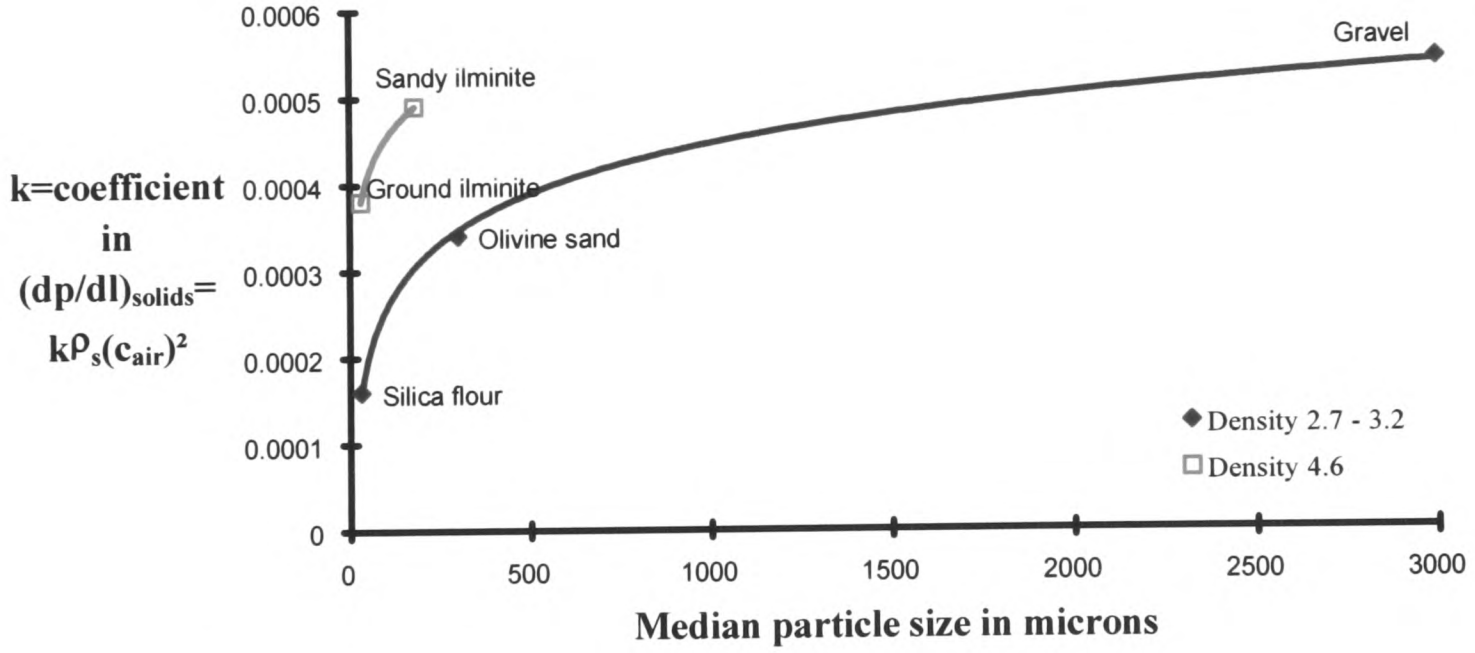

Graph 6.12: showing the results of the materials which have particle density in common.

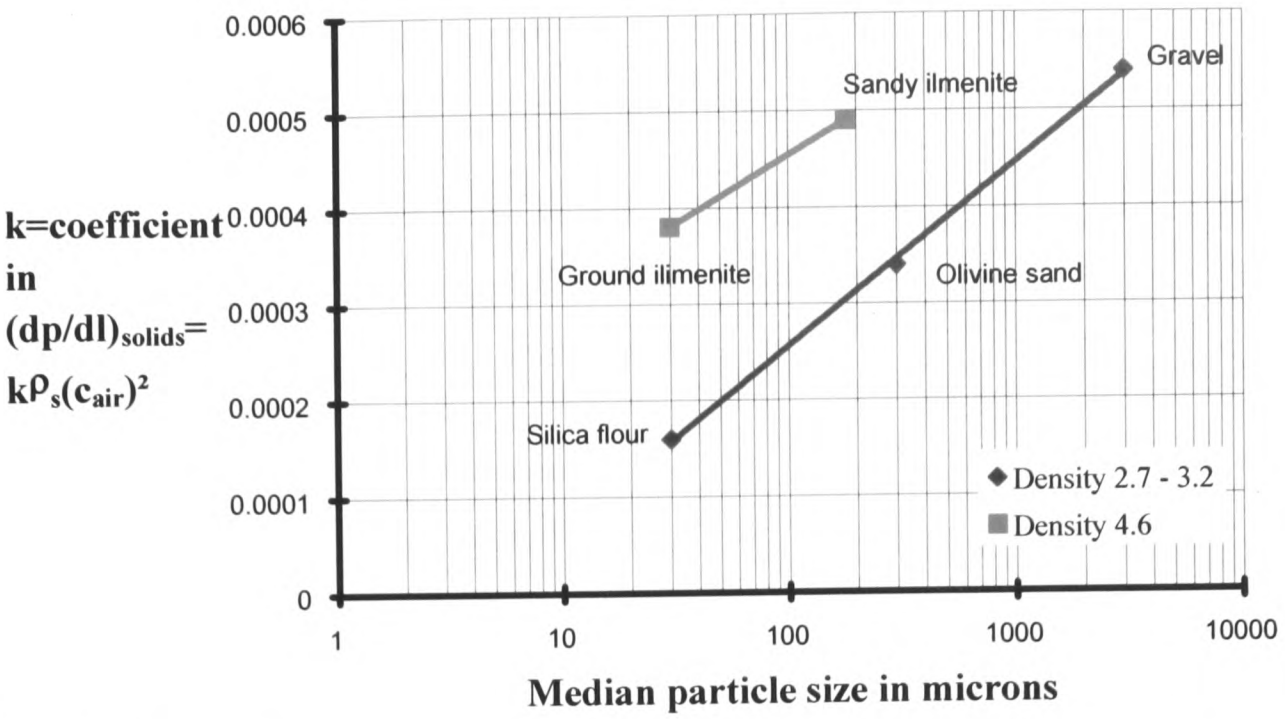

Graph 6.13: showing the results of the materials which have particle density in common, plotted using a log scale on the x axis.

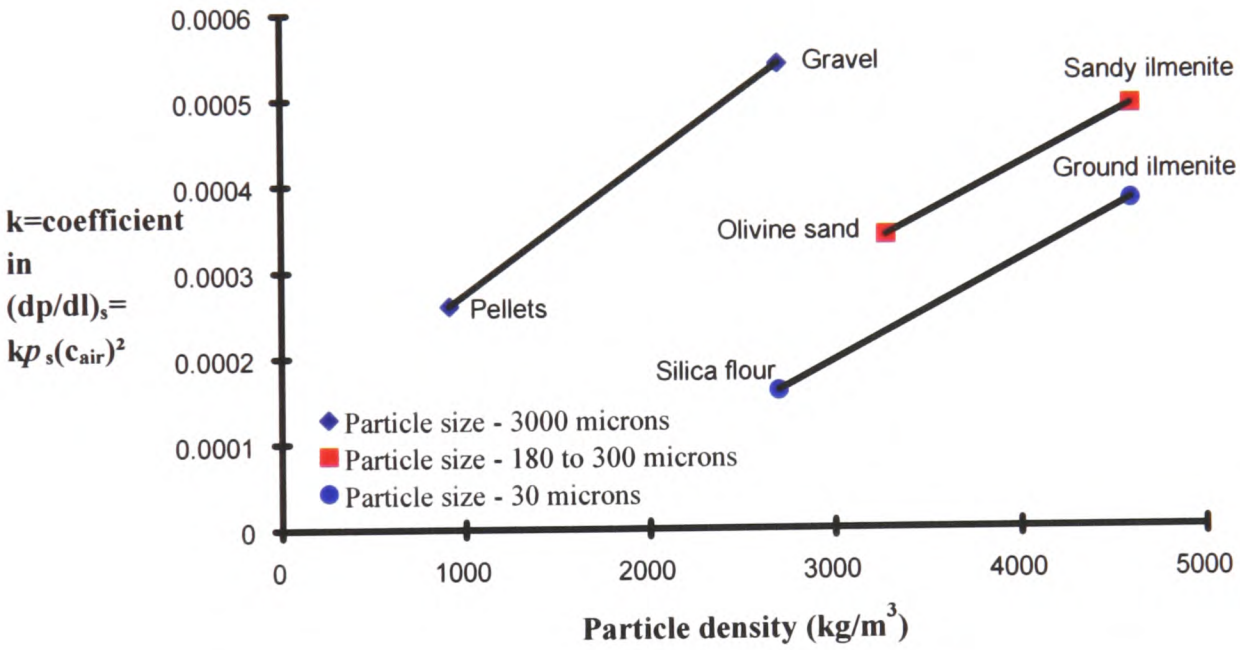

Graph 6.14: showing the results of materials tested that have the particle size in common.

Some useful information was obtained from graphs 6.12 to 6.14, which helped to form graph 6.15. Graphs 6.12 and 6.13 clearly displayed the need for a logarithmic scale of particle size. In addition, there were clear trends for the coefficient (k) to increase consistently across the particle density and median particle size. Ways of plotting the particle density, median particle size and coefficient (k) on one graph were explored. With three variables, there are clearly three possible presentations in terms of abscissa, ordinate, and a third variable represented by contours or a 'family' of curves. Graphs 6.13 and 6.14 were two of the three possible presentations, and graph 6.15 was the other one.

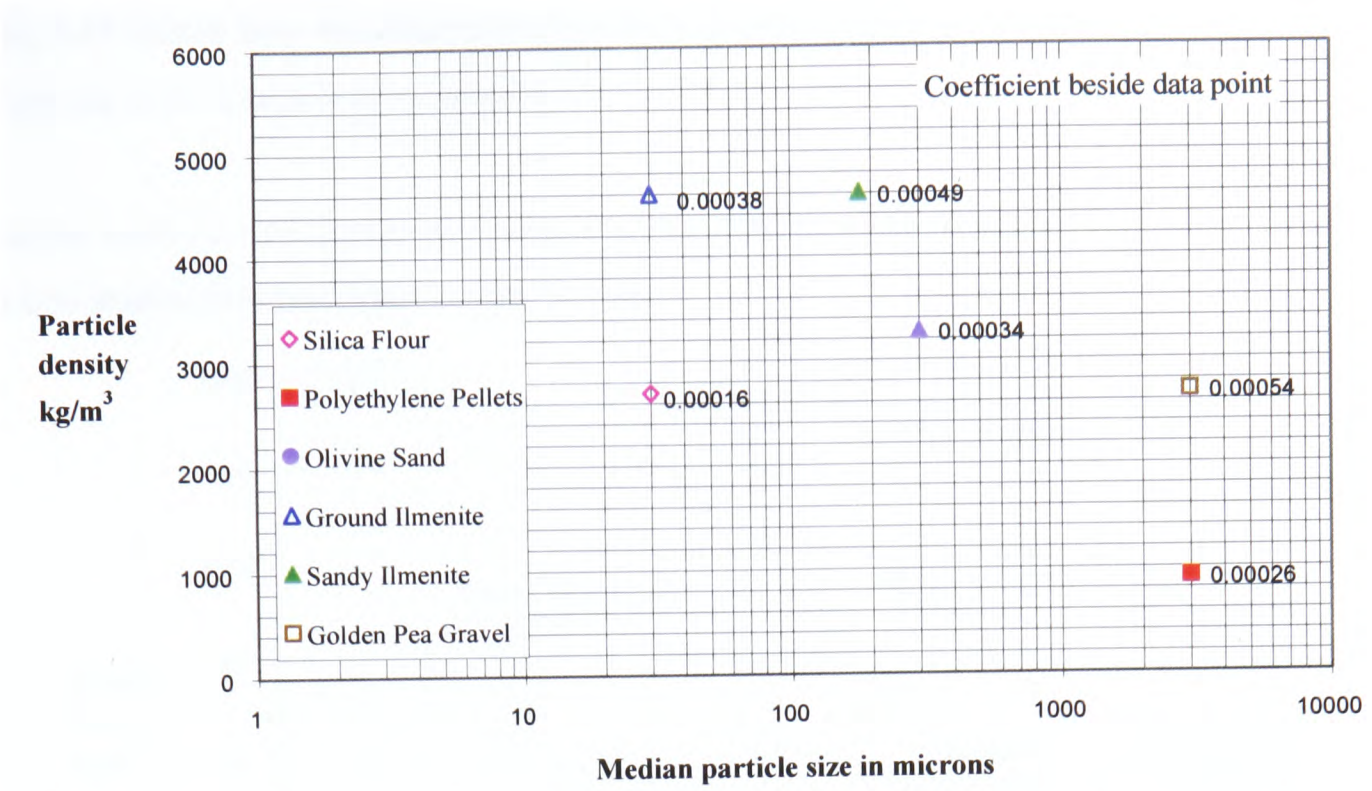

Graph 6.15 displaying the coefficient (k) values for each test material, when particle size is plotted against particle density.

As with all the previous graph plotting, the data points were displayed and links between the data points added as straight lines or curves. Graph 6.15 started as the preceding graphs in that at first glance the data did not appear to show a useful way of linking the data in a positive manner. However, the change in coefficient (k) could be related to the difference in particle density for these combinations, to produce extrapolated points. This enabled interpolated lines to be drawn between the data points as shown on graph 6.17.

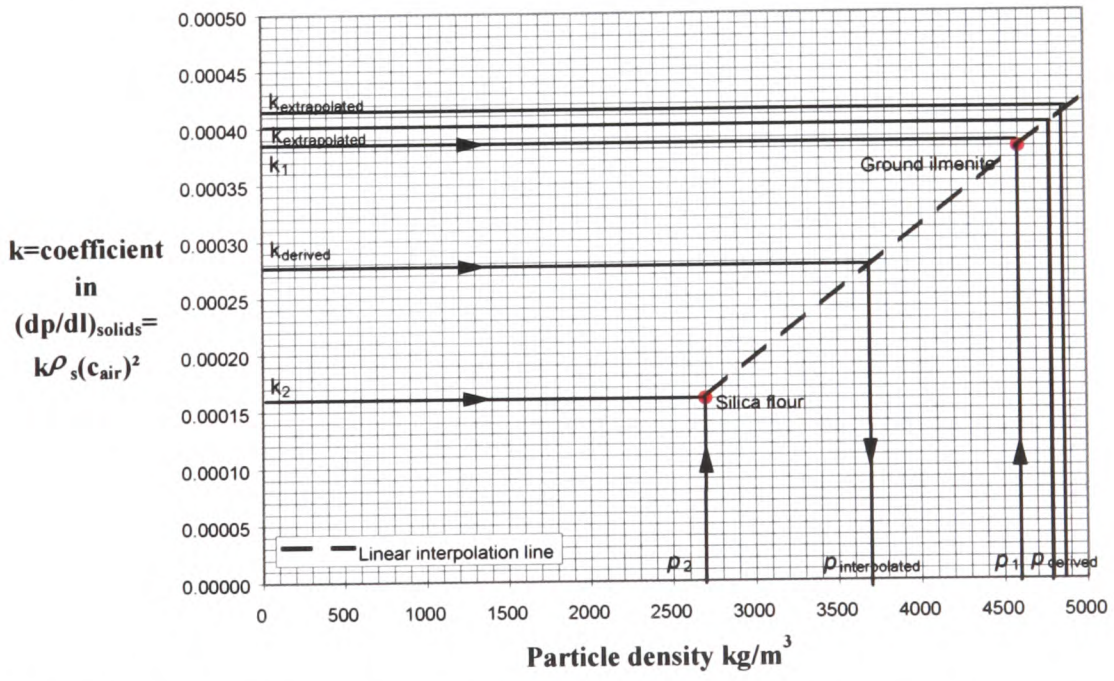

Graph 6.16: Using the data from the silica flour and ground ilmenite, both having a median particle size of 30 microns, the derived values for the coefficient (k) and the particle density were determined.

Graph 6.16 shows how the interpolated points were determined to enable contours to be drawn through the solid data points on graph 6.17.

A similar exercise was carried out using the polyethylene pellets and golden pea gravel data, as they also shared the same median particle size.

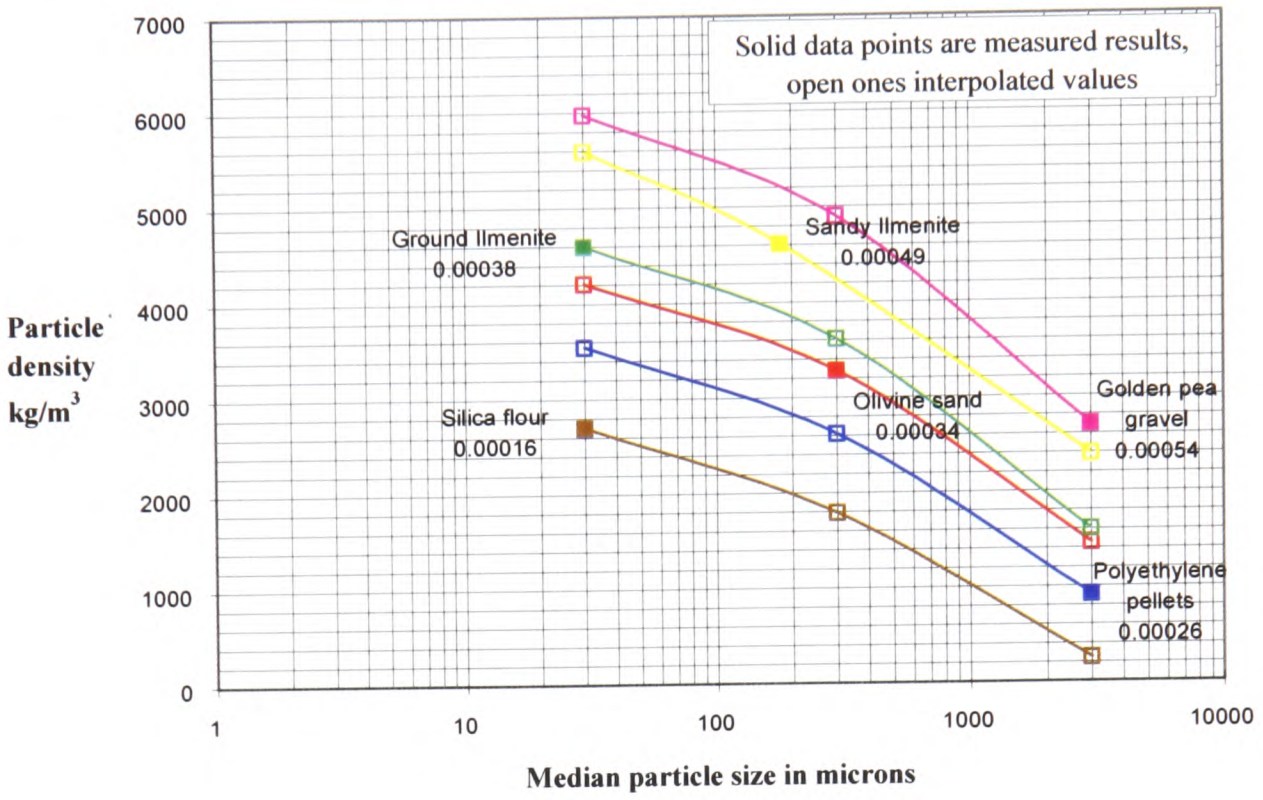

Graph 6.17: with interpolated contours of coefficient values drawn through the data points, using the particle size versus the particle density.

The objective of the analysis was to determine the optimum way of representing the data to provide an empirical method for determining a coefficient (k) for each material, from its particle density and size. Graph 6.17 appeared to fulfill this objective, with curves representing coefficients (k) from plotted data points.

In order for graph 6.17 to be used for predicting the pressure gradients along the straight section of a pipeline, the median particle size and particle density of a material need to be identified. The point where the two values meet would enable the coefficient (k) to be determined from the curves, which would then be used in the pressure loss prediction method, for the straight sections of pipeline only. The initial limitations of using the graph were that most of the material particles used to develop graph 6.17 were all more or less of a rounded shape (although the ground ilmenite and the silica flour were more irregular shaped than the rest) and the size range of the materials was confined to 50:1. It was thought that these may limit the application of graph 6.17 immediately.

Following the discovery of the apparently consistent relationship between the particle density, median particle diameter and the pressure loss coefficients (k) of solids shown in graph 6.17, the decision was taken to test the relationship by testing some other materials that did not necessarily have any particle properties in common with the original test materials, and see whether their coefficient (k) values would be close to the predicted values, as determined from graph 6.17.

Chapter 7

Additional test programme and analysis

7.1 Introduction

7.1.1 Objectives for further test materials

The initial test programme involved testing and analysing data from six carefully selected materials. The aim was to compare the differences between the pressure loss of the materials when they were pneumatically conveyed along a pipeline, under similar conveying conditions. A graph was produced from the results that enabled the user to obtain a coefficient for any material using the particle density and median particle size. The coefficient could then be used in a pressure loss prediction method to obtain the pressure gradient along straight sections of pipeline for that particular material.

The graph was produced from the data arising from the initial six materials, all of which were chosen because they would convey easily without too much degradation, were fairly free flowing, and were each related to at least one other material in the group by particle size or particle density. A detailed description is found in chapter 4.

As the graph was produced from the results of the initial six materials, it was necessary to verify the findings of the graph by further test work. This was achieved by testing additional materials that would not have fitted in as well with the original test materials. This would confirm if the graph was useful for materials other than those used in the initial test programme. From the test work, the coefficients for each material were determined, and compared to those predicted using the graph.

7.1.2 Additional test materials

The selection of further materials that could be pneumatically conveyed, would ideally be limited to those already stored in the laboratory, in order to keep the costs down. Many such materials had previously been utilized for other test work, so the degree of degradation of any material for the test programme, was an important factor that had to be considered. The degradation of particles, usually meant that the particle size and shape was altered by fracturing. This action increased the amount of finer particles within the materials, thereby altering the particle size distribution. To

utilize the graph, the particle size range should be known, therefore the particle median size was an important selection factor.

7.1.3 Selection of first material

Investigating the materials available, a number of products were identified that could be used for the test programme. If any of the products bore similarities to those in the original test schedule, it would be advantageous when comparing the differences between the test materials. Conversely, materials that were completely different to those already tested, would also examine the validity of the graph at conditions not previously tested.

A total of three materials were selected as possible products that could be tested. They were granulated sugar, boral lytag and glass beads. The first two had been used previously in another project, and the third was unused and ready for utilization.

The materials were tested in an order similar to that of the original materials, i.e. to test the less abrasive materials first, so that the pipeline bends would not wear out so quickly. Although the wear of bends was inevitable when considering the nature of materials tested previously and those selected for the additional test work, data from completed test runs could be analysed while a worn bend was being repaired or replaced. Therefore, it was important to get as much test work as possible completed before a bend wore through, which meant conveying the most abrasive products last. Full details of the additional test materials may be found in chapter 4.

7.2 Granulated sugar test work

The first product to be tested from the additional materials, was granulated sugar. The sugar had only been used once previously, over a short conveying distance, thereby very little degradation had taken place, as confirmed by a size analysis exercise. However, this material was expected to degrade rapidly and the number of test runs would be limited. It did have the added advantage that when the material had degraded beyond its usefulness, additional conveying around the test rig at high velocities could be used to "grind" the material even further until it was of the size of icing sugar. This would be advantageous to the test programme, as further tests could produce additional data for a material of the same particle density, but of a smaller particle size and different shape.

The intention was to limit the degradation of the sugar so that as many test runs as possible could be carried out, and the conveying characteristics of the sugar determined before the particles degraded too much. Therefore, the test runs with the lowest conveying air velocities were to be completed first. In addition, once a test had completed scanning the channels for data over the predetermined time period, the screw conveyor could be stopped and the air turned off while another test was set-up. This would allow more than one test to be completed for one batch of material in the blow tank.

7.2.1 Problems conveying granulated sugar

When conveying all the previous test materials, if the time period for a test run had finished and there was still enough material in the blow tank, the screw was stopped and the air shut off. This enabled more than one test to be completed using a single batch of material in the blow tank. Once the transducer readings had been transferred from the data logger to the host computer for storage, the valve allowing air to enter the blow tank was turned on, the screw conveyor started, and another test was set-up and performed using the remaining material in the blow tank.

It was during the second test performed on this way, after the initial test run had been completed, that the screw jammed and could not be rotated, even by manual methods. It was suspected at that point, that the sugar had compacted under the pressure in the blow tank, thereby requiring a higher torque than the motor was capable of to rotate the screw feeder. A fault finding exercise identified that the variable speed drive unit had failed. This necessitated the purchase and installation of a new drive unit.

Once the rig was up and running again, it was decided that the sugar should not be left in the blow tank to compact, but conveyed back to the receiving hopper after each test. Resulting from the drive unit failure, it was thought likely that the compacted sugar created too high a force for the screw conveyor to start up against. However, this would reduce the number of test runs that could be performed, because of the rapid degradation of the sugar, and limit the range of conveying conditions that could be compared to the rest of the test materials, Therefore, due to the limited number of test runs allowed, the length of each test run was extended from 150 to 200 seconds. This allowed enough time to begin a test run using one mass flow rate of solids, start recording a test when the material had settled down to a steady state period, and then increase the mass flow rate of solids to capture a second test run at a different solids flow rate.

There obviously had to be enough time left after the second mass flow rate of solids was set, for the blow tank air and pipeline pressures to settle into a steady state period if the data was to be useful. If the increase in the mass flow rate of solids was too late in the test run time period, the pressures could not settle down in time to record a steady state period. It was impracticable to increase the time period further, as this had been tried and the data storage software package was incapable of transferring all the data for analysis.

This process allowed two different mass flow rates of solids to be recorded. In other words, for one complete cycle of the test material, two separate conveying conditions could be measured. The exceptions were for higher mass flow rates of air, where it was only possible to record one set of conveying conditions before the material ran out.

Samples of the sugar were taken after every five cycles to monitor the particle size degradation. When the percentage of fines in the samples went up to 40% after 15 cycles of the conveying system, compared to only 5% of fines at 10 cycles, no more tests were recorded using the material as granulated sugar. The 'fines' were particles less than 200 microns, as measured using the Malvern laser particle sizing equipment [R6].

7.2.2 Analysis of granular sugar test runs

The coefficient of 0.00049 determined from the processed and analysed data was almost three times as great as would be predicted by the graph, which was around 0.00020, as shown on graph 7.1. Therefore, the analysis on the granulated sugar, did not confirm the usefulness of the graph as a tool for predicting pressure loss. The initial thoughts were that as the sugar was changing some of its particle sizes from one test run to the next, this may have affected the median particle size position on the graph. However, on examination, the coefficient was too far removed from where the particle size would have to be to 'fit' onto the graph, as shown below.

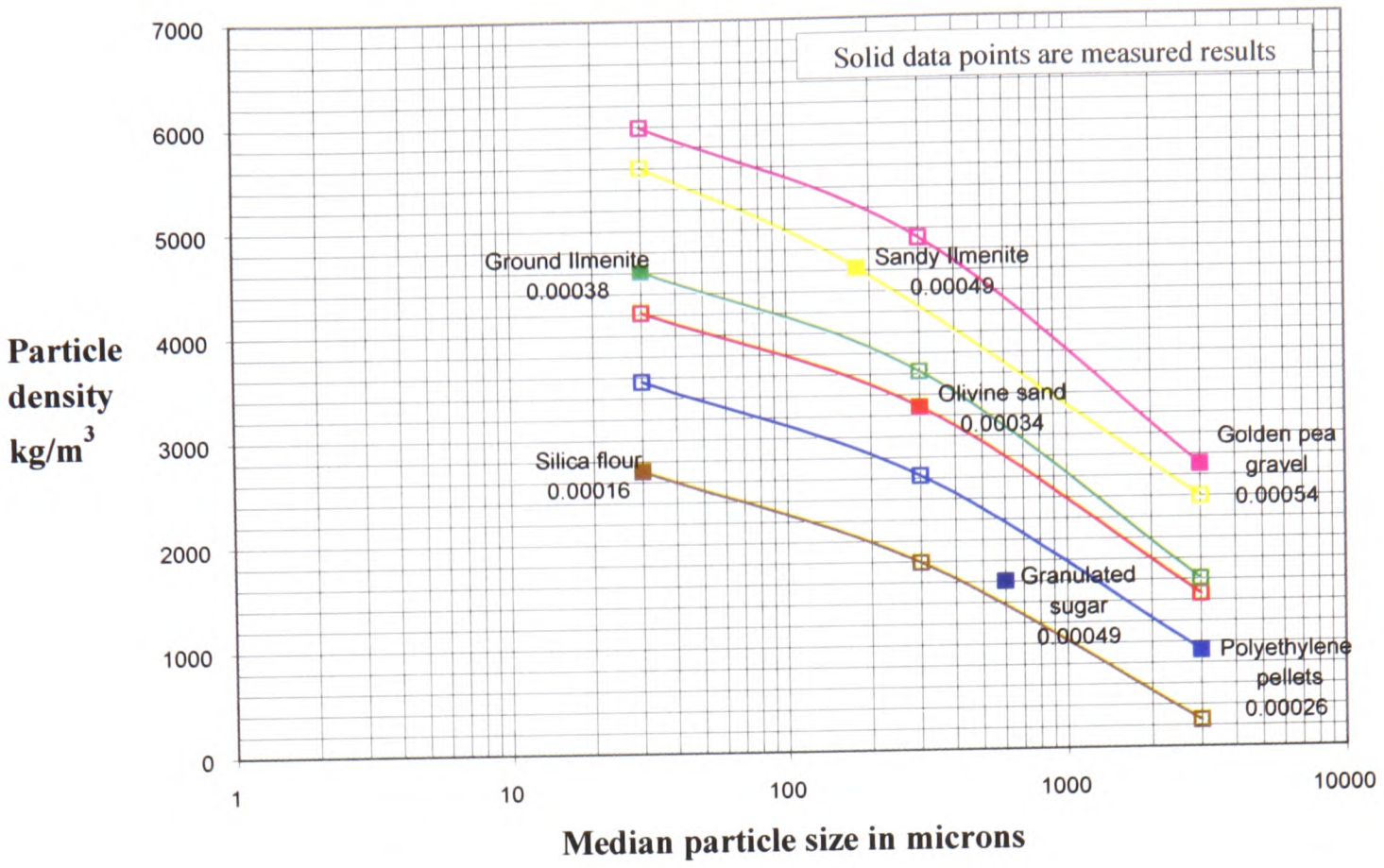

Graph 7.1: Particle density versus particle size range, with interpolated contours of coefficient values drawn through the data points.

As the sugar was degrading relatively fast from each test run, the analysis process was repeated using only the first half of the test run results. This would show whether the changes in particle sizes had affected the value of the coefficient, because in the first half of the tests the particles were relatively unchanged, but fortunately had also been conveyed over the majority of conveying conditions.

Taking the results from the first 13 test runs, and analysing them using the usual method to determine the coefficient, produced results which confirmed the original coefficient had been correct. It also suggested that increasing the amount of test runs has little change on the graph. However generally, when there are fewer data points at higher or lower air velocity ranges, the coefficient curve does not fit the data points as closely as the rest of the data points. The results from this investigation are shown on graph 7.2.

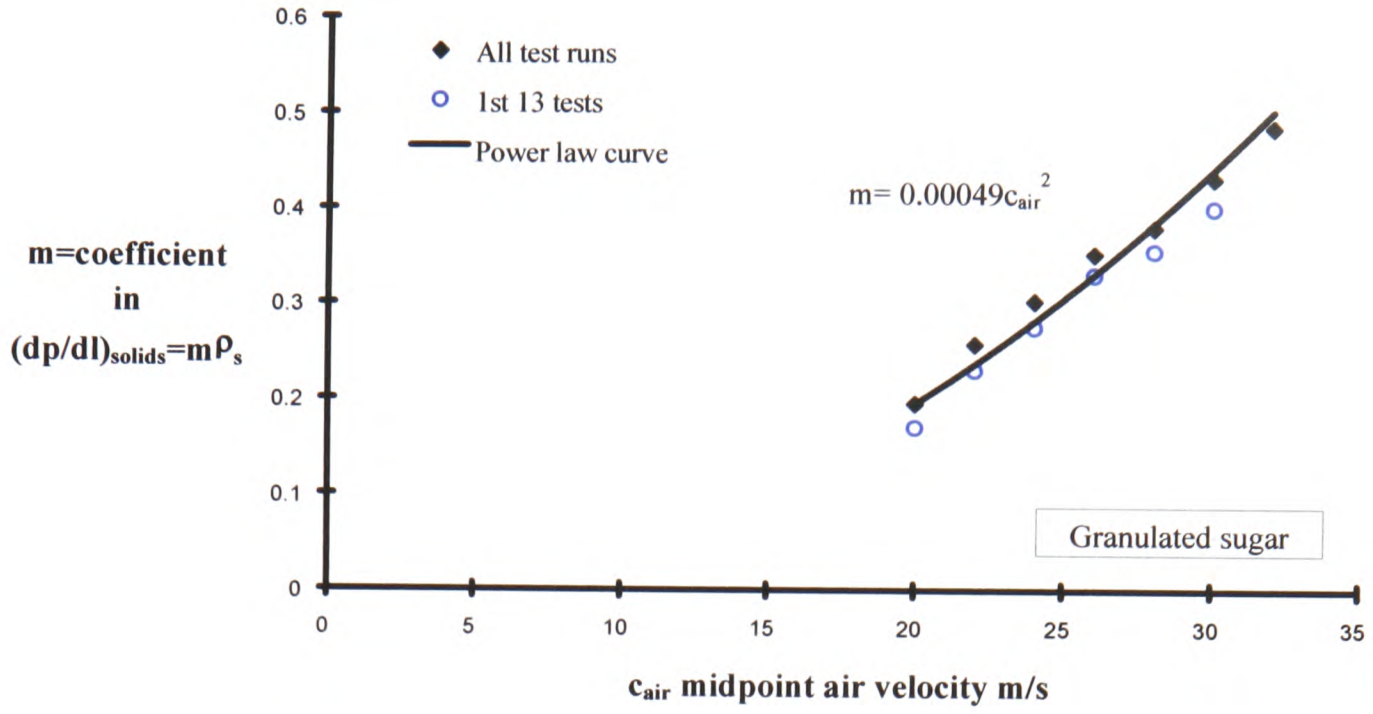

Graph 7.2: Results of individual graphs of pressure gradients for solids only, versus the midpoint suspension density, for the granulated sugar.

7.2.3 Comparing the results of the graphs coefficient and the test work coefficient, to that of the measured pressure loss data.

An exercise was carried out to see what pressure losses were suggested when the coefficient predicted from the graph was used in the prediction method. This was to confirm that the pressure loss predictions made using the coefficient determined from the graph, would be incorrect for the granulated sugar. The pressure drop predictions using the coefficient determined by the test work, were compared with the measured pressure losses across the test section, shown on graph 7.3. The predicted data points are scattered each side of the measured results. However, when the coefficient determined by the graph was used in the pressure loss prediction method, the pressure losses were almost all under predicted, and are also shown on graph 7.3. This is unacceptable; it is advisable to over predict the pressure losses a system is likely to encounter, to ensure that the system will transport the material along the entire pipeline. Otherwise blockages may occur as a consequence when there is not enough pressure for the material to be conveyed along the complete pipeline system.

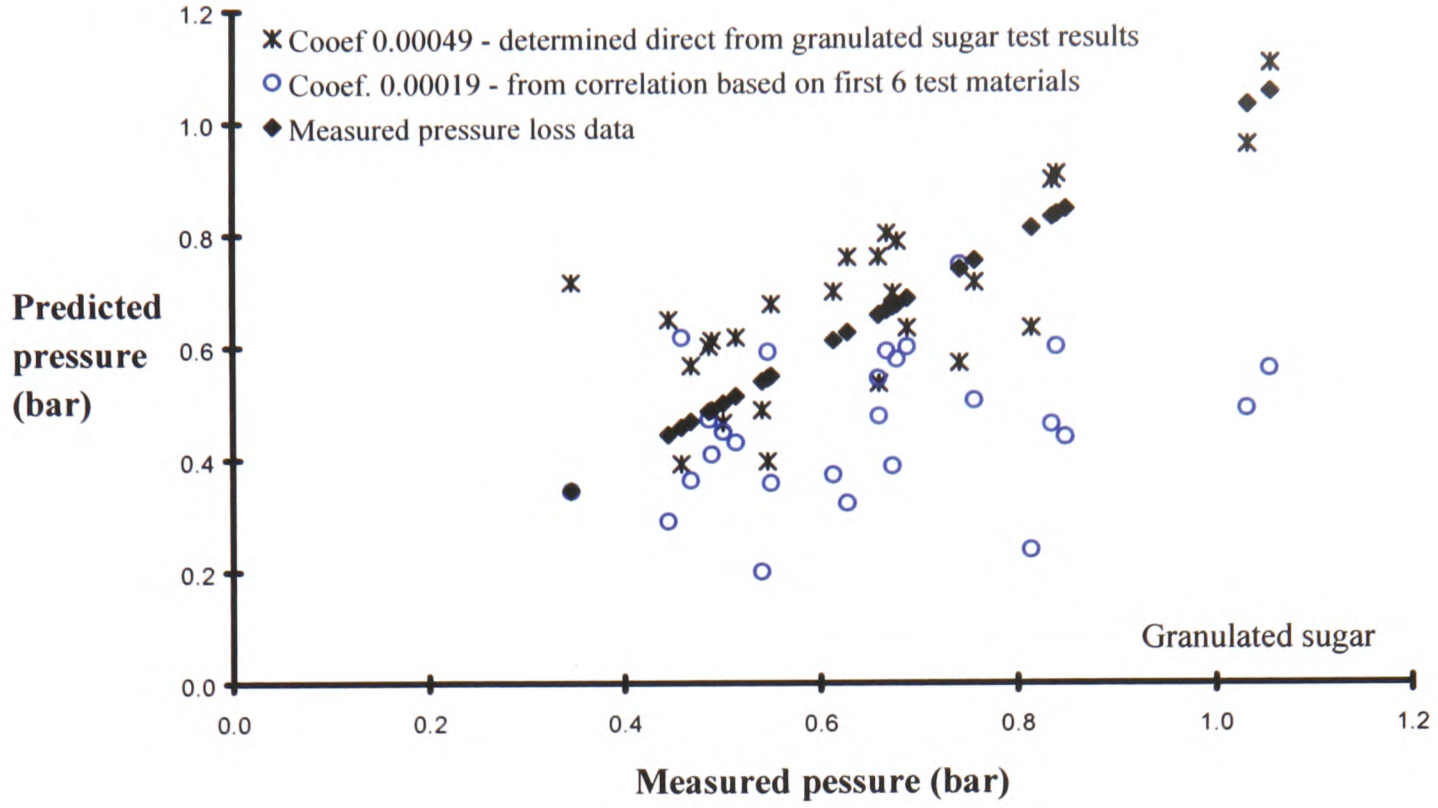

Graph 7.3: The measured pressure losses compared to the predicted pressure losses, using coefficients determined from the test work and using the graph.

Examining the reasons for the higher coefficient determined from the test work, delayed the test programme. So after re-examining the raw data and the analysis process, it was thought that testing the sugar at a smaller particle size may provide some clues. Therefore, the granulated sugar analysis was put to one side in order to carry on with the test programme.

The material was then conveyed many more times around the system at very high air velocities, in order to degrade all the sugar particles until they were reduced to icing sugar size. When samples taken after several test rig cycles, showed the size was not reducing noticeably further, the material was considered ready to be conveyed as icing sugar.

7.3 Icing sugar

7.3.1 Particle size analysis for icing sugar

Although the granulated sugar was conveyed until it had degraded enough to pass as icing sugar, not all of the particles degraded at the same rate. Therefore some large particles were still in the icing sugar. Initial analysis on the samples using the Malvern laser particle sizing equipment confirmed that there was nearly 40% of granules over the particle size of 100 microns.

(Note: The granulated sugar, once reduced in particle size by this means, was referred to as icing sugar for identification purposes. The particle size range of manufactured icing sugar has not been identified so a comparison has not been made.)

The newly degraded, icing sugar material, proved to be the product that produced the most problems. After each conveying test, the material was stored in the receiving hopper until the valves are opened between the receiving hopper and blow tank, allowing the material to fall down into the blow tank under gravity. As the sugar broke down due to degradation, more fines were produced and it became harder to discharge the material from the receiving hopper into the blow tank. As the finer sugar was harder to discharge, the test work was slow. A manual aeration lance was effective at encouraging discharge of the sugar from the receiving hopper into the blow tank.

7.3.2 Analysis of icing sugar results

The processed and analysed data for the icing sugar, brought the same conclusions as the granulated sugar test results, i.e. that the coefficient determined from the test data, was far removed from what the graph drawn up from other materials would suggest. However, in relation to each other, they followed the same pattern as previously tested materials that had the same chemical composition and particle density in common, in that the higher coefficient belonged to the material with the larger median particle size.

7.3.3 Summary of the sugar results

Comparing the coefficient values from the test work to those predicted by the graph, the sugar results were disappointing. However, the sugar is a product most unlike any of the others in the test programme. It is very friable, it is a food product, and can absorb moisture. There were the problems as stated earlier regarding discharging of the product into the blow tank. This made it apparent that this may be related to the reason why so much more energy was required to convey this product than all the others. Further analysis of possible reasons why this product did not fit the trend is made later, in section 7.7.

One of the findings from the results of the initial test work, identified that when materials of a similar particle density are conveyed in two particle size ranges, the larger particle size range will produce a higher pressure drop along the straight sections of pipeline than the smaller particle size range. The larger the particle size, the greater the coefficient that is used in the prediction method. This trend was also confirmed from the analysis on the granulated and icing sugar test results.

7.4 Boral lytag

A product called boral lytag was available, that had been used for some test work, but not pneumatically conveyed around a pipeline. The material had already been sieved into selected particle size ranges. As there was not enough material to convey along the pipeline and obtain sufficient results from one size range, a combination of two size ranges was used for the conveying tests. The boral lytag did not degrade in the usual way with the particles breaking into smaller fragments, but generated dust with little change in the median particle size during conveying. For this reason, the number of test runs was limited.

Samples were taken every five test cycles to monitor the amount of dust in the material. However, after only 17 complete cycles of the test rig, almost a third of the material had turned to dust and was clinging to the hopper walls. This was determined by the load cells when the product was dropped through the valves from the receiving hopper to the blow tank before each test run commenced. The receiving hopper is seated on top of three load cells, and the total weight from all three load cells is recorded by the data logger unit. At the start of each test, the load cells usually read 0kg, and the weight increases on the load cells as the material is being conveyed around the pipeline and back into the receiving hopper. The dust was allowed to build up in the receiving hopper during the tests and not dislodged into the blow tank for conveying. This allowed the amount of fines in the conveying material to be kept to a minimum, so as not to affect the median particle size.

During the conveying, there were two punctures of bends. One bend (not in the test section) was repaired, but the other was a test bend, so all three test bends were replaced. This was the third time that all three test bends had been replaced during the test programme.

7.4.1 Analysis of test results on boral lytag

The processed and analysed data produced a coefficient that was of the same value to that predicted using the graph. This was the first encouraging additional data since the development of the graph. When the coefficient determined by the results and the graph was used in the prediction method (which was of the same value) the predicted pressure losses across the test section was over predicted by up to 13% on all the data points when compared with the measured data.

7.5 Glass Beads

Some test work using glass beads had been carried out for another project, where the particle size range of the beads had been very specific. The glass beads had been sieved and separated into precise size ranges, which resulted in over half a tonne of new, unused glass beads being available for this project if required. The glass beads were reportably robust and would therefore not degrade too much during conveying. Hence a decision was made to convey the glass beads as the tenth and last test material for this project.

The conveying tests were carried out using the same method as the sugars and boral lytag, in that the extended test run period allowed two different test conditions to be monitored during one complete system cycle, to reduce the degradation of the product during conveying runs. There were no problems conveying the glass beads, which acted like a liquid when poured into a heap. However, as the glass beads were colourless and spherical, spillages were hazardous because the beads were transparent and like ball bearings when walked on.

During the conveying trials, another two non-test bends wore through and they were repaired. Some non-test bends had been repaired for the fourth time by the end of the test programme. It was apparent that once a bend has worn through, repairing it by placing another piece of metal plate across the hole and welding it together, is not as effective as replacing the complete bend. This is because when plating and welding, the rate of wear in a repaired bend increases [B4].

7.5.1 Analysis of test results on glass beads

The coefficient determined from the processed and analysed test results did not exactly match that expected from plotting the particle density and median particle size on the graph. However, at 0.00023 it was not too far removed from the value of 0.00030 predicted by the graph. This may have been attributed to the rounder particle shape of the glass beads. The predicted pressure losses across the test section, varied from the measured results by ±16%.

7.5.2 Sieve analysis on glass beads

During the test work using glass beads, material samples were taken at least every five test rig cycles. The samples were measured using sieves to determine the particle size degradation during the conveying runs, and shown on graph 7.4. The results show that the particle size reduction was very small, possibly because of the limited number of test runs undertaken. The percentage of larger particles reduced from 20 % to 2 %, but there was little dust generated from the breakages.

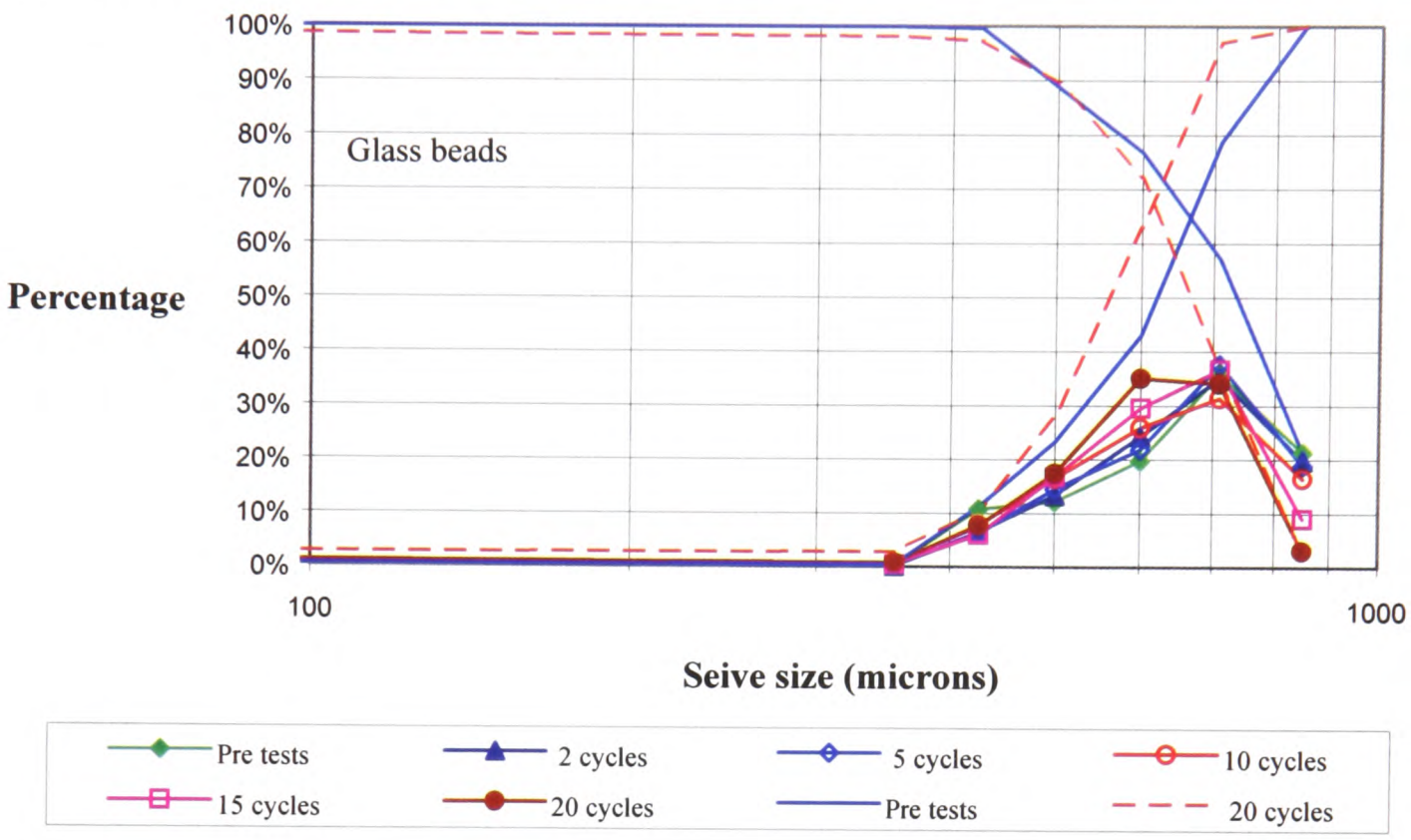

Graph 7.4: Sieve analysis on glass beads. Results shown are from six samples taken periodically during the conveying trials.

7.6 Analysis on the four additional test materials

The particle size is important for the purposes of plotting the data on graph 7.5, which is used to determine the coefficient of the material when using the prediction method. Of the four additional materials tested, only one of the coefficients fitted perfectly on graph 7.5. That was the boral lytag material. The coefficient for the glass beads obtained from the test work, was quite close to where it was predicted to be if using the graph, taking into account the range in the particle sizes. Unfortunately, the coefficients for both grades of sugar did not fit on to the graph at all, in that their coefficients were almost three times greater than what they should be if the graph were to be used as a guide to eliminate test work on a material.

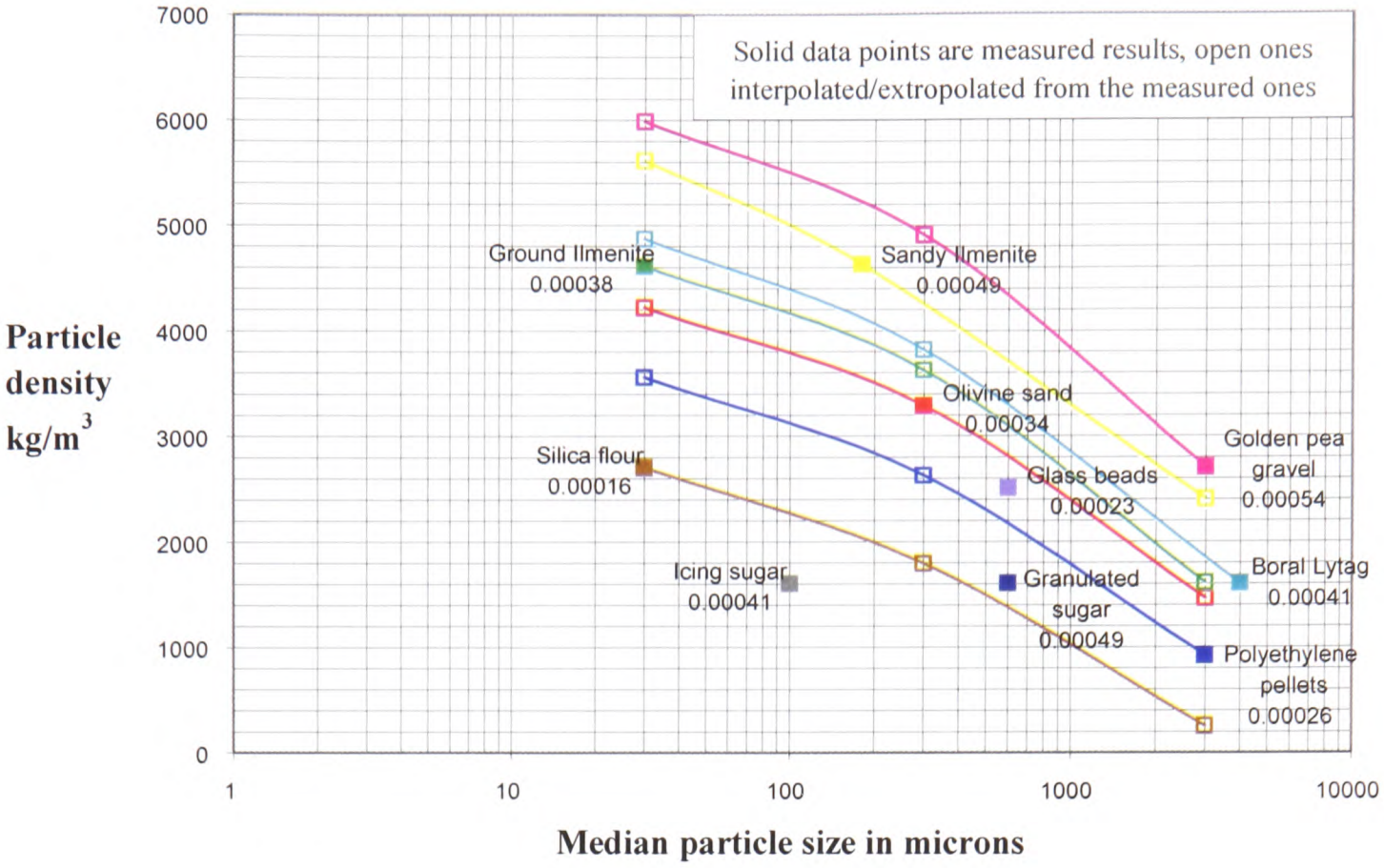

Graph 7.5: All ten test materials displayed with interpolated curves drawn through data points.

7.7 Investigation into why the sugars do not fit on to the graph

Out of all the ten materials in the test programme, the sugars were the only materials that gave a coefficient not fitting the pattern of relationship to the particle density and median particle size, observed by all the rest. Sugar is very friable, and breakages soak up energy, which may account for the higher than expected pressure losses. An investigation into a possible explanation for this deviation was required, so that the limitations of the graph could be identified. A list of all particle characteristics which were thought could affect the pressure losses was drawn up. This was to try and identify anything which might identify a characteristic of the sugar that is in any way different from the other materials. It was intended to establish whether or not this characteristic may have a significant effect on the pressure drop. It was considered that a list of particle characteristics would possibly highlight something that could be measured using the sugar in other tests (i.e. not pneumatic conveying) and compared with the other materials. The particle characteristics identified are listed below, and also whether or not the ability to measure each property could be established.

7.7.1 Particle size

When measuring a particle, derived diameters are determined by measuring a size dependent property and relating it to a linear dimension. The most widely used of these are the equivalent spherical diameters. For example, if an irregularly shaped particle is allowed to settle in a liquid, its terminal velocity may be compared with the terminal velocity of a sphere with the same density under similar conditions. The size of the particle is then equated to the diameter of a sphere which has the same terminal velocity. Thus, many different equivalent diameters can be applied to the same particle, which is not a unique a value[S5]. Therefore, the measurement of the equivalent diameter for the number of materials used in this project, was determined by one method for the smaller sized particles of less than 560 microns, and a second method for particle greater than 560 microns. This was due to the limitations of the particle sizing equipment.

The methods used to measure the larger particle sized test materials were sieving, and for the smaller sized particles, a laser particle sizer was used. Sieving measures the second largest dimension of the smallest cuboid box around a particle. The Malvern laser particle sizer determines an equivalent sphere for light scattering, and measures particles up to 560 microns.

Most of the test materials were measured using the Malvern particle sizer, because their particles were within the range for that equipment. Although two different methods were used to measure the particles in the test programme, the distance between the sizes of those measured meant that any differences between the accuracy of the two methods would make very little difference to the results on the graph.

7.7.2 Size distribution

The particle size used on the graph is the mass median particle size determined from the Malvern or sieve analysis. Some materials had a wider size range than others tested, and in addition both the median size and size range could change during conveying as the particles degraded. The level of degradation was monitored by taking samples of materials known to degrade during pneumatic conveying, at regular intervals of five complete test cycles. Once the size distribution began to move across to a smaller size range, the test work on that material was finished. For example, the effect of the particle degradation of the sugar was limited to prevent the changing size range from affecting the analysis.

7.7.3 Particle density

The particle density measurement has less room for variability in measurements than particle size and shape. This is because the particle density is constant regardless of size, provided all the particles are made of the same material (and unless the particles are hollow). The particle density for the test materials was determined by using the air comparison pycnometer. Due to the density being measured in thousands of units, small errors would not make much difference to the coefficient curve when using the graph.

The accuracy of the measurements is divided between two pieces of equipment, i.e. the scales on which the mass of the solids are measured, and the test balls used in the pycnometer. The tolerances on the test balls were ± 0.015 c.c. (0.00175% of the balls) and the resolution on the scales ± 0.1 g. The average sample weight of material used in the sample cup, was 29g (of which 0.1g represents 0.00345%), which gives a nett error of ± 0.0052%.

7.7.4 Particle shape

7.7.4.1 Particle shape definition

Particle shape influences properties such as the flowability of powders, and the interaction with fluids. A definition of particle shape is found in the British Standard 2955, and gives terms and a description of shape e.g. Angular - sharp-edged or having roughly polyhedral shape. However, if shape factors are to be incorporated into equations concerning particle properties, then it is necessary to measure and define shape quantitatively.

As stated previously, the main factors affecting the pressure losses along a pipeline were expected to be the particle size, density and shape. To reduce the problem of trying to measure the differences between various shapes, the aim originally was to only test materials with rounded particle shapes. However, this concept could not be tested when the sandy ilmenite was reduced to ground ilmenite by the size reduction processing. The particles that were originally rounded (see photograph 7.1) changed to angular shapes amongst tiny dust particles (see photograph 7.2) by the grinding method used to reduce the particle sizes.

Photograph 7.1 Sandy ilmenite

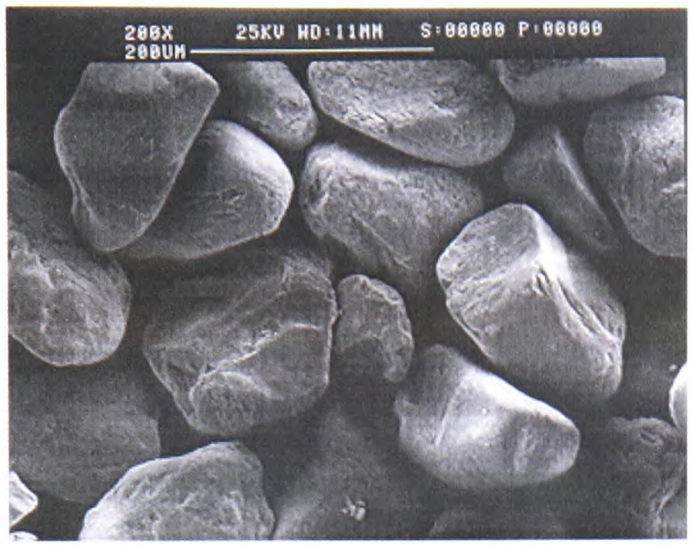

Photograph 7.2 Ground ilmenite

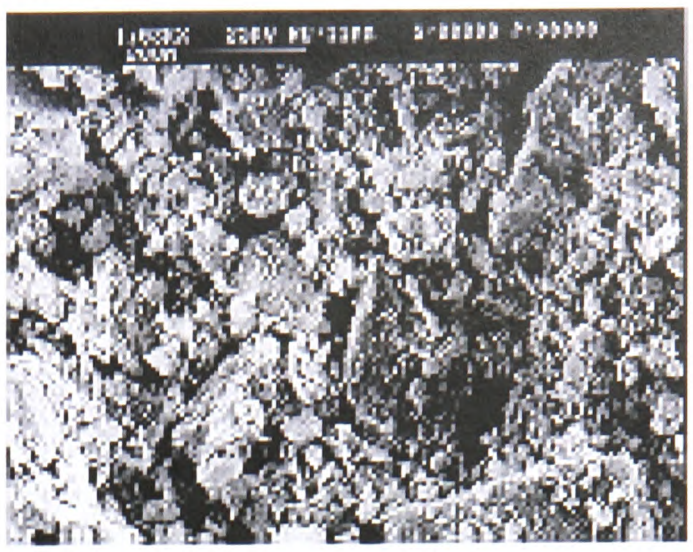

7.7.4.2 Surface area analysis

To measure the particle shapes to see how they relate to a spherical particle, a number of exercises were carried out. For the first test, samples from each of the test materials were used in a Micro meritics surface area analyzer. The device takes five point surface area measurements by using liquid Nitrogen as an adsorption gas. The machine measures the amount of nitrogen adsorbed by the particles to identify the surface area of the particles. Unfortunately, most of the particles were too large for the equipment which meant that the surface area was too low a value to obtain a reading. The icing sized sugar sample, although containing appropriate particle sizes, was not suitable for the test because a vacuum is formed to equilibrate the chamber, and this action removed the moisture from the sugar particles which upset the test procedure.

7.7.4.3 Fractal dimension

A different approach was used for the shape analysis exercise. It was based on work from Mandelbrot[M9] and involved taking a photograph of one or more of the particles from each test material, and measuring the perimeter (P_λ) of each shape using a set of dividers. By counting the number of steps (λ) and multiplying by the divider setting, the perimeter of the shapes were determined. Each particle photograph was scaled to fit an A4 sheet of paper, so that each particle was of a similar dimension. The setting of the dividers were set at a distance of 20mm, (the percentage of each particle diameter varying from 10 to 14%) and reduced by steps of 5mm (varying from 2.5 to 3.5% of each particle diameter) for each measurement, until 4 sets of values were obtained. The results are plotted on graph 7.6 shown below. Reducing the divider setting, increased the perimeter distance (P_λ) for irregular shaped particles, but for spherical shaped particles, the values barely changed. The angle of the slope of the straight line drawn through each

set of results (δ) is the indicator of the fractal dimension and gives an indication of the sphericity of each shape. The steeper the angle, the more irregular the particle shape. Where the particle shapes were varied amongst a material, i.e. granulated sugar, several particles were used to determine an average fractal dimension.

P_λ = total length of inscribed polygon ≡ perimeter estimate

λ = step length

δ = slope = fractal dimension of each particle

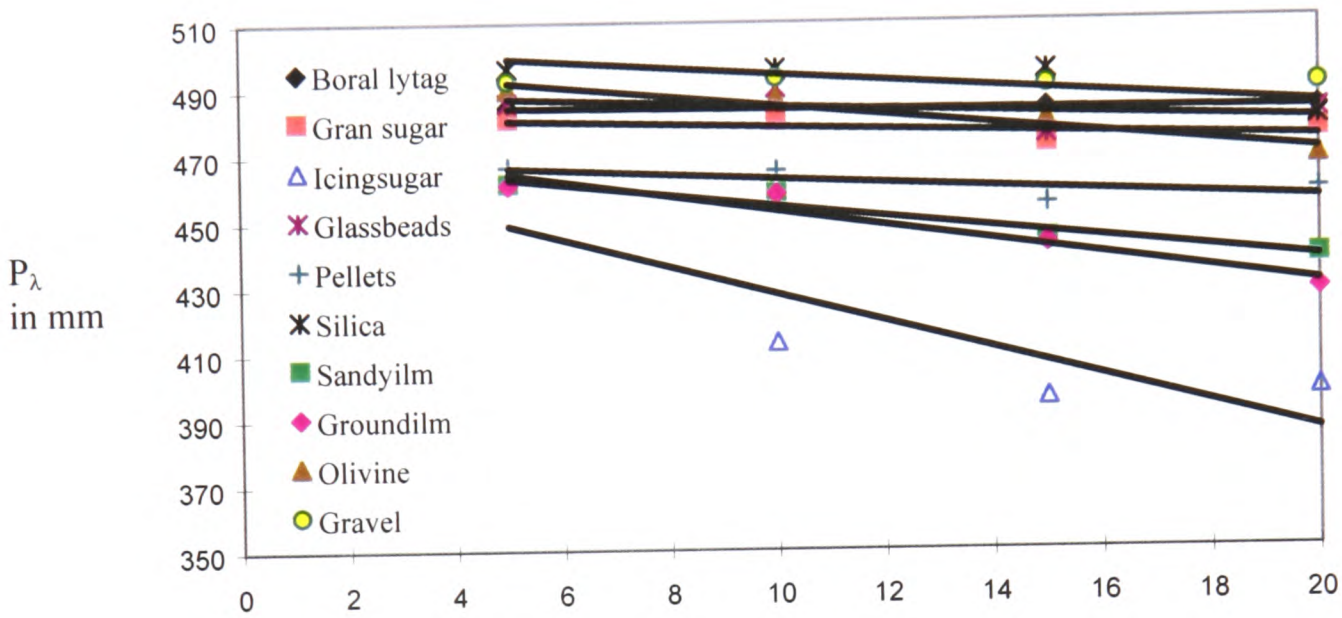

Graph 7.6: The total length of the inscribed polygon of each particle, against the step length of each particle shape, are plotted to determine the fractal dimension of the particles for each test material.

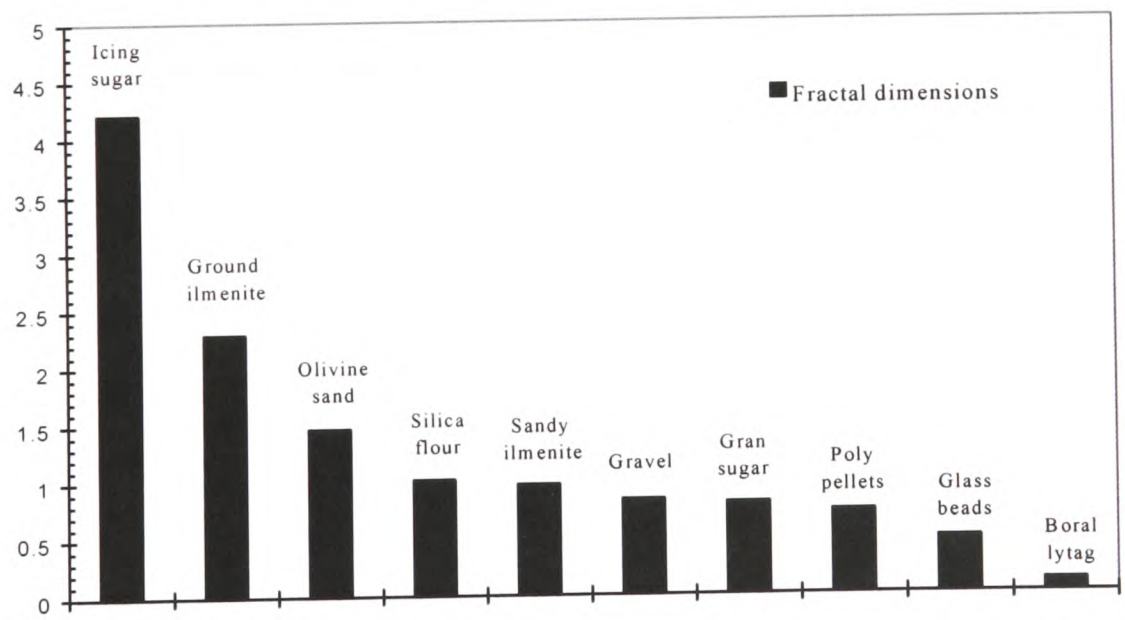

Graph 7.7: shows the results of each materials indicator of fractal dimension. The higher the reading indicates the more irregular shape.

7.7.7.4 Equivalent diameter

The area of each shape was measured using graph paper, to determine its outlined area, and the maximum diameter of the profile (known as the Ferets diameter) drawn across the particle and measured. The outlined area of each shape was used to calculate the proposed diameter, if the shape was spherical. The ratio of the diameter for a sphere, and the dimension of the longest line drawn though the particle shapes, was used to indicate the roundness of the particles.

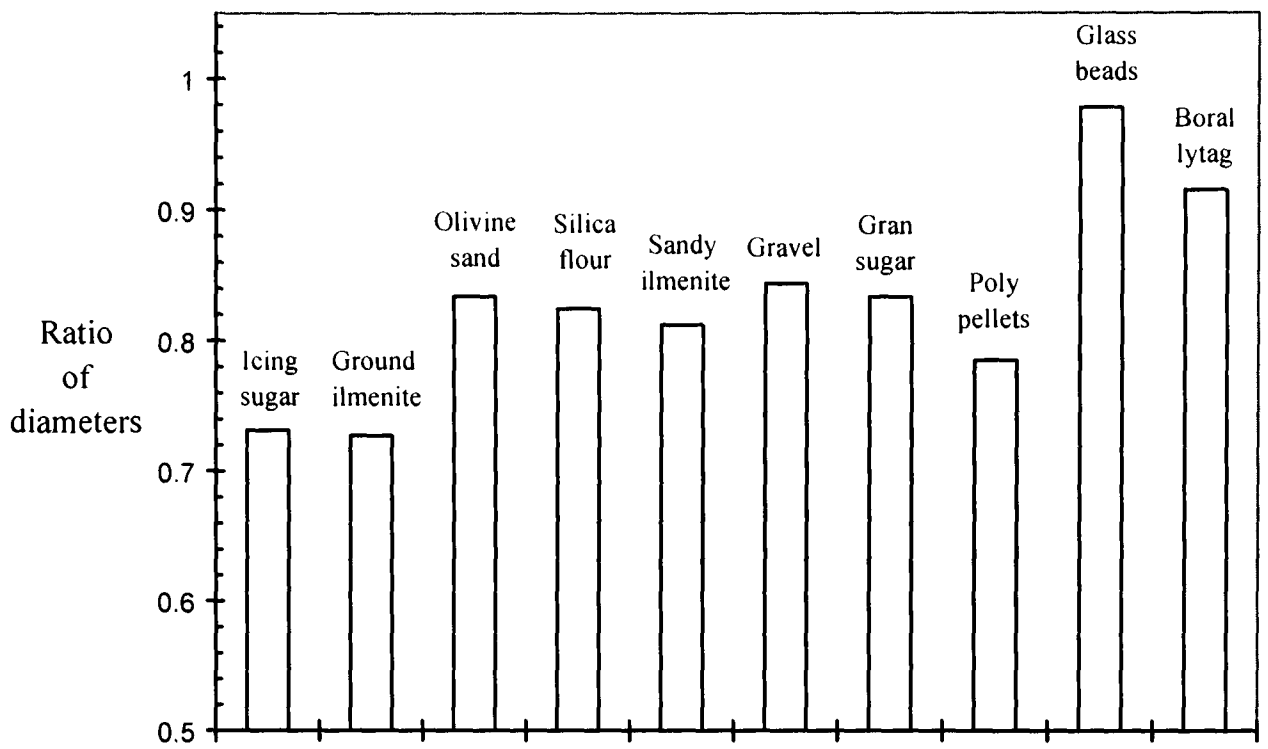

Graph 7.8: The ratios of the maximum projected length of a profile in any given direction (F_D), to the diameter of a sphere using the calculations from the outlined area of each shape. The lower readings indicate the more irregular shape.

Comparing the results on graphs 7.7 and 7.8, to those on graph 7.5, There does not appear to be any connection between the shape of the particles for both the sugars, to explain why the coefficient determined from the graph is far removed from the coefficient determined from the analysis of the test results. The icing sugar indicator of fractal dimension was very much higher than all the other particles, but as the granulated sugar was not noticeably different from the rest, the shape of the particles were not thought to be responsible for the differences.

Although the shape factor was considered important, as the majority of the test materials had rounded particles as indicated on graph 7.8, particle shape was not included in the analysis.

7.7.5 Hardness

Relative hardness is usually measured on the Mohs hardness scale. The scale is based on the ability of a mineral to scratch other minerals. The test materials were not measured to determine their hardness values.

7.7.6 Fragility

The ease at which the particle breaks, or is worn. A fragile material like the sugar breaks up easily during pneumatic conveying, and therefore only a limited amount of test runs were useful for a specific size range. A method to test this property has not been used to date.

7.7.7 Elasticity

The elasticity of the particle would affect the rebound properties of the material when a particle collided with the pipe wall or other particles. The only method available to measure particle elasticity, is to find the coefficient of restitution, by holding an individual particle at a certain height and dropping it on to a surface, then measuring the height to which it rebounds. This method is suitable for the larger particle greater than 500 microns, but the silica flour particles are approximately 30 microns. Holding a handful of this material and dropping it from a height just causes a dust cloud to emerge, as air drag is so great in relation to gravitational and inertial force, for such fine particles.

As the objective was to compare the sugar with all the materials in the test programme, measurement of the elasticity on the larger sized particles was considered unnecessary, because the icing sugar could not be measured due to its particle size.

7.7.8 Hydroscopicity

The amount of moisture a particle can absorb. This will make a difference to the flow properties of a material, like the sugar. The sugar was the only material that would absorb water and dissolve.

7.7.9 Surface texture

The surface texture would be likely to have some effect on the drag coefficient of the particle. The only means of identifying this property would be under a microscope visually. All the materials were photographed in this way for the thesis, so the differences between the materials could be identified. The sugars did not appear to be any different from other materials within the test programme, as can be seen in appendix 7.

7.7.10 Wall friction

As part of the investigation into the differences between the sugars and the majority of the test materials, the frictional characteristics between the bulk solid and the pipeline wall material were measured. This is known as the angle of wall friction [D2] and is not a constant value for a bulk solid, but depends on the smoothness and material of the wall surface against which the bulk solid is moving. The angle of wall friction measurement was achieved by using the Jenike[J2] shear tester.

To use the Jenike shear tester, a shallow circular ring was placed on a flat sample of wall material. The sample was made from a mild steel material representative of the test rig pipe wall, with a comparable internal wall surface roughness. Kilogram loads were applied incrementally to the cell using a gravity loading system. An electro-mechanically driven loading stem moved horizontally to push the ring across the wall, providing a shearing action. The shear force corresponding to the applied normal load was measured with a load cell and indicated on a chart recorder.

The wall friction was considered a useful entity to study because the particles as they move along the pipeline are likely to hit the pipe walls at some point. As the shearing force is what is measured in the wall friction test, it would be relevant to the energy loss in collisions, and therefore the pressure loss in the pipeline.

A graph plotted from the results using the values of shear load against the normal load, determines the angle of wall friction for the material. The angle of wall friction for each of the ten materials were plotted all together on several graphs to compare the differences between them, and search for the correlations against pressure loss coefficient values.

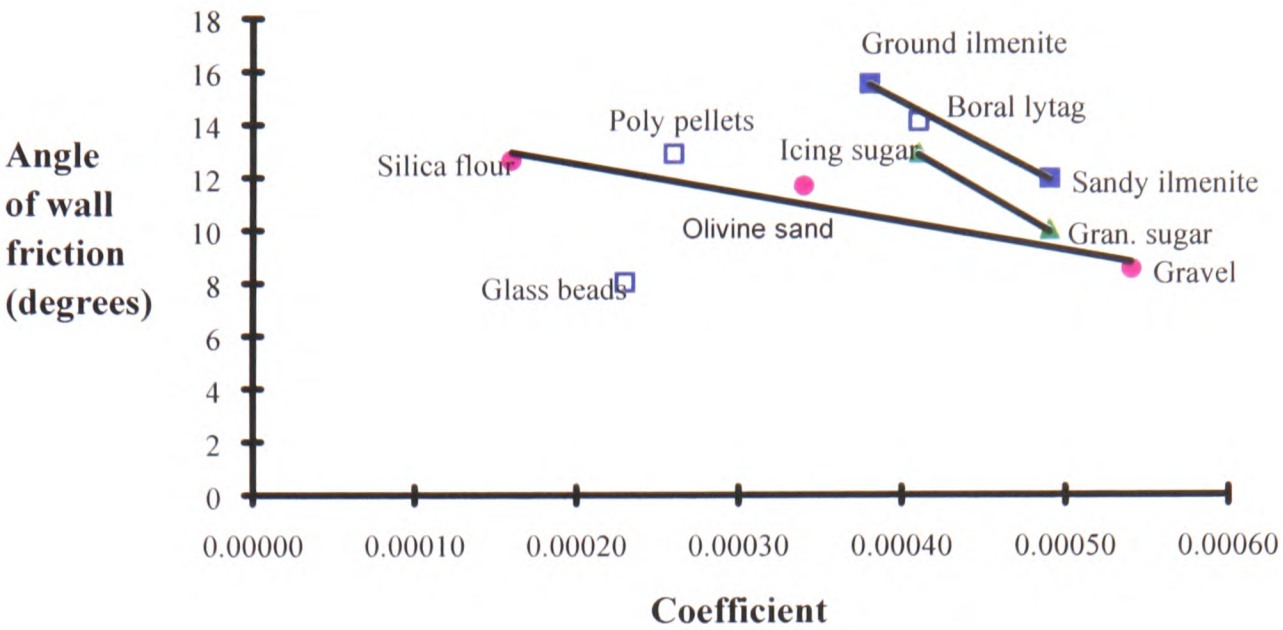

Graph 7.6: Results of wall friction tests using the Jenike shear cell, versus the coefficient derived from measured test results.

The results in graph 7.6, show that for each set of sizes of one material, the finer the particles, the higher the wall friction, yet the lower the pressure drop. This can be seen in the decline in the coefficient value, which represents a decrease in the pressure losses across the test section.

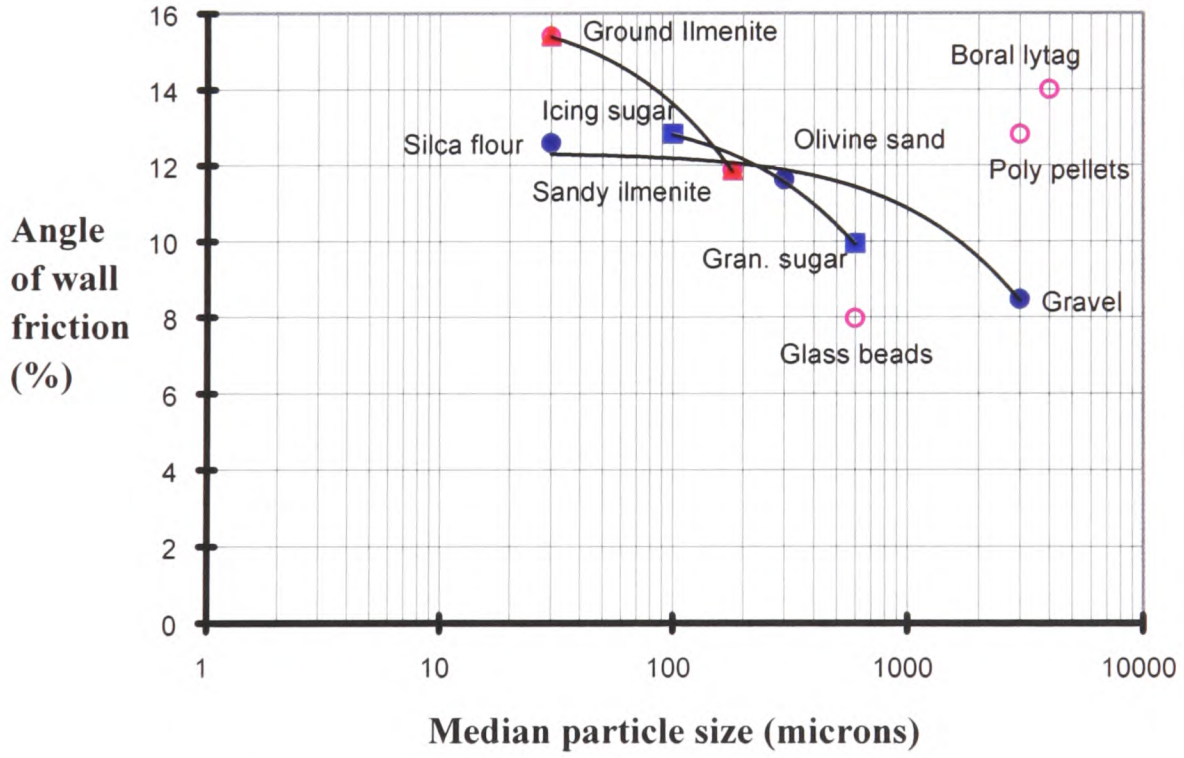

Graph 7.7: Results of wall friction tests versus the average particle size, for all the test materials. The relationship between particle size and wall friction can be clearly seen.

Graph 7.7 shows that the increased surface of the smaller particles, leads to higher wall friction of these materials. Since the higher wall friction of fine particles was in opposition to the lower pressure drop, it suggested strongly that pressure drop is not significantly dependent on wall friction.

In spite of the fact that the glass beads have a similar chemical composition to the olivine sand, silica flour and golden pea gravel, the beads did not fit along the same line. The reason was thought to be because the glass beads were very smooth and almost like ball bearings with regard to frictional properties, and so spherical in shape they just rolled over the wall surface. The particle density of the glass beads is 2500, compared to 2700 for the gravel and silica flour, and 3200 for the olivine sand.

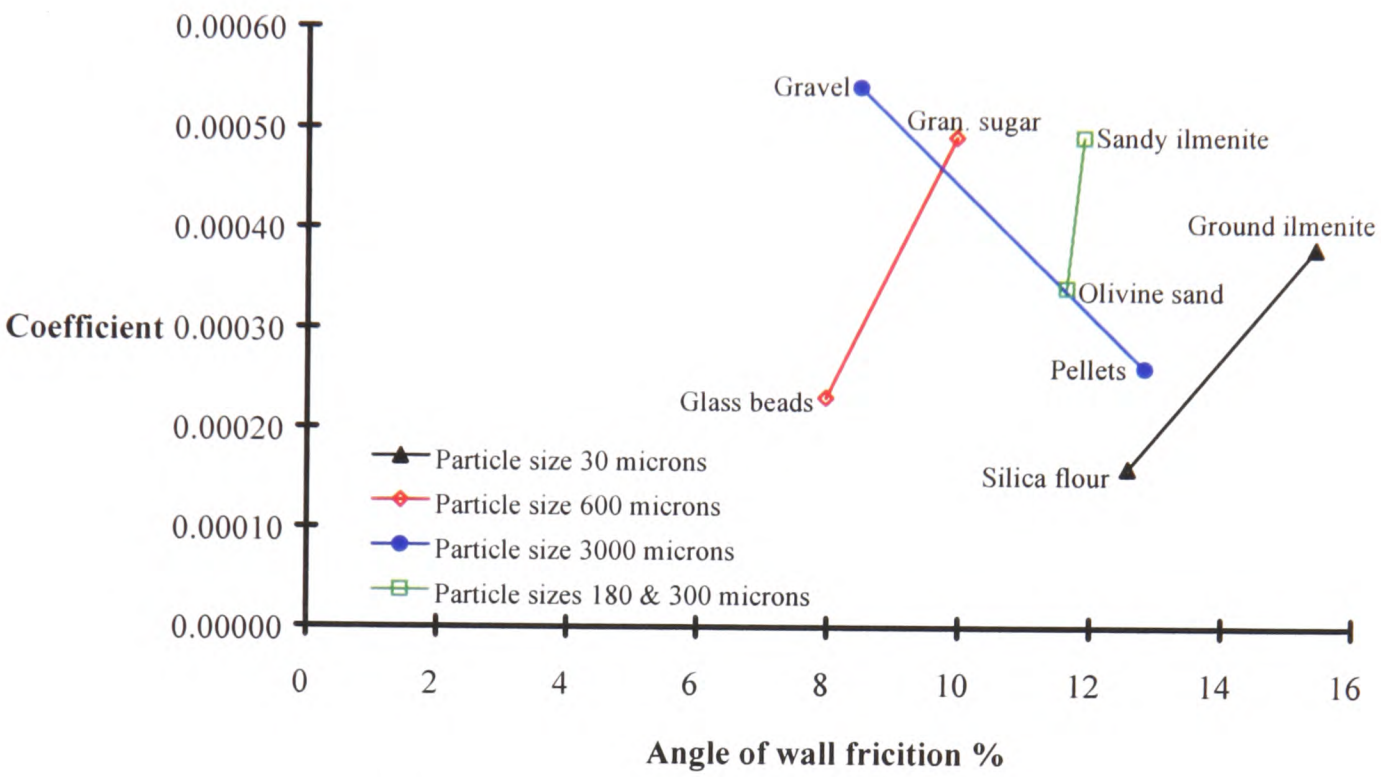

Graph 7.8: The coefficient versus the angle of wall friction, for particles of the same median size, but different materials.

Graph 7.8 was plotted to show the relationship between the coefficient, which represents the pressure losses along the straight sections of pipe, against the angle of wall friction, for groups of material with their median particle in common. With exception to the 3000 micron particle group, the remaining three groups show a coefficient value which increases as wall friction increases.

It appears that the effect of density over-rides the effect of friction. In every case except sugar, the higher coefficient value occurs with the higher particle density.

7.8 Conclusions on particle characteristics investigation

The investigation into why the loss coefficient obtained for sugar from the test work, did not compare consistently with the coefficient determined from the graph, was not productive. It was thought that the amount of time spent investigating possible reasons was adequate. Therefore, the investigation was stopped and it was concluded that no clear differences were found that could be measured easily. Apart from the noticeable issues stated previously, i.e. that the sugar was more friable than the other materials; it was the only food material, and it absorbs moisture easily, no other reasons were found for the departure from the trend identified for the other test materials.

7.9 Final survey and summary of findings, and some conclusions

The amount of data produced by the test work on ten materials enabled comparisons between materials of different median particle sizes, yet of similar particle densities and shapes, to be made. The results of this were included in a paper found in appendix 8. To summarize, as the particle median size increases, the pressure losses along the pipeline also increase. This effect was consistent with all densities, but the increase of change for each group was not at the same rate for the other groups in the test programme.

The comparison between materials of different particle densities, having similar median particle sizes and shapes, was also determined from the project work. The results also show that for material of similar particle sizes, the pressure losses increase as the particle density increases. Even though the effect is consistent across all particle sizes, the rate of change varies between each set of materials. However, the main conclusion of the test programme was the formation of a graph that may be used to help predict the pressure losses in straight sections of pipeline.

A limitation of using the graph was demonstrated with the additional work using the sugar. It indicated that the graph was not suited for use with all materials. The characteristics of the original six test materials from which the groups was formed, were mainly mineral and non-organic. Therefore, using the graph to predict the pressure gradients would appear to be limited to similar materials where the particles are firm, with mostly rounded particle shapes (although some of the original particles were angular at the edges), do not absorb moisture, and not easily friable during pneumatic conveying.

Chapter 8

Conclusions

8.1 Achievements of this project

The prediction of pressure losses when conveying solids and air along a pipeline, has been investigated by many researchers. Experience has shown that when solids are pneumatically conveyed, each material will behave differently in terms of its pressure drop and minimum conveying conditions. It is clear that these differences in behaviour must arise from differences in the particles, however it has never been possible to form direct links between the particle characteristics and their behaviour in a conveyor. The main objective for this project was to compare the pressure differences between several materials to discover if there is a correlation between pressure gradient and the particle properties of the materials. To achieve this, a methodical investigation was conducted, using ten materials, into how the particle size and density affects the pressure drop in straight sections of pipe. The intention at the start of the project was to measure the pressure losses from the minimum to the maximum conveying conditions within the confines of the test rig, which usually suggests from dense to lean phase conveying. However, due to the limitations of the volumetric feeder, dense phase was not possible for some materials, so the full analysis was restricted to lean phase conveying only.

The particle properties that this project was intended to investigate, were the particle median size, density and shape. The particle median size and density were relatively easy to evaluate, but the particle shape was difficult to measure due to the wide range of particle sizes used. Therefore, the original plan was to eliminate the comparison in particle shape, by using only rounded particles in the test work. However, this proved very difficult to achieve when materials obtained for the test programme had been through a size reducing process such as grinding, that altered the particle shape. An assessment of the particle surface texture was carried out, which gave some indication of shape, and concluding that most of the test materials, although not altogether spherical in shape, were fairly rounded.

By using a structured approach, the project has achieved its objective, as a link between the particle density and pressure gradients, and the particle median size and the pressure gradients, has been identified between the materials used in this project. A graph has been developed plotting particle density versus the particle median size of materials, with lines drawn representing contours of

pressure loss of coefficient values. The graph gives the user a coefficient that can be used in a simple equation, to predict the solids contribution towards the total pressure gradient along straight sections.

To obtain the pressure gradient results for each material, a test rig was used that included a pipeline loop, blow tank and receiving hopper. The rig originally available was instrumented with pressure tappings along two straight sections, separated by a 90° test bend. Modifications were made to this rig to fulfill the project objectives. A volumetric feeder was installed to control the feed rate of solids into the conveying line; and additional pressure tappings were fitted so that four consecutive straight sections of pipe could be used to monitor the pressures along the pipeline. Three identical bends were placed in-between the four straights sections, and the computer data logging, storage and retrieval system was upgraded.

The number of consecutive straight sections of pipeline fitted with pressure tappings, enabled a far longer length of pipeline to be instrumented than in previous work. Earlier research had measured the pressure drop along two straight sections and across one bend. This indicated what was happening in a small section of a conveying pipeline, and systems have been designed using those results. However as the majority of the modified test rig was instrumented to give pressure readings, measured data obtained from the test rig gave a more detailed view of what was happening to the pressure during pneumatic conveying over a greater distance. The main advantage of this arrangement was that any mechanical effects of a single straight test section or bend are not so significant, as only part of the test section is affected. Whereas in the event of a mechanical defect in a system with a limited test section, all the results are affected. This gave a clearer picture of the actual flow conditions during pneumatic conveying.

Most of the work for this project was experimental, as the initial objective was to compare the results from six materials, but ultimately ten materials in total were used. At the start of the project, it was intended that the pressure losses caused by the bends were to be examined, as well as the pressure gradients along the straights. However, after the first three materials had been tested, the information obtained from instrumenting four straight sections, produced such a large amount of data, that it became obvious that an analysis of all the results would be too great a task for one project. Consequently, the data produced from pressure losses caused by the bends, was put to one side for use and analysis in a further project.

The work involved in completing this project, led to the discovery of many things. Firstly, as this was the first time that four consecutive straight sections had been fitted with pressure tappings, it allowed a profile of the pressure losses along a test section of 57m, with three identical test bends,

to be monitored. The pressure gradient along the straight sections of pipeline before and after a bend, are rarely the same, because the pressure losses caused by a bend are generally higher per unit length, in comparison with the pressure losses per unit length along straight sections. This is because the change in direction of the bend, slows the particles down as they collide with the pipe walls and each other, and as they leave the bend, the particles are re-accelerated to try and reach the velocity of the conveying air. As a result, the pressure is significantly lower after a bend than before, the air density is also considerably lower. Consequently, air velocity is higher and suspension density lower. For this reason, it should be expected that the pressure gradient will not be the same before and after the bend, even in the regions of fully developed flow some distance from the bend, and this was confirmed by the results of the experimental work.

One of the problems early on in the commissioning stage, was trying to fit sensible progression straight lines through all the gradients, but taking the pressure losses caused by the bends into account. This was achieved by using the measured pressure gradients from each section (calculated from data taken after the acceleration zones) and applying a linear fit progression through all four gradients. Taking the midpoint value of each gradient also allowed the midpoint air velocity and suspension density to be determined, thereby giving four different conveying conditions for each test run.

One of the advantages of instrumenting four straight sections of pipeline with pressure transducers at regular intervals, was that this enabled a considerable amount of data to be obtained from relatively few test runs. It also allowed a full understanding of the relationship between the pressure drop, flow rate of solids and flow rate of air to be achieved. The reduced number of test runs would naturally lower the costs involved when conducting pilot scale test work on a new product.

The analysis of the test results produced new findings in two areas. The first area covered the declared objective of the research, which was to investigate the difference in pressure loss between the materials with different particle characteristics. The differences between the particle characteristics was further divided into the effect of particle size, and the effect of particle density, upon the pressure gradient in lean phase transport along straight pipes. The second area was the development of a consistent model for use in a data analysis and pressure drop prediction method.

Such an examination of the differences in pressure drop caused by the differences in particle characteristics had not been undertaken before in a comprehensive, systematic way. Careful choice of the test materials allowed the effect of particle characteristics to be seen much more

clearly than ever before. The analysis of the test results shows a clear link between these properties and the pressure drop.

The materials used to measure the effects of size, fell into of three groups. They were (i) the silica based materials (silica sand, olivine sand and golden pea gravel) (ii) ground and sandy ilmenites and (iii) granulated and icing sized sugars. All materials in each group had a similar chemical composition, but their sizes differed. The results show that as the particle size increases, the pressure losses for the solids contribution to pressure gradient along straight sections also increases. This effect is consistent in both magnitude and direction.

Three groups of materials were also compared to establish the particle density effects, which were similar in particle median size, and all fairly free flowing. They were (i) silica flour and ground ilmenite, (ii) olivine sand and sandy ilmenite, (iii) golden pea gravel, polyethylene pellets and boral lytag. The comparisons between these materials of similar particle median size, but with different particle densities, also show that as the particle density increases, so do the pressure gradients.

With respect to the model developed from the analysis, a consistent model, reduced the entire lean phase pressure loss characteristics of each material in a straight pipe, to a single value. This was used in a prediction method. To develop the model, several steps were taken, described as follows. When all the test work on a material was completed, the solids contribution to straight pipe pressure gradients were isolated (by subtracting a notional "air contribution" for each test condition, established from a Darcy/Fanning approach but using a Moody friction factor determined from measurements on the conveying pipeline). Then the results were plotted on a graph displaying the pressure gradient versus the suspension density. Due to the scatter of these results, the data was filtered down into air velocity ranges in order to find a correlation that could be used for further analysis. This was achieved in terms of a simple linear relationship between solids contribution to pressure gradient, and suspension density, the proportionality coefficient having a characteristic value for each range of air velocity. From the individual graphs, a further graph was drawn to show the variation of the proportionality coefficient with air velocity, to which a square law curve was fitted. The scaling coefficient of the curve was then used in a model to predict the pressure losses along horizontal straight sections of pipe during lean phase conveying, varying only by the scaling coefficient for each material.

The prediction method calculates the pressure losses along a conveying pipeline in a step-by-step method, starting at the outlet where conveying conditions such as air velocity and suspension density

are known. The pressure losses along each straight section are calculated using the model and the coefficient for the material, and across each bend is calculated by using the existing pressure loss data. The pressure losses are accumulated along the pipeline. Each time a new value for the pressure is calculated, the conveying conditions change accordingly and the old conveying conditions are replaced by the new current values for the next straight or bend position along the pipeline. The procedure is applied for each section or bend until the inlet of the conveying line is reached, and the pressure at inlet is determined.

It was intended to test the method of predicting pipeline pressure drop using the model and coefficient for each material, by comparing pressure loss results from each test run using the prediction method, against the measured test results. This was achieved by starting the prediction method at the last pressure transducer position towards the outlet of the test rig, and finishing at the first pressure transducer at the beginning of the test section. At both points, the pressure had been measured during each test run using the pressure transducers along the test section, so the conveying conditions (i.e. air velocity and suspension density) were known. Using the scaling coefficient for the material being compared in the prediction method, the pressure gradient was determined for the straight section leading up to the last transducer. The pressure losses caused by the each test bend were added to the new pressure values, (taken from the measured bend losses because the analysis of the bend data has not been accomplished). The process was repeated until the beginning of the test section was reached, at the first pressure tapping. Hence the total predicted pressure losses across the test section were determined and compared to the measured data.

The correlation between the measured pressure losses, and those determined by the prediction method, was good. There was some scatter of predicted data points either side of the measured results, indicating an over prediction or under prediction of the pressure losses along the test section, the magnitude of which varied for each material, but generally, the differences were within 20% either way.

From the analysis of the test work on the original six test materials, a graph was plotted to link the particle density, the median particle size, and the scaling coefficient of each material. With a single data point for each material, correlations and extrapolations produced curves representing the scaling coefficients over a wide range of particle size and density. Using this graph could in principle eliminate the need for pilot-scale tests for predicting the pressure gradient along straight sections of pipeline, because it enables the coefficient to be determined from the particle median size and particle density of the material that any new system will be designed to convey. Until the analysis of the work for the pressure losses caused by the bend has been analysed, pilot scale test

work will still be necessary to determine the pressure losses caused by the bends, for the material the system will be transporting. However, due to the fact that more test bends then usual were installed in the test rig, the number of tests necessary to obtain data on pressure losses caused by the bends over a wide range of conveying conditions, was greatly reduced.

All the materials initially chosen to develop the graph, were free flowing, fairly robust, do not absorb moisture and are reasonably rounded in shape. To substantiate the validity of the graph, further materials that did not necessarily fit the profile of the original materials, were added to the test programme. The four materials selected for this purpose, were boral lytag, glass beads and granulated and icing sized sugars. The analysis of test results for these materials was varied. For the sugars, the scaling coefficient values predicted using the graph, were far removed from values determined by analysing the test work. Using the graph to predict the scaling coefficient for the glass beads was not dissimilar from that determined from the test work, while the boral lytag values fitted exactly. Analysing the additional material characteristics, the boral lytag showed properties similar to those from the original test materials, and the glass beads, although silica based like other materials in the programme, were spherical and very free flowing, almost like ball bearings. The sugars however, are very different chemically. They are a food product, absorb moisture, are very friable, become very cohesive when degraded and have a bimodal size distribution. There is a possibility that the sugar may have melted on impact with the pipe walls during conveying, thereby causing an increase in friction. This would account for the high pressure losses during the test work. Several tests were conducted to measure the differences between the sugars and all the other test materials, however some properties were too difficult to measure, and the tests that were performed, did not enable any conclusions to be reached.

From the work on the additional test materials, it is evident that the graph is not valid to predict the scaling coefficient for all materials. However, it has worked for some of the new materials introduced after the initial development test work, where these have generally similar characteristics of shape, hardness, robustness and are free flowing (e.g. boral lytag and glass beads).

The work using the ten materials in this project, represents a small selection of the varied materials that are pneumatically conveyed in industry. An investigation into what materials are suitable for use with the graph, can only be carried out by testing materials that are both similar to those used in this project, and those that differ only slightly. Products like the sugar differ in many ways, and have too many particle variables that deviate from the other materials in the test programme. This made it difficult to identify why the sugars were unsuitable candidates to determine their coefficient from the graph alone.

8.2 Recommendations for further work

More research is needed that concentrates on the differences between materials with regard to their effect on the pressure losses during pneumatic conveying. From the separate groups of materials used in this project to measure the effect of the particle median size, and the effect of the particle density on the pressure losses during pneumatic conveying, only one group had three material data points from which to correlate. The other groups had just two data points for comparisons, which are permissible when used with the other groups, but are not as satisfactory as materials with three data points.

The identification of how the particle shape affects the pressure losses should be explored in more detail. This could be achieved by using a product such as plastic pellets, that may be obtained in cylindrical and spherical shapes. In addition, other particle properties such as surface texture, hardness and melting point, to name but a few, could be examined using pairs or groups of materials that are similar except for the characteristic under investigation, to identify the effect that property has on the pressure losses during pneumatic conveying.

In addition, research needs to be carried out regarding the mechanisms in which particles are carried in the air stream within the pipeline. Variables such as the coefficient of restitution and the degradation of the particles, and their affect on the pressure losses need to be determined. A high degree of energy is transferred during the breakage of particles, and a correlation between the rate of degradation and the pressure losses could identify a wider range of materials that could be used with the graph, which cannot be identified at present. The friability of the types of sugars tested was thought to be a major factor that accounted for the higher pressure losses.

The particle size range of the test materials was reduced to a single value, and classified by their median size. This was appropriate because of the narrow size range of the products used to develop the graph. However, apart from the median size of particles, other size measurements could be investigated for their evaluation for use with the graph. For example, it may define whether or not a material with a wider particle size range could be used to determine its scaling coefficient.

An examination into the measurement methods to determine a particle's coefficient of restitution value, would also benefit the work carried out as part of this thesis. The reason for this relates to the fact that the greater a particle deflects on impact, the longer it takes to rebound back to its original shape, or in the case of friable product, permanent damage takes place. The coefficient of

restitution of a particle would most likely have an effect on the frictional pressure losses of materials conveyed along pipelines, because that property would affect the amount of energy transferred to the pipe walls and other particles during collisions. Measurements of the differences in the coefficient of restitution between all the test materials used in this project would be useful, as the first group of materials used to develop the graph contained fairly robust particles.

One aspect of the project that was not fully explored due to the large amount of data and analysis involved, was that of the pressure losses caused by the bends. Each test run produced results for the pressure losses caused by the effect from three identical test bends, but for different conveying conditions. The data is stored in databases, for future evaluation and analysis.

The limitation of this test programme, is that only a small number of the many varied materials that are pneumatically conveyed in industry, have been used to predict the pressure losses using the technique devised in this project. However, based on results relating to these materials, the conclusions give real expectations that a reliable prediction method from particle properties may be possible with some additional work, and that the work that has been undertaken for this project provides a sound base upon which to build further.

Appendix 1

Literature review

A.1.1 Introduction

Previous work on the modelling of pressure drop across bends and along straight sections for two phase gas-solids flow, highlighted the fact that little research had previously been undertaken into the measured pressure drop differences between materials of different particle size, shape or density. Of the work that had been carried out in that particular area, the main areas of research have related to the differences in particle size from only a handful of coarse materials. Other workers have used a number of different products for their work, but were investigating other aspects of pneumatic conveying, so their findings are not directly related to this research. Never the less, papers relating to this work are included in this review for their contributions. In addition, the prediction of pressure losses for pneumatic conveying systems, are obviously of interest, in particular where the author takes account of the particle characteristics in their prediction methods.

A1.2 Review of papers on pneumatic conveying

A1.2.1 Pressure drop modelling comparing different materials

In 1948, Vogt and White [VI] used four different materials, sand, steel shot, clover seed and wheat, to look at the pressure drop due to friction of solids during pneumatic conveying. The sand was sieved into four distinct size ranges, which enabled the results of the difference in size for one material to be compared. The small scale test rig was constructed of 12mm diameter pipe, with a rather primitive method of controlling the feed rate of solids into the conveying line. It consisted of a feed hopper 150mm in diameter, 300mm high, connected to the air line by a large rubber hose. The rate at which the solids fell into the air stream was regulated by adjusting a screw clamp on a large rubber hose that connected the feed hopper to the air line. The pressure readings were taken at 90mm intervals along a pipeline of less than 15m in length, which also included two bends. As the straight lengths of pipe were not long enough for fully accelerated flow to be measured, the significance of the test results is doubtful. Vogt and White concluded that the data from their investigation indicated that the pressure drop could be represented by the following type of equation, but should not be used for fine particle materials in large pipes.

$$\alpha - 1 = A\left(\frac{D}{d}\right)^2\left(\frac{\rho}{\omega}\frac{r}{\mathrm{Re}}\right)^{\kappa}$$

where A and k are empirical functions of the dimensionless group

$$\sqrt{\frac{1/3(\omega-\rho)\rho g d^3}{\mu}}$$

α = relative pressure drop

ρ = fluid density, lbs/ft^3

ω = Solid density, lbs/ft^3

μ = viscosity of fluid, lbs/ft^3

A graph displaying all the results, showed that the particle size does have an affect on the pressure losses, as the pressure loss increases with the increase in particle sizes.

Clark et al [C2] (1952) measured the pressure drop for 5 granular materials in a 25mm dia. brass pipe. The test rig consisted of two straight lengths of pipe, up to 13.7m in length, separated with a 180° bend and instrumented with pressure tappings at suitable intervals. The pressure gradients along the straight section were obtained from measurements from one straight only. Particle velocity was also measured by trapping material in a section during conveying, and measuring the contents. Unfortunately, an insufficient number experiments were carried out for a complete correlation of the pressure drop for all materials, and no pattern could be made from the graphs plotted that showed a relationship between the mean diameter of the particle and the pressure losses. The authors had hoped that an index could be used to relate pressure gradient to the physical properties of the material.

In their study of the pressure drop during pneumatic conveying using glass beads, Mehta et al [M1] (1957) used two distinct particle sizes of 97μm and 36μm, and also included the particle velocity measurements. The test rig comprised of a 12mm dia. pipeline, with a vertical and horizontal test section from which measurements were taken. The main problem was that both test sections were much too short at less than one and a half metres long. However, from a graph plotting the solids friction factor against the Reynolds number, the larger of the two particles friction factor was 10 times higher than the smaller particle, indicating a distinct change in type of flow, but mostly bend effects - albeit not fully developed.

Following on from the work from Clark et al [C2], Richardson et al [R5] (1969) identified the limitations of the test pipe rig and techniques adopted, so modifications were made to the rig. In addition, the method of measuring the solids velocity was replaced with a more accurate approach that did not interrupt the conveying. The changes in the pipeline resulted in a very long straight horizontal pipe, 35m in length, from which both pressure drop and solids velocity measurements were taken. Instead of the batch wise method of pneumatic conveying Clark et al had used, continuous conveying of the material was achieved by installing a return feed line, cyclone separator and rotary valve, to enable a steady flow rate to be reached before measurements were taken. Pressure measurements were taken using mercury manometers. Before taking any measurements, the material was conveyed between 30 and 45 minutes to determine if the readings changed with time. Some materials produced an electrostatic charge after lengthy conveying, which resulted in an increased pressure drop. Sight glasses enabled visual observations during the conveying of the ten materials used in the test programme. The results from the solids velocity measurements, indicated that at high velocities, the relative velocity between the air and the particles was constant, independent both of feed rate and of air velocity. At low velocities, the solids fell into three classes.

Class A included particles such as lead, polystyrene, brass powder and rape seed, for which the relative velocity at both low and high velocities was constant. The size distributions were narrow and the ratio of sizes of the smallest and largest particles, was less than 3. Class B materials included some coals, which had a wide size distribution, an average size greater than 1.02mm, and the relative velocity was around 0.6m/s more at low than at high velocities. Class C materials included aluminum powder and some coals with a wide size distribution an average size of less than 1.02mm. At low velocities, the relative velocity is dependent on the feed rate of solids.

The pressure drop correlation equation for the solids only, included a numerical constant that was determined from the experimental results over a 22m straight section of pipe, during dilute phase conveying. The difference between the pressure drop of the various materials was not shown, but the pressure drop due to the solids was directly related to the free fall velocity and other variables, including the particle density. As all the test work was carried out using a 25mm diameter pipe, the effect of the pipe diameter was not investigated.

This paper was particularly interesting because of the length of the straight section used, and the continuous conveying tests. The results showed that the pressure gradient along the horizontal section was not a straight line, but a wave type curve. A mean straight line was drawn through the

curve to obtain consistent and reproducible results. This procedure confirms that drawing a straight line through the data points along each of the four straight sections, as used in this project, is the best method of dealing with data that is not always in alignment.

Mendies et al [M2] (1973) carried out an investigation using three plastic materials of similar particle shape and density, but with different particle sizes. They evaluated the solids velocity by measuring the particle velocity and pressure distribution in a pilot test plant, which consisted of 11 metres of horizontal pipe, and 6 metres of vertical pipe, using maximum solids loading ratios (SLR) of 9.

From a graph representing their results, the fully accelerated flow from the inlet to the conveying line, was only just reached. However, as the results showed, fully accelerated flow was reached near the end of the straight pipe. Mendies et al used the data from the last set of tappings in the horizontal section for their results. The results plotted on a graph indicated that the particle size had an effect on the solids velocity, as it showed that the smaller the particle, the higher the solids interstitial fluidising velocity. However, no comparison was made of the pressure losses between the test materials. It was also found that the air velocity and SLR did not influence the acceleration length of the material, which took 4 to 5 metres. This is in agreement with Rose and Duckworth [R3] (1969).

Rubber pellets and polypropylene nibs were two materials used by Scott [S1] (1978) to investigate the influence of particle properties on the pressure drop during pneumatic conveying. Particle size, shape and density, as characterised by the terminal free fall velocity were considered important, so both the materials he used had similar terminal free fall velocities. He used a test rig made from aluminum pipes of 80, 100 and 155mm internal diameter, 135m long. The results show that in fully accelerated horizontal flow, the overall pressure drop is greater with the rubber pellets than the polypropylene nibs. The pressure drop in fully accelerated horizontal flow is only shown for the rubber pellets, so comparisons could not be made between the two materials. Separating the pressure drop due to the solids only in horizontal flow, two models were used that are dependent on the velocities either above or below the velocity transition zone. Below the transition zone, the particles are sliding along the bottom of the pipe, above the transition zone is where particles are suspended in the air stream. The models include the slip velocity, terminal free fall velocity and the drag and resistance forces on a particle.

In suspended flow regimes, Scott states the extra pressure drop attributed to the solids only above the transition zone, rises because the particles are retarded on collision with the wall and

subsequently re-accelerated by the gas stream. In addition, at higher gas velocities, the ratio of radial to axial particle velocity is important. At low air velocities, the extra pressure drop for the solids is due to the free fall velocity and sliding friction. In conclusion, the observations and models were in good agreement, provided that the solids were fully suspended along the pipe. The two materials used in this study shared a similar terminal velocity, with the rubber pellets being higher than the nibs, but their size and shape was different. The rubber pellets were roughly spherical and the nibs, cylindrical. The particle density of the rubber pellets were 20% higher than the nibs. The higher pressure drop measured for the rubber pellets, indicates that the free fall velocities are not sufficient in predicting the pressure drop in pneumatic conveying, and the difference may be due to the higher particle density. However, the obvious difference in the particle shapes and size may also have increased the pressure losses for the rubber pellets. The big difference in the size and shape of the particles, render the results outlined in the paper of no use to this author.

Chen [C3] (1978) used a horizontal pipe, 37m in length, to measure the solids velocity of the same two materials as Scott [S1]. He found at high air velocities, the pressure drop from rubber pellets was much greater than with polypropylene nibs. His proposed model has particle free fall velocity and particle/wall friction coefficient as parameters, and includes a ratio of radial to axial particle velocities, which requires further investigation. The same conclusions are applied to that of Scotts paper above.

Raheman and Jindal [R1] (1993) carried out experiments in vertical and horizontal conveying of rough rice, milled rice and soy bean for solids ratio of 0.7 to 3.5 in 54, 68 and 82mm inside dia. pipes. The length of each straight section is not supplied with this paper. The pressure gradients were measured using 'U' tube manometers, with water as the working fluid. The particle sizes ranged from 3 - 7 mm, but due to the very low solids loading ratios, from 0.7 to 3.5, a large proportion of the pressure drop was due to air only. The total pressure drop was separated into the pressure drop of the air plus the solids pressure drop. The Fanning equation was used to estimate the air contribution to pressure drop in both the horizontal and vertical pipelines. An equation similar to Fanning's equation involving a solids friction factor, dispersed solids density and solids velocity was used to represent the solids contribution. Three graphs were produced which plotted the total pressure drop results of the tests for each material, as a function of the superficial air velocity. The pressure drop along the horizontal sections was greater for the soybean compared to the rough rice, which in turn was greater than the milled rice. The soybeans particle equivalent diameter was twice the size of the rices, it's solids density and terminal velocity was also greater than the rices. The rough rice particle volume and particle weight was greater than the milled rice,

but the solid density of the milled rice was greater than the rough rice. This indicated that the rough rice was porous, because the terminal velocity of the milled rice was also greater than the rough rice. These results compare well to the results of this project, because the increase in particle size increases the pressure losses along the straight sections.

Even though the authors examined in this section used several materials in their work, few compared the pressure losses between the materials, or even the differences between the particle properties of the materials. In view of this, the papers were not as beneficial to this author as they first appeared. However, some aspects of the papers were useful, confirming that the effect of particle characteristics on the pressure drop needed further research. For example, the differences in pressure losses or air velocity attributed to the particle sizes, were covered by Vogt and White[V1], Mendies et al[M1], Mehta et al [M1], Scott [S1] and Raheman and Jindal [R1], regardless of the fact that the acceleration length along the straights was either overlooked or not long enough, or very low solids loading ratios were used. The work by Richardson et al [R5] was useful because the results of his work using a very long length of instrumented straight section, showed that the pressure fluctuates as the air velocity increases and is not a straight line, but fitting a straight line through the data points is a satisfactory method of representing the gradient. The analysis on the results of the pressure gradients in this project, also displayed scattered data points, which were represented by plotting a straight line through the data, which may indicate why the measured and predicted pressure gradients showed good results.

A1.2.2 Particle properties - computer simulations

Modelling the behaviour of particles during pneumatic conveying has been undertaken by workers such as Tsuji [T1] (1993), and Govan et al [G1] (1990). Work using computer simulation to predict the particle motion in a pipeline, has shown that the amount of memory and processor power for such programs can be extensive. The two methods of numerical multiphase flow, are classified as Eulerian or Lagrangian, depending on how the particulate phase is modelled. The Eulerian method regards the particulate phase as a continuum, and the method is further divided into one fluid and two fluid models. The Lagrangian method computes the motion of individual particles, but as the number of particles increase, large memories and long computation time are needed. To avoid the demerits of the Lagrangian method, Tsuji [T1] applied the Direct Simulation Monte Carlo (DSMC) method to multi phase flow, which was developed in molecular dynamics. Trying to predict the interactions between particle to particle, particle to wall and particle to fluid, is a complicated process, and the calculations are discussed in his paper. The particle size, density, coefficients of restitution and friction, are used to predict the trajectories of a particle in a horizontal channel.

The particle shape was considered in the calculations, regarding the irregular bouncing of particles along the pipeline. The relationship between the particle velocities before and after collision with each other and the pipe walls, was attributed to the irregularity of the non-sphericity of particle shape. A calculation method was used for three dimensional collision of a non-spherical shape.

Govan et al [G1] (1990) describes the experimental measurements and numerical predictions of the motion of particles, 500-800μm in diameter, in a 20m long vertical tube. The experiments used three types of particles, in very lean phase. The numerical model was a Lagrangian simulation of the motion of each particle, that assumed because of the very lean phase, there were no particle to particle interactions, and that the particles had little affect on the air flow. They found discrepancies between the simulations and measurements, but attributed this to the non-idealities in the particle bounce behaviour.

The work on using a computer to predict the pressure losses, highlighted how difficult it is to measure all the variables that are involved in pneumatic conveying. The complicated process requires that very lean phase is used in the process, with spherical shapes, and still requires a vast amount of memory and processor power. These papers indicate the need for pilot scale test work to obtain the necessary variables for computer simulations, and that the technique is still a long way from being useable for design of industrial systems.

A1.2.3 Papers comparing different materials but investigating issues other than straight pipe pressure gradient

Werners [W5] (1983) work, looked at the effect that the particle size distribution has on dense phase conveying. He found that changing the particle size distribution, but keeping the average particle size of the solids constant, affected the friction factor and velocity ratio of the air-solid phase. He achieved this by conveying several different particle diameters of glass balls, all sharing the same density, in three small diameter sized pipelines, of 10, 20 and 30mm diameter. The initial tests used one sized particles, and for subsequent tests, fine and coarser particles were added at increasing percentages for each test, keeping the average particle size constant. He concluded that in horizontal conveying, a wide particle size distribution decreased the friction factor while increasing the velocity ratio. In vertical conveying, both parameters decreased.

Jones [J1] (1988) research investigated the effect of product properties on pneumatic conveying performance, using several different materials to achieve his objective. A high pressure blow tank was used as a feeder, in order to measure a high product throughput of each material. He used his

results and correlations to produce a phase diagram based on product properties that involved product/air interaction, which were classified into three groups. The first group were materials that are highly retentive of air which will convey in both lean and dense phase. The second group included those which are highly air-permeable, and are also likely to be conveyable in both lean and dense phase. The last group were materials in between, which would be likely to be limited to lean phase transport only. His phase diagram with the mass throughput correlation gives a method of predicting whether or not a material is likely to be conveyable in dense phase or not.

Bell [B2] (1990) discusses the importance of material characteristics when designing conveying systems, and reviews the most important characteristics. He says that particle size and shape combine with particle density to determine the minimum conveying velocity in dilute phase regimes. He points out that the size of particles are also important with relation to the inside pipe diameter of the conveying pipeline, i.e. that the conveying pipeline diameter should be at least three times the dimension of the maximum particle size. He lists a particle shape classification table which defines particle shapes below 1mm in size, as shape is a descriptive, rather than a measured term. His paper illustrates the effect that the characteristics of a material have on the pneumatic conveying regimes of either dense or dilute phase, and the effect the characteristics have on the system performance. Bell concludes that full scale testing remains the best method of determining the conveying criteria and observing flow patterns, and that internationally agreed standards are needed in classifying material characteristics to remove subjective characteristics.

Hitt [H2] (1994) used several materials to compare the air velocity required for low velocity pneumatic conveying. He commented on the difficulties encountered in measuring product characteristics, and the significant variation in the measured values obtained from using different techniques to measure the same variable, such as the coefficient of internal sliding friction. He concluded that particle size and cohesion are factors which determine the flow regime in dense phase pneumatic conveying. He also noted that the pressure gradient is dependent upon the product, but independent of pipe length to produce a given flow rate.

Williams [W4] (1983) equations are based on the established equation used to predict the pressure losses in single phase flow for air only. He represented the higher pressure drop during the conveying of solids by means of an equivalent length of pipe which would give the same pressure drop when handling air only. The equations for relating total equivalent length to mass flow rate of solids for any given pressure drop for dilute phase only, have a factor that varies for each type of material which changes with the material shape. However, the factor is the same for most powdered and granular material, because tests showed that materials with a good percentage of

fines or powders in relation to spheres, most often will act as powdered or granular materials. There was no guide as to how this factor may vary or how its value may be determined for any particular material, and no indication as to how many materials were tested.

The minimum conveying velocity was determined for several different materials, by Cabrejos and Klinzing [C1] (1992), in order to determine the pick-up and saltation mechanisms of solid particles. They tested a wide variety of materials to assess the effect of particle size, particle density, and particle shape on the pick-up mechanism. Only coarser particles >100μm were used in this paper, as they behaved differently from fine particles. This is because the behaviour of fine particles is more complicated due to their dominant cohesive forces and ability to get trapped inside the boundary layer of the pipe. All the test work was conducted using very low solids loading ratios, no greater than 6. The work of Cabrejos and Klinzing presented some simple correlations to determine pick-up and saltation velocities for coarse materials, but they concluded that further work was necessary to fully understand the effect that material characteristics and other variables have on the particle velocity, before a general correlation could be attempted.

In both their papers, Pan et al [P1, P2] (1994) looked at the boundaries between dilute phase, the unstable zone, and dense phase conveying of fine and granular materials. In granular materials, the unstable zone causes pressure fluctuations and vibrations in the pipeline, which are best avoided. Four different granular products (2 plastic pellets, wheat and duralina) and five fine products (4 coals and flyash) were used in pipelines ranging from 53 - 105 mm in diameter, and 96 - 556 m in length. From their work, they presented two correlations to calculate the boundaries between the phases, as well as a new model for the prediction of the pressure drop in dense phase conveying. There was no comparison shown between all the test materials in order to determine the relationship in behaviour between the different materials.

Raherman and Jindal [R2] (1994) studied the effect of the dispersed solids density in pneumatic conveying. The test work involved the use of three different materials, rough rice, milled rice and soybean for solids-to-air ratio of 0.7 to 3.5, in three pipe sizes, ranging from 54mm to 82mm inside diameter. The particle equivalent diameter of the soybean was twice that of the rice, although they did not specify how the particle equivalent diameter was calculated. They studied both horizontal and vertical conveying, using a sampling device that was manually slid into the conveying line during a steady state period to collect the solids. The solids were then weighed and the dispersed solids density was determined by dividing the weight of the sample by the volume of pipe section. The full test rig was not detailed in their paper, but due to the description of the simple mechanical sampling device, it could not have been a high pressure system. Their results

showed that the increase in particle size and possibly the shape of grains, along with the solids-to-air ratio, influenced the solids concentration in their pneumatic conveying. The solids concentration in the vertical section for the rough and milled rice, was almost twice that found in the horizontal section, while the soybean concentrations were the same for both pipe orientations. Based on the experimental results, generalized equations were developed for estimating dispersed solids density using step-wise multiple regression with the SPSSX software package, and found to be in good agreement when compared to the test data.

The work in the papers above, was mainly confined to looking at the characteristics of materials that are conveyed in dense phase. The particle size distribution, particle properties and the difficulties in measuring product characteristics were investigated in these papers. The prediction of boundaries between dense and lean phase, were also discussed in some papers, to identify the saltation mechanisms of solids relating to particle size. In addition, the suspension density of granular solids were examined in another paper. The work in these papers identifies the importance of finding relationships between particle properties of different materials, in all aspects of pneumatic conveying, and that graphs are the most appropriate way to represent these differences.

A1.2.4 Pressure profiles along a pipeline comprising of several bends and straights

Many researchers have come to the conclusion that the pressure losses in a pneumatic conveying system transporting solids and air, is usefully represented as the sum of the pressure losses due to the air and the pressure losses due to the solids [B1, A3, M7,R5,M1].

The method used by Bradley [B1] (1990) in his research into the prediction of pressure losses during pneumatic conveying, consisted of fitting parallel straight lines to averaged measured pressure values along two straight test sections that were fitted with pressure tappings. The pressure gradients were calculated from the parallel lines. The pressure gradients along both straights were taken to be identical, and the difference between the two parallel lines at the apex of the test bend, was measured and said to be the pressure drop caused by the bend. The total pressure loss was separated into two regions, the solids contribution to the total pressure loss, and the air contribution to the total pressure loss. This approach was adopted by several authors, some of whom are mentioned in this section.

As the solids travel along the pipeline, the velocity increases as a result of the pressure drop due to friction losses. If there is a measurable pressure drop across a bend, (Owen and Pankhurst [O1]) it is

not unreasonable to expect the pressure gradients to differ each side of the bend due to the change in air pressure and hence flow conditions. Such previous work demonstrated to this author that in order to obtain a more accurate picture of what actually happens to the pressure gradients along a system with bends as well as straights, pressure transducers should be installed along several sequential straight sections, as in the present project.

No other researcher has instrumented four consecutive straight lengths of pipeline to determine the pressure gradients along sequential straight sections and across three similar bends. Where other researchers have instrumented a pipeline with bends (Marcus, Hilbert and Klinzing [M3]) the pressure drop has been taken over the whole test section, with an allowance taken for the bends as a whole, rather than dealing with bends and straights separately. In their paper, Marcus et al paid particular attention to the acceleration zone immediately downstream of a bend and after a rotary valve fitting. They used three different bends and measured the pressure losses across the system to identify if the radius of a bend affects the degree of pressure losses. They concluded that the short radius bend, appeared to show the lowest pressure losses for fine powders.

The Engineering Equipment Users' Assoc. [E1] (1963) also recommended dividing the pipeline into sections starting at the delivery end first where the value of pressure is known, and working out the pressure drop in that section before moving on to the next section. This would give a new pressure value to begin the process again. This is a similar method to that used by Bradley [B1] except that Bradley recommended dividing the proposed design pipeline into components (i.e. bends and straights) rather than arbitrary sections.

Tsuji [T2] (1982) proposed a method for predicting the pressure drop in dilute phase systems. The results were limited to air velocities greater than 10 m/s with coarse particles >500μm. His design method is based on the equation of particle motion, which is based on Newtons second law of motion using force, mass and acceleration of particles, with some empirical constants. Values were taken from previous experiments consisting of vertical to horizontal pipe, with a bend in between, to determine the constants. He stated that the calculations could be performed by using an electronic hand calculator, but the equations are complicated with many unknown variables which would make this difficult to achieve.

The concept employed by Wirth and Molerus [W6] (1982) predicts the pressure drop during pneumatic conveying when the solids are conveyed with sliding particle strands. Their aim was to predict the pressure drop in steady state conveying, which they describe as uniform suspended flow with sliding strands. Several dimensionless groups were applied in the mathematical models

used to form a state diagram where the pressure loss predictions for sliding particle strands can be obtained. Due to the extremely high angular velocities of the particles due to wall collisions, the rotary motion of the particles was taken into account. Therefore, non dimensional presentation for suspended flow was derived in which a normalised pressure drop, was combined with a particle Froude number and a Froude number that contained the particle fall velocity and pipe diameter. The pressure drop prediction then used both the derived state diagrams for fully suspended flow and sliding particle strands to calculate the pressure drop. The results compared well with those carried out experimentally using wheat and polystyrene particles.

Pan and Wypych [P4] (1993) examined the pressure gradients along both horizontal and vertical straight sections for this paper. They stated that the pressure gradient along a straight section could not be constant, particularly over a long distance (as confirmed by Richardson et al's [R5] work) due to the increasing air velocity and decreasing pressure as the mixture moves along the pipeline. Most authors use a straight line through data points to determine the pressure gradient along straight sections, whereas they used empirically determined results from one test pipeline, to predict the pressure gradients along other test pipelines of varying lengths and diameters. The results showed good correlations. A comparison between the results of the pressure gradients was also made, which concluded that the ratio of 2 which is commonly used, is not sufficient, as the vertical to horizontal pressure drop is a function of pipe location, diameter, air and solids mass flow rates.

Saccani's [S2] (1996) test plant measured the pressure losses and solids velocity in a 75mm bore diameter pipeline. The test rig had two bends separated by a straight section of no more than 5 metres. Both bends had the same radius initially, and then the first bend was changed for a smaller radius bend. Sand was the only material conveyed for the test work. The pressure losses were measured along the straight sections using a number of static transducers. The solids velocity was measured using a pneumatic probe together with techniques based on laser and phase Doppler anemometry. Only four tests were carried out, and the test results were compared with those using a simulation program. However, from a graph showing the pressure losses versus pipeline distance, the complete pipeline is only ten metres in length, and believed to be too short to establish steady flow conditions.

The above work clearly established that different configurations of pipeline produce different total pipeline air pressure drops, e.g. Arnold, Wypych and Reed [A3] (1994). Prior to the current project, the method of design based on detailed pressure measurement results from one test bend and two

straights was the closest to a reliable method for gathering pressure drop data for the purposes of system design.

A1.2.5 Pressure losses - scaling from pilot plant to industrial plant

Keys and Chambers [K1] (1993) used results from their previous work to form a method to scale pneumatic conveying characteristics of a powder measured on a pilot scale, to that of a full scale system. Their method was restricted to scaling lean phase and 'moving bed' flows only, which was based on empirical correlations. They used their method and another concept based on Mills [M8] (1992) work, with input from Weber [W8] (1982) to compare the results. They found the method based on Mills ideas and others working in this area, did not work out when scaling more than 1.5 times the test pipe length. Their model calculated the pressure losses along a straight pipe in small lengths for a more accurate prediction, starting from the pipe outlet, so that several calculations are performed for one section. A simplified correlation accounted for bend losses, that included the experimentally determined pipe pressure loss, and an iterative method to calculate a bend loss coefficient.

The design of test rig used by Pan and Wypych [P5] (1992) consisted of two long and one short straight section of pipeline and two bends. They measured the pressure drop along the two straight sections of pipe and used the data in their equations to predict the pressure drop caused by bends and straight sections of pipe. From their results, the exponents in empirical formulae were determined, and they were then able to accurately predict the pressure drop in straight sections and bends, allowing for the influence of location and number of bends, as well as the influence of relatively short sections of straight pipeline. Measured data was used for the exponents of friction factor used in the equations, and can only be used for the material tested in the test rig. However, as their measurements covered two bends and one short straight section of 6.5m, no data was obtained to ensure that the effect of two bends close together did not affect the pressure prediction method used for a single bend.

A1.2.6 Re-acceleration length versus pipe straight length

Generally, the pressure drop increases remarkably in the downstream pipe immediately after a bend. This is because the particles which are decelerated in the bend due to the collision with the walls, are accelerated after the bend. This was also shown by Tsuji [T2] (1982).

Rose and Duckworth [R3] (1969) used four different materials conveyed in air, along a 32mm diameter pipeline, 9.75m long, to measure the pressure gradient along a horizontal pipe. Their objective was to determine the point at which the flow became fully established, so that the acceleration length could be established. Pressure tappings connected to manometers, were spaced at 1.2m intervals along the pipe. The test work was in very lean phase only, but the length of pipe required to accelerate particles was clear from the plotted results, and an equation was produced that predicted the acceleration of material before fully suspended flow is acquired. They showed no comparison of results between the materials, but stated that all the particles in the materials used were spherical and closely graded in size. As experimental work of others that used non-spherical shaped particles, were correlated and showed good agreement with their results, they considered that the particle shape was of minor importance.

The acceleration length after a bend is often excluded, e.g. Marcus, Hilbert and Klinzing [M3] (1985). The acceleration length of material after a feeder was predicted using the equation by Rose and Duckworth [R3] (1969). Marcus et al concluded that the pressure losses associated with the flow through bends and acceleration zones are significant, but did not measure them individually. Instead, they characterised the pressure loss across bends indirectly using the whole system rather than individual bend losses. They achieved this by only using one particular type of bend during each set of tests, and then changing the bends with another in the test programme. In that way, they associated the difference in the overall system loss as a consequence of the type of bend used.

Mendies et al [M2] (1973) found that the air velocity and solids loading ratio did not influence the acceleration length of the material, but took 4 to 5 metres regardless, which was in agreement with Rose and Duckworth [R3].

The conclusions drawn from the papers in these sections are as follows. The pressure losses along straight sections are often separated into the air and solid contributions to the total pressure losses [B1, A3, M7,R5,M1] and this seems to be useful. A suitable length of straight pipeline that takes account of the acceleration zone before any measurements are taken to determine the pressure gradient, is also recommended [R3,M2,M3,T2]. Separating the pipeline into sections to take account of the difference between the pressure gradient along the straights, and the pressure losses caused by the bends, appeared to be the most promising method of predicting system pressure losses [E1,B1].

A1.2.7 Bend pressure drop - methods of use

Morikawa et al [M6] (1978) carried out all their test work in very lean phase of solids loading ratios up to 8, at high air velocities. They used plastic pipes, with an 8m length of pipe downstream of the test bend, and conveyed polyethylene pellets. Measurements of bend pressure drop were taken from the inlet to the outlet of the bend, which would not have taken into account the re-acceleration pressure drop caused by the bend as shown by Rose and Duckworth [R3].

Ower and Pankhurst [O1] showed the importance of losses downstream of a bend and modelled the pressure loss at a bend with k factor.

Park and Zenz [P3] (1980) used 145μm median diameter glass beads and measured the pressure losses across three horizontal-to-vertical bends in their paper. In a 102mm bore pipeline, they fitted three pressure tappings at 1.5m intervals, upstream and downstream of the bends at very low solids loading ratios (up to 5). They measured the number of velocity heads lost due to gas friction, without solids in the line, and used the results in their equations. In that way, the step loss caused by each bend was determined, which were described as a coefficient times the dynamic pressure of the air flow (for the 'air only' loss) plus a coefficient times the dynamic pressure of the flowing suspension. The downstream effect of the bend was accounted for by fitting the pressure tappings, 6 m downstream of the bend. Their results cannot be compared to the work carried out on glass beads for this project, because the straight section after the bend in this paper, is in a vertical orientation.

Marcus, Hilbert and Klinzing [M3] (1985) used a test rig with a number of bends, four horizontal to horizontal, and two that were horizontal to vertical and vertical to horizontal. The measurements were taken using a 188m recirculating test loop, with pressure measurements taken just downstream of the fluids-solids pump that fed the system. They obtained their results by measuring the pressure across the system with and without a bend. Using their results, they found that a linear relationship existed between the pressure drop caused by a bend and the mass flow rate ratio.

Westman, Michaelides and Thomson [W7] (1987) used four different materials to measure the pressure losses caused by different bends, all having the same median sized particles, but of varying particle density, and three sharing a similar shape. All the results are shown together so any differences between the materials are not displayed. They used a 102mm diameter pipe with 6.4m lengths either side of a test bend in a horizontal configuration. They claimed that the length

of pipe downstream of the bend was long enough for fully accelerated flow to be reached, but a longer distance would have ensured the required flow conditions. All the tests were for low solids ratios. To measure and store their results, they used a similar system to Bradley [B1] but their transducers scanned once every ten seconds, for ten times. The data was then averaged and processed. They found that the long radius bends resulted in lower pressure losses when compared to the other bends in the test programme.

Michaelides and Lai [M7] (1987) conveyed five materials in a test rig consisting of two 9m horizontal straights, and a 180° bend in between. The straights had a length of 9m upstream and downstream of the bend, and instrumented with pressure transducers. The bend pressure drop was measured from the inlet of the bend, to the outlet of the bend, but the graphs from which they showed the pressure loss across the bends were ambiguous. They measured the pressure profile along the straights by fitting a least square fit method through the transducer data points, but omitting the acceleration and recovery regions which they found to be around 3m downstream of the bends. The bend losses were represented as a coefficient times the dynamic pressure of the air flow, which was then separated into air and solids parts. Comparing their results with others, they concluded that doubling the pressure loss for one 90° bend over-predicts the pressure loss for a 180° bend. No comparisons between the different materials were shown in their work.

Bradley's [B1] (1990) test rig was the same test rig used for this project, before any modifications were carried out. Bradley developed a measurement method which determined the pressure drop across a bend from the gradients in the straight pipes either side, as opposed to Morikawa et al [M6] (1992) who measured pressure at the inlet and outlet of the test bend, and consequently missed the downstream effect of the bend.

Bonnin and Bouard [B5] (1990) measured the pressure drop using pressure tappings along a horizontal and vertical straight pipe, with a test bend in between. They tested four bends in order to compare the generated pressure losses, in an 80mm internal diameter pipeline, 36m in total length, with a 6m vertical section. The materials used during the tests were Portland cement and glass beads, using solids loading ratios up to 15. Static pressure tappings suffered from blockages occurring during test runs, therefore the measurements may not all be accurate. They concluded that results carried out in experimental facilities cannot be appropriate for industrial plants.

Levy and Mason [L1] (1998) used a three dimensional simulation of gas-particle flow in a pipe system, consisting of three horizontal straight sections and two bends, to carry out a numerical investigation into the effect that a bend radius has on the particles as they leave a bend. The

equations used were based on the Inter-Phase Slip Algorithm (IPSA). There were two materials of different particle sizes used in the calculations, polyethylene pellets and pulverised coal. The results showed that as the bend radius increases, the cross sectional particle concentrations were different, and the paths the particles followed varied, depending on the particle sizes. The numerical simulations predicted that the rope region increased in size as the pipe radius increased. Only two straights and one bend were used in the equations, and no experimental results were taken to compare with the numerical study.

Many researchers have used two straight sections separated by one bend, to measure the pressure losses caused by the bend [L1,B1,M7]. Lean phase was used for the measurements [M6,P3,M3,W7] in several papers. Some of the straight sections were in a horizontal to vertical orientation [B5,P3,M3], but most used both horizontal straight sections. The methods used for measuring the pressure losses varied, i.e. from the inlet to the outlet of the bend, and from across the entire test section and comparing any differences by changing the bend and repeating the test. However, the most logical method took account of the acceleration zone downstream of the bend, before any values were determined [B1,R3,P3].

A1.2.8 Papers looking at pressure losses in systems

The design of pneumatic conveying systems was discussed by Soo [S3] (1980). The paper examined the individual factors that must be taken into account when predicting the pressure losses in a conveying system, such as the mode of flow, the friction factor, minimum conveying velocity, bends losses etc. The paper also looks at the electrostatic effects, erosion and attrition of particles of material during conveying, plus the work of others and subsequent equations developed. It is a general paper that tries to look at all aspects involved when designing a system in a cost effective way, and concludes that the most economical one is likely to be a dense phase system.

Alberti et al [A2] (1991) also looked at system design in their work, describing guidelines for a pilot plant centre and integrated computer aided system that they were using. They described their guidelines in stages. The first design stage involved obtaining information about the product to be conveyed. The second stage sizes the conveying equipment based on the required performance. The final stage includes a drawing of the proposed conveying system design using CAD. The aim of the pilot plant is to continuously increase the database that stores details of the optimum conditions for handling various products, which can then be used for new types of conveying or plant improvements and subsequently tested in the pilot plant. This paper sounds like an advertisement for their test centre, and does not offer anything new.

Wypych [W3] (1999) suggested that the problems with pneumatic conveying systems are often due to a lack of appreciation and understanding of the relevant fundamentals. His paper examines some of the main issues often overlooked in the design stage, and in the analysis when problems occur. For example, predicting the total pipeline pressure drop, requires measuring particle characteristics, some of which cannot always be defined or characterised properly. Pilot plant testing is recommended for those materials. The determination of the minimum conveying velocity for the material to be conveyed, is important if the product is to be conveyed in a specific phase, or to minimize degradation, pipe wear and power consumption. Correlations from a number of authors were used by Wypych to determine the minimum conveying velocity, but he found a wide scatter of data when comparing the results. Several reasons were put forward, e.g. the definition of the minimum transport conditions was different for some researchers, some models showed good agreement for particular applications only, limitations in the range of products and pipe diameters by authors, and the test rig and configuration used by researchers could affect the accuracy of results. In his paper, Wypych also used case studies as examples of industrial problems and the solutions and results.

A1.3 Papers related to test rig design

A1.3.1 Volumetric feeder

A major modification to the test rig involved the installation of a volumetric feeder. Workers such as Selves [S4] (1995), Burnett [B4] (1996) and Wypch [W2] (1990) had all used screw conveyors in their pneumatic conveying rigs to control the feed rate of material into the conveying line. Wypch used a screw feeder for accurate metering of coal from a blow tank into the conveying pipeline, which was suitable for both fine and coarse materials. He used a variable speed drive attached to the screw to control and vary the feed rate of the material into the conveying line, and showed that it was an effective method.

Bates [B3] (1986) designed the screw used in the volumetric feeder, which was confirmed by others such as Roberts [R4] (1996) and G. Haaker et al [H1] (1994) in their specifications for an effective screw design. A design methodology used by Roberts [R4], determines the pitch, screw diameter and shaft diameter to meet specified draw-down objectives, for volumetric efficiency. The specification for an effective screw design is important because it determines the mode of flow of material as it leaves the end of the screw, and consequently dictates the flow pattern generated in the hopper above the screw. By gradually changing the screw geometry, uneven withdrawal of material from the hopper, segregation of the particles, and deterioration of the material in stagnant

zones, can be prevented. The design of the screw used for this project, incorporated the recommendations found in these papers.

A1.3.2 Drop out box

As the solids leave the end of the screw feeder, the material enters the conveying line which is injected with air at a pressure high enough to move the material along the pipeline. The conveying pipeline was positioned below the screw conveyor to enable the material to fall under gravity into the conveying line. The connecting section between the screw conveyor and the conveying line is known as a drop out box. Kessel [K2] (1986) looked at the initial mixing of the air and solids in a chamber formed by a drop out box, which was based on the relationship between a rotary valve and conveying line. He concluded that for the maximum entrainment efficiency of 90% solids to air, the position of the conveying line should be at least two conveying pipe diameters in depth from the bottom of the rotary valve. Based on his calculation, the drop out box was designed as shown in section A2.4.5.

Appendix 2

Numerical comparison with the data of other authors

A2.1 Introduction

This section compares the methods applied to characterise the straight pipe pressure gradient, using the coefficients developed in the modelling process. Little previous work had been carried out into the measured pressure losses between materials of different particle size, shape or density, so that comparisons between the work in this thesis and other authors were limited. However, to enable a direct comparison on a numerical basis, the results and correlations of the work contained in this thesis were compared to the work contained in two separate papers. The first is the work of Keys and Chambers, the second is the work of Molerus.

A2.2 Comparison of results

A2.2.1 Results of the work by Keys and Chambers

Keys and Chambers [K1] (1993) used results from their previous work to form a method to scale pneumatic conveying characteristics of a powder measured on a pilot scale, to that of a full scale system. Their method was restricted to scaling lean phase and 'moving bed' flows only, which was based on empirical correlations. They used their method and another concept based on Mills [M8] (1992) work, with input from Weber [W8] (1982) to compare the results. Their model calculated the pressure losses along a straight pipe in small lengths for a more accurate prediction, starting from the pipe outlet, so that several calculations are performed for one section. The equations used for comparison from their paper, were for lean phase conveying only.

A2.2.1.1 The concept of solids and air contributions to total pressure gradient

The complex interaction involving the two phases along a pipeline are often represented as a model displayed below,

$$\left(\frac{dp}{dl}\right)_{total} = \left(\frac{dp}{dl}\right)_{air} + \left(\frac{dp}{dl}\right)_{solids}$$

where $\left(\frac{dp}{dl}\right)_{total}$ = pressure gradient observed in pipe.

$\left(\frac{dp}{dl}\right)_{air}$ = pressure gradient when solids are absent, predicted using conventional means e.g. an equation similar to the Darcy or Fanning equation, or an equation produced by tests using air only along the pipeline.

$\left(\frac{dp}{dl}\right)_{solids}$ = Additional pressure gradient, in principle caused by the addition of the solid particles to the air.

Note: The results from the test work in this thesis is presented in units of mbar per metre.

The model is purely a concept used as a convenient means of thinking about why the pressure drop increases when solids are introduced, and storing the data.

The pressure losses along straight pipelines due to the 'solids contribution' are commonly used in data analysis because it is considered that the 'air only' pressure contribution to the total pressure losses are small in comparison. Under certain conditions, i.e. very low suspension densities and high air velocities, and in pipes of small size, the air only contribution can become larger and more significant.

As the data for each test material in this thesis was analysed, and its database completed, the data points from which the coefficient (k) for each material was determined, was plotted on a graph together with data from the other test materials. Graph A2.1 is an example of such a graph, and shows the differences between the materials in terms of the values of k in,

$$\frac{dp}{dl}_{solids} = k\rho_s\left(c_{air}\right)^2 \qquad [1]$$

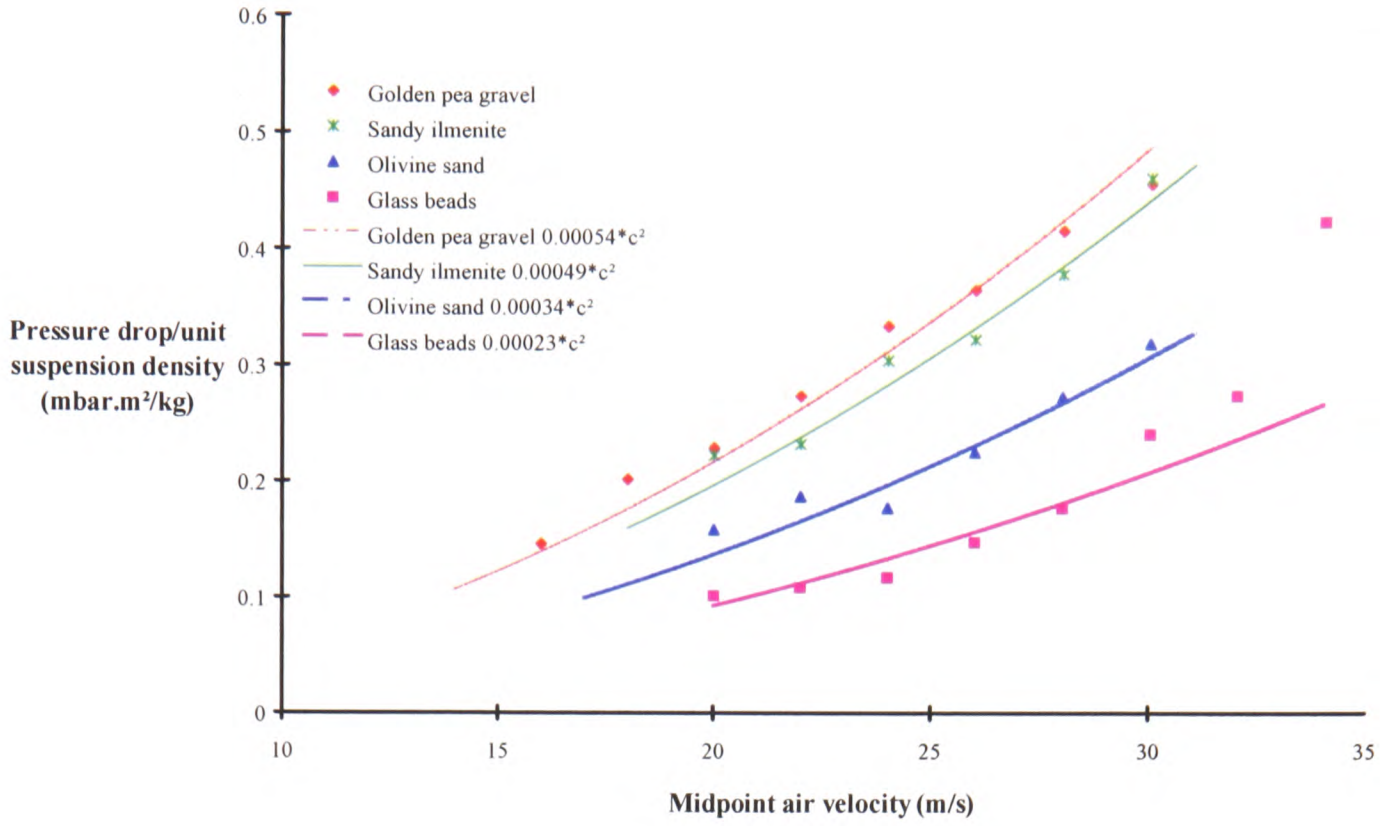

Graph A2.1: Plot of pressure drop per unit suspension density against midpoint air velocity, for four of the ten test materials.

Data from the work of Keys and Chambers [K1], and Weber [W8, W9] in terms of an air alone friction loss λ_f and a particle friction loss $m^*\lambda_s$, in the pipe loss term, where:

(Keys and Chambers [K1]) Pipe loss, $P_L = \rho_a V^2 L(\lambda_f + m^* \lambda_s)2D$ [2]

ρ_a = density of air

V = air velocity

L = pipe length

D = pipe diameter

m* = mass flow ratio

(Weber [W8]) $\lambda_f = 1.325/[\mathrm{Ln}\{\varepsilon/3.7D\}+5.74/\mathrm{Re}^{0.9}\}]^2$

N.B. $\varepsilon = 0.045$ for commercial steel

(Weber [W9]) $\lambda_s = 2.1F_s^{0.25}(D/d_i)^{0.1}/(m^{*0.3}F)$

when $d_i < 0.5$mm

d_i = particle mean diameter

F = Froude number

F_s = Particle Froude number

(Weber [W9]) or $\lambda_s = 0.082F_s^{0.25}(D/d_i)^{0.1}/(m^{*0.3}F^{0.86})$

when $d_i > 0.5mm$

Inputs to above λ_s are:

(Weber [W8])

$$F = V^2/gD$$

$$F_s = W^2/gd_i$$

W = Solids settling velocity based on d_i and ρ_b

$$W = [4gd_i(\rho_b-\rho_a)/(3C_d\rho_a)]^{0.5}$$

ρ_b = bulk density of solid

C_d = coefficient of drag

<u>Assuming particle sphericity:</u>

$C_d = (24/Re_{di})(1+3Re_{di}/16)$ for $Re_{di} < 1.0$

$C_d = 0.4 + 26/(Re_{di})^{0.8}$ for $1.0 < Re_{di} < 1000$

$C_d = 0.4$ for $Re_{di} > 1000$

Now, considering the total pressure drop and the relationship with the conveying air velocity:

$$P_\rho = \rho_a V^2 L(\lambda_f + m^*\lambda_s)2D$$

The coefficients arrived at in this thesis by the foregoing measurement and graphical methods can now be checked against the theoretical relationships which have been defined; as follows:-

Pressure drop per metre/suspension density (ρ_{susp}) = coefficient . midpoint air velocity^2

- from [1]

Pressure drop per metre = P_L / L - from [2]

Suspension density = $\rho_{susp} = \dfrac{\dot{m}_s}{\dot{V}_a}$

As mass flow rate ratio, m* is defined as: $m^* = \dfrac{\dot{m}_s}{\dot{m}_a} = \dfrac{\rho_s \dot{V}_s}{\rho_a \dot{V}_a}$

Then: $m^* = \dfrac{\dot{m}_s}{\rho_a \dot{V}_a}$

Therefore: $\rho_{susp} = m^* \rho_a$

i.e. $(P_L/L)/(\rho_{susp}) = \text{coefficient} \cdot V^2$

where P_L is from ref W8,W9 & K1, and the coefficient is from the work in this thesis.

Therefore, for a known material the coefficient can be estimated by the following, if all the properties are known:

$$P_L = \frac{\rho_a V^2 L}{2D}\left(\lambda_f + m^* \lambda_s\right) \qquad [3]$$

As the pressure gradient used in the graphical methods are for the solids contribution to the pressure losses only, the air friction term was omitted from the pressure loss equation, to give:

$$P_{solids} = \frac{\rho_a V^2 L}{2D}\left(m^* \lambda_s\right)$$

Comparing to the coefficient (k) determined empirically from the data, where the pressure gradient was measure in mbar/m,

$$\frac{dp}{dl}_{solids} = k\rho_s\left(c_{air}\right)^2 \quad \Rightarrow \quad \frac{dp}{dl}_{solids} \cdot \frac{1}{\rho_s\left(c_{air}\right)^2} = k \qquad [4]$$

Where $\left(c_{air}\right)^2 = V^2$ in [2] and [3]

The equivalent coefficient can be obtained from:

$$P_{solids} = \frac{\rho_a V^2 L}{2D}\left(m^* \lambda_s\right) \Rightarrow \quad \frac{P_{solids}}{L} \cdot \frac{1}{\rho_a m^* V^2} = \frac{\lambda_s}{2D} \qquad [5]$$

As both the left hand terms in [4] and [5] are the same, the right hand terms in both equations must also be the same.

Therefore, the coefficient for the solids contribution to the total pressure losses, determined from the modelling is,

$$\text{Coefficient} = \frac{\lambda_s}{2D}$$

A2.2.1.2 Comparison of measured and modelled coefficient

The value of the coefficient for the various materials determined by empirical means and by modelling from refs K1,W8 & W9, are shown on table A2.1. To compare the value of the modelling coefficient to the coefficient determined from the test results, data from each test material database was selected. In order for the comparison to be made for each material, the conveying conditions were as similar to each as possible. The mass flow rate ratio for all the materials were between 14.5 and 15.9. The inlet air velocities ranged from 13.6 to 16.5 m/s^2.

Material	Coefficient value	
	Empirical	Modelling
Silica flour	0.00016	0.00111
Ground ilmenite	0.00038	0.00179
Icing sugar	0.00041	0.000956
Sandy ilmenite	0.00049	0.00121
Olivine sand	0.00034	0.00102
Granulated sugar	0.00049	0.000092
Glass beads	0.00023	0.000072
Polyethylene pellets	0.00026	0.000101
Golden pea gravel	0.00054	0.000086
Boral lytag	0.00041	0.000068

Table A2.1: Results of empirical and modelling values for each test material.

Comparing the graphically determined and modelling values of the multiplying coefficient does not indicate a reliable correlation. However, the materials used in the original test work in

references K1,W8 and W9, on which the modelling equations were based, used fly ash of various sizes and did not venture into the realms of extending the model to other materials.

In addition, the comparison of the results shown on table 1, show that the coefficient from the model of refs K1,W8 and W9, used in the modelling, display a reverse trend for the particle sizes. That is, the true coefficient is greatly over predicted for the smaller particles, and under predicted for the larger particles.

It was also found that the model predicted that the coefficient would change with conveying conditions, so to explore this it was necessary to plot some graphs showing the model coefficient against air velocity. Three of the graphs (A2.2, A2.3 and A2.4) are shown, for the silica based materials, which vary from each other by their median particle size. It can be seen when comparing the power law curve drawn through the sets of data, that they do not follow a pattern relating to their particle size.

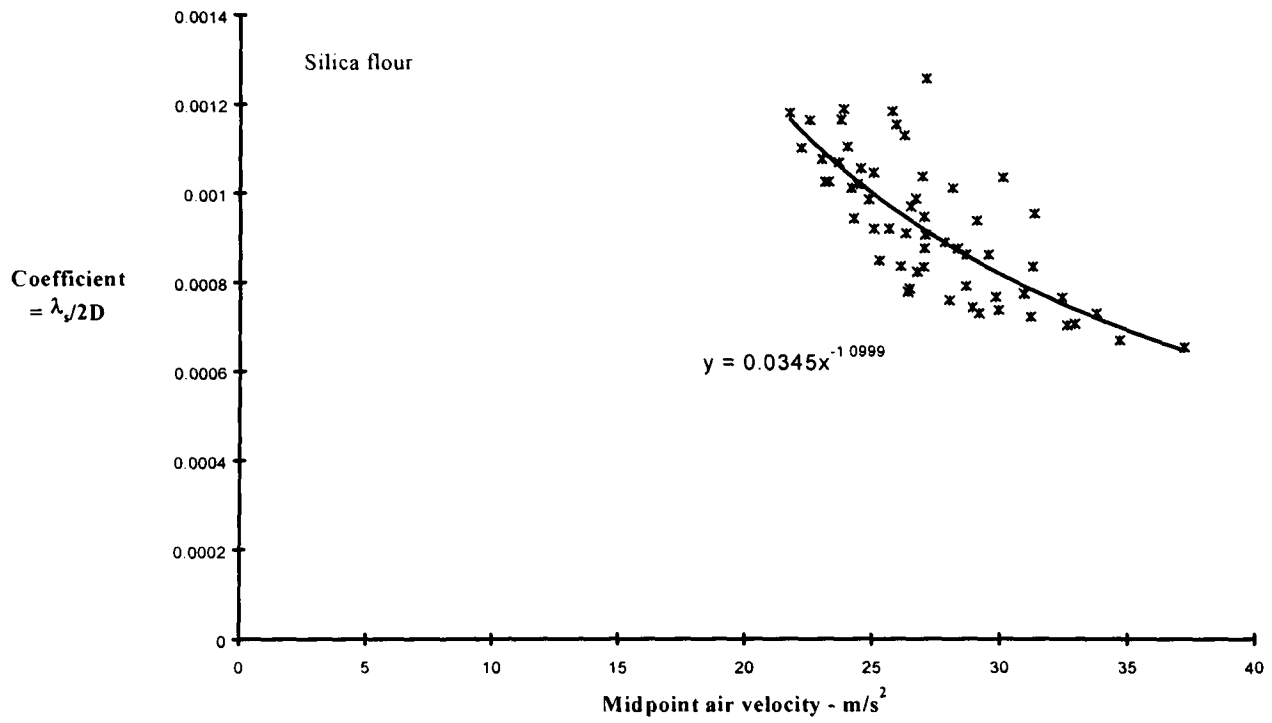

Graph A2.2: Modelling coefficient using test data conveying conditions for the silica flour, versus midpoint air velocity. Measured coefficient value = 0.00016.

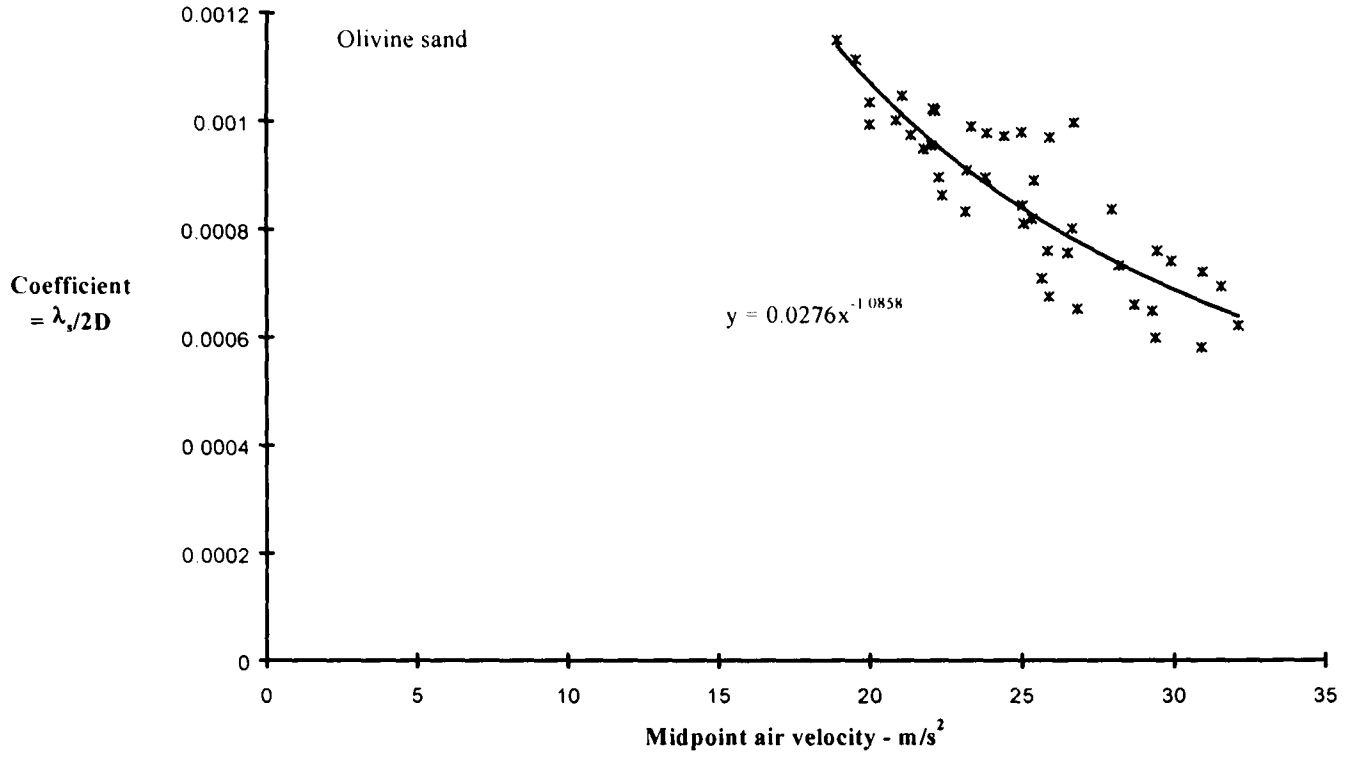

Graph A2.3: Modelling coefficient using test data conveying conditions for olivine sand, versus midpoint air velocity. Measured coefficient value = 0.00034.

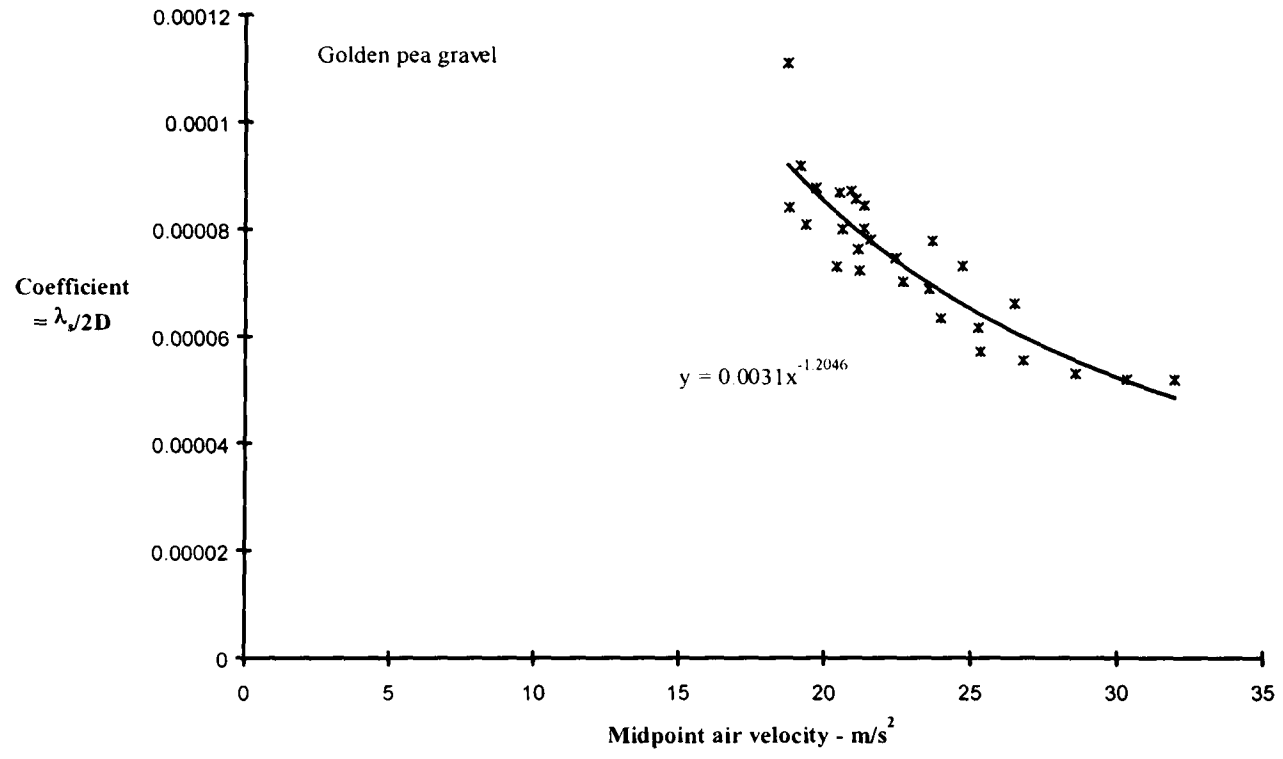

Graph A2.4: Modelling coefficient using test data conveying conditions for the golden pea gravel, versus midpoint air velocity. Measured coefficient value = 0.00054.

As shown in graphs A2.2, A2.3 and A2.4, the modelling indicates that a different coefficient should be used as the air velocity changes, whereas from the analysis on the empirically determined data for each material, the conveying conditions for each material were reduced to a single coefficient over the wide range of conditions tested.

A2.2.1.3 Summary of comparison with Weber, Keys and Chambers

The coefficient values determined from the measurements of the flows of the ten materials have been compared with a widely-quoted model of Keys and Chambers [K1] based on Weber [W8 & W9] and Streeter and Wylie [S6], and it is apparent that they deviate by as much as one order of magnitude in either direction. This is believed to be due principally because the model of Keys and Chambers, and Weber was constructed using data from only one material.

A2.3 Comparison of the pressure gradients using the results by Molerus

A paper by Molerus [M10] looked at the pneumatic transport of coarse grained particles in horizontal pipes. The paper looked at the slip velocity between the particles and the conveying fluid, for the fully suspended and strand flow types of conveying. Equations were developed for both types of flow, that separated the total pressure gradients into the pressure gradients caused by the particles and the pressure gradients relating to the fluid. The equation developed for the particle pressure losses in a fully suspended type of flow, is shown as follows:-

$$\frac{\Delta P_p / \Delta L}{\rho_s g} x \frac{v_f - v_f^*}{v_s} = \lambda_p \frac{(v_f - v_f^*)\sqrt{\rho_s / \rho_f v_f}}{Dg} \qquad [6]$$

where λ_p = impact factor

v_f = superficial fluid velocity

v_f^* = plugging limit velocity

v_s = superficial solid material velocity

ρ_s = density of solids particle

ρ_f = density of fluid

Rearranging for the particle part of the pressure gradient, $\frac{\Delta P_p}{\Delta L}$

$$\frac{\Delta P_p}{\Delta L} = \frac{\lambda_p (v_f - v_f*)\sqrt{\frac{\rho_s}{\rho_f v_f}}}{Dg} \frac{v_s}{v_f - v_f*} \rho_s g \qquad [7]$$

the pressure gradient can be predicted and compared to the results using equation [1]. The data used in the pressure gradient prediction methods, was obtained from the empirical test data using two of the test materials from test program. Two of the materials used in the Molerus test work, were glass beads and angular quartz sand particles. This enabled a comparison against the test work in this thesis using the glass beads and olivine sand data.

The value of the superficial solid material velocity, does not differ to a great extent from the superficial fluids velocity for fully suspended flows such as is studied in this thesis, as found by Woodhead [W10]. Therefore, $v_f = v_s$ is taken in the comparison calculations.

The value for the plugging limit velocity of 14 m/s for the glass beads, and 12.5 m/s for the olivine sand, was taken from observed and measured values, during the assessment process of the limitation of the conveying conditions that was performed on each test material.

The values for the pressure gradients using equations [1] and [7], were determined and the results plotted on graphs A2.5 and A2.6.

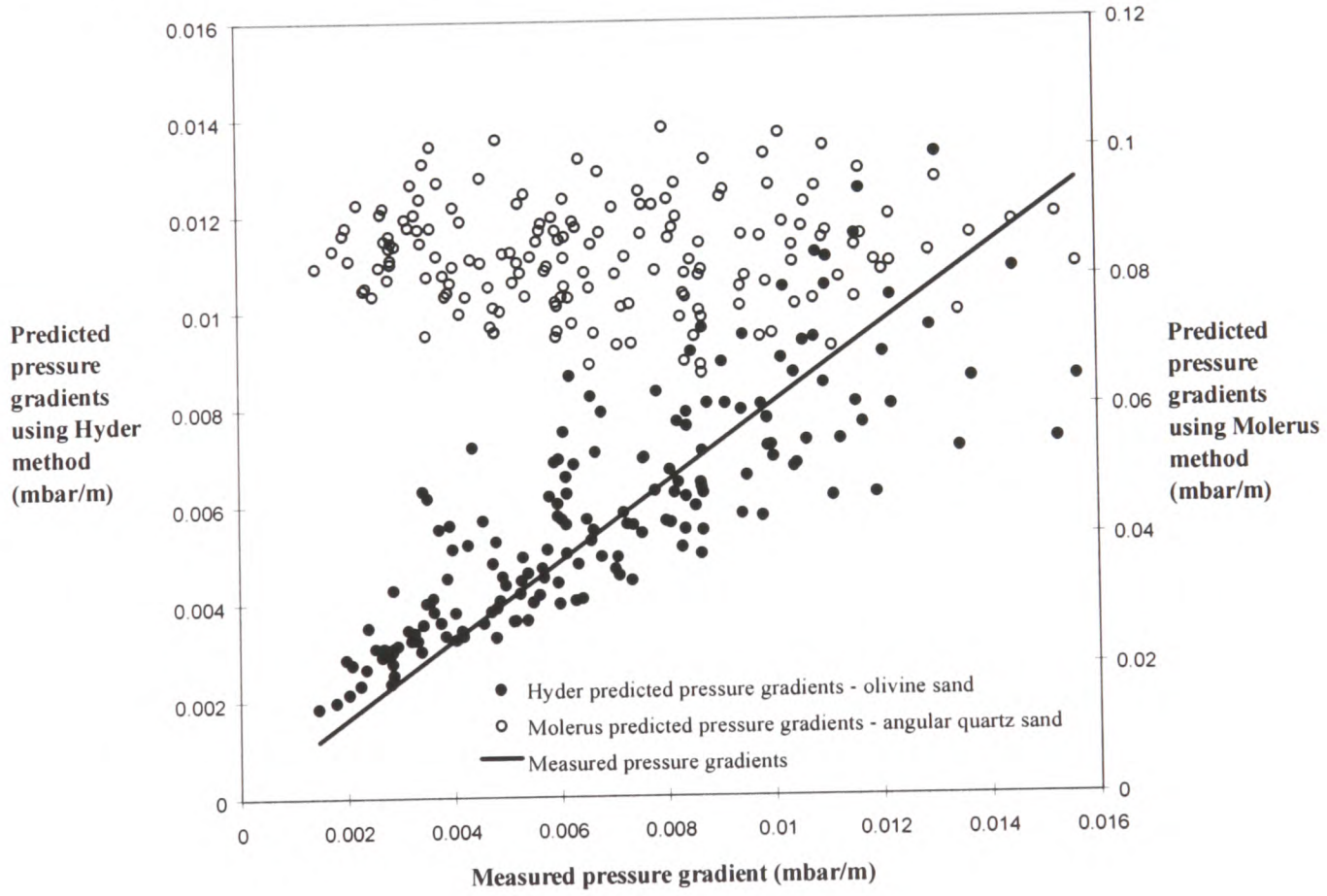

Graph A2.5: The predicted pressure gradients using the empirical test data in Molerus and Hyder equations, to compare the results with the measured pressure gradients using olivine sand. Note the scale is different for the Molerus results.

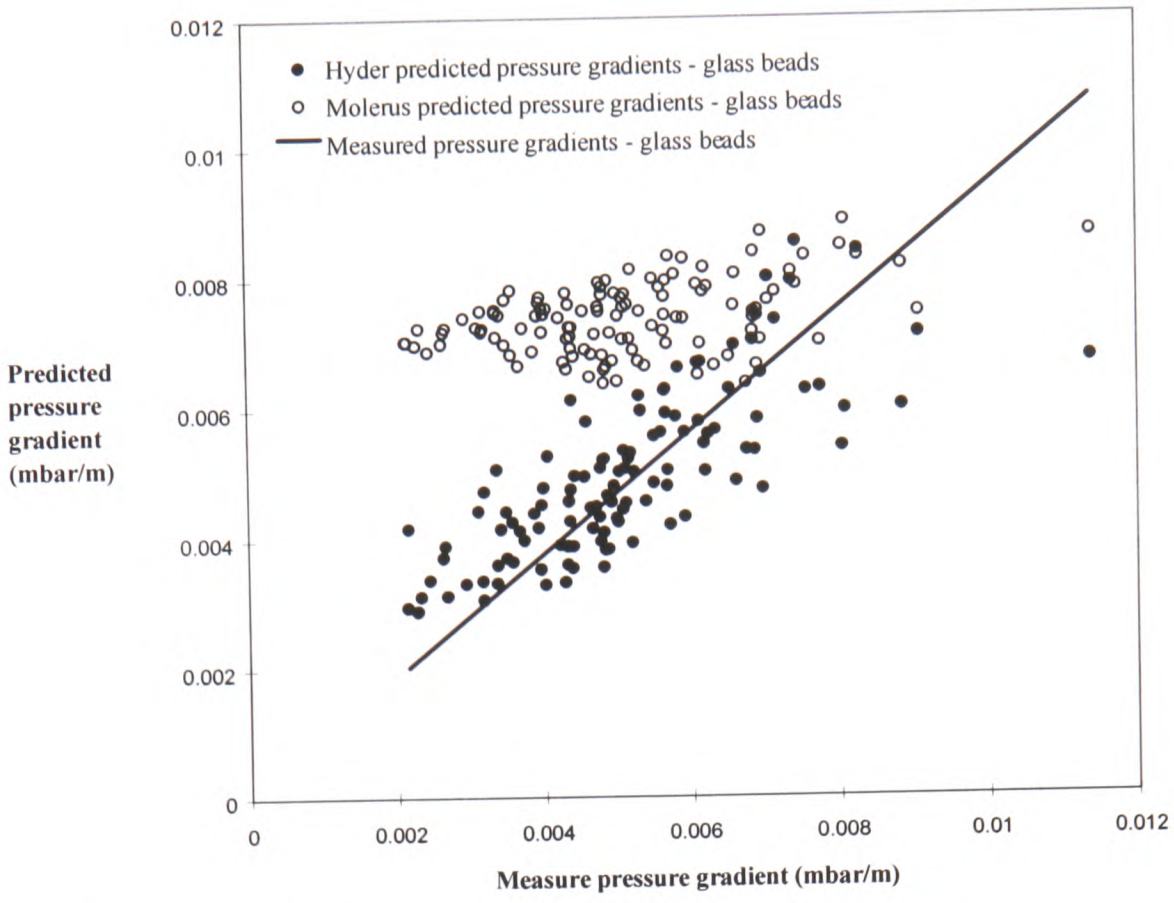

Graph A2.6: The predicted pressure gradients using the empirical test data in Molerus and Hyder equations, to compare the results with the measured pressure gradients using glass beads.

The conveying conditions for the test data are shown below. These values were taken from the analysis of the test materials in this thesis.

Material	**Inlet air velocity at start of test loop**		**Min. suspension density**	**Max. suspension density**
	m/s		kg/m^3	kg/m^3
	Min.	Max.		
Olivine sand	12	23	7	85
Glass beads	14	22	17	67

A2.3.1 Discussion on the comparison between Molerus and the results from this thesis

The particle size of the materials in the Molerus paper, were 1mm for the angular quartz particles and 0.7 mm for the spherical glass beads. The paper does not indicate how the particles sizes were determined, but that the materials had a similar particle density and hardness, with distinctly different shapes. Graphs A2.5 and A2.6, show that the glass bead predictions are of similar orders to the predictions and measurements in this thesis, whereas the

olivine sand and quartz pressure gradients are not of the same order. The Molerus method over predicts the pressure gradients determined from the quartz sand results.

The glass beads used in this thesis had a median particle diameter of 660μm, which compares well with the glass beads used by Molerus of 700μm. Therefore, the impact factor determined by Molerus for glass beads should be appropriate for use in his equation, when using the test data determined from the work in this thesis.

The angular quartz sand particles had a diameter of 1mm, while the olivine sand had a median particle diameter of 320μm. The difference in size and the fact that the olivine sand has more of a rounded shape, may account for the fact that the comparison between these material results were not as close as those of the glass beads.

The Molerus equation [6] does not take account of the mass flow rate of solids when predicting the pressure gradient during pneumatic conveying. Therefore, the results shown on graphs A2.5 and A2.6 do not account for the change in the suspension density when conveying, or the difference in the range of conveying conditions for any material. The value determined for the impact factor allows for the solids mass flow rate, but the impact value is constant as stated in the following equation from the same paper:-

$$\frac{\pi}{4}\frac{\left(\Delta P_P / \Delta L\right)D^3}{\sqrt{\rho_s / \rho_f}\,\dot{M}_s v_f} = \lambda_P = const.$$

The constant impact factor value used in equation [6] explains why the Molerus results do not alter very much across the range of suspension density (or solids flow rate), when compared to the measured pressure gradients taken from the test data in this thesis. This appears to be a fundamental deficiency with the equation of Molerus

A2.3.2 Conclusion of Molerus equation

The work of Molerus acknowledges that the particle material and particle shape influence the particle velocity, and thereby the pressure gradient for fully suspended types of flow. Therefore, an impact factor determined from experimental data is used in his equation to determine the pressure gradient for fully suspended types of flow. There is no differentiation to take account of the particle size of materials, but the particle diameter of 0.7mm for the glass

beads and 1 mm diameter for quartz sand particles are fairly close. This may indicate why the difference in particle size is not accounted for in the Molerus equations.

The wide range between the impact factor of the two materials, would explain why the quartz sand results over predict the pressure gradients by a factor of ten, while the glass beads are of the same order. However, the issue of variation in solids flow rate during pneumatic conveying in fully suspended types of flow, have not been addressed in the Molerus equation, which does not make the equation useable for designing pneumatic conveying systems over a wide range of conveying conditions.

A2.4 Overall conclusion of numerical comparisons

Keys and Chambers paper included equations by Weber for predicting the pressure losses for solids only, and were based on data obtained from the test work and analysis using one material of varying particle densities over a very limited range. The results of the numerical comparison using the equation derived from the work in this thesis, does not correlate well with the equations used in the Keys and Chambers paper. The coefficient determined from their equation, varies with the changing air velocity, whereas the coefficient determined for each material in this thesis, is constant for the range of air velocities as stated in this thesis.

The equations used in the Molerus paper is independent of the solids flow rate, which clearly is not indicative of the conveying conditions that are used in industrial pneumatic conveying systems. Therefore, a comparison between the equation derived in this thesis, which is based on the test work covering an extensive range of solids mass flow rates, cannot be compared to Molerus equation which clearly does not take account of the variable conveying conditions used in industry.

Appendix 3

Test rig development

A3.1 Introduction

An existing test rig was available which had been used for previous research. It was considered that this was reasonably suitable for this project. However, some modifications were needed to adapt the rig to the requirements of this project. This chapter explains the pre-existing test rig alterations to the test rig and the additional pieces of equipment.

A3.2 Test rig requirements

A3.2.1 Fundamental requirements

Some work had been carried out but not in a systematic way, comparing the differences caused by particle properties during pneumatic conveying. Mainwaring [M4], looked at the effect of particle properties on the slugging behaviour in dense phase conveying, while Jones[J1] also looked at material characteristics effects on the minimum conveying velocities. The main objective of this research project was to assess how particle properties affect the pressure drop. In order to achieve this objective through a structured approach, several materials were carefully selected for the research project. Initially, the decision was to test at least six materials for comparison purposes, which would mean considerable test work, and as a result, a considerable accumulation of data. Consequently, the test data should be as reliable and repeatable as possible to reduce the number of test runs necessary to cover the full range of conveying conditions. Work of other authors [D1], had shown that it can be difficult to obtain repeatable and reliable results for the pressure measurements in pneumatic conveying, due to fluctuating pressures. Therefore, those issues would need to be addressed.

A3.2.2 Arrangement needed

The most relevant research to date had concentrated on measuring the pressure loss caused by a bend and in adjacent straight sections, by fitting pressure transducers along two straight lengths of a conveying line with a bend in between [B1]. By measuring the pressure profiles along the straight sections, the pressure loss caused by the bend was determined. This seemed an effective method of measuring the pressure losses along a pipeline, providing the pressure transducers were situated

at regular intervals over a reasonably long length of straight pipeline, to ensure the pressure gradient had recovered from the effect of the bend. It was thought that for the purposes of this project, equipping additional straight sections with pressure transducers would produce further data points from each test tun, as the conveying conditions change with reducing air pressure as the material moves along a pipeline. This would serve several purposes;

- it would reduce the number of test runs required to obtain a full data set for each material,
- it would give a clear picture of the pressure changes along a pipeline with several bends, and
- it would give an opportunity to interchange the test bends, to see whether the nominally identical bends would give indistinguishable pressure losses when operating under the same conveying conditions.

Pressure readings should be taken for the widest range of conveying conditions possible if the conveying characteristics of the materials were to be measured fully. The full range of conveying conditions range from the lowest air velocities possible to convey the product, to the highest air velocities and mass flow rates of solids that were possible using the test rig equipment. Some of the materials chosen for the test work were known by experience to be incapable of being conveyed in dense phase. However, all the materials were capable of lean phase conveying, and as the purpose of the test program was to compare the results of tests carried out under similar conveying conditions, the fact that some materials could not be conveyed in dense phase was not perceived as a problem.

The test rig arrangement preferred for use with this project, would allow pressure transducers to be fitted along four consecutive straight sections of pipeline which would enable the pressure drop across three test bends and four straights to be measured.

Instrumenting four straight sections of pipeline would involve a substantial number of pressure transducers. There were 12 transducers already fitted along two of the horizontal pipelines separated by a 90° test bend, thus an additional 12 transducers were obtained to be installed along the two remaining consecutive horizontal straight sections in the test rig. They were also separated with 90° test bends (nominally identical test bends).

Monitoring the pressure simultaneously at twenty four positions along the test pipeline would allow the pressure profiles in four straights to be determined. In order to capture the amount of data expected, a computerised data acquisition system was required.

A3.2.3 Existing test rig

An existing test rig that had been used for two other research projects was available which could accommodate the necessary modifications. The rig incorporated a 53mm nominal bore pipeline loop, made up of straight sections and bends, 81 metres in length. The majority of the pipe line was in a horizontal orientation. The first two long (17 metre) lengths of horizontal straight sections were fitted with pressure transducers at 2 metre intervals, with a 90° test bend in between. A blow tank was acting as a feeder at the beginning of the conveying line, with a receiving hopper at the end of the line, situated above the blow tank and mounted on load cells. The flow rate of solids was determined by monitoring the gain in weight in the hopper via the load cells, over a known period of time.

The air flow rate was regulated by a bank of choked flow nozzles installed in parallel. The nozzle bank consisted of eight choked flow nozzles of different sizes in "times two" geometric progression that could be used to make up any chosen flow rate, up to the maximum with them all open [B1]. The rig was controlled from a mimic panel and the instruments were connected to a data logging system. The pressure readings were recorded using the data logging system, and transferred at the end of each test to a computer for processing.

A3.2.4 Modification to the existing rig to achieve the project objectives

The existing test rig required several modifications before test work could commence. The existing rig was capable of using any one of three different sized internal diameter pipeline loops. The nominal diameter of the pipes were 50, 80 and 100mm. For this project, the 50mm pipeline was considered most suitable to use because less material would be needed for the conveying runs. Work by Ashenden [A1] had shown that the largest diameter particle to be conveyed during the test work would not be affected by the pipeline diameter, as the pipeline nominal bore diameter should be at least three times larger than the largest particle diameter. Work previously carried out using the original test rig using all three pipeline loops [B1] had shown that the results obtained from a 50 mm nominal bore pipeline could be scaled to suit larger diameter pipes successfully.

The major changes were the installation of a volumetric feeder to provide a steady flow rate of material from the blow tank into the conveying pipeline, and the placement of additional pressure transducers along the pipeline loop to monitor the pressures along most of the conveying pipeline.

Some pipeline modifications were also required to obtain four long straight sections of pipeline for the test section.

The volumetric feeder was required because a blow tank does not always provide a steady flow rate of solids into the conveying line due to pressure pulsation [A4]. In addition, without a volumetric feeder, it is difficult to preset the blow tank discharge rate accurately.

With the additional data that would be obtained from each test run by the numerous pressure transducers, an upgrade of the existing data processing equipment would be necessary. The existing data acquisition unit that received the transducer signals was not fully utilized, and had the capacity for several more input channels. In addition the original host computer was incapable of processing all the data simultaneously from the input channels, and using the extensive range of software presently available.

A3.3 The pipeline and bends

A3.3.1 Pipeline

The pipeline to be used for this project was part of a previously used test rig, and therefore only required minor alterations. It was constructed from 50 mm nominal bore medium weight seam welded steel pipe (bore 53mm).

The existing pipeline loop was mainly made up from four straight lengths of pipeline as shown in fig A3.1. The first two long straight sections were fitted with pressure transducers and were connected by a 90° bend. The layout of the pipeline made it possible to fit the remaining horizontal straight sections with pressure transducers, and to install 90° tests bends in between the straight sections. The end of the conveying line required extending so the last straight test section was of a suitable length, as it was originally too short to enable the solids in the conveying air to reach a fully-accelerated condition. Solids slow down when they enter a bend due to collisions with the pipe as it changes direction. When the pipeline straightens out again, the particles are then re-accelerated by the velocity of the air in the pipeline, until they reach as near as possible, the same velocity as the conveying air.

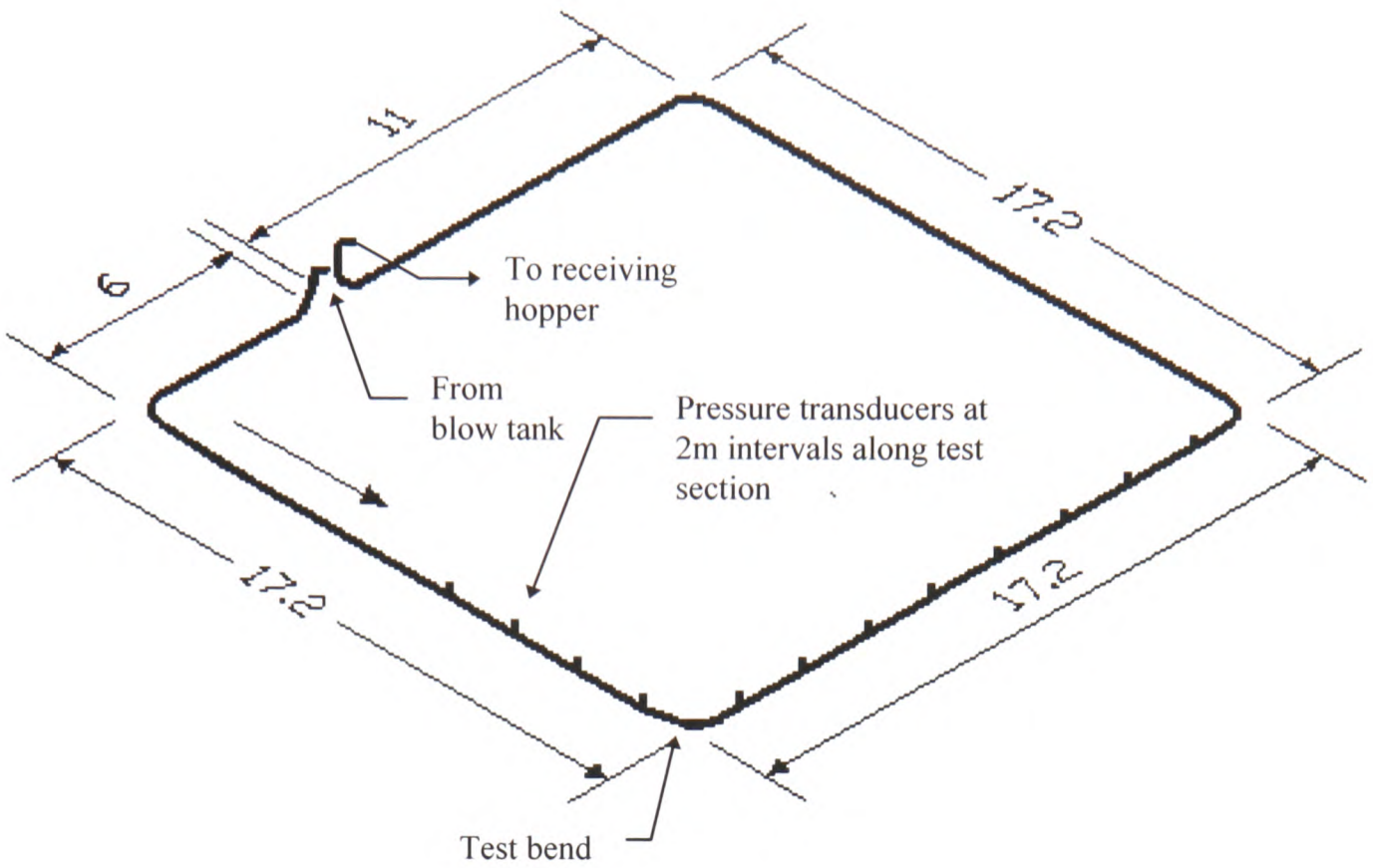

Figure A3.1: Diagram of loop before modifications

The length of a straight section to ensure a fully-accelerated flow is dependent on the conveying air velocity, but is a usually around 5 metres. Research by Rose & Duckworth [R3], Bradley [B1] and Jones [J1], had shown that recovery of the particle velocity to a value approaching its terminal value after a bend in suspension flow, appears to occur at a minimum of 5 metres, although this distance can rise to 8 metres depending on the air velocity. This was inferred from observations that the pressure gradient first reached a steady value at this distance, after the disturbance caused by the bend. Therefore the first transducers in the new straight test sections were fitted at a distance of 5 metres from the apex of the test bends.

Consequently, the fourth straight section was extended to match the three existing straight sections of 17 metres in length.

A3.3.2 Modified test loop

A diagram of the extended conveying pipeline with the additional pressure transducers is shown in fig A3.2. The first transducer positioned after the second and third test bends, are 5 metres after the apex of each bend, which is the minimum re-acceleration length of the solids conveyed in air[R3] for the air velocities anticipated in the test work.

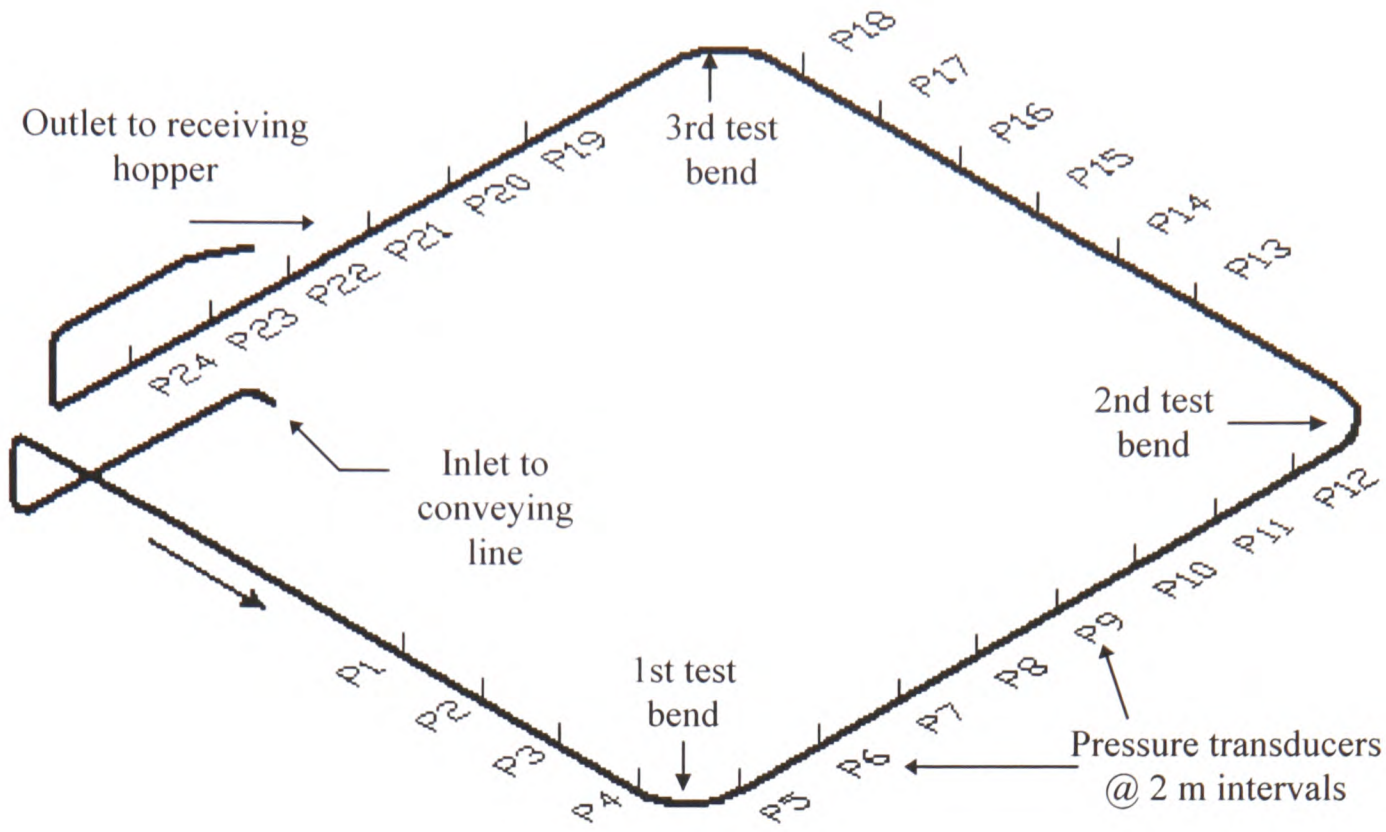

Figure A3.2: Layout of the test rig pipeline showing the positions of the pressure transducers and test bends.

A3.3.3 Bends

Only one bend type was used for the test work, and all three test bends were manufactured to the same specifications and from the same length of pipe, to ensure that they were as similar to each other as possible. During the project it was found that bend wear was a problem with some conveyed bulk solids. As expected with wear of bends [B4], it was always the last test bend, where the velocity of the air and material were highest, that wore through first. A total of three sets of bends were used for the project. When a bend wore through, all three were replaced at the same time, which were constructed to the same specifications.

The bends used in the test rig were the type most commonly used in conveying pipelines. They had a relatively long radius and were made from pipe of the same specification that was used for the straight sections, by bending. The pipe was bent in stages using an hydraulic pipe bender moving the pipe bender between marked points on the pipe in turn. This gave a smooth finish to each bend. By carefully noting the positions that the pipe was bent at, it was easy to make identical bends. Each bend had a radius of 711 mm ± 5 mm to centre line. This gave a bend radius to pipe bore ratio of 13.9, which is typical of industrial practice.

In most commercial systems, bends are fitted into a pipeline using either flange or sleeve couplings. The bends in the test program were fitted into the pipeline using sleeve (Morris) couplings. This type of fixing was chosen because it clamps on the outside of the pipe, providing an internal smoothness of joints, with no gap between the pipe ends or misalignment if installed carefully.

A3.4 The feeder

The feeding device introduces material into the conveying line. It had to be capable of reaching the desired flow rate of material into the line, yet achieving a high turn down so that the widest range of conveying characteristics could be examined. High flow rates of product are only achievable with a high pipeline pressure drop. Therefore a high pressure feeder was needed; the only suitable option was a blow tank.

A blow tank is a pressure vessel that is loaded with material and then pressurised in order to force the product into the conveying line. At that point, additional air is normally injected to create the required product to air ratio. The blow tank that was installed as part of the original test rig had a $1.5m^3$ capacity, with a pressure rating of 7 bar, discharging into a 50 mm pipeline. Above the blow tank, a hopper of a similar capacity was mounted on load cells, with an air filter on top. The blow tank was charged with material from the hopper, through two DN200 butterfly valves. The valves were separated with a flexible hose so that the weight of the hopper was de-coupled (the hopper being mounted on load cells). The top valve held the material in the hopper, whilst the lower valve sealed the pressure in the blow tank. The entry point into the hopper at the outlet of the conveying line, was fitted with a flexible hose to de-couple weight transfer from the conveying line. The blow tank was also fitted with a valved vent line to enable air to escape into the hopper during charging and de-pressuring. This was also fitted with a flexible section to ensure weight de-coupling, as shown on photograph A3.1.

During a conveying cycle, the material leaves the blow tank and is conveyed along the pipeline loop to the hopper above the blow tank. The flow rate of solids is calculated by monitoring the gain in weight in the hopper over a known period of time.

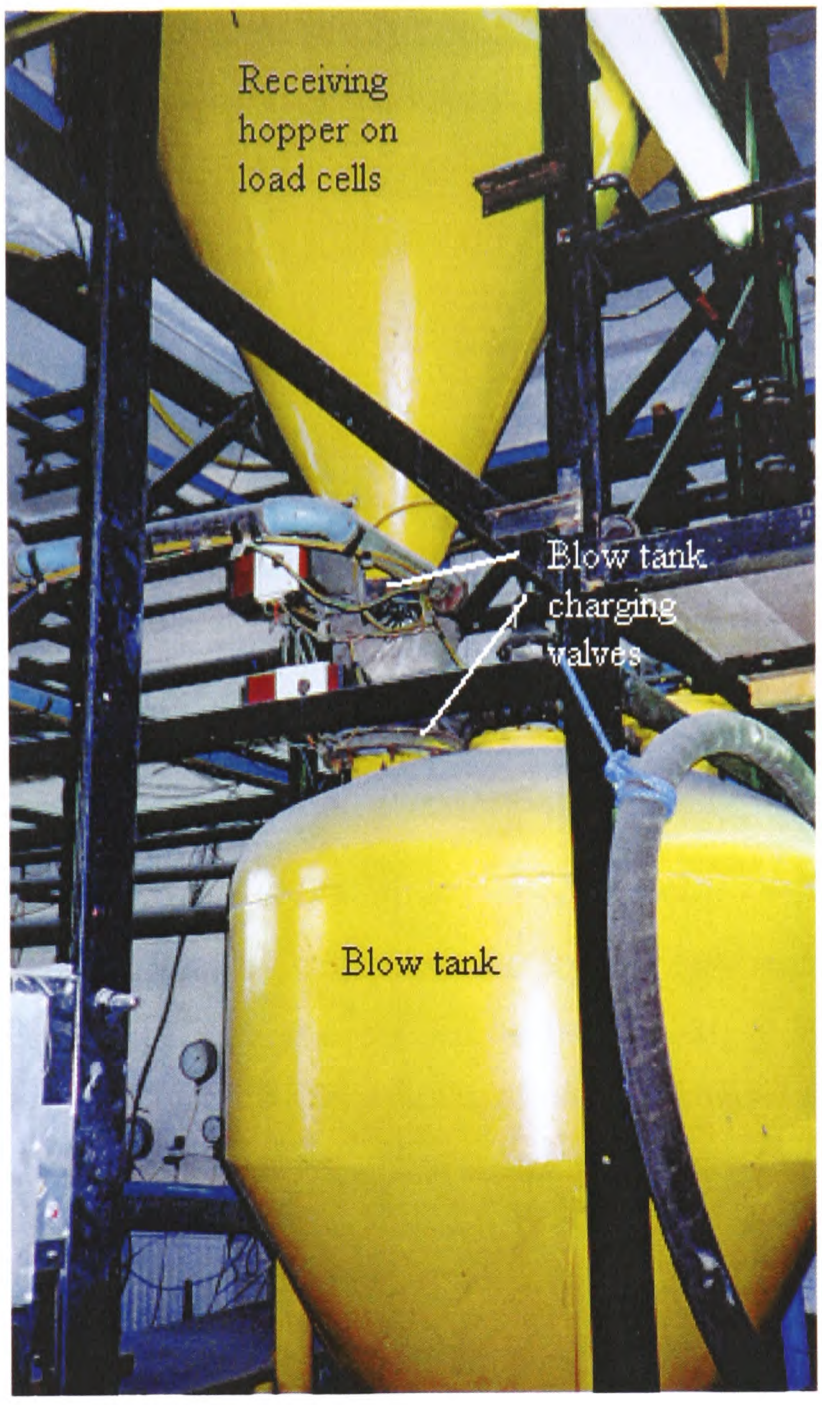

Photograph A3.1 Receiving hopper, blow tank and charging valves.

A3.4.1 The volumetric feeder

Originally the blow tank was designed to discharge from the top. However, feed rate fluctuations that are a consequence of using a blow tank as a feeder, limited the repeatability and consistency of the data obtained from test runs carried out under similar conveying conditions with this arrangement. As stated previously, repeatability of test data requires a steady flow-rate of material into the conveying pipeline from the blow tank which needs also to be readily controllable. For these reasons, a volumetric feeder was needed and a screw feeder was selected as the most suitable device. Rotary valves and high pressure rotary valves were also considered, but discounted primarily because of the types of material used for the project. Rotary valves are not particularly suited to handling abrasive material [K2]. Products harder than 3 on the Mohs scale can cause rapid increase in the clearances between rotor and casing, which would affect the air

leakage through the valve. That would in turn impede the product flow rate into the rotor pockets and thereby reduce the feed rate. In addition, the material discharge from a rotary valve pulsates into the conveying line more so than a screw feeder would.

A3.4.2 Design of the screw feeder

The introduction of a screw feeder required a major alteration to the blow tank, and this modification had to be capable of withstanding the high operating pressure used within the tank. A housing unit for the screw was designed to the same pressure specifications as the blow tank and manufactured as a pressure vessel. The initial design of the screw and housing unit was commissioned to Ajax Equipment Ltd. This company were also responsible for the manufacture of the screw. However, it was later decided to arrange for another subcontractor to manufacture the housing unit because of cost considerations.

The specification for the design of the screw and the housing unit required that it should be capable of conveying the test materials at a maximum mass flow rate of 20 tonnes per hour. The minimum flow rate would be as slow as the screw control system could operate. As the test rig was already operational and only required modifications, the design had to fit in with the existing arrangement.

The screw feeder geometry was carefully considered so that active draw-down of material from the entire cross-section of the hopper would be achieved to avoid dead material. Dead material would give rise to core flow and attendant problems of segregation, variable bulk density and irregular discharge rate, all of which would compromise consistency of flow rate and material quality.

For mass flow (active draw down of material across the entire hopper cross section) to be achieved, the capacity of the screw needed to increase, in a controlled way, in the direction of feed. The capacity of the screw was made to increase by use of an increasing pitch and stepped shaft. Roberts [R4] gives guidance on the correct design of screw feeders involving the selection of combinations of variable screw diameter, shaft diameter and pitch to produce the necessary volume increase along the screw.

The final design of the screw is shown below in figure A3.3, and incorporates most of the factors quoted by Roberts [R4] as significant for an optimum design. The 200mm diameter, mild steel screw had graduated flight pitch, on a stepped shaft. The design included a clearance of 10mm between

the screw and housing unit to prevent the largest particle predicted to be used in the conveyor, from getting trapped.

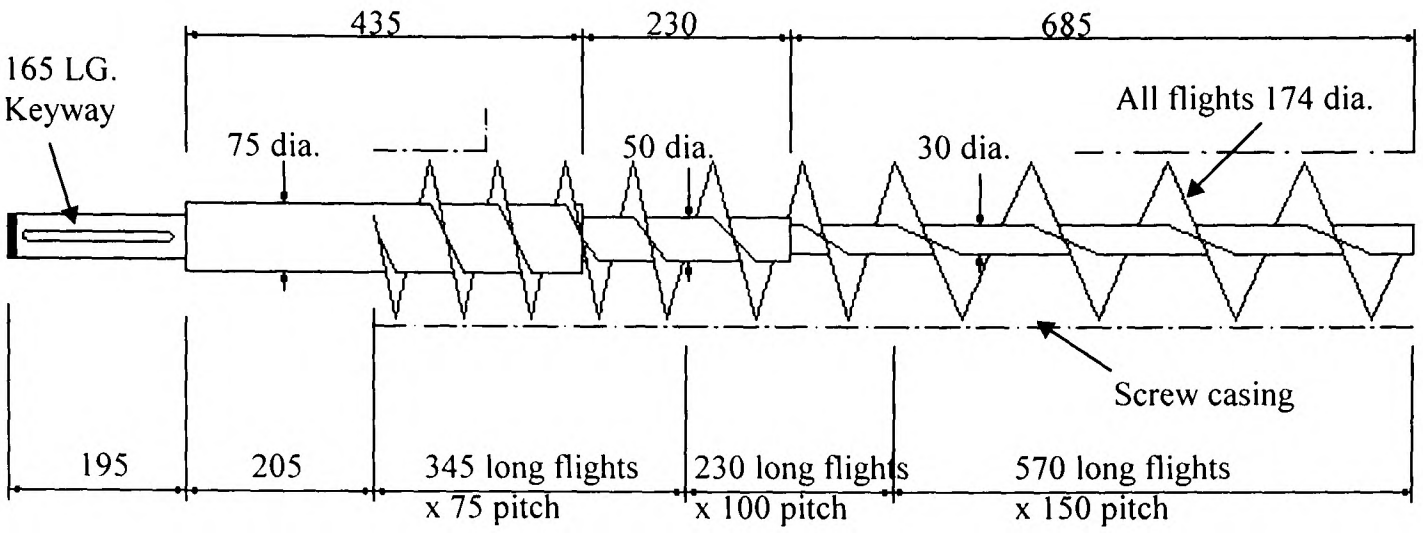

Figure A3.3: Drawing of screw

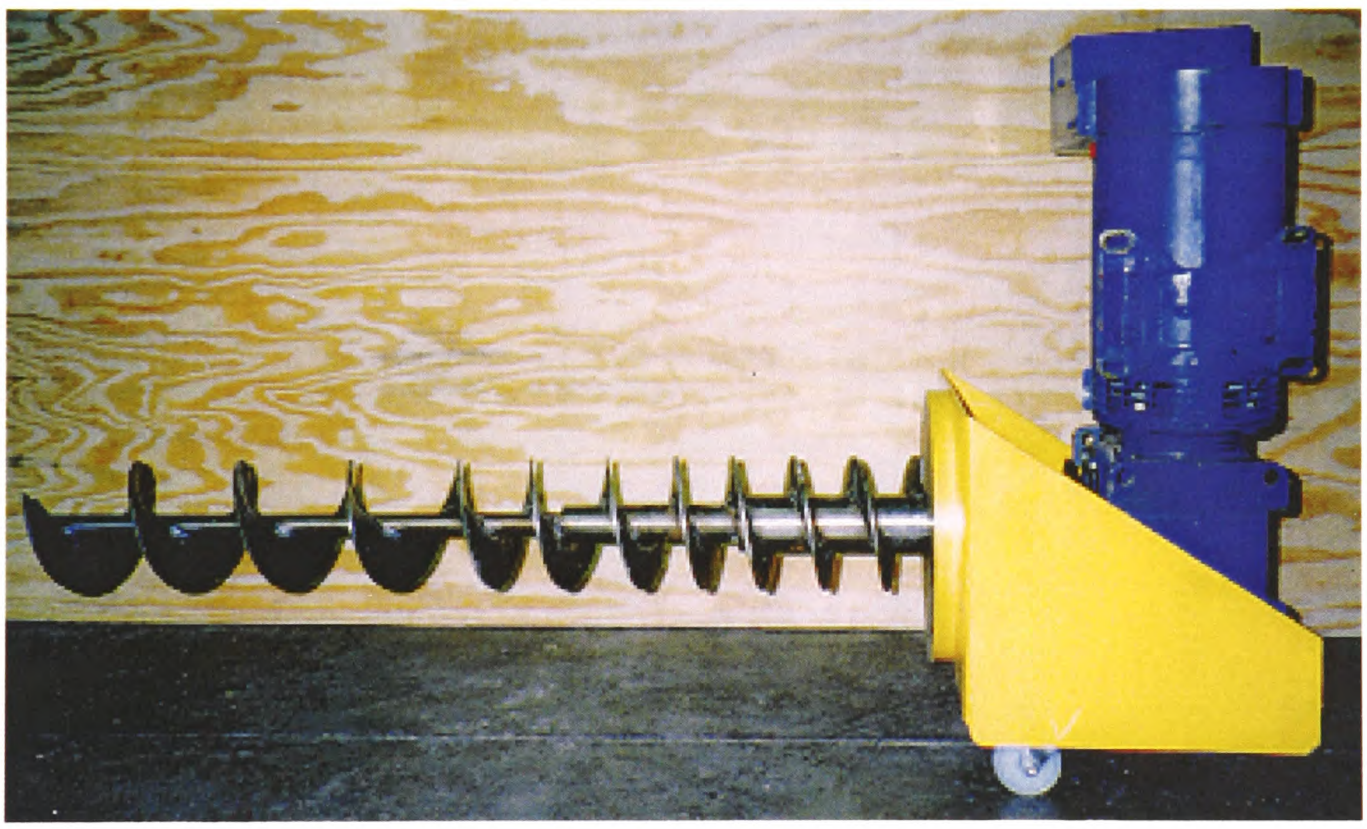

Photograph A3.2: Photograph of screw showing the variable shaft diameter and variable pitch, fitted to motor and gear unit.

In order to modify the blow tank to accommodate the screw and housing unit, it was necessary to remove the bottom of the blow tank and transform it from a top discharge to a bottom discharge vessel. This limited the head room for the housing unit because the blow tank and hopper above it, were heavy components that would be cumbersome to raise up if extra height was needed.

With the installation of the screw feeder, the design had to allow the air pressure across the screw to be balanced, otherwise the material would be forced past the screw into the conveying line, thereby defeating the object of achieving accurate control over the flow rate purely by means of screw speed.

To achieve an air balance, the air supply to the blow tank and conveying line was re-designed so that the inlet air supply was divided into three. The air to the blow tank was directed to a manifold connecting the top of the blow tank, the screw feeder housing unit just above the screw, and the pipeline under the drop out box where material fell from the screw discharge into the pipeline. Figure A3.4 shows the layout of the air supply.

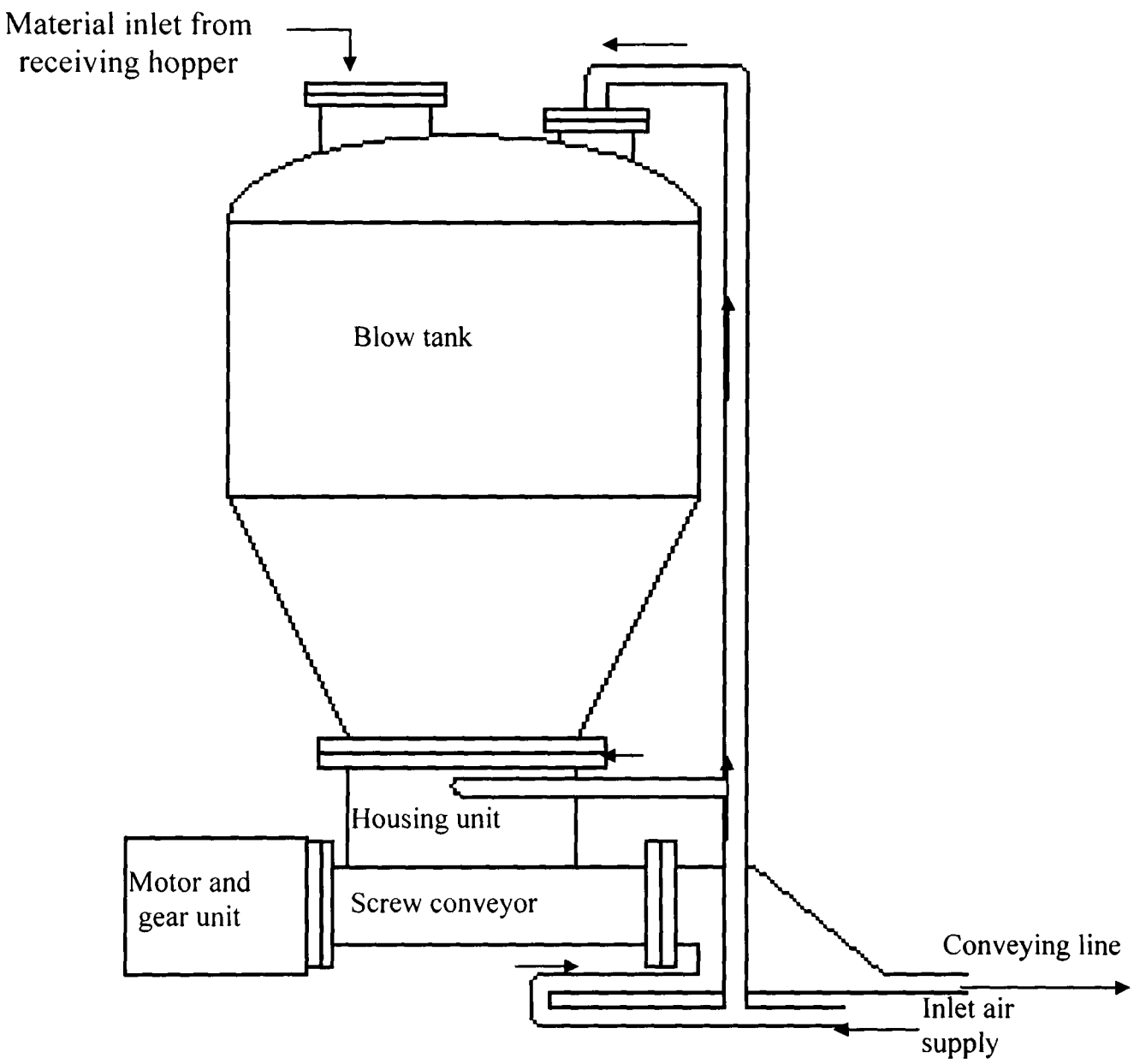

Figure A3.4: Diagram of air supply to the rig

A3.4.3 Housing unit for the feed screw

The flow properties of the test materials had to be carefully considered in the design of the housing unit, as the angle of the housing wall had to be chosen to promote a mass flow of the

materials in the converging section above the inlet to the screw. With mass flow, the bulk material is in motion at essentially every point of the hopper whenever any material is allowed to flow through the outlet [D2].

In order to ensure that mass flow was achieved when using the feeder, the types of materials that were in the test program and their median particle sizes, plus the angle of wall friction obtained from two of the materials that were already stored in the laboratory to be used in the test programme, were given to the screw housing unit designers. They were also given the dimension of the blow tank outlet the unit was going to be connected to, and the headroom available beneath the blow tank and the floor of the laboratory. Their final design allowed for the full range of materials to be used in the unit for the required flow pattern and mass flow rates of solids.

Upon completion, the housing unit was pressure tested to 7 bar and certificated for insurance.

Photographs A3.3 & A3.4 of screw housing unit

A3.4.4 Liner for converging section above screw

A smooth steel liner was also designed to fit inside the housing unit. It was of a similar shape to the converging section and stopped just above the top of the screw. The purpose of the liner was to distribute the air supply evenly around the bottom of the discharge section, and it followed the shape of the housing unit walls. The liner was also intended to promote mass flow in the section above the screw by presenting a smoother surface than the inside of the steel outer body, so that the bulk solid would discharge in mass flow and be presented to the screw in as consistent a condition of bulk density and size distribution as possible [B3]. Figure 5 below, shows the screw housing unit and liner. The angle was determined from wall friction analysis.

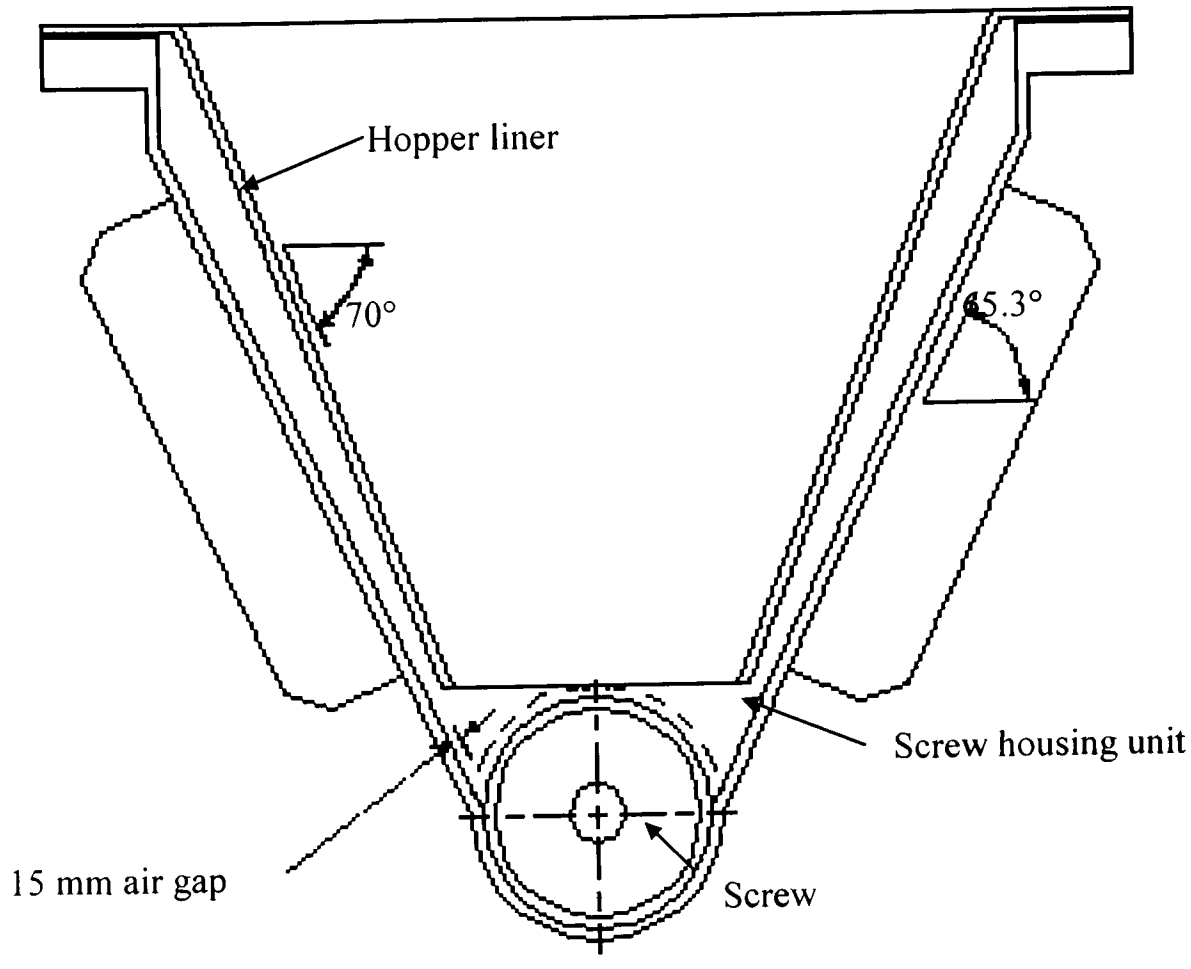

Figure A3.5: Drawing of screw housing unit and liner

A3.4.5 Drop out box

When designing the screw and housing unit, consideration was given to the transfer of the material from the end of the screw into the conveying pipeline. This was achieved with a drop-out box, the design of which enabled the material leaving the screw to become entrained in air before entering the conveying line.

The work of Kessel [K2] on rotary valves and drop out boxes, concluded that the minimum height for a drop out box is twice the diameter of the conveying air line. Bates [B3] confirmed a minimum wall angle of 70° from the top of the screw to the conveying pipe line was essential. With these dimensions, a drop out box was designed to fit the limitations of the modified test rig that would include the screw conveyor housing unit (photograph A3.5).

The drop out box was fabricated in house, and fitted to the housing unit. As mentioned previously, the air supply was re-directed into the blow tank and beneath the drop-out box, to balance the air pressure across the screw.

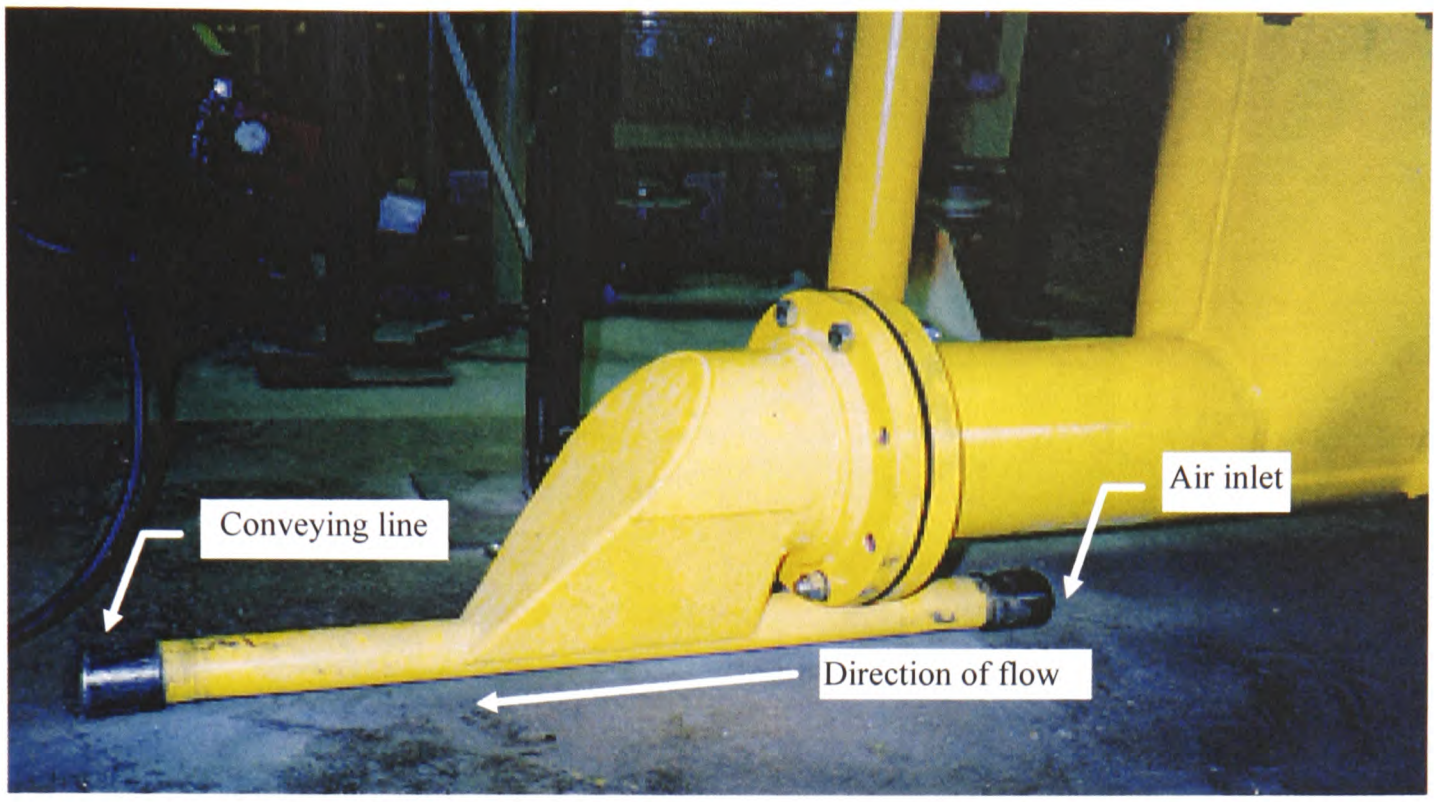

Figure A3.5:. Photograph of the drop out box

A3.4.6 Screw feeder control system

The installation of the screw feeder required an instrumentation and control system to drive and monitor the screw rotation under load. A G.E.C. 3.3kw DC motor with a top speed of 2000 revs per minute, and worm reduction (20:1) gear unit, was recommend by the designer of the screw, and installed. A three phase electrical supply was used to power the control system, which comprised of a thyristor drive unit to control the speed of the D.C. motor.

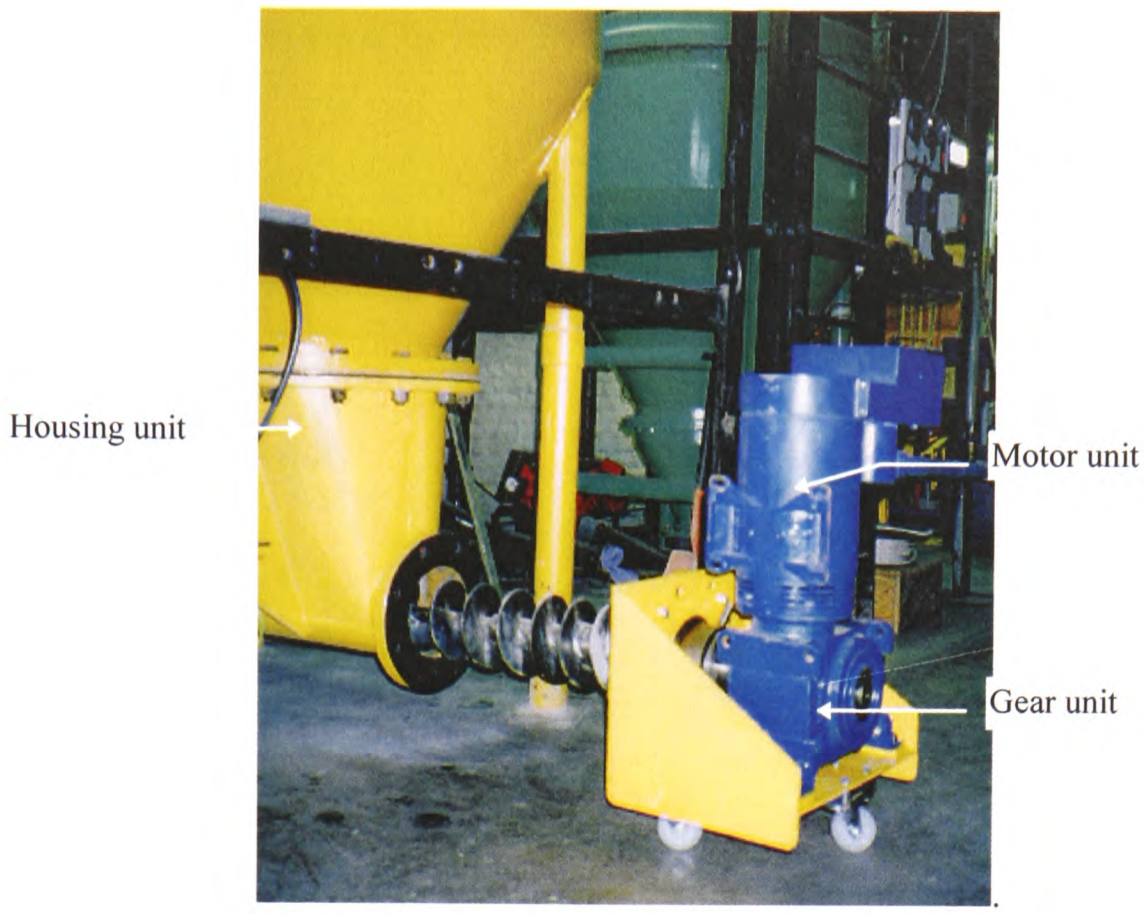

Photograph A3.6: Screw, housing unit, motor and gear unit. The motor, screw and gear unit were on wheels to enable the screw to be withdrawn from the housing unit for cleaning. After the conveying trials for each test material had completed, the material was removed from the rig and the equipment cleaned.

A3.4.7 Tachometer

An encoder disc was attached to the screw shaft in order to determine the speed of the screw, by counting the rate at which holes around the edge of the encoder disc passed a sensor. The output of the sensor was connected to a tachometer on a mimic panel controlling the test rig. The thyristor drive unit, controlling the speed of the motor, was operated using a potentiometer that was also mounted on the same mimic panel.

A3.5 The air supply

The laboratory air supply comprised of three Broom and Wade V200DA oil free reciprocating air compressors giving a total capacity of 0.33 kg/s (5.5 m^3/min free air) at 7 bar, and feeding one receiver (figure A3.6). From the receiver, the air passed through a pressure regulator before reaching a bank of choked flow nozzles of different sizes. A fixed pressure upstream of a choked flow nozzle, gives a constant known flow rate irrespective of downstream pressure, up to an absolute pressure ratio (downstream/upstream) of about 80% (ref Bradley [B1]). To obtain different air velocities in the

pipeline, the air flow rates could be varied from run to run by selecting different combinations of nozzles.

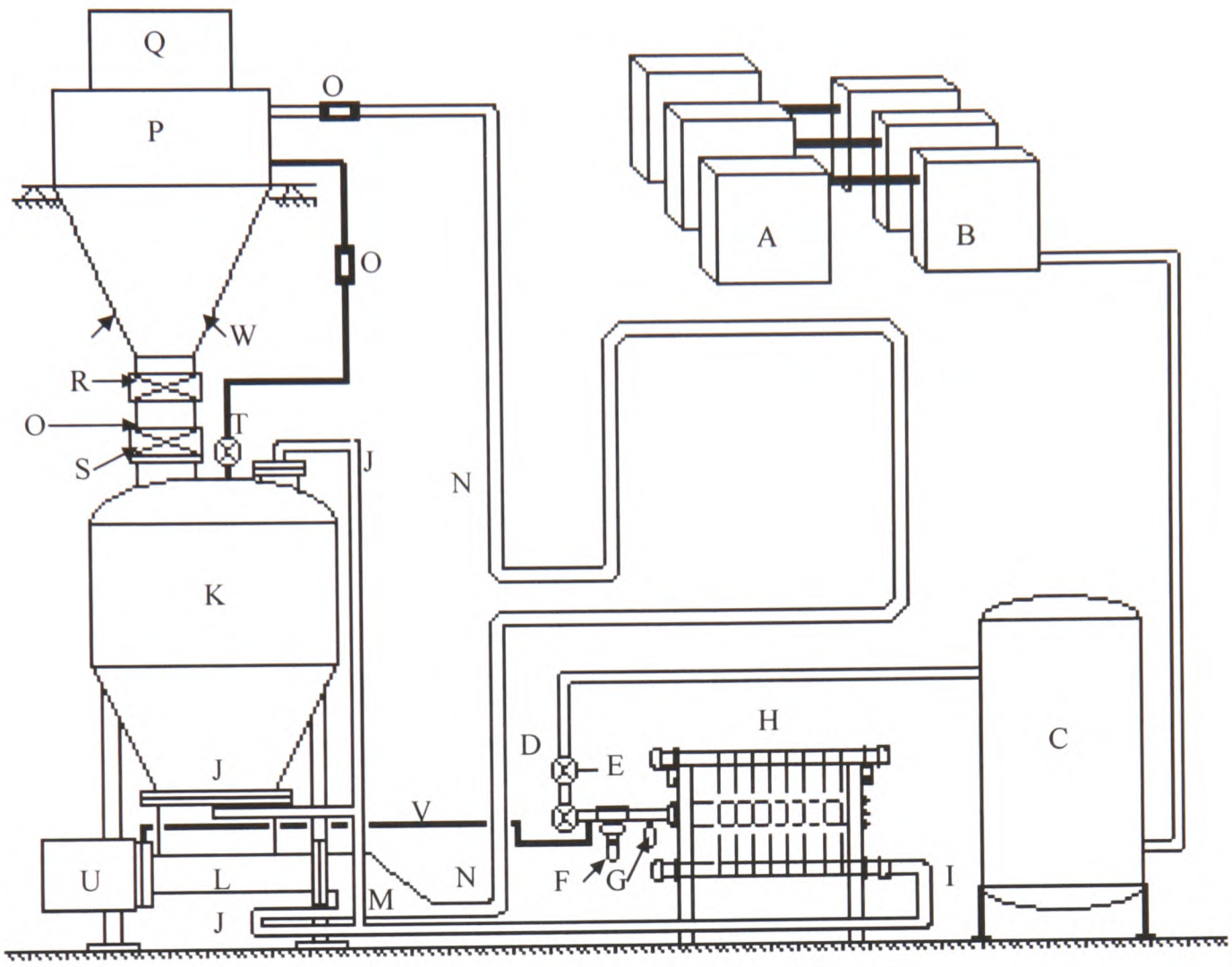

Figure A3.6:. Diagram or schematic of air supply

Key to code letters

A Compressors (in enclosure on roof)
B Aftercoolers (in enclosure on roof)
C Air receiver
D Manifold
E Air takeoff to pneumatic control equipment
F Filter/water trap
G Pressure regulator
H Choked flow nozzle bank (figure A3.7)
I 50mm nominal bore pipe
J Blow tank injection point
K Blow tank
L Screw feeder
M Drop out box (photograph A3.5)
N Conveying line
O Rubber sleeve for weight decoupling
P Receiving hopper
Q Exhaust air filter
R Upper charging valve
S Lower charging valve
T Blow tank vent valve 50mm
U Motor and gear unit for screw feeder
V Air line to screw shaft seal
W Air injection to aid discharge from hopper

The actual air flow rates were determined by the selection of the choked flow nozzles after the valves. A computer program that indicated which nozzles should be selected in order to obtain the

desired air flow rate, was used to aid the nozzle selection for a required mass flow rate of air. The nozzles were in a "times two" geometric progression so that they could be used to make up any chosen flow rate, to the maximum which is achieved with them all open, and with a resolution equal to the flow rate of the smallest nozzle. Detailed diagrams of the nozzle bank and nozzles are shown below in figure A3.7, A3.8a and A3.8b.

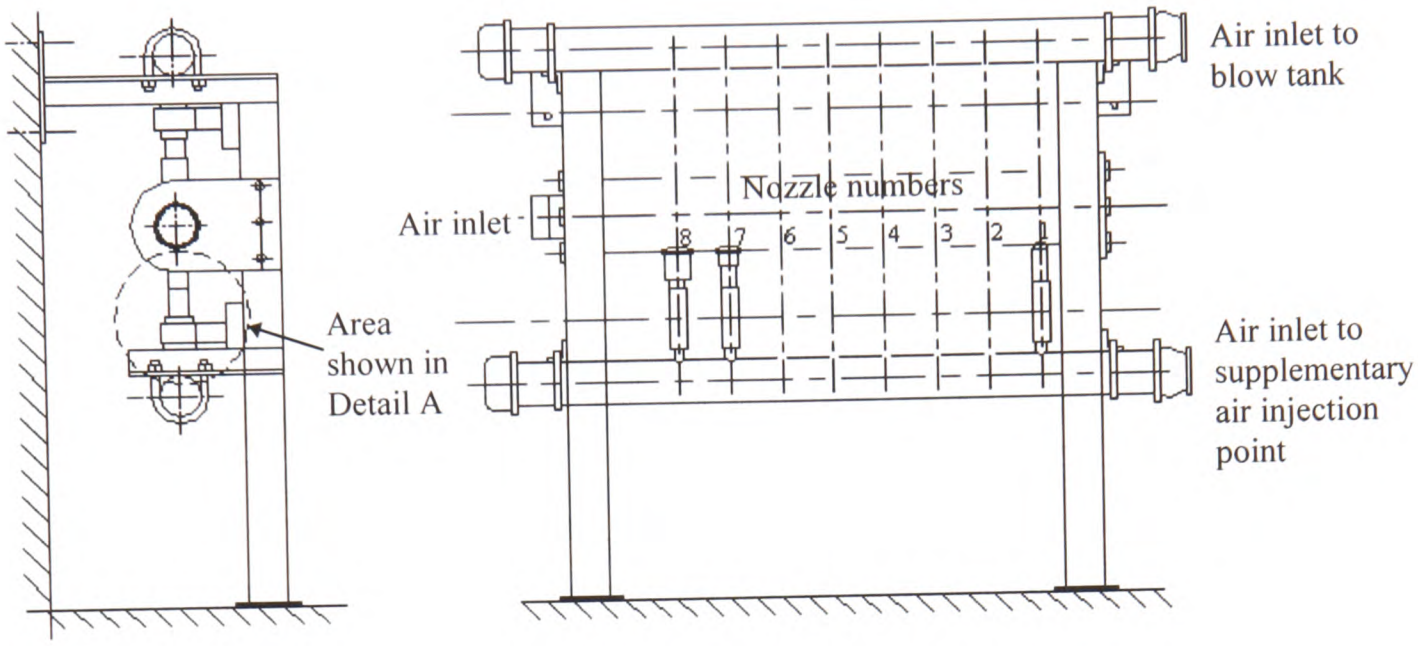

Figure A3.7. General assembly diagram of the choked flow nozzle bank

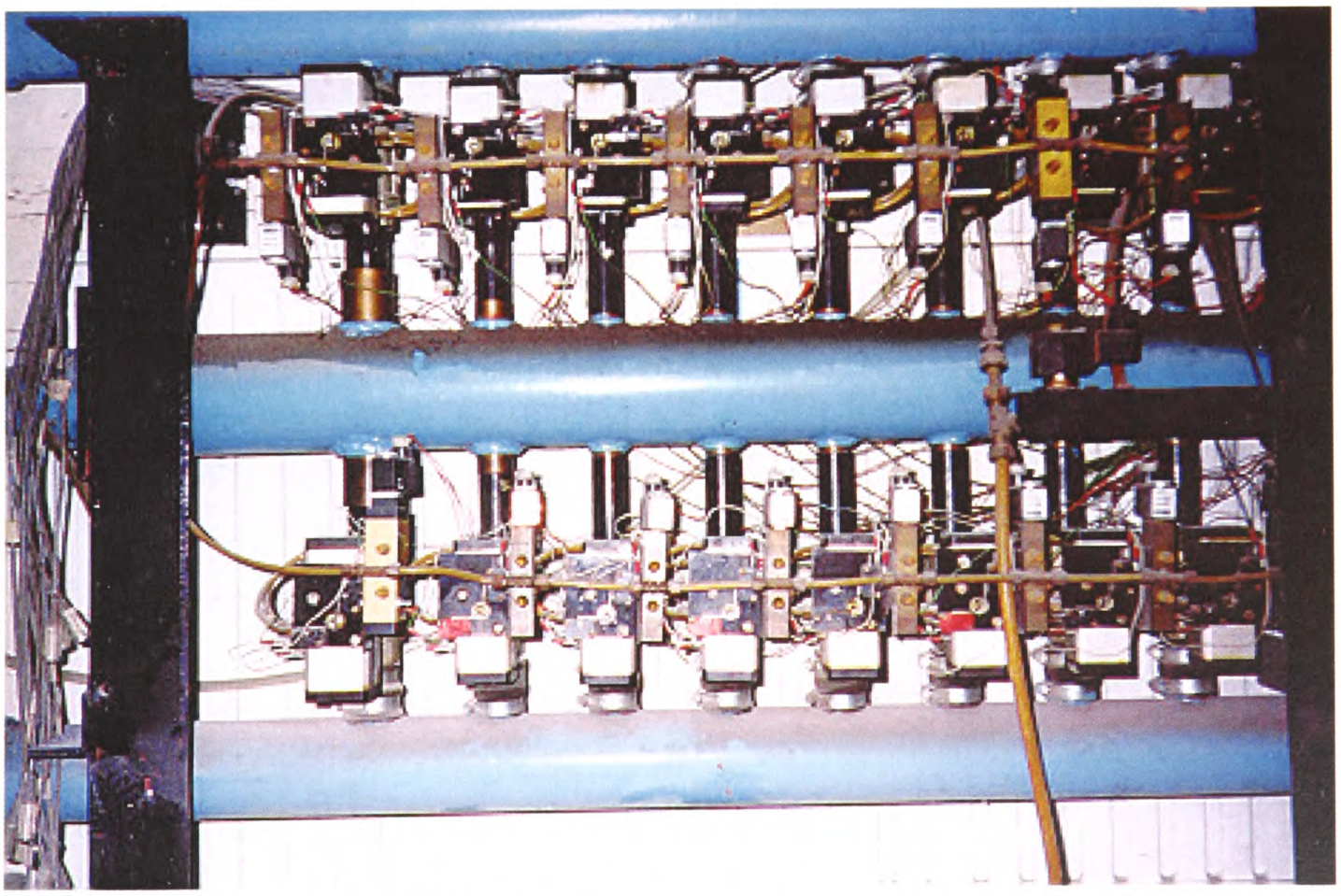

Photograph A3.6: Nozzle bank as shown in figure A3.7.

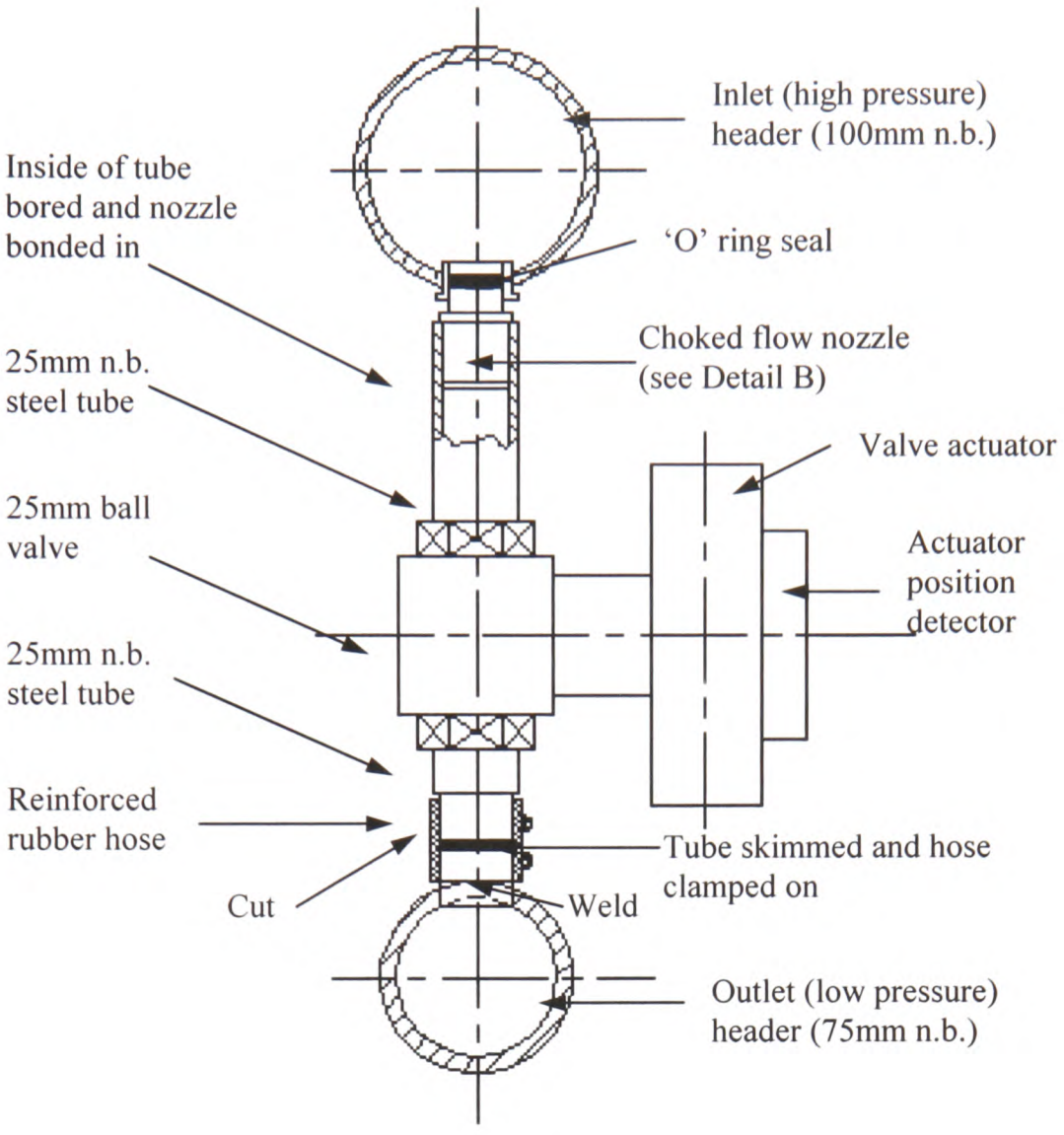

Figure A3.8a. Detail A. (relates to figure A3.7) Layout of valves and nozzles and outlet headers

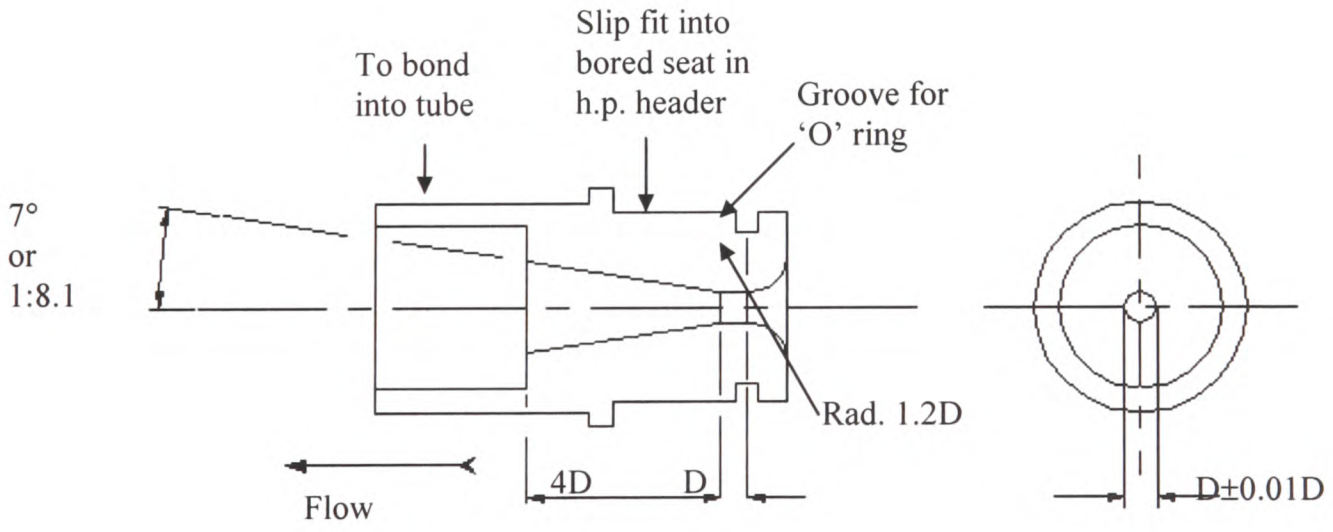

Figure A3.8b. Detail B. Functional dimensions of the choked flow nozzles No.5 shown.

A3.6 Instrumentation and control

The quantities that would need measuring during test runs were mainly the pressures at tappings along the four straight sections, and the weight of product in the receiving hopper which was mounted on load cells. In addition, the pressures upstream and downstream of the choked flow nozzle bank that were used to control the air flow to the blow tank, needed monitoring. The final arrangement of all the instrumentation and control systems are shown in figure A3.9.

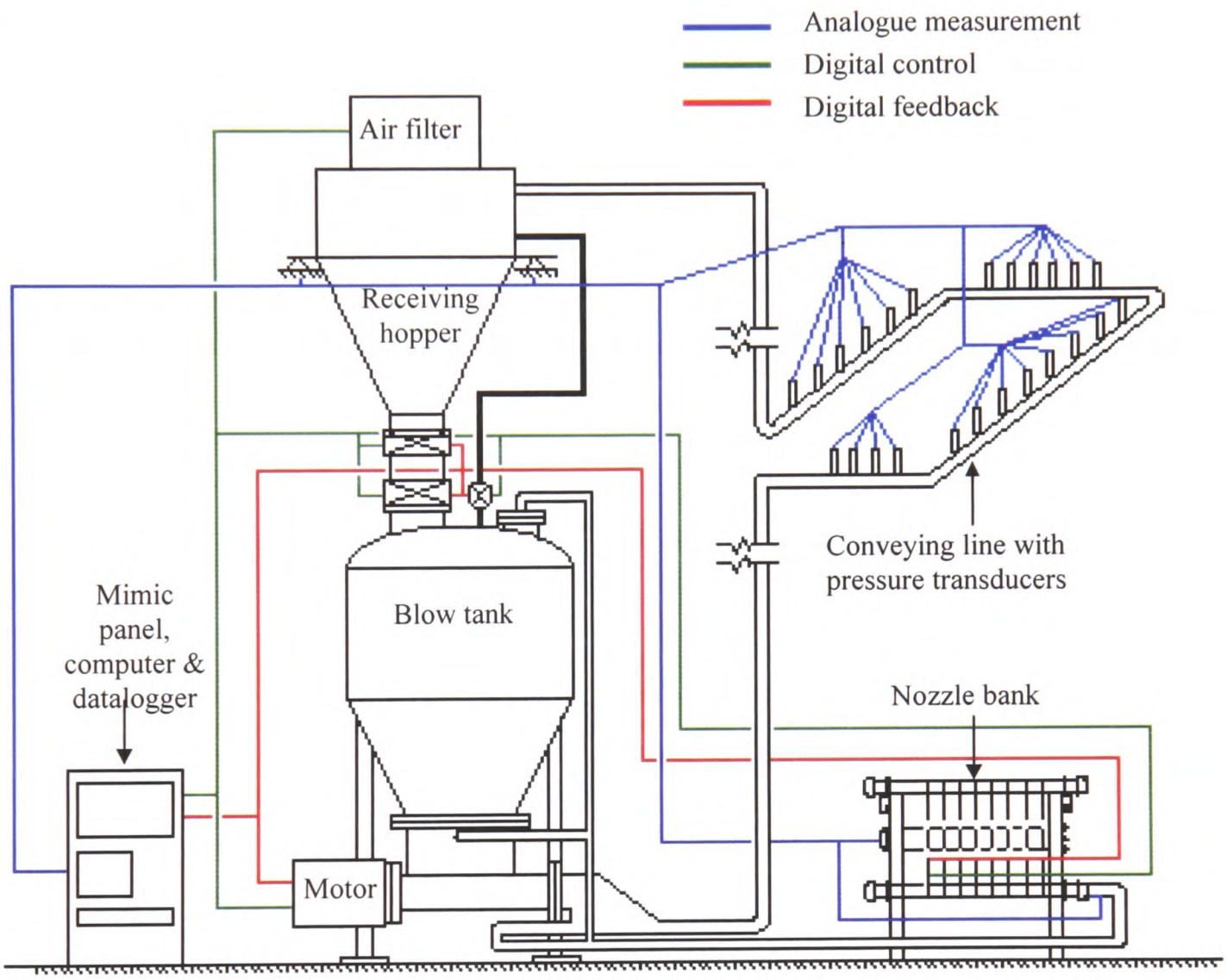

Figure A3.9: Diagram of instrumentation & control systems

A3.6.1 Load cells

The receiving hopper was mounted on three load cells, all of which were connected to a power supply unit that also incorporated amplification, and applied an offset to the signal received from the load cells to remove the tare signal. The voltage output from the load cells which was transmitted from this unit to the data logging system, was proportional to the weight of material in the hopper.

A3.6.2 Control

The original test rig was operated remotely using a mimic panel in a control room, where the data acquisition equipment was sited (photograph A3.7). The mimic panel displayed a schematic diagram of the rig, and a switch for every valve that could be operated automatically, but could also be opened or closed manually. The position feedback circuits would operate lights on the display panel to indicated the status of each valve.

As a consequence of the modifications, the additions to the mimic panel consisted of a potentiometer to control the speed of the screw conveyor; a digital counter to display the actual speed of the screw via an encoder disc on the screw shaft; on/off buttons for the motor and fan for the screw conveyor, and a reset button should the motor stall. The switches also had indicator lights to confirm their status. The additional solenoid valves that purge the pressure tappings were connected with the existing switch so that all the tappings could be purged simultaneously (see next section, A3.6.3).

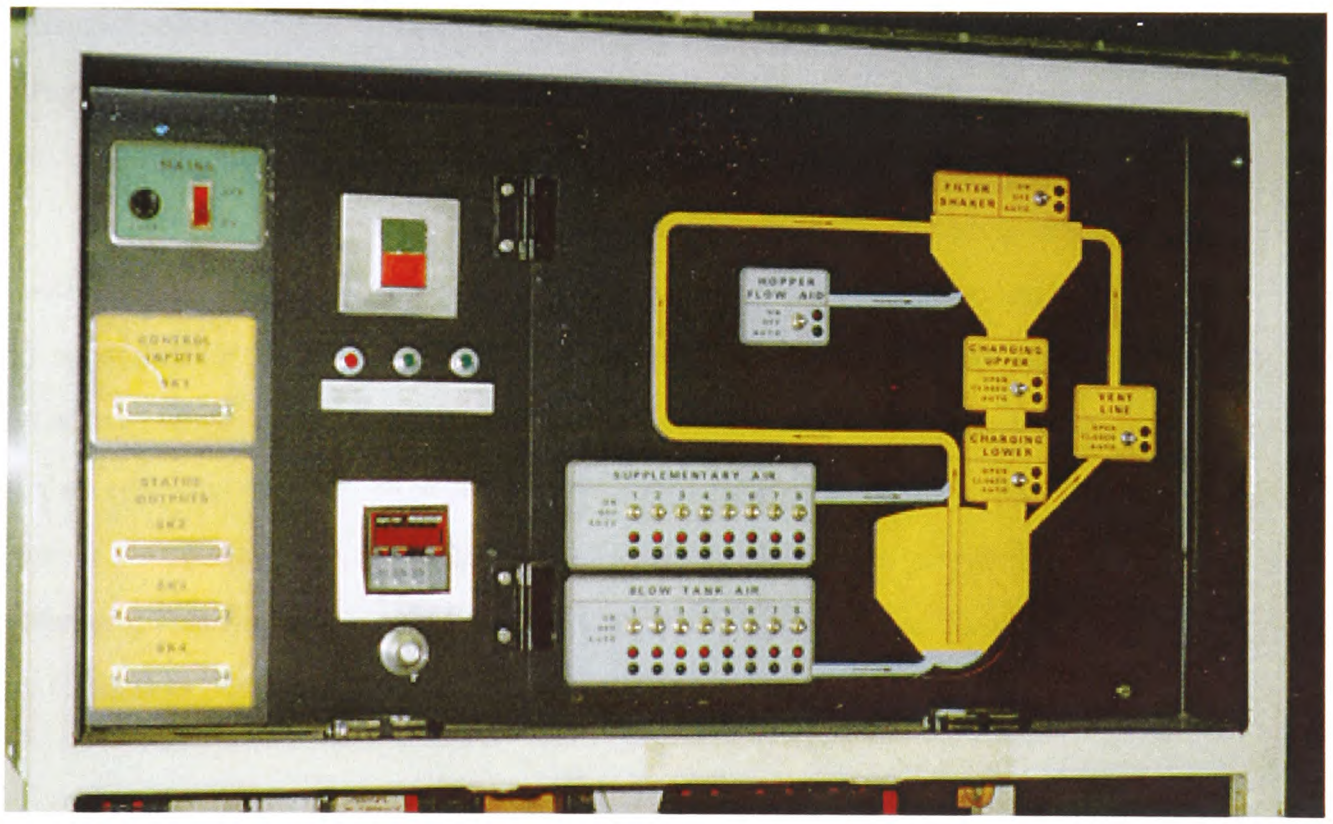

Photograph A3.7: Mimic panel in control room

A3.6.3 Pressure transducers and tappings

The original test rig was designed to measure the pressure gradient along two straight sections of pipeline with a test bend separating the two straight sections. Twelve pressure transducers had been used, spread at equal intervals along the straight sections of pipeline in order to measure the pressure profile along the pipeline. To enable monitoring the two additional straight sections, further instrumentation consisting of another twelve pressure transducers would be needed along the two

subsequent straight sections of the pipeline. These were also separated by bends of identical angle and design to the test bend. The installation of these transducers allowed pressure measurements to be taken along four straight sections, separated by three 90 degree test bends.

The transducers already installed and used on the original test rig, were of a silicon diaphragm design manufactured by Druck of Germany. Due to their reliable performance whilst in use for the previous project, the additional transducers installed were of the same type, but had a lower specification of 3.5 bar_g compared to 7 bar_g of the original. The lower pressure rating was sufficient for the estimated pressures that would be reached during the test work. The original 12 transducers were chosen for their combined accuracy (linearity, hysteresis and repeatability) specification of 0.1% with an over pressure capability of x4 without change in calibration. The output was a differential voltage of 30mV full scale, which was enough to be reasonably immune to noise over the distance from the data logging system to the furthest transducer, provided that screened cable was used.

All the transducers were of a flush diaphragm type, PDCR 810. This type was specified for the conveying line measuring stations so that there would be no cavity to clog should any powder enter the tappings.

The positioning of the tappings around the pipe was already documented by Bradley [B1] who had decided upon deliberation that it was at the top of the pipe that the tappings should be made. This was for convenience of access because it was deduced that along the steady gradient of straight pipeline, no one side of the pipe would be uniquely subject to more or less bouncing of the flow at any place. It was considered that the effect of gravity, increasing pressure in the bottom of the pipe and decreasing it at the top, would have no bearing on the decision to site the tapping at the top of the pipe. This was because it would be consistent from one tapping station to the next.

The original tappings were designed to accommodate the M14 x 1.5 threaded mounting of the transducer, while the additional tappings required ¼ BSP 60° internal thread. A nylon filter pad made from a carpet tile (held in place by a sintered bronze permeable disc) was used to protect the transducer from powder. The nylon pad and the sintered bronze disc prevents the solids from entering the tapping. The carpet pad filter filters out the solids to prevent the bronze disc from blinding which they have a tendency to do very easily. A solenoid valve was also fitted to the tapping, which introduced a high pressure air supply to blow powder out of the filter after use. The arrangement is shown in figure A3.10.

The tappings were welded onto the pipe over pre-drilled holes, and the filters, transducers and solenoid valves fitted. Once the plastic airline tubes were attached, the pipeline was blocked and pressurised and the tappings checked using soapy water to ensure there were no air leaks which would give rise to an air flow through the filter. This in turn would produce a pressure drop across the filter consequently giving a false reading.

Purging of the filters was carried out after each test run. The pressure drop across the filters when purging between runs was occasionally checked for consistency, to ensure they were not blinded or punctured.

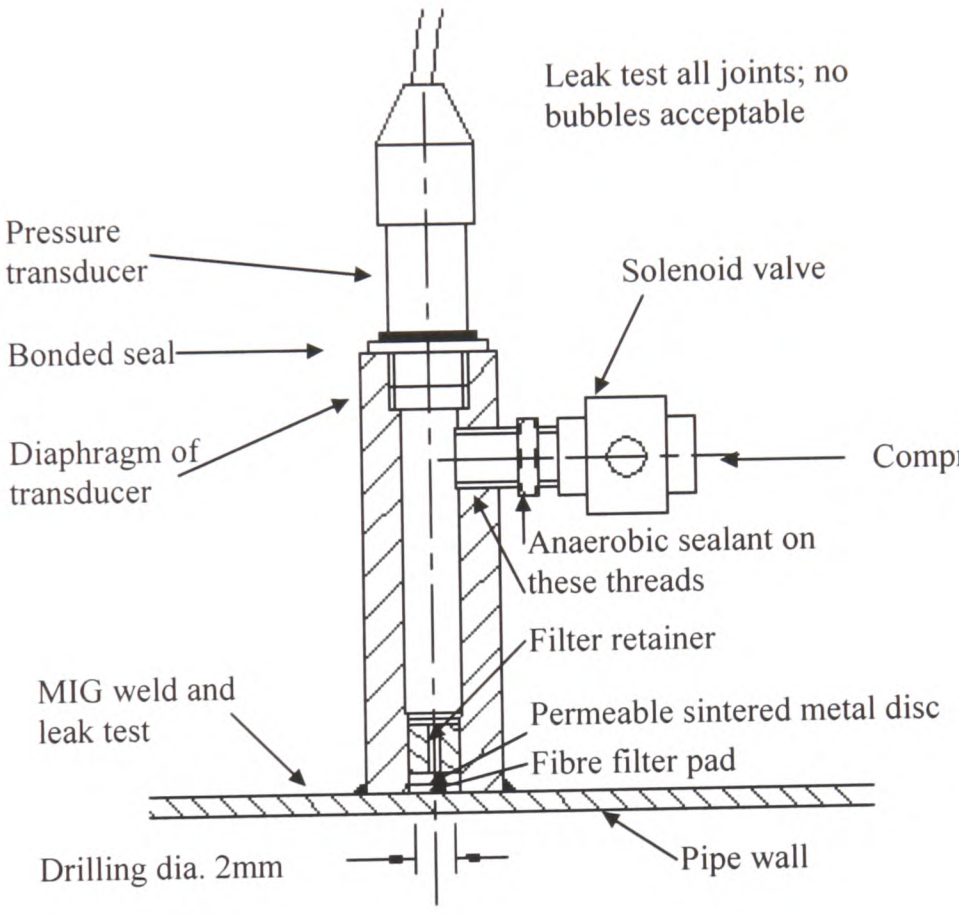

Figure A3.10: Drawing of pressure tappings

A3.6.4 The data logging system

Recording of the data from the pressure transducers and load cells was achieved using a data logging unit linked to a computer. The system was capable of controlling the frequency of scanning, enabled data to be taken and processed, and performed calculations required by the operator. The computer used prior to this project was a BBC Master, and the data logger was a Mowlem Microsystems ADU unit.

The Mowlem Microsystems ADU had an on board intelligence giving it the ability to run measurement and control programs on its own under instruction from a host computer through an RS423 communication link. The beneficial features included the gain and configuration of the analogue input channels being set by software from the host computer, those channels being multiplexed into an analogue to digital converter of twelve bit resolution (1 in 4096 or 0.02%) preserving the resolution of the signal from the transducers. Also, the input channels would accept the transducer signals with no need for any pre-conditioning, and the unit supplied the excitation voltage for the devices. The channel scan rate of up to 100 channels/second was in excess of the original test rig requirements, and with the additional 12 pressure transducers would still have surplus channels available.

The system worked well and was adequate for the existing test rig, but the modifications necessitated upgrading the data logger to accommodate the additional channels for the new pressure transducers, and an IBM compatible computer and updated software, to handle and process the increased volume of data.

To upgrade the data logger and its software, it was only necessary to purchase and install an additional 8 channel input card, upgrade microchip and IBM compatible software. These were obtained from ELE international (commercial successors to the original manufacturers, Mowlem Microsystems). An IBM compatible computer was also purchased and installed at the same time. Photograph A3.8 of the control area is shown below.

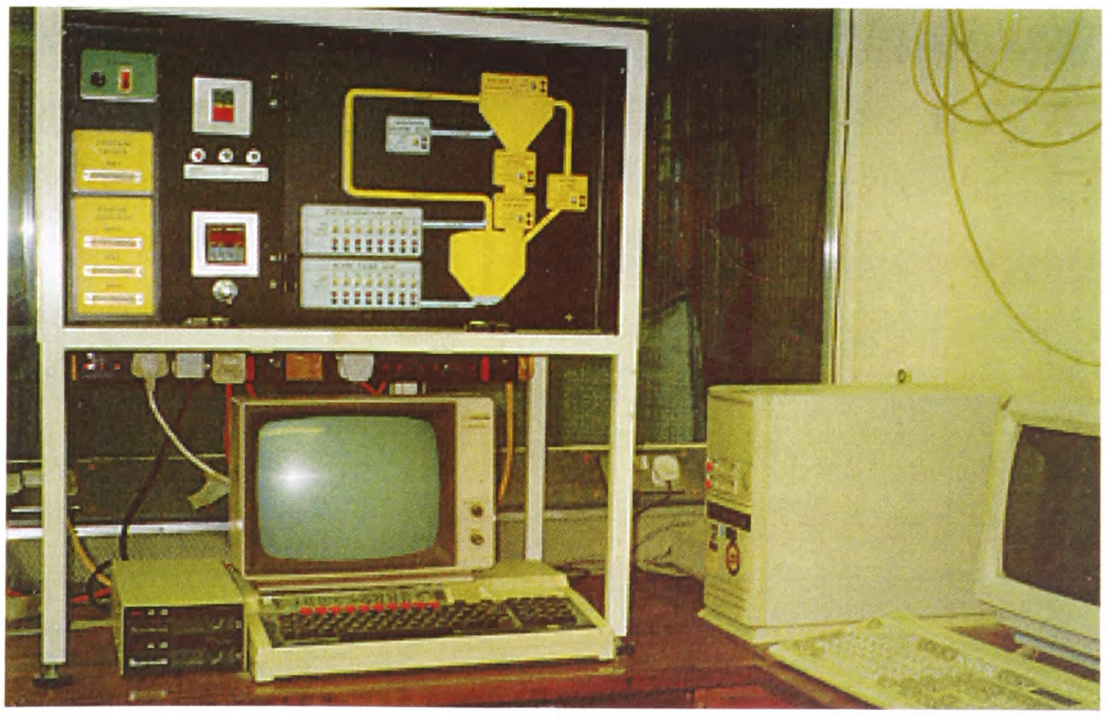

Appendix 4

Commissioning of the test rig

A4.1 Introduction

Modifications to the original test rig included the installation of a new screw feeder together with a motor and drive unit to control this, fitting 12 additional pressure transducers to the pipeline and re-arranging the air supply to the rig. The consequence was that a commissioning period was required in which the rig could be operated to ensure everything was working as desired before the project work commenced.

A4.2 Selecting the initial test material

Having selected several materials for the test program (chapter 4) the initial test product would also be used to commission the modified test rig. Therefore, the first test material would have to endure numerous tests until the performance of the system was capable of fulfilling the research objectives. Consequently the initial test material would have to be robust to ensure the particles would degrade as little as possible.

Degradation of a particle includes the fracture of the whole particle in to pieces or in half, or just the corners breaking off during conveying so that the particle shape alters. Either of these change the size distribution of the product and increase the amount of fines in the material. Some product particles also wear down so that their shape remains the same while the particle size reduces, resulting in a high proportion of dust being generated. An example of such a product is boral lytag which was one of the materials tested later in the project.

One of the materials selected for the test program was polyethylene pellets which fulfilled the requirement for robustness. Some plastics are known to hold a significant electrostatic charge whilst conveying, which can present other problems and change the conveying characteristics. However, this is not the case with the polyethylene pellets, as discovered during previous test work by other researchers using this material [B1,J1]. As the pellets had also been used for other test work, the material was conveniently on the premises and ready for use in the test rig. In addition, the data obtained from the previous test work for the product was available [B1] and could be useful for comparison purposes. For these reasons, the polyethylene pellets were used as the initial test material whilst commissioning the rig.

A4.3 Primary test program - teething problems

Once the modifications had been completed, the conveying line was blocked at its outlet and pressurised with air only, so that the readings from the pressure transducers could be observed on the monitor of the host computer. This task permitted the operator to view which channels were displaying a reading before the pressure transducers were calibrated. There were some problems with some of the newly installed transducers, but the faults were due to wrongly connected electrical wiring and quickly solved. The calibration of the transducers was achieved using a pressure test gauge connected in parallel with all the pressure transducers, with the blocked conveying line pressurised at set levels. The readings from the transducers were compared to the pressure gauge readings. Once the transducers were calibrated, the first test was prepared for instigation.

A4.3.1 Commissioning of the test rig

To commission the test rig, test runs were performed to determine that all the equipment and instrumentation on the rig was working correctly in order to achieve the project objectives. This included the mechanical, electrical, computer and software aspects of the rig. Therefore, the initial tests were kept as short and simple as possible so that minor problems would come to light before the main test program commenced. The important task was to convey the product under stable controlled conditions, produce results which could be relied upon, and process the data. To cover the full range of conveying conditions, the minimum air velocity at which the material could be conveyed without blocking the pipeline, needed to be established. This is usually achieved by conveying first at an air velocity and suspension density where the material is generally certain to convey. Subsequent tests at reduced air velocities, are then performed until the line is blocked with material, to determine the minimum air velocity at which the material will convey.

In order to ensure the line would not block during the initial test runs, the air velocity selected to convey the material was twice the expected minimum conveying velocity [J1], i.e.20 m/s, together with a very low suspension density of less than 10 kg/m^3.

Having determined the air velocity and suspension density values for the initial tests based on previous work by Jones [J1] and Bradley [B1] the first batch of tests were carried out to determine the optimum frequency and duration at which to scan the channels on the data logger, and the ideal number of readings to take for a reasonable assessment of each test. If an insufficient number of

readings were taken during each test run, any pressure fluctuations that occurred during the conveying run would not be observed; and the period from which the steady state period is selected when processing the data, would not be a true representation of constant conveying conditions.

For the initial test run the air was turned on, the screw feeder was set at 10 rpm and the data gathering test initiated. A total of 20 scans of the transducers and load cells were taken at 2 second intervals. The results were stored and further tests were run using the same air velocity, but increasing the speed of the screw feeder. This action increased the suspension density (i.e. the mass flow rate of product per unit volume flow rate of air). At the end of each test, the screw feeder was stopped whilst the results were stored and the next test prepared. This enabled several tests to be performed using the same batch of material. A total of 5 tests were completed using the initial batch of material in the blow tank.

After the initial test results were processed, the number of readings taken were increased to 50, at 1 second intervals, to obtain more data points taken over a longer period. The air velocity was reduced in an effort to approach the actual minimum conveying air velocity for the material, so that the limits of the conveying characteristics could be determined. The line blocked when the mass flow rate of air was set at 0.04968 kg/sec and the solids mass flow rate was increased to 1.0825 from 0.8644 kg/sec. The inlet pressure at blockage was measured at 1.49 $bar_{g,}$ at which pressure the superficial air velocity was 12 m/s. The air flow was reduced even lower and blocked the line again, thereby confirming the minimum conveying velocity.

The decision was made to run further tests on the same principle as the initial test runs, keeping the mass flow rate of air constant for several tests, but to increase or decrease the feed rate of material into the pipeline, depending on whether or not the material showed signs of blocking. The signs are usually that the pressure starts to rise along the pipeline and then suddenly drops, followed by loud noises as the pipeline vibrates as slugs of material arising from saltation, travel along the line and hit the bends. The results were stored from each test run, to be examined at a later date when several test runs had been completed.

A4.3.1.1 Pressure data scanning rates - initial investigation

Upon examination of the commissioning test results, it was apparent that about half the data was unusable; a steady state period could not be identified as the pressure was fluctuating unacceptably. This appeared to be because the time period programmed for taking pressure readings for each test run, was insufficient for gathering the data before the pressure stabilised after the start-up transient. Therefore, the time interval for scanning the pressure transducer channels for data was increased from 1 to 2 second intervals for the next series of tests, for the same number of readings. The subsequent results were also unsuitable in that they were unsteady during some periods, and the tests were therefore repeated. On that occasion 200 readings were taken at 2 second intervals, which recorded almost the complete test run. Only one test was completed and processed, and it was relatively easy to find a steady state period. However, there was a problem when it came to printing graphs that used all the processed data, in that there was insufficient memory for the task, and therefore most of the data had to be deleted. As a consequence, a reduced number of 150 readings were taken during subsequent tests at 5 or 7 second intervals.

A4.3.1.2 Cycling effect on test results

At low solids feed rates occurring with a speed of less than 20 r.p.m. using the screw feeder, a cycling pattern appeared on the raw data graphs at a period between 60 to 70 seconds. To discover the cause of this effect, an investigation was carried out. The obvious explanation of pulsations from the screw feeder was at this stage rejected, as the period of oscillation of pressures was much larger than that of the rotation of the screw (60 to 70 seconds as opposed to 6 seconds for a screw speed of 10 r.p.m).

Initially, it was thought that the cycling was attributed to the air compressors periodically cutting in during a test run, as the timings seemed to coincide with the pressure peaks. Three compressors were used to supply compressed air to the rig, and the compressed air was stored in an air receiver. The compressors turn on and off continually during operation to keep the pressure of air in the receiver within limits, then a regulator is used to keep the pressure constant at the choked flow nozzle bank which meters the air to the test rig. To prevent the compressors turning off, the exhauster vent on the top of the air receiver was opened slightly to damp the excess air from the compressors, so that the pressure in the air receiver could not reach the upper limit and cause the cut out of the compressors. However, although this action guaranteed that the pressure upstream of the nozzle bank did not fluctuate, it did not eliminate the pressure fluctuations along the conveying pipeline. The exercise

was also repeated with the regulator fully open so that the air was not regulated from the compressor. Again, this had no effect on the results.

A4.3.1.3 Air only tests

A series of tests were carried out in order to confirm whether or not the compressors were responsible for the pulsations on the pressure transducers. Each test from **a** to **d** below was repeated for two different mass flow rates of air, without conveying any material during each test. As no solids were being conveyed, the scanning rate of the pressure transducers was reduced to 1 second intervals because it was not necessary to obtain data over a long period.

a air only
b air only and screw rotating
c air only with the exhauster vent on the air receivers open
d air only with a pressurised blow tank and the screw rotating

In every case, all the pressure transducer signals were stable with the pressure in the pipeline. Therefore, it was concluded that the use of compressors, or the motor controlling the screw conveyor, had no effect on the pressure signals.

A4.3.1.4 Alterations of air line to blow tank

When material is in the blow tank, there is a relatively large amount of empty space between the product and the top of the tank. When the product is discharging into the conveying line, the vacated space is increasing. It was thought that the increased empty space in the blow tank may have affected the pressure balance across the screw, causing the pulsations. For this reason, the air into the top of the blow tank was blanked off to see if it would eliminate the pulsations, or at least reduce them (see diagram of air distribution to the blow tank in appendix 3).

Seven conveying tests were completed after the air to the top of the blow tank had been sealed off. The results were compared to identical tests carried out before the alteration to the air line. The results showed that there was very little difference between them, so the airline was reconnected to its original configuration.

A4.3.1.5 Conveying line improvement

At the start of the conveying line, material fell into a drop out box from the screw feeder. Air was introduced into the drop out box, which entrains the material and carries it into a 50 mm nominal bore pipeline. At the end of the drop out box, a bend rising to a vertical pipe was the beginning of the conveying pipe line (see diagram A4.1).

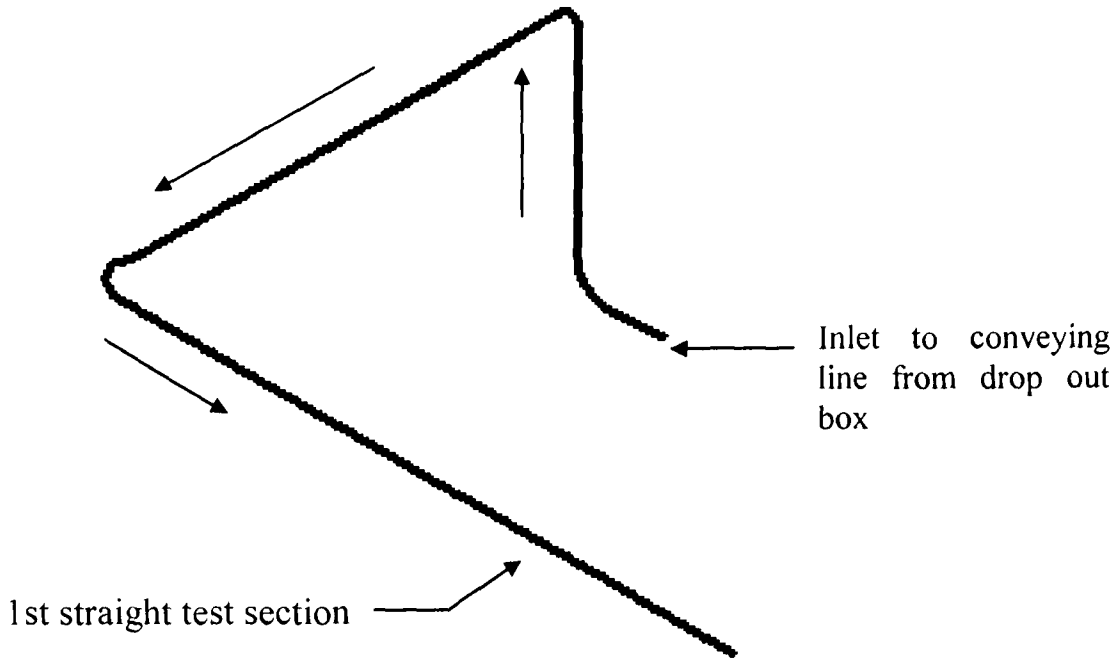

Diagram A4.1: Conveying line from the drop out box to the 1st straight section

It was thought that the pulsations may have been due to the vertical pipe being too close to where the material was introduced into the conveying line. The suspicion was that if the material has not reached the same velocity as the air (or as near as can be [L3]) the material may be building-up at the bottom of the vertical pipe. Once material has blocked the line, the pressure behind the obstruction would build up and force the material along the conveying pipeline, thus causing a cyclical build-up and drop-off in pressure.

In order to overcome this suspected problem, the design of the conveying line from the drop out box was altered. Instead of a vertical bend leaving the drop out box section, a horizontal bend leading into 3 metres of horizontal pipeline was installed (see diagram A4.2). A large radius bend then led into a vertical section to bring the pipeline to the elevation of the test section.

Following the alterations, several test runs were completed. The results showed that the pulsations still occurred.

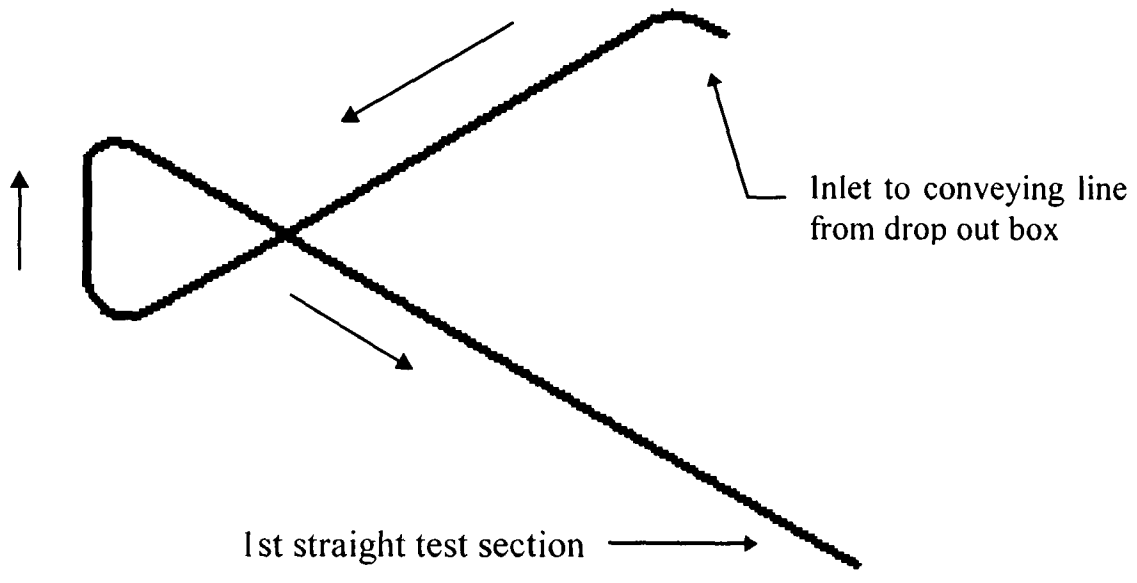

Diagram A4.2. Revised conveying line inlet sections from drop out box to 1st straight section

A4.3.1.6 Aliasing effects in pressure signals

In the continuing search to discover why the pressure pulsations occurred during each test, the frequency of the scanned data was re-examined. The cycling period of the data was 58 seconds. In order to obtain results for each test run over a long time period, and still be able to plot the data, the time intervals for each scan had been set between 5 and 7 second intervals per test run (from the investigation in section A4.3.1.1). However, during the air only test runs, the transducer scanning time intervals had been set at 1 second over a shorter period, because it was not necessary to obtain as much data as possible if no solids were conveyed.

A solids conveying test was carried out which scanned at 1 second and also at 7 second intervals. Graph A4.1 shows the data from pressure transducer number one which was scanned every 7 seconds. This appears to show a cyclical fluctuation at a period of 49 seconds. Graph A4.2 shows data from the scanning intervals of both 1 and 7 seconds. The graph of data taken at 1 second intervals reveals a cycling frequency of 7 - 8 seconds. The 7 second interval signal has been overlaid on the 1 second scanning signal, and the data points clearly show how delaying the scanning rate gives misleading results, suggesting a cyclical variation with a 49 second period which is actually not present.

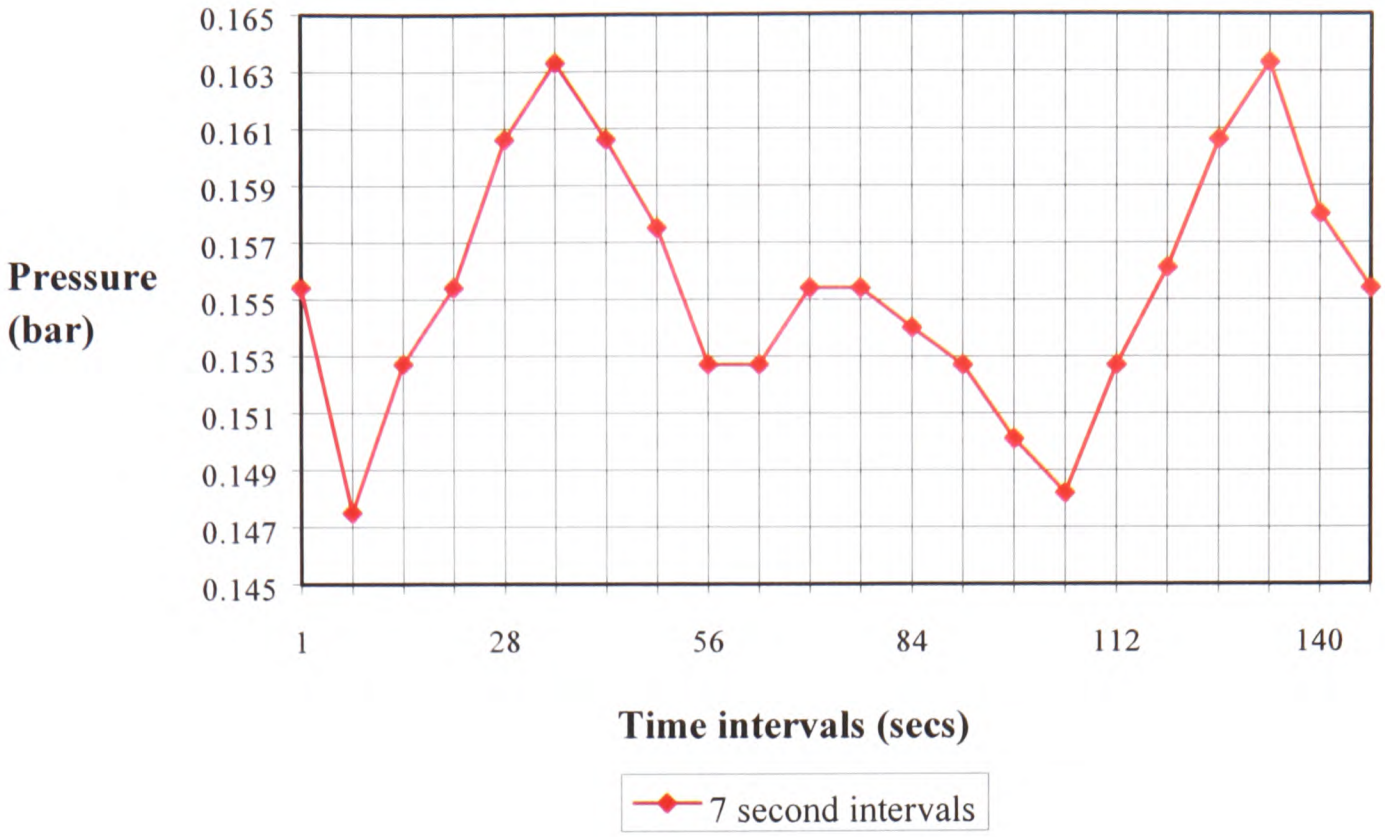

Graph A4.1: Data from pressure transducer number 1, scanned at 7 second intervals.

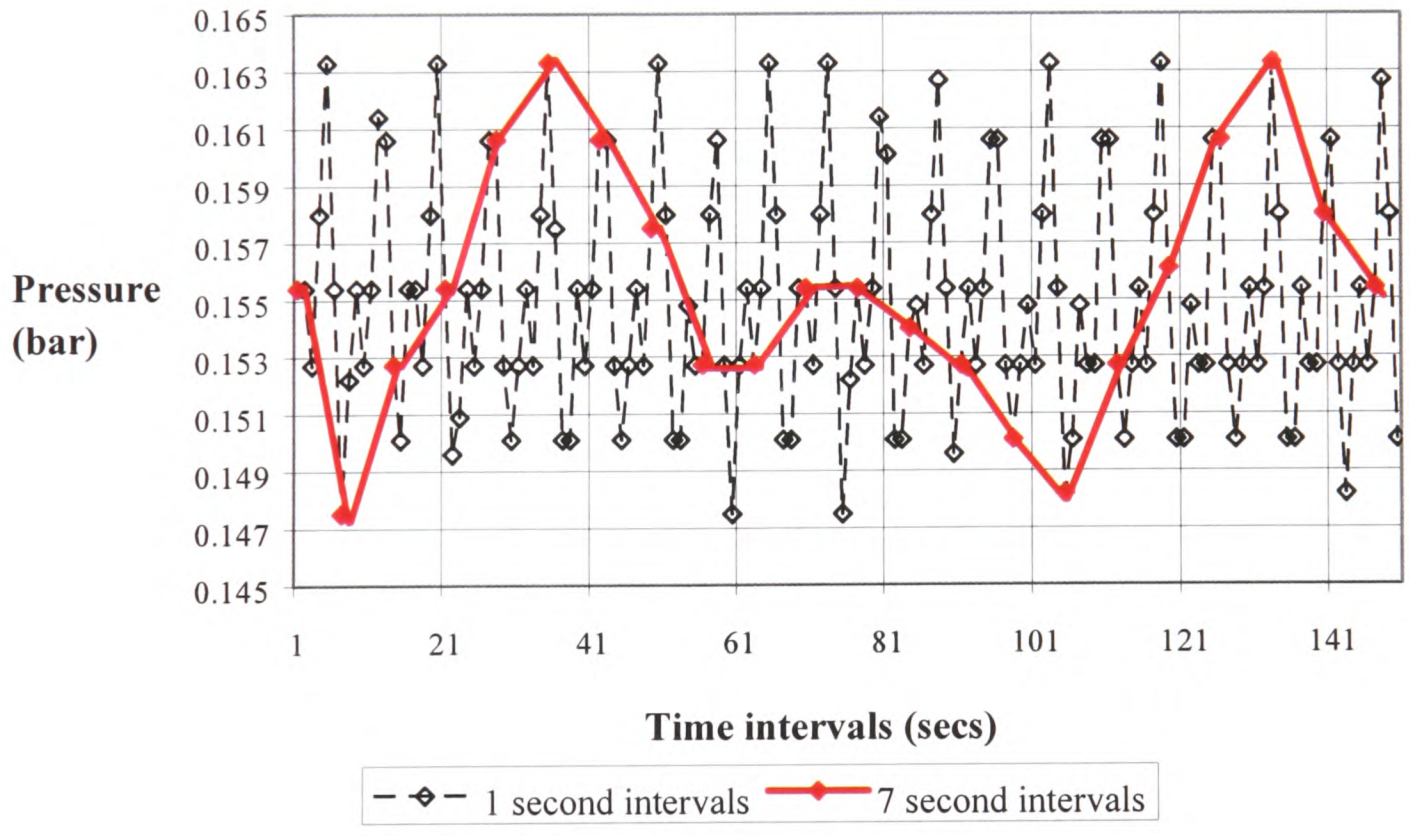

Graph A4.2: Results of scanning transducer number one at 1 and 7 second intervals during a test run.

The cycling visible on the graphs with 7 second scanning intervals, appeared to be of a low frequency, whereas it was actually much higher i.e. equal to that of the rotation of the screw. The rotation of the screw gave pulsations in the discharge of solids into the conveying line, which had appeared as pulsations in the pressure along the pipeline.

During the test, the screw rotation was set at 8 r.p.m. This gives a period of 7.5 seconds for one revolution of the screw. The generation of false signal frequencies caused by sampling at a rate lower than the Nyquist rate or two times the maximum signal frequency is known as Aliasing. The Nyquist frequency is the maximum signal frequency allowed in a sampling process before the reconstructed signal is aliased, 1/2 the sampling frequency.

The problem was explained and all future scanning rates were set at 1 second intervals to eliminate the aliasing effect.

A4.3.2 Blockages in bends

A4.3.2.1 Conveying line alterations and limitations on conveying conditions

During the commissioning of the modified test rig, it was found that the pipeline blocked at air mass flow rates much higher than the expected minimum conveying velocities of 4 m/s for the pellets (based on the experience from the previous user of this material). The blockages started at the end of the pipeline, and the pipeline configuration was thought to be part of the problem. During the commissioning test runs, at the end of the conveying pipeline, were two 90 degree bends separated by a short length (less than one metre) of vertical pipe, which was closely followed by a slightly longer length of vertical pipe leading into the receiving hopper.

When material fully entrained in air enters a bend, the impact of the material hitting the bend reduces the velocity of the particles as energy is transferred from the particles to the pipe wall [B4]. On leaving the bend, the particles accelerate to almost the velocity of the conveying air, if the straight section following the bend is of a sufficient length [R3]. Therefore two bends close together give the material inadequate time to recover from the impact of the first bend before entering the second bend. As a result, the material leaves the first bend travelling slowly and is almost immediately slowed even further by the second bend. In turn this gives rise to an area of excessively high concentration of particularly slow moving material just after the second bend, which is then a preferential place for blockages to develop.

For the reason stated above, the two separate lengths of vertical pipe were replaced with one vertical section, using larger radius bends and a long sweeping bend leading into the receiving hopper. To reduce the number of bends, an additional entrance to the receiving hopper was also created. The changes to the pipeline are illustrated in diagrams A4.3 and A4.4, shown overleaf.

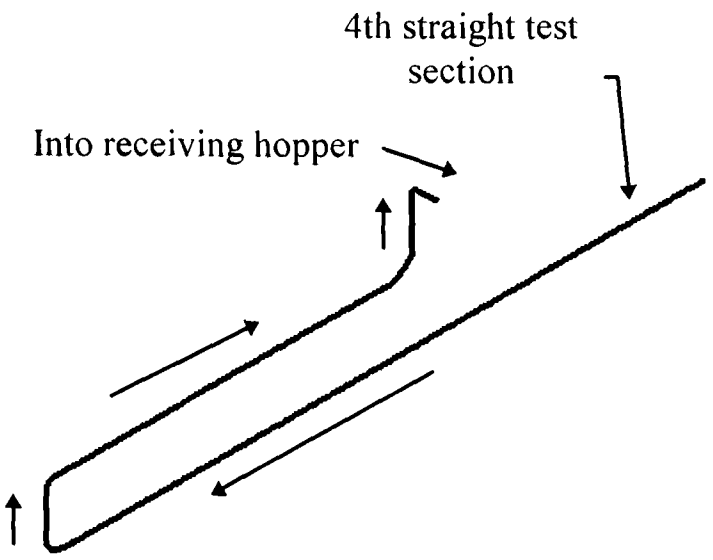

Diagram A4.3. Previous layout

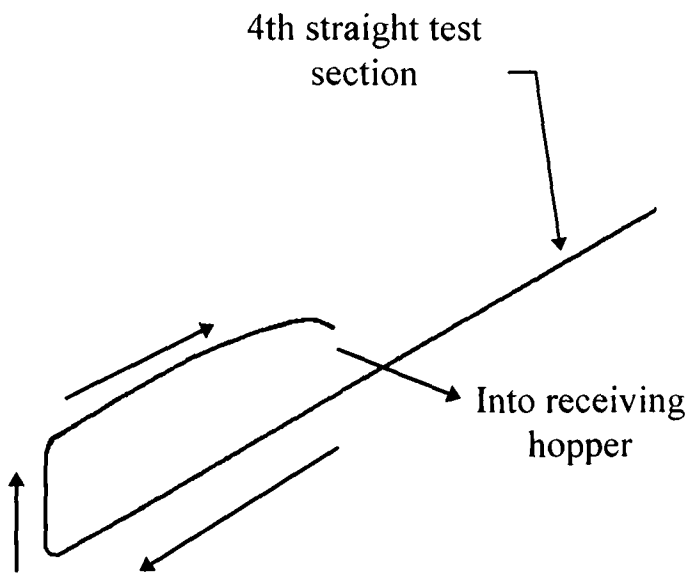

Diagram A4.4. Revised layout

Once the alterations had been completed and test work resumed, the pipeline still blocked at air velocities much higher than previously observed when the same material was pneumatically conveyed during previous research. It was concluded that the modified test rig with the screw feeder replacing the blow tank as a feeder, would not convey this particular material in 'dense phase' at input velocities of less than 10 m/s, with solids loading ratios not greater than 7. It would still be possible to convey this material over the expected range of lean phase conditions, but not the dense phase conditions.

The term 'dense phase' or 'non-suspension' flow refers to the mode of conveying in which the particles are not fully suspended in air while being conveyed along the pipeline, but travel out of suspension along the bottom of the pipeline, or in "slugs" or "plugs". 'Lean phase' or 'suspension flow' conveying is the term applied to a flow in which the solid particles are fully entrained in a gas in an almost homogeneous suspension during pneumatic conveying.

The consequences of measuring 'lean phase' conveying conditions only for the initial test material, meant that the full range of conveying conditions could not be compared for all the materials in the test program. It was also known that at least two other materials in the test program would not convey in dense phase either, based on the experience of others who had conveyed the material for other projects. Therefore, the comparison between all the test materials would be limited to 'lean phase' conveying only, although tests on each material would try to convey in dense phase so that a full range of conveying conditions for each material would be available for future use.

This did not present a problem to the test program, because although more research has been completed for 'lean phase' conveying, comparisons between as many materials as planned for this project, had not been researched even in lean phase only.

A4.3.3 Straight sections pressure gradient

The rig employed a pipeline that had four consecutive straight sections with a number of pressure tappings along each section. During each test run, the pressure at each point along the pipeline was recorded as material was conveyed.

The results of the initial tests showed that the pressure gradient for each straight test section was different. This was not altogether unexpected before the tests were carried out, because of the change in conditions from one straight section to the next. That is to say, as material is conveyed along a pipeline the air velocity increases while the pressure, suspension and air densities decrease. However, it was expected that the pressure gradients in the four straight sections would follow a pattern, in that the pressure gradients would either consistently increase due to the increased air velocity, or consistently decrease due to reduced suspension density.

An example of the pressure gradients from an early test run (10100) is shown in graph A4.3 and is representative of all the processed test data up to this point. The gradients appear inconsistent in their pattern along the four straights of the test section, which makes it difficult to decide how to fit a gradient rationally to all four straight sections. The initial view that the first two gradients along the straight sections may be similar, was based on the work by Bradley [B1] who using one test bend between two straight sections, fitted the same gradients to both straight test sections in order to determine the pressure losses caused by a bend.

From the results shown in graph A4.3, for the 1st and 2nd test sections, the pressure gradients increase, but the 3rd section shows a reduced gradient compared with the previous section. The 4th pressure gradient is in keeping with the 1st and 2nd sections gradient in that it has a further increase in pressure gradient in keeping with the first two sections. The values for the pressure gradients are shown below, calculated using the least square best fit method through the averaged data points from each transducer.

Number of straight section	1	2	3	4
P gradient of straights (bar_g/m)	-0.002228	-0.003513	-0.003123	-0.004339

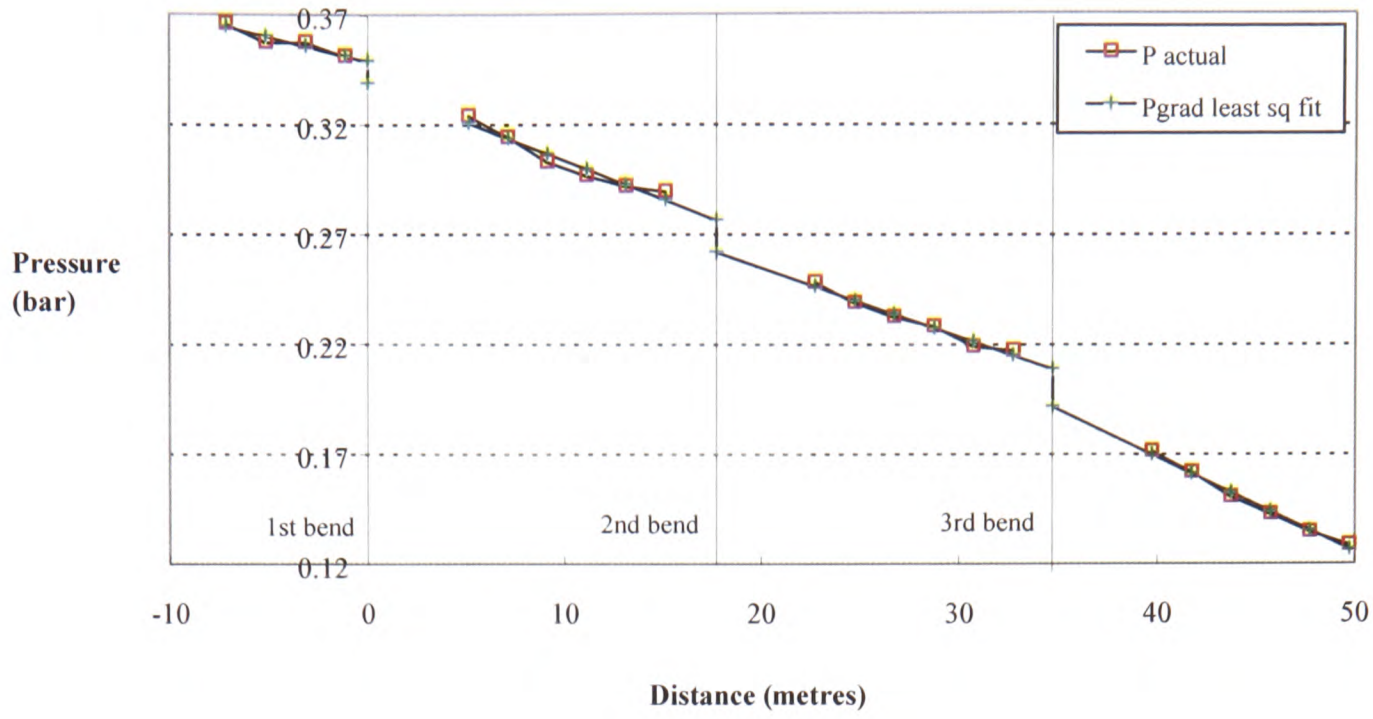

Graph A4.3: Showing the pressure transducers versus distance, with straight lines drawn through the data points for each test section. The test number was 10100 using polyethylene pellets.

A4.3.3.1 Investigation of possible causes of irregular gradients

There were three possible explanations as to why the pattern of pressure gradients appeared as described and shown on graph A4.3. They were:-

1. The pressure transducers were incorrectly fitted on to the tappings and giving false readings.
2. The assembly of the test rig could be causing these effects through misalignment, and/or variations in the horizontal pipeline level.
3. This could be a true representation of what really was happening in the conveying system, in that the pressure gradients do not follow a consistent reduction or increase in pressure for consecutive straight sections.

The conveying pipeline was made-up from several straight lengths of pipelines and bends. When the test rig was modified, this necessitated the installation of some new sections of pipeline and bends. All three bends within the test section were formed in an identical way from the same length of mild steel pipe. Most of the original pipeline joints used screw fittings, while all the test bends and the newly installed straight sections were joined using 'Morris' sleeve couplings. These couplings enabled a relatively smooth internal fitting to be achieved if installed carefully, as well as being fairly easy to install. As the intention during the test program was to interchange bends, and the

replacement of test bends when they wore out would be necessary considering some of the abrasive materials in the test program, this was an important factor. A diagram of the test section is shown below.

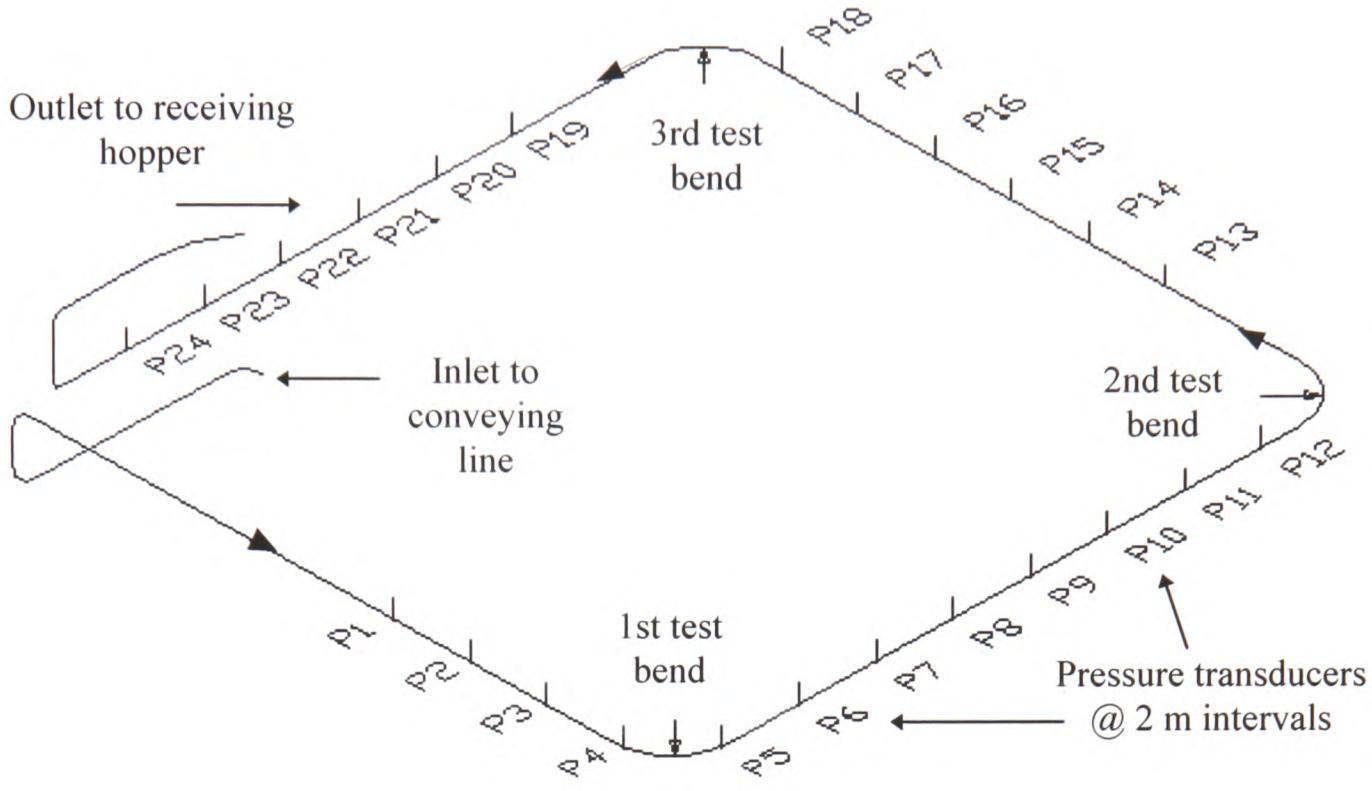

Diagram A4.5: Layout of the pipeline loop.

To try and discover the reasons for the irregularity of the pressure gradients, a number of options were identified for investigation and are listed below,

a. Interchange all the pressure transducers on the 3rd test section with those on the 4th section.
b. Interchange test bends 2 and 3 and repeat some test runs to compare the results.
c. Examine the test section of the conveying pipelines in detail. In particular the wall thickness of each section of pipe, joins, internal pipe surfaces, internal seam positioning and internal seam roughness. This exercise would also identify any gaps between the pipe ends at the joins, the positioning of the pipe seams in relation to the pressure tappings, and the degree of roughness of the internal seams and internal pipe surfaces.
d. Change the initial test material of polyethylene pellets to another product. If the same pattern of pressure gradients occured, this would show whether or not the problem is a function of the system or the conveyed material.
e. Revert back to the original blow tank system to compare the pressure gradients. This would involve taking the screw feeder out and putting the bottom of the blow tank back.

As calibration tests on the pressure transducers were carried out after any alterations to the test rig, there did not seem any point in performing the first option. The investigation therefore started with interchanging the test bends.

A4.3.3.2 Interchanged bends

Although all three test bends were as similar as possible, being made from the same length of pipe and formed to identical specifications, the 2nd and 3rd test bends were interchanged to determine any effect on the test results. When the 3rd test bend was installed in the 2nd test bend position, it was found that the bend did not completely meet the connecting straight section. The 2nd straight section of pipe had been moved, and due to the length of 17 metres, made it difficult to move back into position. Thus, a small piece of pipe, 20 mm in length was inserted, to bridge the gap. This was possible because a Morris coupling was already being used to connect the straight pipe and test bend together, and would cover the joins in the pipe, thereby eliminating the previous gap.

The results of the next set of test runs showed that the pressure drop at the 2nd test bend which had always been the greater of all three bends, was now reduced, and this made the pressure drop at the 3rd test bend appear more in keeping with the first two test bends. Before the bends were interchanged, the pressure gradient along the 3rd straight test section almost always appeared to be not as steep as the previous section, resulting in a reduced pressure gradient, for very low solids flow rates, which is explained in appendix 3. However, the pressure gradients in the 3rd and 4th straight sections, had not altered by interchanging the bends. The percentage difference between all the gradients was still similar.

A4.3.3.3 Conveying line inspection

In view of the fact that the pressure gradient in the third straight test section still did not follow the pattern of the other three straight test sections, it was necessary to carry out a more detailed investigation of the pipeline, both internally and externally.

Each straight element within the test section of the test rig was in excess of 16 metres in length. It was not possible to construct pipe runs in continuous lengths, therefore it was necessary to join sections of pipe with either "Morris" sleeve couplings or screw couplings. There was also a mixture of old and new pipe work in some parts of the system, due to the pipeline re-configuration. For these reasons, there was a possibility that the properties of the conveying pipeline varied in different parts

of the rig, and that these variations contributed to the inconsistent pressure gradients. This suggested a closer inspection of a number of areas, listed below:-

- Measure all sections of pipeline to determine whether they all had the same wall thickness, which would affect the internal diameter of the pipe. The pipe used for the rig is manufactured to specific standards of external diameters so that it is uniform and fittings are bound to fit. The primary tolerance is on the outside diameter i.e. ± 0.05mm, and the tolerance on wall thickness is that it should not be less than 3.6mm thick, while the positive tolerance is unlimited. The internal diameter may differ if the thickness of the pipe is not consistent along its length.

- Check all pipes are circular in section.
- Ensure the pipes were butted properly together at joints.
- Measure the pipeline level along each straight test section to ensure that each section is level.
- Determine the internal surface roughness for each straight test section.
- Examine the internal seam for each straight length of pipe, and note the position of the internal seam in relation to a clock position and severity of the flash inside the pipe.

When the above tasks were carried out, it was found that the joints were tightly butted together, the pipes were of the same thickness and the pipes were circular and level. There was a length of pipe on the 4th section that was unsupported for quite a long run. This was rectified by welding a bracket on to the framework and securing the pipe.

The internal inspection of each length of straight pipe revealed that most of the pipeline consisted of old pipe which was still fairly rough to touch on the internal surface, similar to a fine grade sandpaper roughness. There was one new section of pipe along the fourth straight test section, and the bends were also constructed from new pipe. The new pipe was smoother on the walls than the older pipe, but the seams were very jagged with small bits of protruding sharp metal, approximately 1mm high. The seams on the older pipe were almost smooth to the wall of the pipe, having been worn down beforehand during previous conveying of other materials. There was one small section at the beginning of the fourth straight, where the seam was almost completely smooth. There was only one pressure transducer installed in that section.

All three bends had seams on the inside of the bend which were very rough, but as the material accumulates along the outside of the bend, the seam was expected to have little effect on the pressure drop caused by the bends.

The pipe joints were disconnected to determine the positioning of the internal pipe seam, the results for the straight sections were as follows:-

1st straight section

The first four transducers were installed in this section, and the seam was near the top of the pipe at 10 o'clock looking upstream.

2nd straight section

This section had two screwed couplings which made it difficult to take apart for examination. Therefore, the seam position in the middle sections was unknown. However, the two outer sections had seams in the same position at 4 o'clock.

3rd straight section

The seam positions and condition was the one of most interest, as the pressure gradient along this section was not as steep as expected when examining all the results together. The seams were all at the top of the pipe. This may indicate that any material traveling along the lower region of the pipe does not have the problem of the seam to cause additional friction losses.

4th straight section

The last section had a length of new pipe which had a very rough seam. The position of this seam was at the bottom of the pipe at 6 o'clock, and there were three transducers in this section. The pressure gradient in this section was very steep when compared to the previous straight section.

A4.3.3.3.1 Conclusions of internal pipeline seam position investigation

All the seam positions in the third straight were at the top of the pipe, while a length of pipe in the 4th straight had a very rough seam at the bottom of the pipe. This was suspected of possibly being the reason for the inconsistency of the pressure gradients for the pellets between each of the straight sections, i.e. less frictional losses where the seam is at the top of the pipe, in contrast to a very rough seam at the bottom of the pipe in the following section.

A4.3.3.4 Rotation of straight pipe in last test section

The section of pipe in the 4th straight test section which had three pressure transducers fitted on it, had its internal seam positioned at the bottom of the pipe. This was suspected of being the main contributory factor for the pressure gradient along this section being so much greater than for the previous straight test section. For this reason, the section of pipe was rotated by 90° so that the seam position was on the side of the pipe. It was considered that the location of the tappings on the side of the pipe would not affect the pressure readings, as all the material in this section of the test rig would be fully entrained in air traveling at relatively high velocities, and the pressures would be uniform in the cross section.

A4.3.3.4.1 Results of pipe rotation experiment

Seven of the tests carried out before the pipe was rotated, were repeated in order to compare the results and determine whether or not the seam position made any difference to the pressure gradient in the 4th straight section. Graphs plotted showed that the pressure gradient for the last straight section was more as expected in that the gradient was not as steep as the pre pipe-rotation tests. From seven test runs, five tests when compared to those carried out under similar conveying conditions, showed from 3% to 38% reductions in pressure gradients.

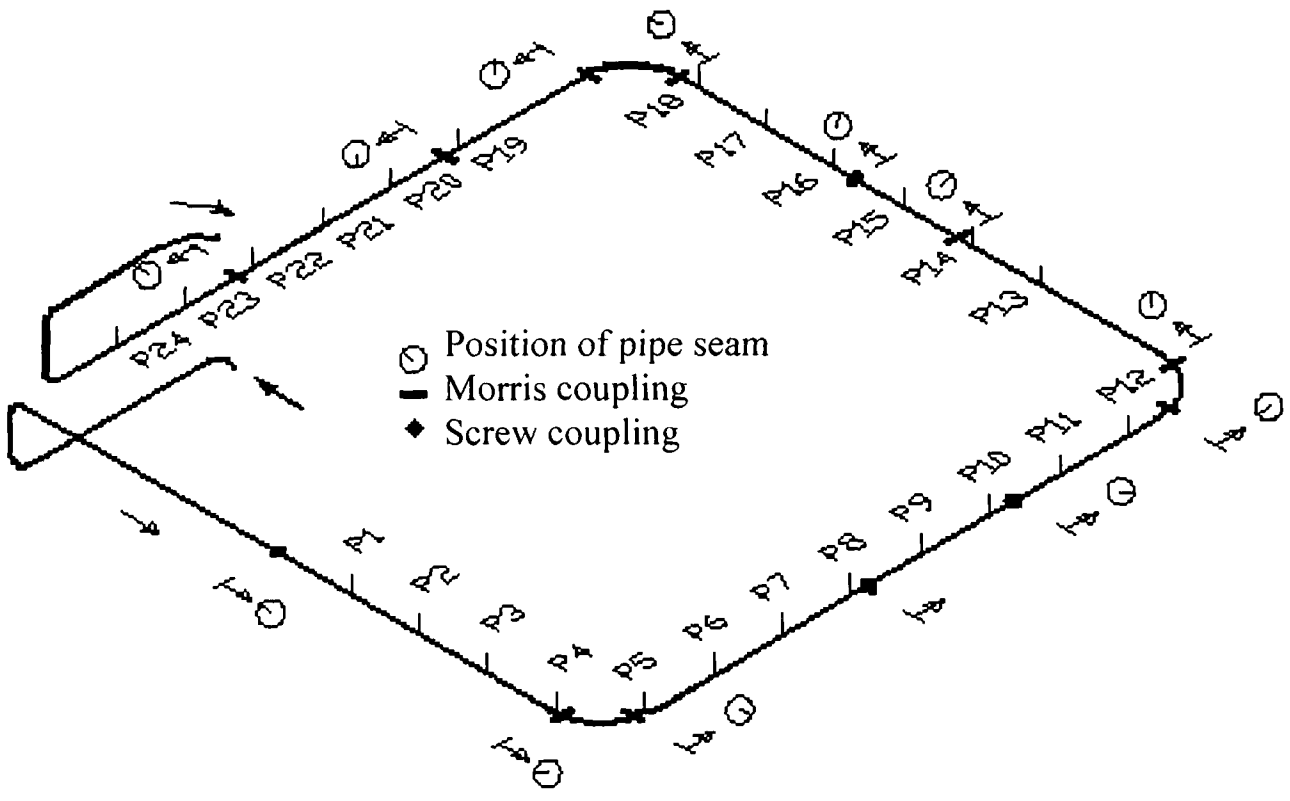

Diagram A4.6 showing pipe seam positions

Table A4.1

Test No.	Pressure gradient (-mbar/m)		Mass air kg/s	SLR	Percentage difference between gradients	
	3rd straight section	4th straight section			Before pipe rotation	After pipe rotation
10105	1.8399	3.01569	.0497	10.3	38%	
10125	**1.95867**	**2.2999**	**.0497**	**11**		**14.8%**
10111	2.88766	3.97711	.0808	7.2	27%	
10131	**3.2917**	**3.78022**	**.079**	**6.9**		**12.9%**
10112	3.68282	4.57158	.0808	11.2	19%	
10132	**3.65929**	**4.03759**	**.079**	**10.3**		**9%**
10102	1.968547	2.03125	.0673	3.2	3%	
10133	**1.688152**	**1.86723**	**.0664**	**3.3**		**9.6%**
10108	2.86193	3.03332	.0673	7.8	5.6%	
10134	**2.51697**	**2.77724**	**.0664**	**8**		**9%**
10100	3.68305	4.19744	.0673	12.8	12%	
10135	**3.22305**	**3.43596**	**.0664**	**12.9**		**6%**
10103	2.47934	2.78966	.0552	10	11%	
10136	**3.22305**	**3.43596**	**.0551**	**15.5**		**6%**

A4.3.3.4.2 Conclusions

71% of the tests repeated showed a marked improvement after rotating the pipe.

A4.3.3.5 Air only conveying tests

The last test on the pipeline was to carry out air only tests with no products being conveyed, to see whether the pipeline configuration was the cause. The results were that some tests appeared to show a maximum pressure difference of ± 4.2 mbar across the second and third test bends. However, the tests showed that the differences between the gradients slightly increase with the mass flow rate of air, as shown on the graph A4.4.

The increase in the pressure gradients at higher mass flow rates of air, did not show cause for concern because of the relatively small increase in pressure. The values for the air only tests are shown on table A42 below, and the results displayed on graph A4.4.

Table A4.2.

TEST	Product	P gradient of straights (bar)				Mass	P loss
No.		1	2	3	4	air (kg/s)	system (bar)
10127	Air only	0.001255	0.001250	0.001245	0.001240	0.06641	0.132
10128	Air only	0.001646	0.001695	0.001745	0.001794	0.07900	0.179
10129	Air only	0.000953	0.000969	0.000985	0.001000	0.05512	0.095
10130	Air only	0.002385	0.002487	0.002589	0.002691	0.09399	0.270

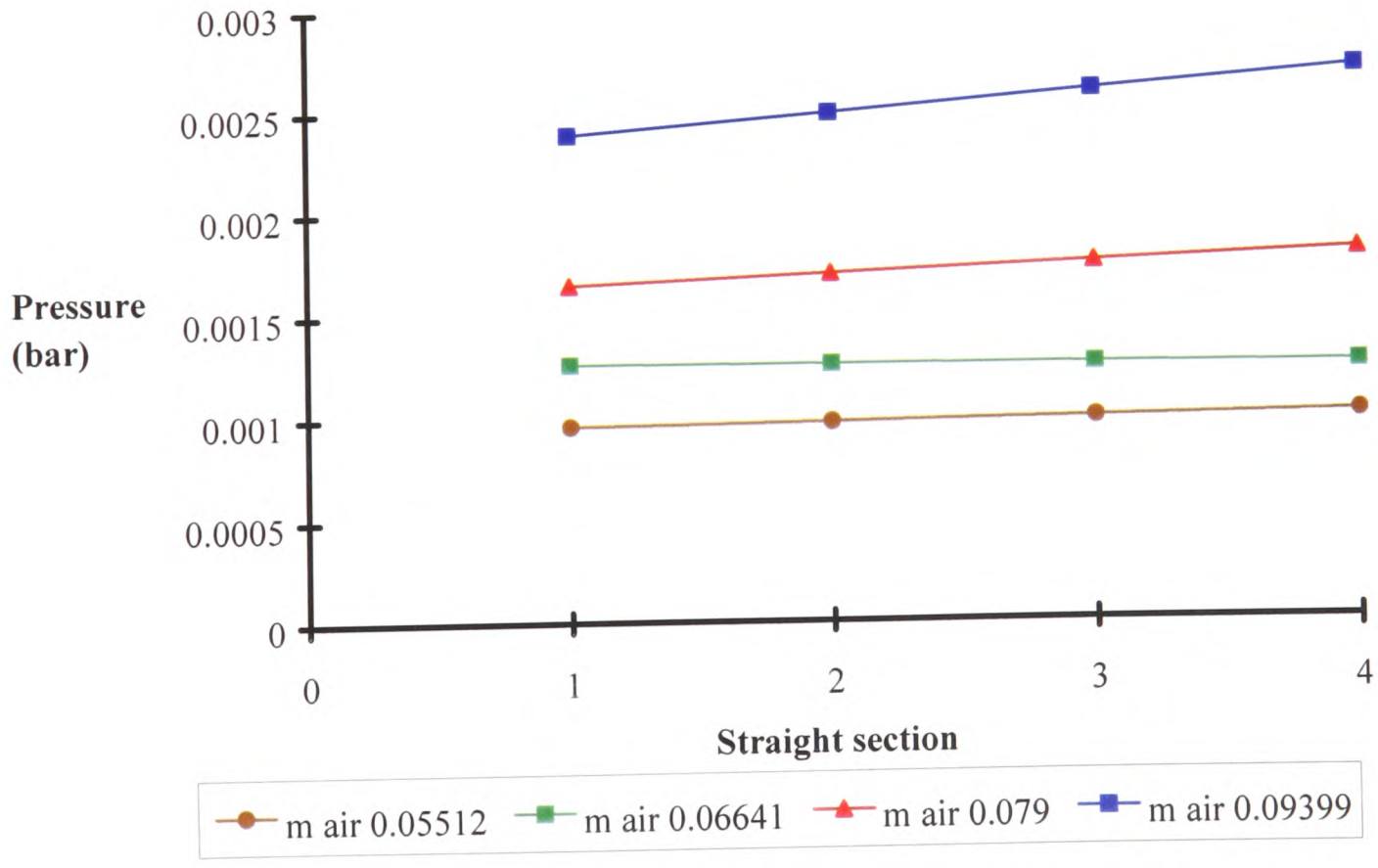

Graph A4.4: Results from the air only pressure gradient tests.

A4.4 Conclusions of trials

Regardless of the fact that the pipe rotation had improved the pressure gradient along the last straight test section, and that fitting the small length of pipe to cover the shortfall between the end of the second straight test section and second test bend, had reduced the pressure losses across that bend, the pressure gradient along the third straight test section was still showing inconsistent gradients when compared to the other test sections.

Following the investigations, the test runs were completed on the pellets and the material changed over. Enough tests had been carried out using the polyethylene pellets to cover the full range of conveying conditions that were possible within the constraints of the test rig. If the test rig was at fault, it could not be identified, so changing the material may induce other ideas on how to eliminate the problem or analyse the results to compensate for it.

In conclusion, the pellets were not altogether the most suitable material for commissioning the rig, because the small pressure losses attributed to this product accentuated the problems with the inconsistent pressure gradients along the straight test sections, and the pressure losses caused by the bends for low solids loading ratios. This made it difficult to find a trend relating to the pressure gradients along all four consecutive straight sections, and finding a suitable way to identify the pressure drop caused by bends. The problem continued throughout all the test work, but was not so apparent with the remaining materials because they gave higher pressure drop values, so that the small inconsistencies were less significant in relative terms.

The commissioning of the modified rig was completed satisfactorily, in that it was capable of measuring the pressures along the extended test section and the screw conveyor produced the consistent and controllable mass flow rates of solids required.

Appendix 5

Software used for data gathering and analysis

A5.1 Introduction

The software that was designed as part of the pre-existing test rig was written to be used with a BBC Microcomputer. This was considered outdated in comparison with the type of computers used at the start of the project, predominantly IBM compatible. The transfer from using a BBC Micro to an IBM computer, not only meant a change in software so that the data logger could communicate with the host computer, but the software used for processing and analysing of data would also need re-developing if the BBC Micro was no longer used with the test rig. The data logger was a stand alone unit which had in-built intelligence, giving it the ability to run measurement and control programs on demand from, but independent of, the host computer. It communicated with the computer via a serial RS423 link.

The software developed can be divided into three areas:-

- for controlling the data acquisition unit,
- for performing the primary processing of data,
- to analyse data and draw graphs.

The software development process was one of evolution using a variety of software packages, which were chosen for practical reasons. The software for control of the data logger was purchased from the company who manufactured the unit; the software for primary processing of raw data had been used already in other research at The Wolfson Centre, therefore some knowledge of using the package was on hand; the graph plotting and analysis software was university standard.

A full copy of the raw data, processed and analysed results are on a CD which accompanies this thesis.

A5.2 Software for controlling the data acquisition unit

The data acquisition unit manufacturers (Mowlem Microsystems) supplied their own software called Dialog. The software had primary functions such as defining signal types for input channels and analogue gain ranges for the analogue input channels; the definition and initiation of tests in the unit, and templates (i.e. calibration factors to be applied to the raw data bits to obtain values in engineering units) and the transfer of measured data from the unit to the host computer for storage.

There were some minor changes from the original BBC microcomputer software, to the IBM compatible computer software, but the main differences were necessitated by the increased number of channels that were to be monitored. A total of 27 channels were to be scanned during each test run. The channels included 24 pressure transducers positioned along the test section, whilst the remaining three channels monitored the pressures at the blow tank and upstream of the nozzle bank, and the load cell output from the receiving hopper. This required three separate tasks to be initiated simultaneously for each test run, because the data logger could not receive the instructions to scan the large number of channels required in one test specification. The raw data from each task was transmitted and stored separately.

A5.3 Primary processing of data

A5.3.1 Software

To store the raw data for processing, a spreadsheet software package called Quattro Pro was used. Four spreadsheets were activated to process and store the data from each test run. These were all linked together so that calculations from one sheet could be automatically imported to the next sheet.

Initially, all three task files from Dialog (the data acquisition unit software) were imported separately into the first spreadsheet, and the data from each channel (usually 150 readings) were displayed. There were 24 transducers providing pressure values on the pipeline, plus blow tank pressure and the pressure upstream of the choked flow nozzle bank. In addition, there were the output readings from the load cells which monitored the mass flow rate of solids in the receiving hopper. An example of the first spreadsheet with all 27 channels and their data values is shown on the following two pages.

A5.3.2 Input data worksheet

Transducer No.	P1	P2	P3	P4	P5	P6	P7	P8	P9	P10	P11	P12	P13
Distance (metres)	-7.13	-5.13	-3.13	-1.13	1.13	3.13	5.13	7.13	9.13	11.13	13.13	15.13	22.73
Average reading (bar)	0.51	0.51	0.50	0.50	0.49	0.46	0.44	0.42	0.42	0.40	0.40	0.39	0.32
Steady state average (bar)	1.16	1.15	1.13	1.12	1.05	1.02	1.01	0.98	0.96	0.93	0.93	0.89	0.73
Time (sec) 1	0.47	0.46	0.45	0.45	0.44	0.41	0.40	0.38	0.36	0.35	0.32	0.33	0.28
2	0.48	0.47	0.47	0.46	0.45	0.42	0.40	0.38	0.38	0.36	0.37	0.34	0.29
3	0.49	0.49	0.49	0.48	0.47	0.44	0.42	0.40	0.40	0.38	0.42	0.36	0.29
4	0.50	0.50	0.50	0.49	0.48	0.45	0.43	0.42	0.41	0.40	0.43	0.38	0.30
5	0.51	0.51	0.50	0.50	0.49	0.46	0.44	0.42	0.42	0.41	0.42	0.39	0.31
6	0.50	0.50	0.50	0.49	0.48	0.46	0.44	0.42	0.42	0.41	0.39	0.39	0.31
7	0.49	0.49	0.48	0.47	0.46	0.43	0.42	0.40	0.38	0.38	0.32	0.36	0.31
8	0.48	0.48	0.47	0.46	0.45	0.42	0.41	0.39	0.38	0.36	0.36	0.34	0.29
9	0.49	0.49	0.48	0.48	0.47	0.43	0.41	0.40	0.39	0.37	0.38	0.35	0.30
10	0.50	0.50	0.49	0.49	0.48	0.45	0.43	0.42	0.41	0.40	0.44	0.38	0.30
11	0.51	0.51	0.50	0.50	0.49	0.46	0.44	0.43	0.43	0.41	0.43	0.39	0.31
12	0.51	0.51	0.51	0.50	0.49	0.47	0.44	0.43	0.43	0.41	0.42	0.40	0.32
13	0.50	0.49	0.49	0.48	0.47	0.44	0.43	0.40	0.39	0.38	0.34	0.36	0.31
14	0.50	0.49	0.49	0.48	0.47	0.44	0.42	0.40	0.39	0.38	0.37	0.36	0.30
15	0.50	0.50	0.49	0.49	0.48	0.44	0.42	0.41	0.40	0.39	0.41	0.37	0.30
16	0.51	0.51	0.50	0.50	0.49	0.46	0.44	0.42	0.42	0.41	0.44	0.39	0.31
17	0.52	0.52	0.52	0.51	0.50	0.47	0.45	0.43	0.44	0.42	0.44	0.40	0.32
18	0.52	0.51	0.51	0.50	0.49	0.47	0.45	0.43	0.43	0.42	0.41	0.40	0.32
19	0.51	0.51	0.50	0.50	0.49	0.45	0.43	0.42	0.40	0.39	0.36	0.37	0.31
20	0.51	0.51	0.50	0.49	0.48	0.45	0.43	0.41	0.40	0.39	0.39	0.37	0.31
21	0.50	0.50	0.49	0.49	0.48	0.45	0.43	0.41	0.41	0.40	0.41	0.38	0.31
22	0.52	0.52	0.52	0.51	0.50	0.47	0.44	0.43	0.43	0.42	0.43	0.40	0.32
23	0.51	0.51	0.51	0.50	0.49	0.46	0.44	0.43	0.43	0.42	0.42	0.40	0.32
24	0.52	0.52	0.52	0.51	0.50	0.47	0.45	0.43	0.43	0.42	0.41	0.40	0.32
25	0.52	0.52	0.52	0.51	0.50	0.47	0.45	0.43	0.43	0.41	0.41	0.40	0.32
26	0.52	0.52	0.51	0.51	0.50	0.47	0.45	0.44	0.43	0.42	0.42	0.41	0.32
27	0.52	0.52	0.51	0.51	0.50	0.47	0.45	0.43	0.43	0.42	0.41	0.40	0.33
28	0.53	0.52	0.52	0.51	0.51	0.48	0.45	0.44	0.44	0.42	0.43	0.41	0.33
29	0.53	0.52	0.52	0.51	0.50	0.46	0.45	0.43	0.42	0.41	0.40	0.40	0.32
30	0.52	0.52	0.51	0.50	0.49	0.46	0.45	0.43	0.43	0.42	0.43	0.41	0.33
31	0.53	0.52	0.52	0.51	0.51	0.48	0.45	0.44	0.44	0.42	0.43	0.41	0.33
32	0.53	0.53	0.52	0.52	0.51	0.48	0.46	0.44	0.44	0.43	0.43	0.42	0.33
33	0.52	0.52	0.52	0.51	0.50	0.47	0.45	0.44	0.43	0.42	0.40	0.41	0.33
34	0.52	0.52	0.51	0.51	0.50	0.47	0.45	0.43	0.43	0.42	0.42	0.41	0.33
35	0.53	0.52	0.52	0.51	0.50	0.47	0.45	0.43	0.43	0.42	0.40	0.40	0.33
36	0.52	0.52	0.51	0.50	0.49	0.47	0.45	0.43	0.43	0.42	0.42	0.41	0.33
37	0.53	0.52	0.52	0.51	0.50	0.47	0.45	0.43	0.43	0.42	0.42	0.40	0.33
38	0.53	0.53	0.52	0.52	0.51	0.48	0.46	0.44	0.44	0.43	0.45	0.42	0.34
39	0.53	0.53	0.53	0.52	0.51	0.48	0.46	0.44	0.44	0.43	0.43	0.42	0.34
to	'	'	'	'	'	'	'	'	'	'	'	'	'
141	0.56	0.55	0.54	0.54	0.53	0.50	0.48	0.46	0.46	0.45	0.45	0.44	0.36
142	0.55	0.55	0.54	0.54	0.53	0.50	0.48	0.46	0.45	0.44	0.43	0.43	0.36
143	0.56	0.55	0.55	0.54	0.53	0.50	0.48	0.46	0.46	0.45	0.45	0.43	0.36
144	0.56	0.56	0.55	0.55	0.54	0.51	0.48	0.46	0.46	0.45	0.45	0.44	0.36
145	0.55	0.54	0.54	0.53	0.52	0.49	0.48	0.46	0.46	0.45	0.44	0.44	0.36
146	0.55	0.54	0.54	0.53	0.52	0.49	0.47	0.46	0.46	0.45	0.44	0.43	0.36
147	0.55	0.55	0.54	0.54	0.53	0.49	0.47	0.45	0.45	0.44	0.42	0.42	0.36
148	0.55	0.54	0.53	0.53	0.52	0.49	0.47	0.45	0.44	0.44	0.43	0.42	0.35
149	0.55	0.55	0.54	0.54	0.53	0.49	0.47	0.45	0.45	0.44	0.45	0.43	0.35
150	0.55	0.54	0.54	0.53	0.52	0.49	0.47	0.45	0.45	0.44	0.45	0.43	0.35

Trans No.	P14	P15	P16	P17	P18	P19	P20	P21	P22	P23	P24	LOAD	NOZZLE	BLOW
Distance	24.73	26.73	28.73	30.73	32.73	39.73	41.73	43.73	45.73	47.73	49.73	CELL	UPSTM	TANK
Average reading (bar)	0.31	0.30	0.30	0.28	0.28	0.21	0.20	0.18	0.18	0.17	0.17	759.2	5.23	0.766
Steady state average (bar)	0.73	0.71	0.66	0.63	0.48	0.42	0.39	0.43	0.46	0.39	0.38	520.9	5.00	1.594
Time 1	0.27	0.26	0.27	0.24	0.24	0.18	0.17	0.15	0.16	0.14	0.14	740.3	5.34	0.748
2	0.28	0.27	0.28	0.24	0.25	0.19	0.18	0.16	0.16	0.14	0.15	740.3	5.34	0.743
3	0.28	0.28	0.28	0.25	0.25	0.19	0.18	0.16	0.16	0.15	0.15	741.3	5.34	0.748
4	0.29	0.29	0.29	0.26	0.27	0.21	0.19	0.16	0.17	0.16	0.16	742.2	5.34	0.764
5	0.30	0.29	0.30	0.27	0.27	0.21	0.19	0.17	0.18	0.16	0.16	743.2	5.34	0.759
6	0.30	0.28	0.29	0.25	0.26	0.19	0.19	0.16	0.17	0.15	0.15	743.2	5.34	0.754
7	0.29	0.27	0.27	0.24	0.25	0.18	0.18	0.16	0.16	0.14	0.14	744.2	5.34	0.754
8	0.28	0.27	0.27	0.24	0.25	0.18	0.18	0.16	0.16	0.14	0.14	744.2	5.34	0.743
9	0.28	0.28	0.29	0.26	0.26	0.19	0.18	0.16	0.17	0.15	0.15	746.1	5.34	0.754
10	0.29	0.29	0.30	0.27	0.27	0.21	0.19	0.17	0.18	0.16	0.16	747.1	5.34	0.754
11	0.30	0.29	0.30	0.27	0.27	0.21	0.20	0.17	0.18	0.16	0.17	747.1	5.34	0.764
12	0.31	0.28	0.29	0.26	0.26	0.20	0.19	0.17	0.17	0.15	0.16	747.1	5.34	0.759
13	0.29	0.28	0.28	0.25	0.26	0.18	0.18	0.16	0.17	0.15	0.15	748.1	5.34	0.764
14	0.29	0.28	0.28	0.26	0.26	0.19	0.18	0.17	0.17	0.15	0.15	749.0	5.34	0.759
15	0.29	0.29	0.29	0.27	0.27	0.20	0.19	0.17	0.17	0.16	0.16	750.0	5.34	0.770
16	0.30	0.30	0.30	0.28	0.28	0.22	0.20	0.18	0.18	0.17	0.17	751.0	5.34	0.770
17	0.31	0.30	0.30	0.27	0.28	0.21	0.20	0.18	0.18	0.16	0.17	751.0	5.34	0.770
18	0.31	0.29	0.29	0.26	0.27	0.19	0.19	0.17	0.17	0.15	0.16	751.9	5.34	0.770
19	0.30	0.29	0.29	0.26	0.27	0.19	0.19	0.17	0.17	0.15	0.15	752.9	5.34	0.759
20	0.30	0.29	0.29	0.27	0.27	0.20	0.19	0.18	0.18	0.16	0.16	753.9	5.34	0.770
21	0.30	0.30	0.30	0.28	0.28	0.21	0.20	0.18	0.18	0.16	0.17	754.8	5.34	0.770
22	0.31	0.30	0.31	0.28	0.28	0.22	0.20	0.18	0.18	0.17	0.17	755.8	5.34	0.770
23	0.31	0.30	0.31	0.28	0.28	0.22	0.20	0.18	0.18	0.17	0.17	755.8	5.34	0.786
24	0.31	0.30	0.31	0.28	0.28	0.22	0.21	0.18	0.18	0.17	0.17	756.8	5.34	0.780
25	0.31	0.31	0.31	0.29	0.29	0.22	0.21	0.18	0.18	0.17	0.17	757.8	5.34	0.786
26	0.31	0.31	0.32	0.29	0.29	0.23	0.21	0.19	0.19	0.18	0.18	758.7	5.34	0.770
27	0.32	0.31	0.31	0.28	0.29	0.22	0.21	0.19	0.19	0.17	0.17	758.7	5.34	0.786
28	0.32	0.30	0.30	0.28	0.28	0.21	0.20	0.18	0.18	0.17	0.17	759.7	5.34	0.775
29	0.31	0.31	0.31	0.29	0.29	0.22	0.21	0.19	0.19	0.17	0.17	761.6	5.34	0.786
30	0.31	0.31	0.32	0.29	0.29	0.22	0.21	0.19	0.19	0.18	0.18	761.6	5.34	0.780
31	0.32	0.31	0.32	0.30	0.29	0.23	0.21	0.19	0.19	0.18	0.18	761.6	5.34	0.786
32	0.32	0.31	0.31	0.29	0.29	0.22	0.21	0.19	0.19	0.17	0.18	763.6	5.34	0.780
33	0.32	0.31	0.32	0.30	0.29	0.22	0.21	0.19	0.19	0.18	0.18	764.5	5.34	0.786
34	0.32	0.31	0.31	0.29	0.29	0.22	0.21	0.19	0.19	0.18	0.18	764.5	5.34	0.791
35	0.32	0.31	0.31	0.29	0.29	0.22	0.21	0.19	0.19	0.18	0.18	765.5	5.34	0.786
36	0.32	0.31	0.31	0.30	0.29	0.22	0.21	0.19	0.19	0.18	0.18	766.5	5.34	0.775
to	'	'	'	'	'	'	'	'	'	'	'	'	'	'
141	0.35	0.34	0.34	0.32	0.32	0.23	0.23	0.21	0.21	0.20	0.20	851.7	5.36	0.823
142	0.35	0.34	0.34	0.32	0.32	0.24	0.23	0.22	0.21	0.21	0.20	852.7	5.35	0.823
143	0.35	0.34	0.34	0.32	0.32	0.23	0.23	0.22	0.21	0.20	0.20	853.7	5.35	0.834
144	0.35	0.34	0.34	0.32	0.32	0.24	0.23	0.22	0.21	0.21	0.20	854.7	5.34	0.839
145	0.35	0.34	0.34	0.32	0.32	0.24	0.23	0.22	0.21	0.21	0.20	854.7	5.34	0.828
146	0.35	0.33	0.33	0.32	0.32	0.23	0.23	0.22	0.21	0.20	0.20	855.6	5.34	0.818
147	0.34	0.33	0.33	0.31	0.31	0.22	0.22	0.20	0.20	0.19	0.19	856.6	5.34	0.834
148	0.33	0.33	0.33	0.31	0.31	0.23	0.22	0.21	0.21	0.20	0.19	858.5	5.34	0.828
149	0.34	0.33	0.33	0.31	0.32	0.23	0.23	0.21	0.21	0.20	0.19	858.5	5.34	0.834
150	0.34	0.33	0.33	0.31	0.32	0.23	0.23	0.21	0.21	0.20	0.20	859.5	5.34	0.834

The spreadsheet displayed all the recorded input data from each test run. However, not all the data recorded during a test may have been under steady state operating conditions. The main reason for this was that when a high mass flow rate of air and solids were required for a test, the amount of material used for the test, did not take long to convey (depending on the amount of material initially loaded into the receiving hopper before the test work commenced). Under such circumstances, the ramp up and ramp down of blow tank and pipeline pressures that occur at the start and end of a conveying test run, would be recorded before and after the steady state period. In addition, pressure fluctuations sometimes occurred during the recording of a tests steady period, which could give a false indication of the pressure readings when averaged.

To look at all the readings measured during each test, a graph was plotted to display the blow tank pressure and a selection of five different pressure transducer readings, versus time. Only five transducers were selected because the software used could only display six series of data on the Y axis of a graph. The selected transducers enabled each of the four straight sections to be monitored, together with the pressure upstream of the blow tank, hence monitoring the blow tank pressure. Graph A5.1 is an example of such a graph. From this graph, the steady state period was selected by the operator and the pressures were averaged over this period. The increase in load cell readings over the steady state period, were then used to find the mass flow rate of solids.

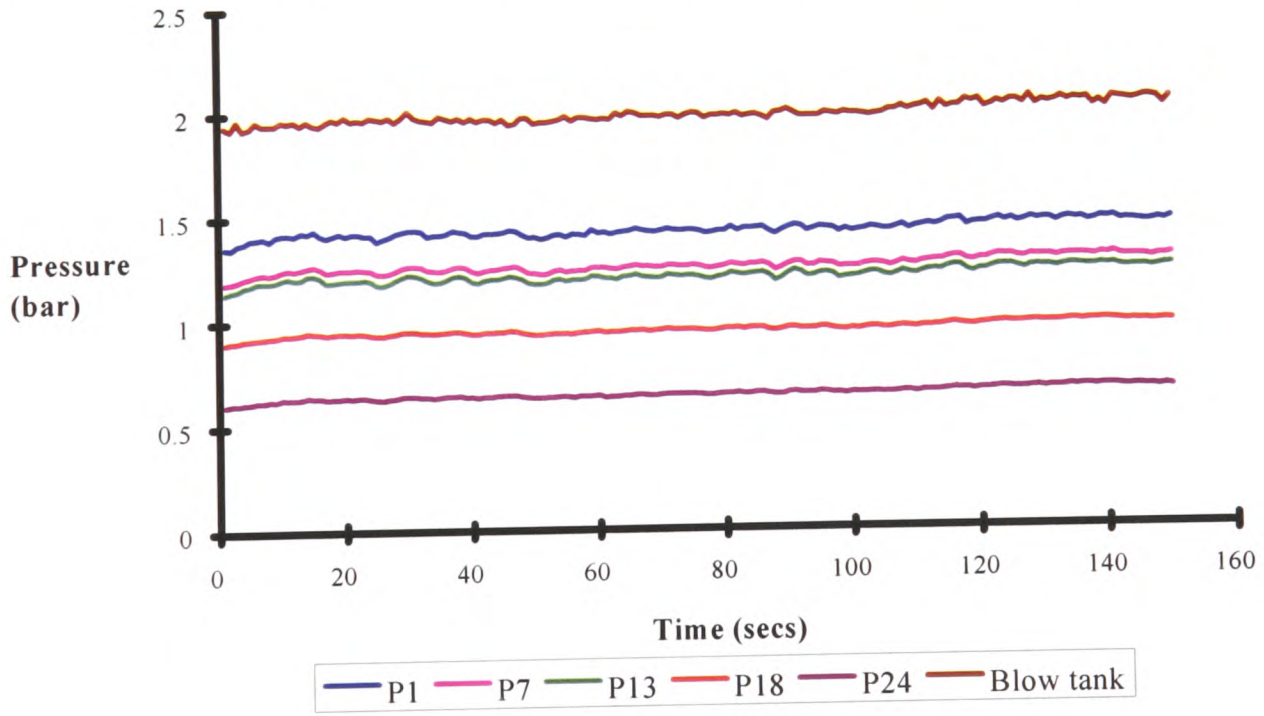

Graph A5.1 showing the blow tank and 5 transducer pressures readings from along the test section, versus time. The steady state time period is selected from such graphs. In this graph, the steady state period would be taken from 40 to 120 seconds.

In addition to using graph A5.1 to view the measured results to determine the steady state period during each test run, a graph displaying the measured weight of solids on the load cells versus time, was also used in the assessment to ascertain the steady state period of the measured results. An example is shown on graph A5.2, and shows how the steady flow rate of the material falling into the receiving hopper was observed.

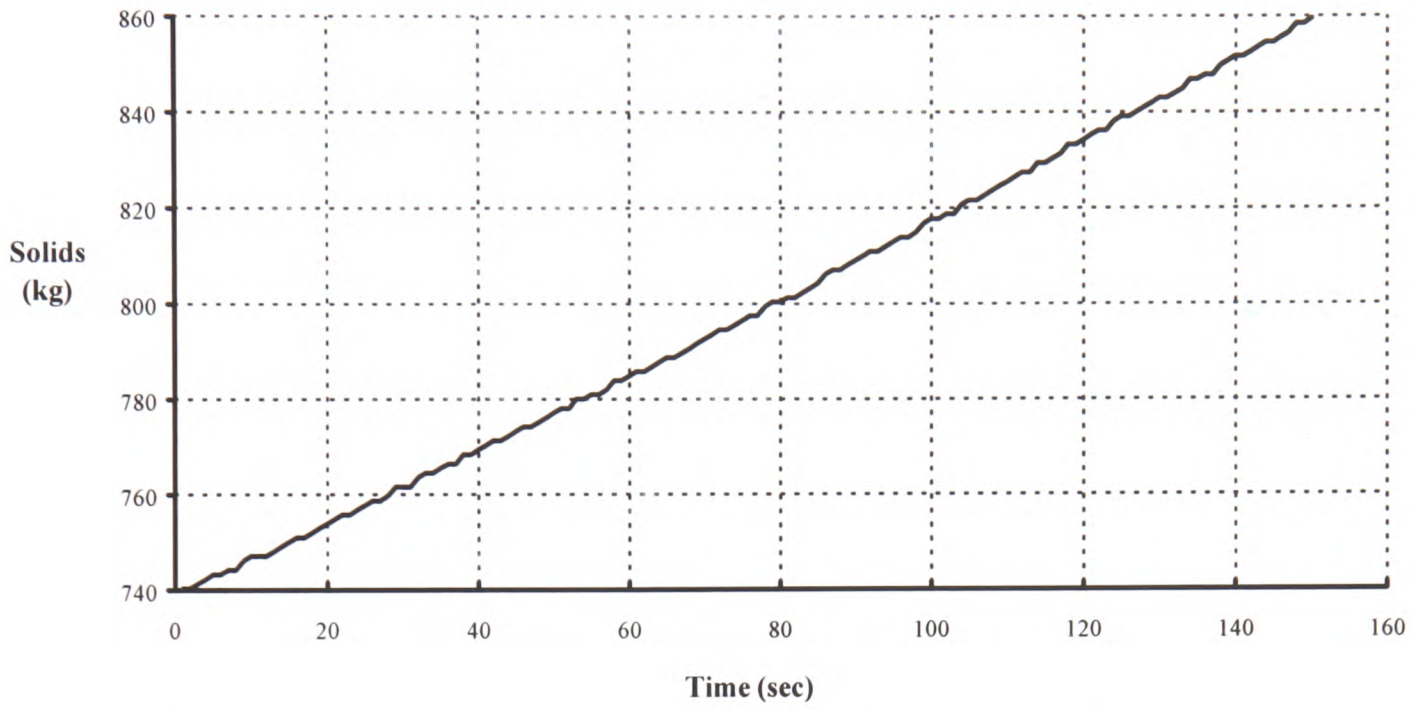

Graph A5.2: The mass of solids into the receiving hopper versus time, is used to determine the mass flow rate of solids for each test run.

To ease the repetitiveness of averaging, calculating and moving data within each spreadsheet, macros were devised to speed the process. All four linked spreadsheets contained several macros. Examples of all the macros can be found at the end of this appendix.

Once the steady state period had been selected and the data processed to obtain an individual value of average pressure or rate of increase in weight from each input channel, the results were exported to a different spreadsheet for further analysis. The calculations in that spreadsheet were applied to the results of the first spreadsheet.

In the results sections, the data for average pressure at each transducer and its distance along the test section was used for the least squares best fit method, to determine the pressure gradient for each straight test section. The values for the averaged data for each transducer were calculated from the identified steady state section, and each new value that the "least square" analysis calculated in order to plot the best fit line through the averaged data points, is also shown on this spreadsheet. The results section of the spreadsheet is shown below.

A5.3.3 Results worksheet for pipeline pressures

Test No. Trans No.	Distance metres	x metre	y bar	X x-xbr	Y y-ybr	X^2	X*Y
1	-7.13	-7.13	0.9938	-3	0.0062	9	-0.0186
2	-5.13	-5.13	0.9947	-1	0.0071	1	-0.0071
3	-3.13	-3.13	0.9851	1	-0.0025	1	-0.0025
4	-1.13	-1.13	0.9768	3	-0.0108	9	-0.0324
	Average	-4.13	0.9876		Sum	20	-0.0607
APEX	0						
APEX	0	0					
5	1.13	1.13	0.9639	-7	0.1020	49	-0.7143
6	3.13	3.13	0.9297	-5	0.0679	25	-0.3395
7	5.13	5.13	0.8959	-3	0.0341	9	-0.1023
8	7.13	7.13	0.8594	-1	-0.0025	1	0.0025
9	9.13	9.13	0.8405	1	-0.0214	1	-0.0214
10	11.13	11.13	0.8156	3	-0.0463	9	-0.1388
11	13.13	13.13	0.8015	5	-0.0604	25	-0.3018
12	15.13	15.13	0.7883	7	-0.0736	49	-0.5150
	Average	8.13	0.8618		Sum	168	-2.1306
APEX	17.73						
APEX	17.73						
13	22.73	22.73	0.6949	-5	0.0475	25	-0.2377
14	24.73	24.73	0.6764	-3	0.0291	9	-0.0873
15	26.73	26.73	0.6583	-1	0.0110	1	-0.0110
16	28.73	28.73	0.6351	1	-0.0122	1	-0.0122
17	30.73	30.73	0.6215	3	-0.0258	9	-0.0774
18	32.73	32.73	0.5977	5	-0.0496	25	-0.2482
	Average	27.73	0.6473		Sum	70	-0.6739
APEX	34.73						
APEX	34.73						
19	39.73	39.73	0.5086	-5	0.0648	25	-0.3242
20	41.73	41.73	0.4823	-3	0.0386	9	-0.1158
21	43.73	43.73	0.4541	-1	0.0104	1	-0.0104
22	45.73	45.73	0.4172	1	-0.0265	1	-0.0265
23	47.73	47.73	0.4125	3	-0.0312	9	-0.0935
24	49.73	49.73	0.3876	5	-0.0561	25	-0.2806
	Average	44.73	0.4437		Sum	70	-0.8510

Distance (m)	Least sq. (bar)	Avg data (bar)	Trans. No.
-7.13	0.9967	0.9938	1
-5.13	0.9907	0.9947	2
-3.13	0.9846	0.9851	3
-1.13	0.9785	0.9768	4
0	0.9751		
0	0.9649		
1.13	0.9506	0.9639	5
3.13	0.9253	0.9297	6
5.13	0.8999	0.8959	7
7.13	0.8745	0.8594	8
9.13	0.8492	0.8405	9
11.13	0.8238	0.8156	10
13.13	0.7984	0.8015	11
15.13	0.7731	0.7883	12
17.73	0.7401		
17.73	0.7436		
22.73	0.6954	0.6949	13
24.73	0.6762	0.6764	14
26.73	0.6569	0.6583	15
28.73	0.6377	0.6351	16
30.73	0.6184	0.6215	17
32.73	0.5992	0.5977	18
34.73	0.5799		
34.73	0.5653		
39.73	0.5045	0.5086	19
41.73	0.4802	0.4823	20
43.73	0.4559	0.4541	21
45.73	0.4315	0.4172	22
47.73	0.4072	0.4125	23
49.73	0.3829	0.3876	24

The data from the results spreadsheet was used to plot a graph of pressure versus distance along the conveying line. At the apex of each of the three test bends, a line was displayed to locate the positioning of each bend along the test section. For the pressure readings in each of the four

straight test sections, a straight line was fitted through the data using the method of least squares. It is at that point that pressure readings from specific transducers could be discounted in the least squares calculations for tangent fitting, if it appeared necessary. Reasons for exclusions may include where the operator considered that it would be inappropriate to use them. For example, if the pressure reading is unusually high or low in comparison to the other pressure readings along the straight section. Or as shown on graph A5.3, the first two readings after the first bend are ignored due to the re-acceleration length after the bend [R3]. This is explained in appendix 1.

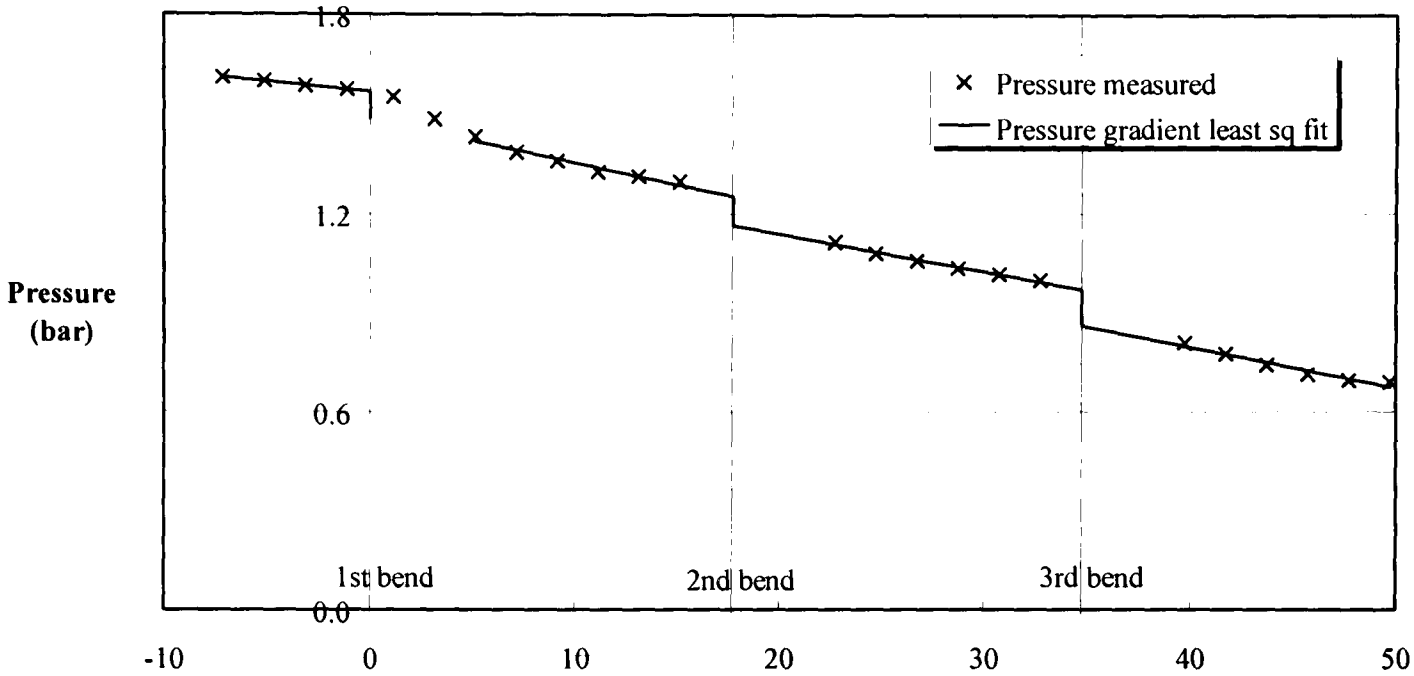

Graph A5.3: Pressure gradients along straight test sections. The first two transducer readings downstream of the first test bend are ignored due to the re-acceleration length.

After the transducer readings had been finalized and the method of least squares had been applied to the remaining data points from each straight section, a linear fit graduation for all the sections was used to adjust the slope of the lines. This was so all four gradients would have a progressive order of slopes for further analysis. A full explanation can be found in chapter 5. From the best fit line through the data, the pressure gradient along each straight section was calculated, together with the pressure drop caused by the bends.

A data sheet was formulated for the results of each test run, which included all the important calculations and data regarding the test. Information such as the mass flow rate of air and the speed control of the screw were typed in to produce a complete print out of the data, and an example is shown on Table A5.1. The information sheet also included a copy of graph A5.3 when a hard copy was printed.

Table A5.1. Results worksheet

Test run number	10442			
Product	Olivine sand			
Particle relative density	3.28			
Median diameter of particles	270 microns			
Straight test section & Bend number	1	2	3	4
P inlet to bend (bar_g)	0.9640	0.7835	0.5732	
P outlet of bend (bar_g)	0.9282	0.7532	0.5739	
P bend = (P outlet-P inlet) (bar_g)	-0.0358	-0.0303	0.0008	
P_{abs} = (P_{bar} bend outlet + P_{atmos}) (N/m^2)	198999.6	180714.0	159401.8	
Bend outlet velocity (m/s)	20.58	22.62	25.17	
Bend outlet suspension density (kg/m^3)	25.36	23.07	20.73	
Bend outlet air density (kg/m^3)	2.34	2.13	1.91	
P gradient of straights (bar_g/m)	-0.0057	-0.0082	-0.0106	-0.0130
P midpoint of straights (bar_g)	0.9876	0.8374	0.6473	0.4437
Midpoint suspension density (kg/m^3)	26.13	24.17	21.69	19.03
Midpoint air density (kg/m^3)	2.41	2.23	2.00	1.76
Midpoint air velocity (m/s)	19.97	21.59	24.06	27.42
P_{abs} inlet = ($P_{blowtank}$+P_{atmos}) (N/m^2)	244695.7			
Mass flow rate of air (kg/s)	0.10663			
Mass flow rate solids (kg/s)	1.15			
Mass flow rate solids (tonnes/hour)	4.14			
Inlet velocity of air (m/s)	16.33			
Outlet velocity of air (m/s)	39.43			
Solids loading ratio	10.80			
Screw feeder (rev/min)	30.00			
Steady state period (sec)	0 to 120			
Nominal C.S.A. of pipe (m^2)	0.002206			
Transducer No.(s) deleted	5 6 7			
Temperature of air (K)	288.00			
Air density at inlet (kg/m^3)	2.96			
P atmosphere (N/m^2)	101325			
Reynolds number (based on average air vel)	144782			

The data from the results worksheet shown on table A5.1, was transferred to another spreadsheet which eventually formed a complete database for the test results from all test runs with one material. The contents of such a database are shown in the following pages. The Reynolds number column was originally used to predict the 'air only' contribution to the total pressure loss.

A5.3.4 Database worksheet

Test No.	Product	P_{abs} in (N/m^2)	Inlet air vel	P loss sys. (bar)	Mass air (kg/s)	Mass solid (kg/s)	Mass solids tonnes/hr	SLR	Reynolds number
10400	Olivine sand	173995	19.97	0.727	0.0928	0.50	1.81	5.43	125659
10401	Olivine sand	195539	17.77	0.942	0.0928	0.79	2.84	8.50	125812
10402	Olivine sand	221091	15.72	1.198	0.0928	1.13	4.05	12.13	126086
10403	Olivine sand	240431	14.45	1.391	0.0928	1.39	4.99	14.94	126400
10404	Olivine sand	193194	18.75	0.919	0.0967	0.67	2.41	6.93	131116
10405	Olivine sand	222627	16.27	1.213	0.0967	1.05	3.79	10.90	131415
10406	Olivine sand	249192	14.54	1.479	0.0967	1.41	5.08	14.59	131663
10407	Olivine sand	268182	13.51	1.669	0.0967	1.72	6.18	17.76	131841
10408	Olivine sand	242262	14.96	1.409	0.0967	2.35	8.47	24.34	132123
10409	Olivine sand	196377	20.35	0.951	0.1066	0.73	2.62	6.83	144584
10410	Olivine sand	248582	16.07	1.473	0.1066	1.48	5.31	13.84	145031
10411	Olivine sand	296737	13.46	1.954	0.1066	2.09	7.54	19.64	145485
10412	Olivine sand	323862	12.34	2.225	0.1066	2.51	9.04	23.54	145726
10413	Olivine sand	202995	21.14	1.017	0.1145	0.76	2.74	6.64	155372
10414	Olivine sand	252076	17.02	1.508	0.1145	1.41	5.08	12.32	155797
10415	Olivine sand	305198	14.06	2.039	0.1145	2.22	7.98	19.36	156243
10416	Olivine sand	352847	12.16	2.515	0.1145	2.94	10.58	25.67	156708
10417	Olivine sand	204924	22.11	1.036	0.1209	0.69	2.48	5.70	164044
10418	Olivine sand	305551	14.04	2.042	0.1145	2.10	7.56	18.34	156080
10419	Olivine sand	209548	21.62	1.082	0.1209	0.77	2.76	6.35	164010
10420	Olivine sand	227114	19.95	1.258	0.1209	1.59	5.73	13.17	164344
10421	Olivine sand	213125	22.60	1.118	0.1286	0.72	2.58	5.56	174432
10422	Olivine sand	266015	18.11	1.647	0.1286	1.48	5.34	11.53	174724
10423	Olivine sand	190790	20.94	0.895	0.1066	1.87	6.74	17.55	145184
10424	Olivine sand	325149	14.81	2.238	0.1286	2.35	8.45	18.26	175233
10425	Olivine sand	341091	14.12	2.398	0.1286	2.54	9.15	19.76	175381
10426	Olivine sand	211115	20.33	1.098	0.1145	1.13	4.08	9.89	155452
10427	Olivine sand	244746	22.41	1.434	0.1464	0.97	3.49	6.62	198765
10428	Olivine sand	274161	20.01	1.728	0.1464	1.44	5.20	9.86	198878
10429	Olivine sand	282628	19.41	1.813	0.1464	1.53	5.50	10.44	198982
10430	Olivine sand	326417	16.80	2.251	0.1464	2.31	8.33	15.80	199414
10431	Olivine sand	296937	12.20	1.956	0.0967	2.17	7.82	22.46	132019
10432	Olivine sand	308262	19.93	2.069	0.1640	1.91	6.87	11.64	223099
10433	Olivine sand	358039	17.16	2.567	0.1640	2.45	8.80	14.91	223531
10434	Olivine sand	294590	20.86	1.933	0.1640	1.57	5.66	9.58	222876
10435	Olivine sand	379460	16.19	2.781	0.1640	2.67	9.63	16.31	223637
10436	Olivine sand	282036	15.22	1.807	0.1145	1.67	6.01	14.59	156359
10437	Olivine sand	221320	18.05	1.200	0.1066	1.03	3.72	9.70	144665
10438	Olivine sand	209490	17.30	1.082	0.0967	0.94	3.37	9.68	131147
10439	Olivine sand	271139	17.77	1.698	0.1286	1.69	6.07	13.12	174934
10440	Olivine sand	250797	17.11	1.495	0.1145	1.38	4.96	12.04	155604
10441	Olivine sand	244696	19.69	1.434	0.1286	1.15	4.14	8.95	174570
10442	Olivine sand	311815	12.81	2.105	0.1066	2.18	7.86	20.47	145605

Test No.	Steady state period (sec)	Transducers deleted	P gradient of straights 1	2	3	4	P midpoint of straights 1	2	3	4
10400	20 to 150	5 6 7 13	-0.0028	-0.0033	-0.0038	-0.0044	0.4491	0.3572	0.2494	0.1528
10401	20 to 150	5 6 7	-0.0035	-0.0040	-0.0045	-0.0051	0.5838	0.4481	0.3380	0.2147
10402	0 to 150	5 6 7	-0.0051	-0.0059	-0.0067	-0.0074	0.7470	0.5663	0.4268	0.2680
10403	0 to 150	5 6 7	-0.0056	-0.0070	-0.0084	-0.0097	0.8928	0.6702	0.4951	0.3067
10404	0 to 150	5 6 7	-0.0041	-0.0043	-0.0046	-0.0048	0.5831	0.4703	0.3442	0.2179
10405	0 to 150	5 6 7	-0.0058	-0.0064	-0.0070	-0.0075	0.7773	0.6068	0.4561	0.2906
10406	0 to 150	5 6 7	-0.0068	-0.0084	-0.0099	-0.0115	0.9689	0.7595	0.5712	0.3595
10407	0 to 150	5 6 7	-0.0079	-0.0092	-0.0106	-0.0120	1.0943	0.8602	0.6423	0.4061
10408	30 to 80	5 6 7 23 24	-0.0093	-0.0118	-0.0144	-0.0170	1.3940	1.1239	0.8285	0.5186
10409	0 to 150	5 6 7	-0.0035	-0.0044	-0.0053	-0.0062	0.6223	0.5103	0.3764	0.2350
10410	0 to 150	5 6 7	-0.0059	-0.0073	-0.0087	-0.0101	0.9921	0.8033	0.6108	0.3966
10411	0 to 150	5 6 7	-0.0081	-0.0096	-0.0111	-0.0126	1.2980	1.0569	0.7835	0.5100
10412	0 to 150	5 6 7	-0.0090	-0.0108	-0.0126	-0.0144	1.4965	1.2084	0.9024	0.5917
10413	0 to 150	5 6 7	-0.0044	-0.0050	-0.0056	-0.0062	0.6674	0.5473	0.4022	0.2477
10414	0 to 150	5 6 7	-0.0065	-0.0071	-0.0077	-0.0083	1.0127	0.8227	0.6241	0.4062
10415	0 to 150	5 6 7	-0.0043	-0.0070	-0.0097	-0.0124	1.3695	1.0993	0.8450	0.5579
10416	0 to 120	5 6 7	-0.0093	-0.0106	-0.0118	-0.0131	1.7277	1.4058	1.0517	0.6713
10417	0 to 150	5 6 7	-0.0037	-0.0047	-0.0056	-0.0066	0.6776	0.5559	0.4105	0.2487
10418	0 to 150	5 6 7	-0.0068	-0.0096	-0.0125	-0.0154	1.3948	1.1439	0.8873	0.6080
10419	0 to 150	5 6 7	-0.0045	-0.0061	-0.0076	-0.0092	0.7291	0.6019	0.4597	0.3027
10420	20 to 80	5 6 7	-0.0054	-0.0078	-0.0103	-0.0127	1.1289	0.9377	0.7402	0.5115
10421	20 to 80	5 6 7	-0.0052	-0.0061	-0.0070	-0.0080	0.7522	0.6226	0.4700	0.3018
10422	0 to 150	5 6 7	-0.0052	-0.0076	-0.0099	-0.0123	1.1420	0.9514	0.7513	0.5164
10423	0 to 30	5 6 7	-0.0056	-0.0082	-0.0108	-0.0134	1.1806	0.9611	0.7383	0.4938
10424	0 to 150	5 6 7	-0.0072	-0.0095	-0.0118	-0.0141	1.5369	1.2776	0.9937	0.6842
10425	0 to 130	5 6 7	-0.0075	-0.0104	-0.0134	-0.0163	1.6492	1.3648	1.0610	0.7286
10426	0 to 60	5 6 7	-0.0048	-0.0065	-0.0081	-0.0098	0.8591	0.7056	0.5519	0.3725
10427	0 to 150	5 6 7	-0.0054	-0.0074	-0.0093	-0.0113	0.9870	0.8273	0.6462	0.4349
10428	0 to 150	5 6 7	-0.0052	-0.0077	-0.0102	-0.0127	1.2001	1.0119	0.8073	0.5613
10429	0 to 150	5 6 7	-0.0060	-0.0078	-0.0097	-0.0115	1.2585	1.0588	0.8408	0.5869
10430	0 to 120	5 6 7	-0.0072	-0.0092	-0.0112	-0.0131	1.5919	1.3361	1.0508	0.7375
10431	0 to 150	5 6 7 24	-0.0068	-0.0096	-0.0123	-0.0151	1.2892	1.0221	0.7663	0.5104
10432	0 to 100	5 6 7	-0.0058	-0.0085	-0.0112	-0.0139	1.4998	1.2725	1.0140	0.7104
10433	0 to 150	5 6 7	-0.0078	-0.0099	-0.0121	-0.0142	1.7999	1.5206	1.1992	0.8427
10434	0 to 120	5 6 7	-0.0051	-0.0078	-0.0106	-0.0133	1.3493	1.1503	0.9199	0.6425
10435	0 to 80	5 6 7	-0.0073	-0.0100	-0.0128	-0.0155	1.9127	1.6175	1.2743	0.9025
10436	20 to 50	5 6 7	-0.0056	-0.0095	-0.0133	-0.0172	1.2864	1.0009	0.7678	0.4998
10437	0 to 150	5 6 7	-0.0036	-0.0054	-0.0073	-0.0091	0.8060	0.6650	0.5185	0.3478
10438	60 to 150	5 6 7	-0.0036	-0.0051	-0.0067	-0.0082	0.6916	0.5606	0.4316	0.2828
10439	0 to 100	5 6 7	-0.0051	-0.0072	-0.0093	-0.0114	1.2261	1.0134	0.7891	0.5389
10440	0 to 150	5 6 7	-0.0050	-0.0066	-0.0082	-0.0099	1.0092	0.8357	0.6507	0.4394
10441	0 to 150	5 6 7	-0.0043	-0.0071	-0.0099	-0.0127	0.9876	0.8210	0.6473	0.4437
10442	0 to 120	5 6 7	-0.0063	-0.0084	-0.0105	-0.0126	1.3652	1.0901	0.8205	0.5504

Test	Midpoint susp. density				Midpoint air density				Midpoint air velocity				Ave. readings	
No.	1	2	3	4	1	2	3	4	1	2	3	4	P1	P24
10400	9.60	9.00	8.29	7.65	1.76	1.65	1.52	1.41	23.76	25.36	27.52	29.80	0.458	0.131
10401	16.43	15.04	13.90	12.63	1.93	1.76	1.63	1.48	21.76	23.78	25.72	28.30	0.596	0.189
10402	25.83	23.18	21.13	18.80	2.12	1.90	1.74	1.54	19.74	22.00	24.13	27.12	0.762	0.234
10403	34.46	30.44	27.27	23.87	2.30	2.03	1.82	1.59	18.23	20.64	23.04	26.33	0.910	0.269
10404	13.38	12.43	11.38	10.32	1.92	1.79	1.64	1.48	22.70	24.42	26.69	29.43	0.595	0.198
10405	23.60	21.35	19.37	17.19	2.16	1.95	1.77	1.57	20.24	22.36	24.66	27.79	0.795	0.256
10406	35.00	31.30	27.98	24.24	2.39	2.14	1.91	1.66	18.28	20.44	22.87	26.39	0.985	0.309
10407	45.27	40.24	35.56	30.49	2.54	2.26	2.00	1.71	17.19	19.34	21.89	25.53	1.112	0.357
10408	70.87	62.92	54.23	45.10	2.90	2.58	2.22	1.85	15.05	16.95	19.67	23.65	1.416	0.474
10409	13.52	12.59	11.48	10.32	1.97	1.84	1.68	1.50	24.43	26.22	28.75	32.01	0.634	0.207
10410	33.59	30.43	27.20	23.61	2.42	2.19	1.96	1.70	19.92	21.99	24.60	28.34	1.005	0.351
10411	54.91	49.19	42.69	36.19	2.79	2.50	2.17	1.84	17.29	19.30	22.24	26.23	1.315	0.462
10412	71.48	63.28	54.56	45.71	3.03	2.68	2.31	1.93	15.92	17.98	20.86	24.89	1.516	0.536
10413	13.51	12.54	11.38	10.14	2.03	1.88	1.71	1.52	25.53	27.50	30.32	34.03	0.679	0.221
10414	30.20	27.37	24.41	21.16	2.44	2.21	1.97	1.71	21.18	23.37	26.21	30.23	1.027	0.371
10415	55.82	49.49	43.53	36.81	2.87	2.55	2.24	1.89	18.01	20.31	23.09	27.31	1.384	0.513
10416	85.11	75.12	64.12	52.31	3.30	2.92	2.49	2.03	15.66	17.74	20.78	25.47	1.747	0.641
10417	11.66	10.82	9.82	8.70	2.04	1.89	1.72	1.52	26.79	28.87	31.82	35.90	0.689	0.221
10418	53.43	47.86	42.17	35.97	2.90	2.60	2.29	1.95	17.82	19.89	22.58	26.47	1.411	0.543
10419	13.38	12.40	11.31	10.10	2.10	1.95	1.78	1.59	26.00	28.05	30.76	34.43	0.741	0.267
10420	34.14	31.10	27.95	24.30	2.58	2.35	2.11	1.84	21.15	23.22	25.84	29.71	1.143	0.452
10421	11.89	11.01	9.99	8.85	2.13	1.97	1.79	1.59	27.28	29.45	32.48	36.63	0.765	0.275
10422	30.07	27.41	24.62	21.34	2.60	2.37	2.13	1.84	22.35	24.52	27.30	31.49	1.154	0.464
10423	46.57	41.91	37.18	31.99	2.64	2.38	2.11	1.82	18.21	20.24	22.81	26.51	1.193	0.448
10424	56.34	50.61	44.34	37.50	3.07	2.76	2.42	2.05	18.89	21.03	24.00	28.38	1.552	0.635
10425	63.65	56.86	49.59	41.64	3.21	2.87	2.50	2.10	18.09	20.26	23.22	27.66	1.668	0.658
10426	22.41	20.58	18.74	16.59	2.26	2.07	1.89	1.67	22.92	24.97	27.42	30.97	0.874	0.324
10427	16.02	14.74	13.29	11.60	2.41	2.22	2.00	1.75	27.42	29.80	33.05	37.87	1.002	0.387
10428	26.41	24.17	21.72	18.79	2.67	2.44	2.19	1.90	24.78	27.08	30.13	34.83	1.214	0.506
10429	28.70	26.17	23.42	20.21	2.74	2.50	2.24	1.93	24.14	26.47	29.58	34.28	1.275	0.538
10430	49.79	44.90	39.45	33.46	3.14	2.83	2.49	2.11	21.05	23.35	26.57	31.33	1.610	0.689
10431	62.57	55.31	48.36	41.41	2.78	2.45	2.15	1.84	15.74	17.80	20.36	23.78	1.309	0.450
10432	35.39	32.19	28.55	24.27	3.03	2.76	2.44	2.08	24.45	26.88	30.31	35.65	1.515	0.648
10433	50.75	45.71	39.91	33.48	3.39	3.05	2.67	2.24	21.84	24.25	27.77	33.11	1.816	0.782
10434	27.39	25.09	22.41	19.20	2.85	2.61	2.33	2.00	26.01	28.40	31.78	37.11	1.362	0.591
10435	57.72	51.90	45.13	37.79	3.53	3.17	2.76	2.31	21.00	23.36	26.86	32.07	1.928	0.835
10436	40.58	35.55	31.43	26.70	2.77	2.43	2.15	1.82	18.66	21.31	24.09	28.36	1.296	0.442
10437	21.34	19.69	17.97	15.97	2.19	2.02	1.85	1.64	21.96	23.81	26.08	29.36	0.814	0.305
10438	19.97	18.44	16.92	15.18	2.06	1.90	1.74	1.56	21.25	23.02	25.08	27.96	0.698	0.246
10439	35.53	32.16	28.60	24.63	2.70	2.44	2.17	1.87	21.51	23.77	26.73	31.03	1.231	0.491
10440	29.45	26.93	24.23	21.16	2.44	2.23	2.01	1.75	21.22	23.21	25.79	29.54	1.019	0.393
10441	21.67	19.87	17.99	15.78	2.41	2.21	2.00	1.76	24.07	26.26	29.01	33.06	0.994	0.388
10442	58.89	52.08	45.40	38.72	2.87	2.54	2.21	1.89	16.80	19.00	21.79	25.55	1.380	0.499

Test	P gradient due to air using Darcy eq.(bar)				Pressure gradient due to solids (bar)				P inlet to bend (bar)		
No.	1	2	3	4	1	2	3	4	1	2	3
10400	-0.00206	-0.00220	-0.00238	-0.00258	-0.00078	-0.00114	-0.00146	-0.00177	0.437	0.335	0.226
10401	-0.00188	-0.00206	-0.00223	-0.00245	-0.00163	-0.00197	-0.00232	-0.00260	0.569	0.421	0.306
10402	-0.00171	-0.00191	-0.00209	-0.00235	-0.00342	-0.00399	-0.00457	-0.00508	0.726	0.527	0.380
10403	-0.00158	-0.00179	-0.00200	-0.00228	-0.00407	-0.00523	-0.00639	-0.00747	0.869	0.624	0.436
10404	-0.00205	-0.00221	-0.00241	-0.00266	-0.00203	-0.00211	-0.00215	-0.00214	0.566	0.442	0.312
10405	-0.00183	-0.00202	-0.00223	-0.00251	-0.00399	-0.00437	-0.00474	-0.00504	0.753	0.565	0.407
10406	-0.00165	-0.00185	-0.00206	-0.00238	-0.00518	-0.00654	-0.00786	-0.00909	0.941	0.704	0.502
10407	-0.00155	-0.00175	-0.00198	-0.00230	-0.00631	-0.00748	-0.00862	-0.00966	1.062	0.799	0.568
10408	-0.00136	-0.00153	-0.00178	-0.00214	-0.00791	-0.01032	-0.01265	-0.01487	1.356	1.034	0.728
10409	-0.00243	-0.00261	-0.00286	-0.00319	-0.00111	-0.00180	-0.00243	-0.00298	0.608	0.481	0.339
10410	-0.00198	-0.00219	-0.00245	-0.00282	-0.00392	-0.00513	-0.00628	-0.00732	0.968	0.755	0.550
10411	-0.00172	-0.00192	-0.00221	-0.00261	-0.00641	-0.00770	-0.00890	-0.00999	1.264	0.984	0.706
10412	-0.00158	-0.00179	-0.00208	-0.00248	-0.00743	-0.00903	-0.01055	-0.01195	1.459	1.137	0.814
10413	-0.00273	-0.00294	-0.00324	-0.00364	-0.00169	-0.00207	-0.00236	-0.00256	0.649	0.514	0.363
10414	-0.00227	-0.00250	-0.00280	-0.00323	-0.00424	-0.00460	-0.00489	-0.00505	0.986	0.776	0.570
10415	-0.00193	-0.00217	-0.00247	-0.00292	-0.00241	-0.00484	-0.00722	-0.00944	1.352	1.053	0.777
10416	-0.00167	-0.00190	-0.00222	-0.00272	-0.00763	-0.00868	-0.00963	-0.01040	1.689	1.336	0.969
10417	-0.00300	-0.00323	-0.00356	-0.00401	-0.00071	-0.00144	-0.00209	-0.00260	0.662	0.525	0.371
10418	-0.00189	-0.00211	-0.00239	-0.00280	-0.00488	-0.00753	-0.01012	-0.01258	1.367	1.080	0.800
10419	-0.00291	-0.00314	-0.00344	-0.00385	-0.00160	-0.00293	-0.00418	-0.00533	0.711	0.562	0.406
10420	-0.00237	-0.00260	-0.00289	-0.00332	-0.00302	-0.00523	-0.00738	-0.00940	1.107	0.886	0.668
10421	-0.00324	-0.00350	-0.00386	-0.00436	-0.00193	-0.00261	-0.00318	-0.00362	0.731	0.582	0.421
10422	-0.00266	-0.00291	-0.00325	-0.00374	-0.00256	-0.00466	-0.00669	-0.00856	1.120	0.901	0.682
10423	-0.00181	-0.00201	-0.00227	-0.00264	-0.00382	-0.00620	-0.00852	-0.01072	1.157	0.907	0.663
10424	-0.00225	-0.00250	-0.00285	-0.00337	-0.00492	-0.00698	-0.00895	-0.01075	1.507	1.215	0.911
10425	-0.00215	-0.00241	-0.00276	-0.00329	-0.00535	-0.00802	-0.01061	-0.01302	1.618	1.296	0.967
10426	-0.00243	-0.00264	-0.00290	-0.00328	-0.00241	-0.00385	-0.00524	-0.00652	0.839	0.663	0.495
10427	-0.00368	-0.00400	-0.00443	-0.00508	-0.00174	-0.00338	-0.00491	-0.00622	0.965	0.779	0.581
10428	-0.00332	-0.00363	-0.00404	-0.00467	-0.00190	-0.00409	-0.00618	-0.00804	1.179	0.961	0.736
10429	-0.00324	-0.00355	-0.00397	-0.00460	-0.00274	-0.00427	-0.00570	-0.00692	1.234	1.007	0.773
10430	-0.00280	-0.00310	-0.00353	-0.00416	-0.00438	-0.00606	-0.00762	-0.00898	1.562	1.276	0.973
10431	-0.00142	-0.00161	-0.00184	-0.00215	-0.00537	-0.00796	-0.01050	-0.01297	1.261	0.959	0.680
10432	-0.00360	-0.00396	-0.00446	-0.00525	-0.00222	-0.00457	-0.00677	-0.00869	1.476	1.216	0.935
10433	-0.00322	-0.00357	-0.00409	-0.00488	-0.00455	-0.00634	-0.00797	-0.00934	1.768	1.455	1.115
10434	-0.00383	-0.00418	-0.00468	-0.00547	-0.00123	-0.00364	-0.00590	-0.00788	1.328	1.099	0.846
10435	-0.00309	-0.00344	-0.00396	-0.00472	-0.00420	-0.00658	-0.00880	-0.01076	1.883	1.551	1.185
10436	-0.00200	-0.00228	-0.00258	-0.00303	-0.00362	-0.00719	-0.01076	-0.01416	1.263	0.938	0.674
10437	-0.00217	-0.00235	-0.00257	-0.00289	-0.00142	-0.00307	-0.00468	-0.00619	0.791	0.629	0.468
10438	-0.00192	-0.00208	-0.00226	-0.00252	-0.00172	-0.00307	-0.00439	-0.00563	0.677	0.527	0.385
10439	-0.00256	-0.00283	-0.00318	-0.00369	-0.00252	-0.00435	-0.00611	-0.00770	1.205	0.966	0.724
10440	-0.00225	-0.00246	-0.00273	-0.00313	-0.00275	-0.00416	-0.00551	-0.00673	0.989	0.792	0.593
10441	-0.00286	-0.00312	-0.00345	-0.00393	-0.00142	-0.00395	-0.00642	-0.00873	0.970	0.774	0.578
10442	-0.00166	-0.00187	-0.00215	-0.00252	-0.00464	-0.00654	-0.00838	-0.01012	1.339	1.035	0.747

Test	P outlet of bend (bar)			P bend=(P out-P in)			Bend outlet vel. (m/s)			Bend out susp density			Bend outlet air density		
No.	1	2	3	1	2	3	1	2	3	1	2	3	1	2	3
10400	0.394	0.292	0.196	-0.043	-0.043	-0.030	24.69	26.63	28.73	9.24	8.57	7.94	1.697	1.573	1.458
10401	0.493	0.383	0.265	-0.076	-0.038	-0.041	23.07	24.88	27.18	15.50	14.37	13.15	1.816	1.684	1.541
10402	0.632	0.493	0.342	-0.094	-0.034	-0.038	21.12	23.07	25.64	24.14	22.11	19.89	1.984	1.817	1.634
10403	0.748	0.579	0.404	-0.121	-0.045	-0.032	19.73	21.83	24.52	31.85	28.79	25.63	2.124	1.920	1.709
10404	0.518	0.390	0.266	-0.048	-0.052	-0.046	23.66	25.82	28.33	12.84	11.76	10.72	1.847	1.692	1.542
10405	0.678	0.526	0.366	-0.075	-0.039	-0.041	21.42	23.54	26.27	22.29	20.29	18.18	2.039	1.856	1.663
10406	0.853	0.670	0.474	-0.088	-0.034	-0.027	19.42	21.52	24.36	32.95	29.73	26.27	2.250	2.030	1.793
10407	0.963	0.748	0.526	-0.099	-0.051	-0.042	18.33	20.57	23.54	42.45	37.84	33.06	2.382	2.124	1.856
10408	1.244	0.973	0.689	-0.112	-0.061	-0.039	16.05	18.24	21.29	66.46	58.47	50.11	2.721	2.394	2.052
10409	0.559	0.429	0.297	-0.048	-0.052	-0.043	25.40	27.70	30.50	13.00	11.92	10.83	1.896	1.739	1.579
10410	0.885	0.698	0.498	-0.083	-0.057	-0.052	21.05	23.35	26.44	31.79	28.66	25.31	2.288	2.063	1.822
10411	1.154	0.895	0.636	-0.110	-0.089	-0.070	18.43	20.94	24.22	51.50	45.33	39.19	2.613	2.300	1.988
10412	1.329	1.029	0.736	-0.131	-0.108	-0.078	17.06	19.57	22.84	66.71	58.16	49.82	2.824	2.462	2.109
10413	0.603	0.458	0.310	-0.046	-0.056	-0.053	26.55	29.16	32.44	12.99	11.83	10.63	1.949	1.774	1.595
10414	0.902	0.701	0.489	-0.084	-0.075	-0.081	22.41	25.03	28.57	28.55	25.56	22.40	2.309	2.067	1.811
10415	1.177	0.942	0.682	-0.174	-0.111	-0.096	19.59	21.95	25.32	51.32	45.80	39.70	2.641	2.357	2.043
10416	1.523	1.170	0.816	-0.166	-0.166	-0.153	16.92	19.65	23.46	78.77	67.80	56.79	3.058	2.632	2.205
10417	0.608	0.467	0.315	-0.054	-0.058	-0.056	27.95	30.61	34.11	11.18	10.21	9.16	1.955	1.785	1.601
10418	1.251	1.012	0.762	-0.116	-0.068	-0.038	18.95	21.18	24.18	50.24	44.95	39.39	2.730	2.442	2.140
10419	0.669	0.536	0.394	-0.041	-0.026	-0.012	26.93	29.25	32.18	12.92	11.89	10.81	2.029	1.868	1.697
10420	1.025	0.843	0.639	-0.082	-0.043	-0.030	22.23	24.41	27.43	32.48	29.59	26.33	2.457	2.238	1.992
10421	0.691	0.540	0.381	-0.040	-0.042	-0.039	28.27	31.00	34.54	11.47	10.46	9.39	2.054	1.873	1.682
10422	1.036	0.851	0.639	-0.085	-0.051	-0.042	23.51	25.84	29.15	28.59	26.01	23.06	2.470	2.247	1.993
10423	1.053	0.846	0.627	-0.105	-0.061	-0.035	19.34	21.49	24.35	43.85	39.47	34.83	2.491	2.242	1.978
10424	1.383	1.112	0.825	-0.124	-0.103	-0.083	20.10	22.67	26.20	52.94	46.95	40.62	2.889	2.562	2.217
10425	1.481	1.195	0.892	-0.137	-0.101	-0.076	19.31	21.82	25.29	59.63	52.79	45.54	3.007	2.662	2.297
10426	0.778	0.633	0.470	-0.061	-0.029	-0.024	23.96	26.06	28.92	21.44	19.71	17.76	2.159	1.985	1.789
10427	0.909	0.740	0.548	-0.055	-0.039	-0.033	28.53	31.29	35.13	15.40	14.04	12.50	2.318	2.113	1.882
10428	1.098	0.910	0.688	-0.081	-0.051	-0.047	25.98	28.52	32.23	25.19	22.94	20.31	2.545	2.318	2.052
10429	1.146	0.938	0.702	-0.088	-0.070	-0.071	25.40	28.12	31.98	27.27	24.64	21.67	2.603	2.352	2.068
10430	1.438	1.162	0.869	-0.124	-0.113	-0.104	22.37	25.21	29.14	46.85	41.58	35.97	2.955	2.623	2.269
10431	1.129	0.890	0.646	-0.133	-0.069	-0.033	16.92	19.04	21.83	58.21	51.71	45.11	2.582	2.294	2.001
10432	1.367	1.126	0.850	-0.108	-0.090	-0.086	25.81	28.72	32.98	33.52	30.13	26.23	2.870	2.580	2.246
10433	1.631	1.320	0.985	-0.137	-0.135	-0.127	23.24	26.34	30.75	47.70	42.09	36.05	3.188	2.813	2.409
10434	1.237	1.026	0.776	-0.091	-0.073	-0.070	27.30	30.13	34.34	26.09	23.64	20.74	2.713	2.458	2.157
10435	1.729	1.402	1.057	-0.154	-0.149	-0.124	22.41	25.44	29.67	54.10	47.64	40.85	3.306	2.912	2.496
10436	1.106	0.901	0.672	-0.157	-0.037	-0.003	20.25	22.42	25.47	37.41	33.78	29.74	2.555	2.308	2.031
10437	0.725	0.591	0.439	-0.066	-0.038	-0.029	22.98	24.90	27.52	20.40	18.82	17.03	2.096	1.934	1.750
10438	0.618	0.498	0.364	-0.059	-0.029	-0.021	22.21	23.97	26.30	19.11	17.70	16.14	1.967	1.822	1.661
10439	1.093	0.882	0.653	-0.112	-0.084	-0.071	22.87	25.42	28.91	33.43	30.07	26.43	2.540	2.285	2.009
10440	0.909	0.733	0.538	-0.079	-0.059	-0.055	22.32	24.57	27.66	28.00	25.43	22.59	2.318	2.105	1.870
10441	0.900	0.746	0.570	-0.070	-0.028	-0.008	25.18	27.38	30.42	20.72	19.06	17.15	2.306	2.121	1.909
10442	1.184	0.926	0.677	-0.155	-0.109	-0.070	18.19	20.61	23.64	54.40	48.01	41.85	2.649	2.338	2.038

All of the relevant information on the results table was automatically sent to the last linked spreadsheet. This sheet formed the database for all the test runs for a particular test material. The database enabled fundamental graphs to be plotted that showed if there were gaps in the test work that needed filling. A list of the database graphs is shown below. Once a complete set of results were obtained because the range of conveying characteristics had been covered, or the test material had degraded so much that further results would be considered unusable, the file was ready to be transferred to another software package for the final analysis.

The total pressure gradient in each straight pipe section was the value transferred to the data base. Once in the database, the pressure gradient for the air contribution towards the total pressure gradient for each straight section, was deducted to obtain the 'solids contribution to pressure drop', as explained in chapter 5. The solids contribution to the pressure drop is the excess pressure gradient, over and above that generated when air alone is flowing. Originally, the Darcy/Fanning equation was used to calculate the air only pressure gradient, but subsequently, another value for the air only pressure gradient was used that was determined from an equation obtained from air only test runs using the test rig, see appendix 3.

A5.3.5 Database list of graphs produced using the Quattro Pro software

The database incorporated macros that transferred the data from each test run into columns, as shown on pages 10 to 14. This enabled graphs to be plotted by selecting two or more columns, for the analysis of the test results. Several graphs were plotted from the database of each material, during the conveying trials. This enabled any gaps in the data to be filled by further test runs, and made it possible to identify results that appeared inconsistent with all the previous data, which may have necessitated repeating that particular test run to compare the results.

The list of variables used to plot graphs using the Quattro Pro software, is listed below.

A	Solids contribution to pressure drop v midpoint suspension density
B	Solids + air contributions to pressure drop v midpoint suspension density
C	Midpoint suspension density v midpoint air velocity
D	Mass flow rate of solids v mass flow rate of air in straight sections
F	Bend outlet suspension density v bend outlet air velocity
G	Pressure drop across bend v bend outlet suspension density

H Pressure drop across bends - linear v bend outlet air velocity

I Solids contribution to pressure drop v midpoint air velocity

A5.3.6 Software to draw graphs, and analyse data

The final databases formed in Quattro pro for each test material, were imported into the software, Excel for Windows. As well as being widely used, this package was considered the most suitable because of the ease of transferring data into word processing documents written in MS-Word.

Using Excel enabled several graphs to be drawn using a combination of the variables stored in the databases. In addition, derived variables were also used to plot graphs in the search to find some order in the results. Eventually, the process was refined so that only a limited number of graphs were needed to be plotted for each material, the others being eliminated because they provided insufficient information value.

From each database, an initial graph was drawn for solids pressure drop (mbar/m) versus suspension density (kg/m^3). Due to the number of data points produced from each test run, it became necessary to filter the results into restricted velocity ranges and plot the results on separate graphs. An example of the final means of processing is shown on graph A5.4. Chapter 5 gives full details of what model was used, and for what reason. The results suggested a linear model drawn through the origin; the suspension density is the mass flow rate of solids divided by the volume flow rate of air, and the absence of solids in the pipeline during a conveying test, would mean zero suspension density. Therefore, no pressure drop due to solids would be measured. Hence any model used could be drawn through the origin.

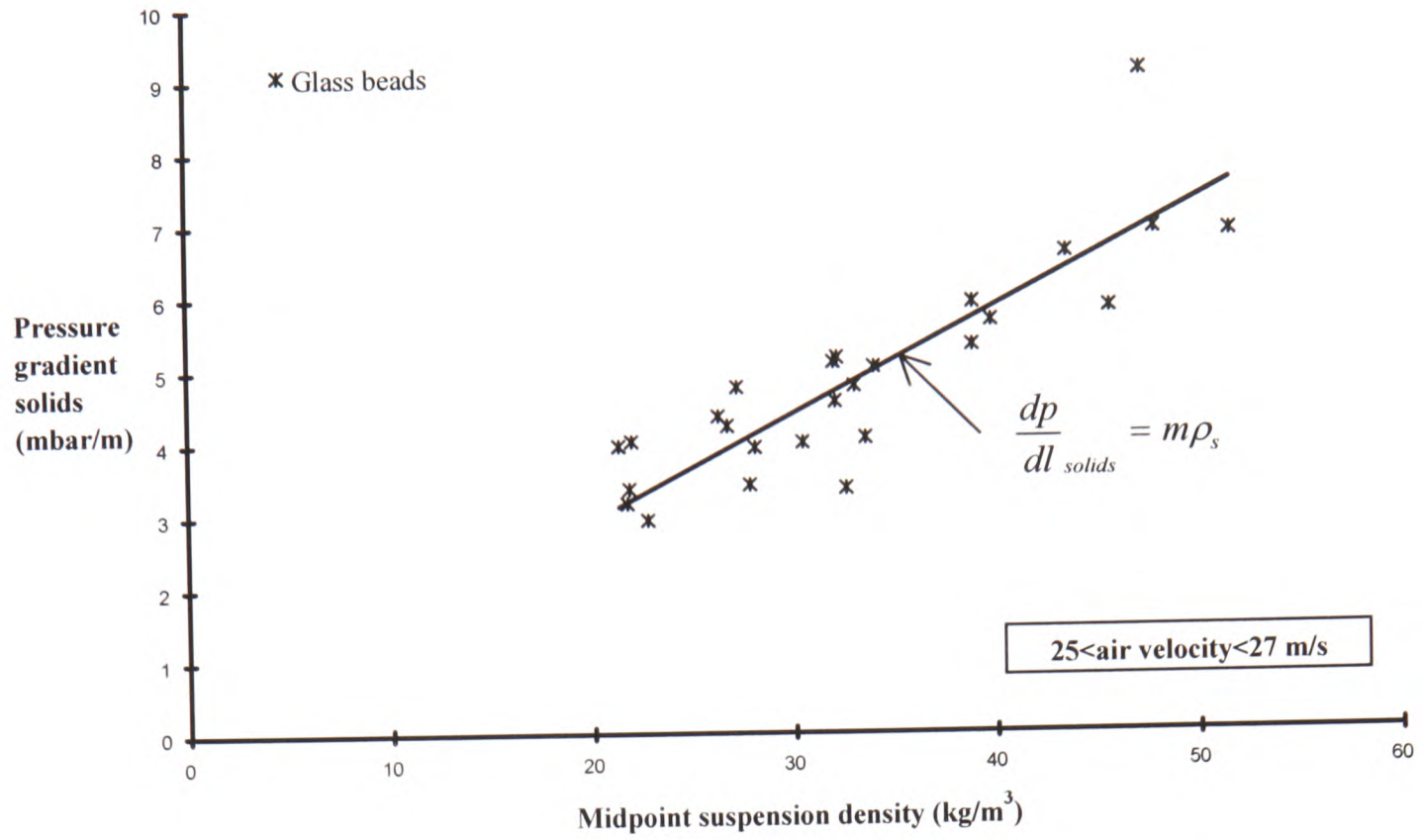

Graph A5.4: showing the midpoint suspension density versus pressure gradients of solids, for an individual velocity range of 25 to 27 m/s.

One graph was drawn for each of the several air velocity ranges, and the slopes of the straight line model fitted to each graph were plotted on a further graph, an example is shown on graph A5.5. That graph plotted the slopes versus the midpoint air velocity range and produced a curve from which a coefficient for that particular material was determined.

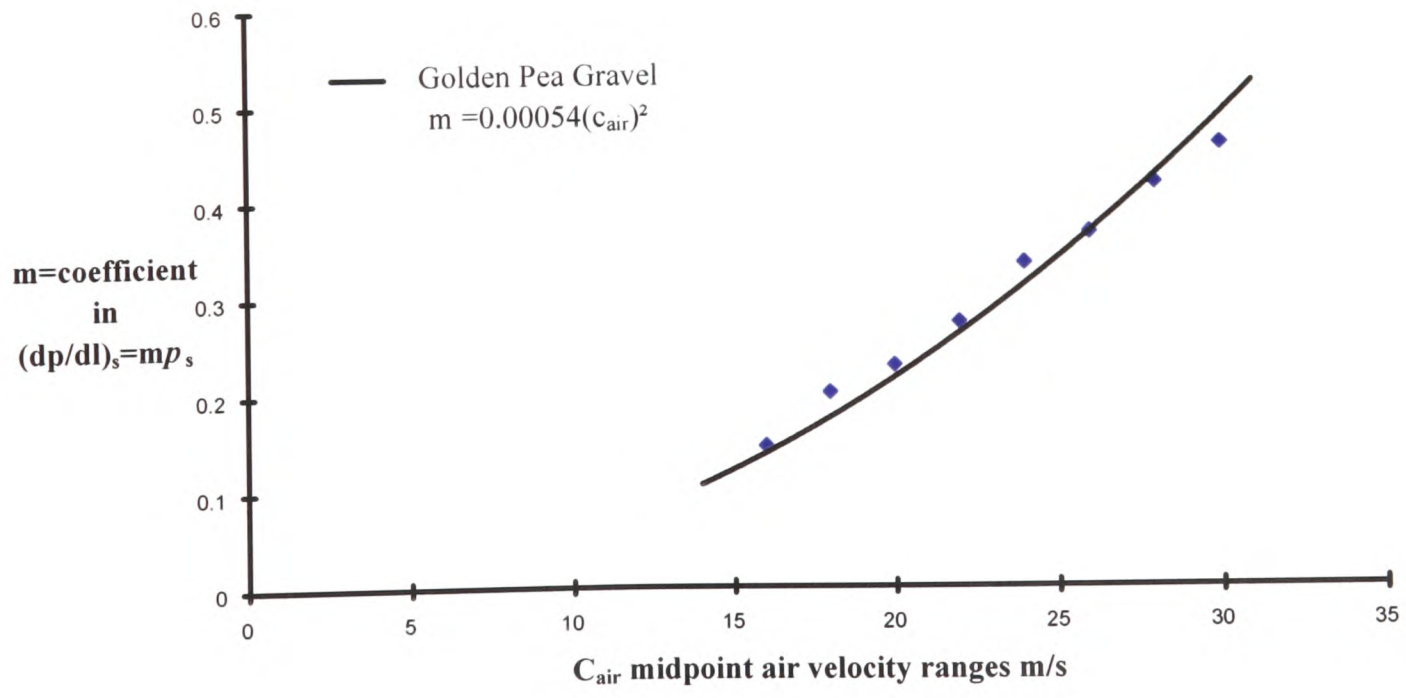

Graph A5.5. Example of graph plotting the m = coefficient values, from each air velocity range graphs, versus midpoint air velocity.

A5.4 Spreadsheet used to predict the pressure losses along straight sections

It was desirable to test the pressure gradient prediction method developed using the coefficients found by the test work, by applying it to a pneumatic conveying system in order to examine the reliability of the correlation method. The most suitable way to test the method was by using the test rig, and data obtained during the test program, and comparing the actual pressure drop over a substantial section including several bends and straights, against the pressure drop calculated using the prediction method. The results of the test program would provide actual measured data between the pressure transducers at either end of the test section, with suitable lengths of straight pipeline and test bends in between.

Using the prediction method for a pneumatic conveying system made up of several straight sections of pipeline and pipeline bends, required a systematic approach similar to that used by Bradley[B1]. Starting at the exit end of the pipeline where the conveying conditions of the air velocity, and suspension density can be found, calculations are employed using known conditions of atmospheric pressure, and the mass flow rate of air. An equation was used to determine the pressure drop along the last straight section, using the atmospheric pressure and density values for air at the outlet end of the pipe. Once values for the pressure and air density at the opposite end of the pipe are calculated, they become the new values to be used in the next set of equations. These new values are then used to calculate the pressure drop along the previous section.

A flow diagram shows the procedure for finding the velocity and suspension density for each step along the pipeline, and is shown as follows:-

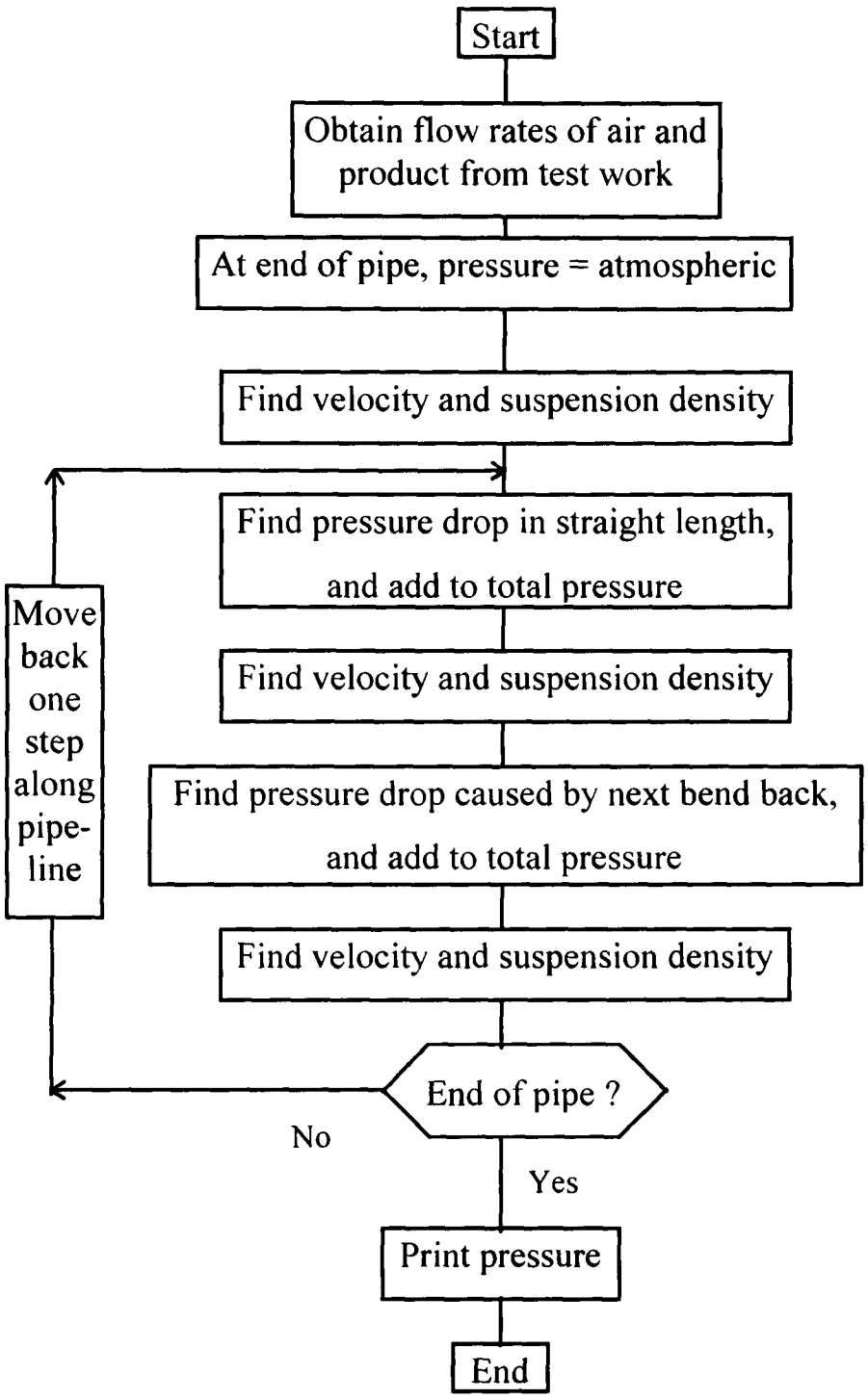

When the pressure losses for the bends at the end of each straight section were due to be calculated, the measured mean value obtained from the test work for each test run, was used. This was because the extent of the test work and analysis on the straight sections of pipeline proved to be sufficient challenge for this Ph.D. project, and a model for the pressure losses caused by the bends had not been developed. The process of calculating the pressure drop along each straight section and bend individually, was repeated until the pipeline inlet was reached.

To speed up the repetitious calculations in the pressure loss prediction process, a spreadsheet was developed to calculate the numerous equations and provide the predicted pressure values at the beginning and end of the test section, situated within the test rig pipeline.

The spreadsheet consists of cells that contain equations in almost all of the cells. The operator has only to type in the coefficient obtained from a particular material, to calculate the predicted pressure loss across the test section. Macros were set up that inserted the mass flow rate of air and solids, as well as the averaged pressure loss caused by the bends, from each test run into the spreadsheet. The macro then proceeded to calculate and produce the pressure drop across the straight pipes and bends, summing them up as it worked along the pipeline for each flow condition to produce an overall pressure drop for that condition, and transferred the information in columns for later use. The spreadsheet is shown in table A5.2, followed by the macros used in all four spreadsheets.

The result was a set of predicted pressure losses across the pipeline section under examination (several straights and bends) for a range of conditions of air and solid flow, which could then be compared to the measured pressure losses for the same conditions. Graph A5.6 below displays the results of the predicted and measured pressure losses.

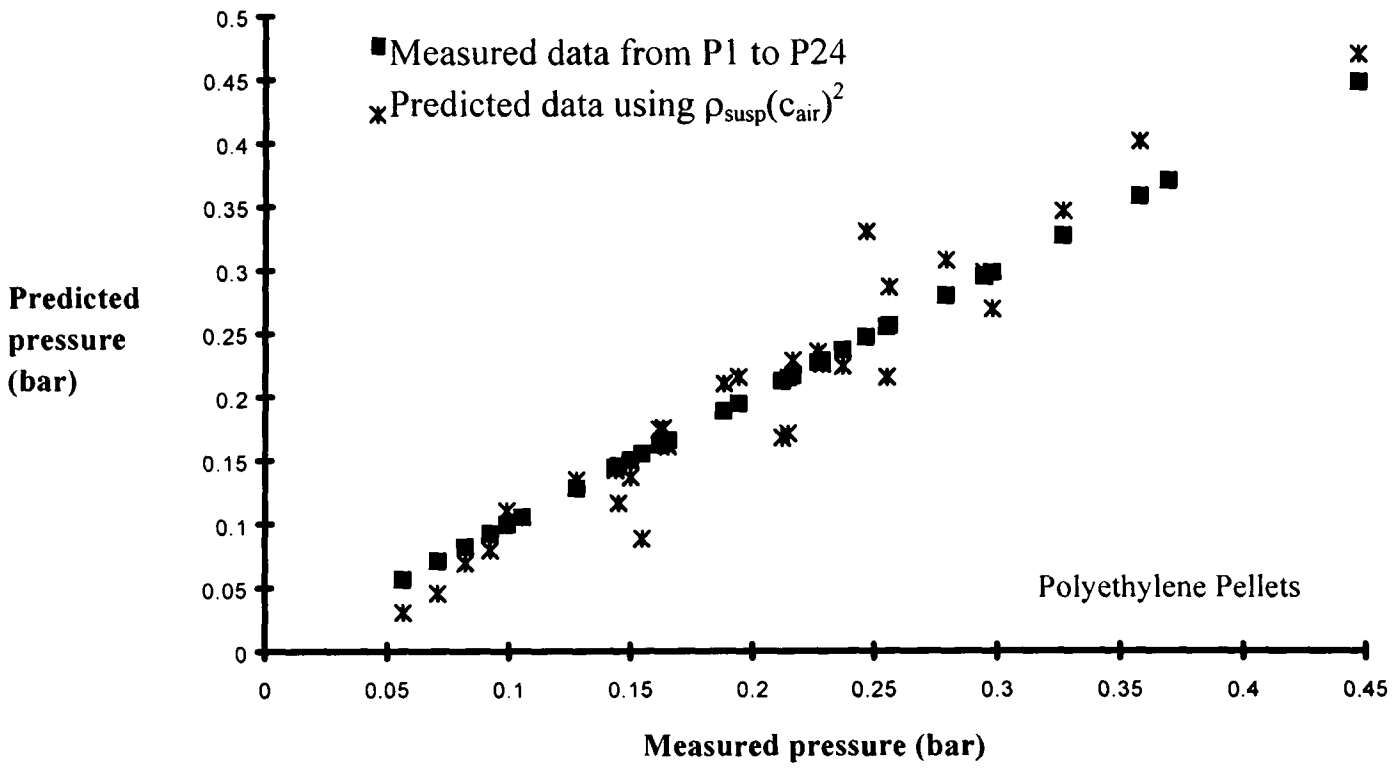

Graph A5.6: Example of the measured pressure loss results and the predicted pressure loss results, for the polyethylene pellets.

Table A5.2. Spreadsheet table to determine the pressure losses along a pipeline for specified conditions

Pipe section		P24 to end 4th straight	3rd bend	3rd straight	2nd bend	2nd straight	1st bend	Straight to p1
Length	(m)	15.0		17.0		17.2		7.1
P outlet	(bar)	1.19462	1.26096	1.37666	1.43843	1.55413	1.60876	1.72446
Vol air	(m^3)	0.0642	0.0608	0.0557	0.0533	0.0493	0.0477	0.0445
C vel	(m/s)	29.088	27.558	25.242	24.158	22.359	21.600	20.151
Model		0.16076	0.14429	0.12106	0.11088	0.09499	0.08865	0.07715
Susp den	(kg/m^3)	14.998	15.831	17.283	18.059	19.512	20.197	21.650
dp/dl air	(bar/m)	0.00201		0.00154		0.00123		0.00101
dp/dl solid	(bar/m)	0.00241		0.00209		0.00185		0.00167
dp/dl total	(bar/m)	0.00442		0.00363		0.00308		0.00268
delta p	(bar/m)	0.0663	0.1157	0.0618	0.1157	0.0546	0.1157	0.0191
P inlet	(bar)	1.26096	1.37666	1.43843	1.55413	1.60876	1.72446	1.74357
Rho air	(kg/m^3)	1.52555	1.66553	1.74027	1.88024	1.94633	2.08631	2.10943
P inlet (bar)	(bar_g)	0.26096	0.37666	0.43843	0.55413	0.60876	0.72446	0.74357

A5.5 Input data macros

\I Import .prn files	{GOTO}A200~{/ File;ImportNumbers} {CLEAR} G:\{?}~ {GOTO}Q200~ {/ File;ImportNumbers} {CLEAR} G:\{?}~ {/ Block;Move}R200..AA350~ {LEFT}~ {RIGHT 10} {/ File;ImportNumbers} {CLEAR} G:\{?}~ {/ Block;Move}AB200..AE350~ {LEFT}~ {/ Block;Move}A200..AC350~ {GOTO}B5~
\M M solids	{GOTO}Ae1~ (AA154-AA5)/(B154-B5)~{BEEP 1} {goto}AD4~{?}~{beep 1} {goto}AE4~{?}~
\A Average	{GOTO}C3~ (@AVG(C5..C154))~ {COPY} {/ Block;Copy}C3~ D3..AC3~
\C Block copy	{GOTO}B5~ {/ Block;Copy}B5..AC154~ AM5..BO154~

A5.5.1 Database macros

\B Move block	{/ Block;Values}A7..BL7 {GOTO}~A6..BL6~
\R Move results	{/ Block;Values}A13..Y16{beep 1} {GOTO}~{?} ~
\L	{/ Block;Values}A6..BL6{BEEP 1}

Import .prn macro

This macro imports the three files from the data acquisition unit into Quattro pro. Each file from the data acquisition unit has the time period of each reading in its first column. This macro also moves the columns across while deleting the first column of data from the second and third files as they are transferred into Quattro pro.

M solids macro

This macro calculates the mass flow rate of solids onto the load cells. It does this by adding the data in the load cell column and dividing it by the time period of the test run. This calculation is revised when the steady state period is determined.

Average macro

The data in all the columns are averaged and the products are put in designated cells using this macro.

Block copy macro

Due to a bug in the software, the block of data containing the newly transferred data is copied across to another area of the spreadsheet.

Move block macro

Moves the latest row of test run data from the results spreadsheet into the top line position on the spreadsheet.

Move results and list data macros

The top line results are copied to other sections of the spreadsheet for further analysis procedures.

A5.5.2 Macro worksheet

#VALUE!	COUNT=	STRTROW =	ROWS=	SUM=	AVG=	COL=
	150	0	149	#VALUE!	#VALUE!	27

```
        \S {GOTO}C2~{BEEP 1}
   STEADY {READING}
    STATE {FOR COL,0,27,1,NSTEP}
    NSTEP {LET SUM,0}{LET COUNT,0}
          {FOR COUNT,STRTROW,ROWS,1,AVERAGE}
          {PUT AVGBLOCK,COL,0,AVG}

  READING {GETNUMBER "ENTER FIRST READING NUMBER
          BETWEEN 0 AND 149  ",STRTROW}
          {GOTO}STRTROW~{?}~
          {GOTO}C2~
          {GETNUMBER "ENTER LAST READING NUMBER,
           HIGHER THAN THE FIRST READING,
           BUT NOT GREATER THAN 149  ",ROWS}
          {GOTO}ROWS~{?}~

  AVERAGE {LET SUM,@CELL("CONTENTS",SUM)+@
          CELLINDEX("CONTENTS",DBLOCK,COL,COUNT)}
          {BREAK}{RETURN}
```

5.3.1 Steady state macro

The macro shown above also involves some sub macros within it. Once the steady state period for the test run has been identified, the macro averages the columns of data and puts the results in specified cells. The results in the designated cells are also transferred to the results spreadsheet which determines the pressure gradients along the straight sections of pipeline.

Appendix 6

Graphs plotted using the test results

A6.1 Introduction

The objective of this exercise was to test predictors of pressure drop made using the prediction method, against measured values of pressure drop, in order to assess the accuracy of the prediction method.

The pressure loss prediction method was used to determine the pressure losses along the test section, which was made up of four straight sections and three test bends, (see diagram A6.1). The pressure losses were determined separately for the straight sections and the bends, so that the pressures along each element of a proposed system could be evaluated. The model containing the scaling coefficient (obtained from the analysis of each test material) was used to predict the pressure gradients along the straight sections. For the bends, actual measured values for their pressure losses, were used in the prediction method. Full details are found in chapter 6.

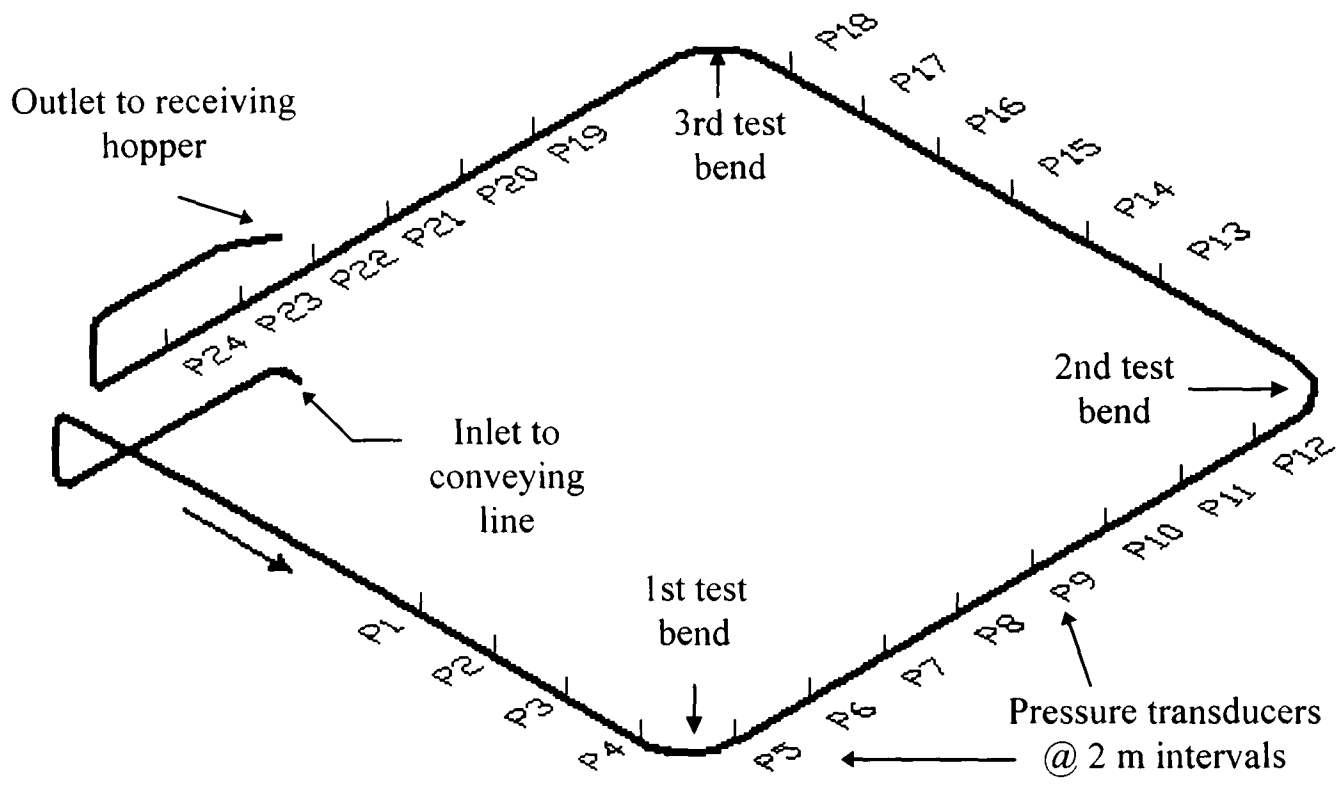

Diagram A6.1: Layout of the test rig pipeline showing the positions of the pressure transducers and test bends.

A6.2 Graphs plotted from the analysis of the test results

The following graphs display the predicted pressure loss values for the test section, together with the measured pressure losses, using data obtained from pressure transducers 1 and 24, as shown on diagram A6.1. In addition, graphs were plotted showing the percentage difference between both sets of results.

A6.2.1 Polyethylene pellets graphs

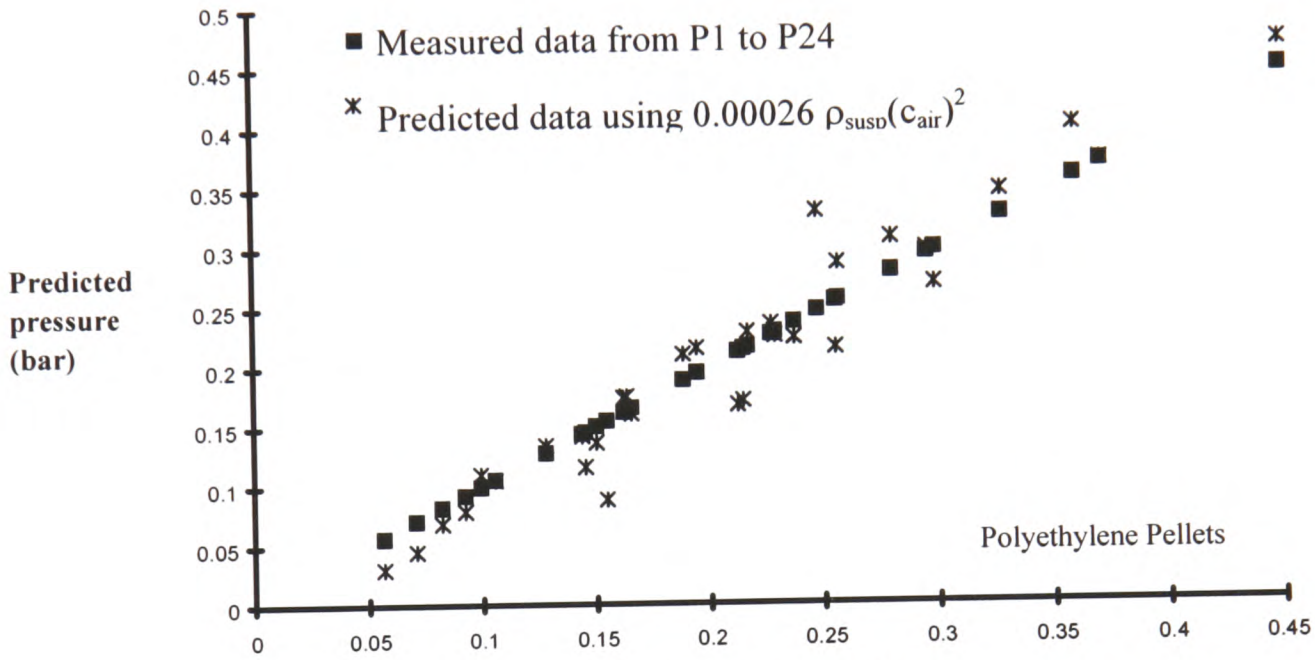

Graph A6.1: Polyethylene pellets - results of predicted and measured losses from pressure transducers 1 to 24.

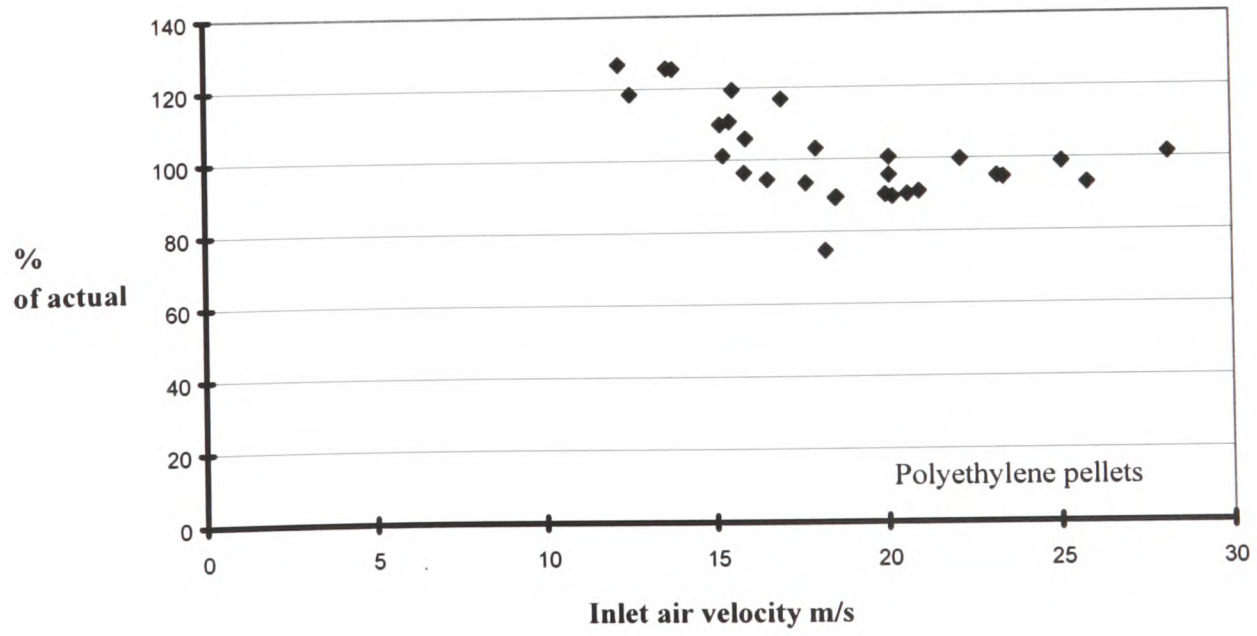

Graph A6.2: Percentage difference between the measured and predicted data for polyethylene pellets.

A6.2.2 Ground ilmenite graphs

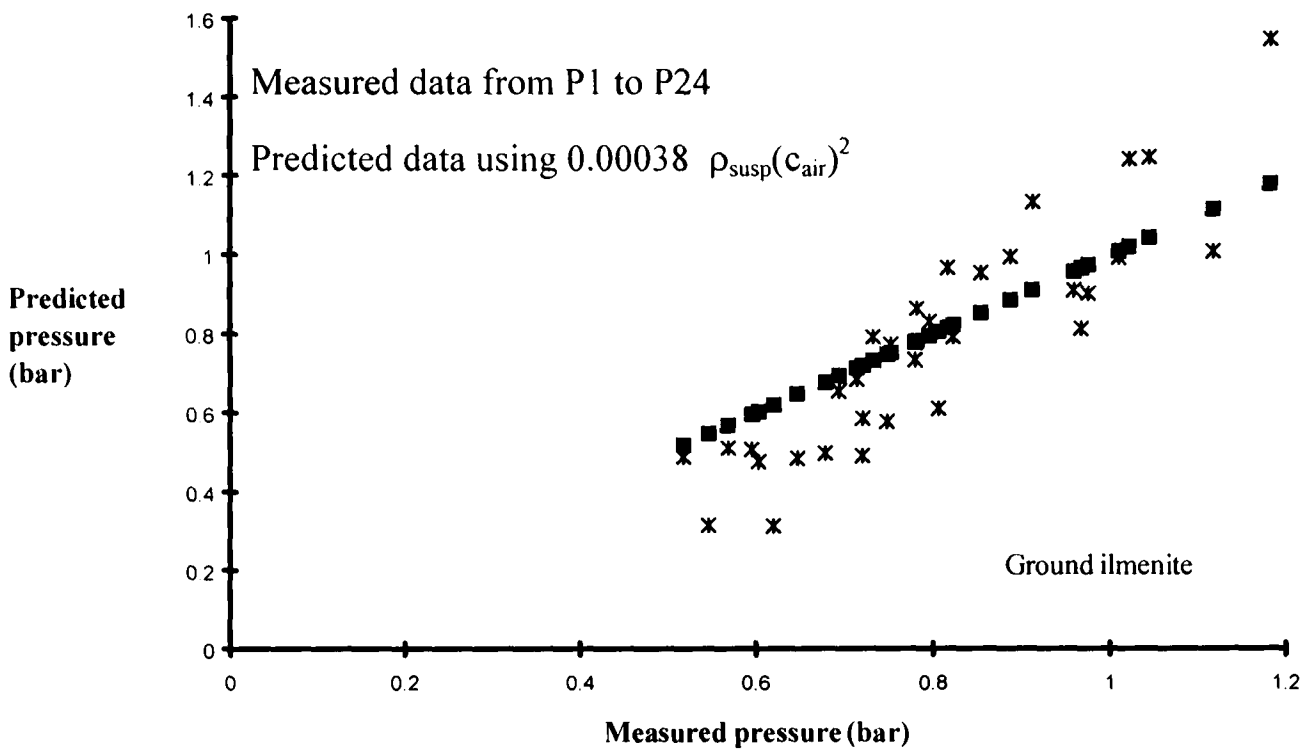

Graph A6.3: Ground ilmenite - results of predicted and measured losses from pressure transducers 1 to 24.

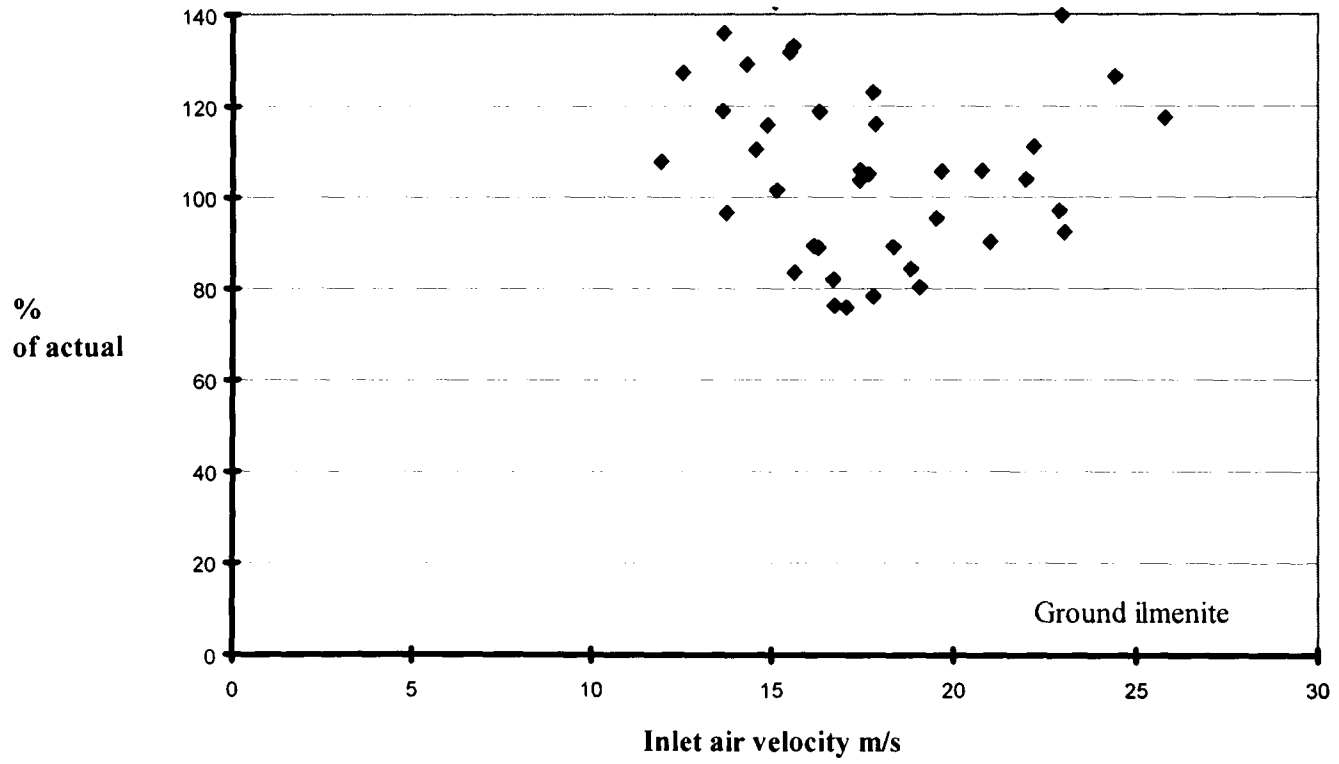

Graph A6.4: Percentage difference between the measured and predicted data for ground ilmenite.

A6.2.3 Sandy ilmenite graphs

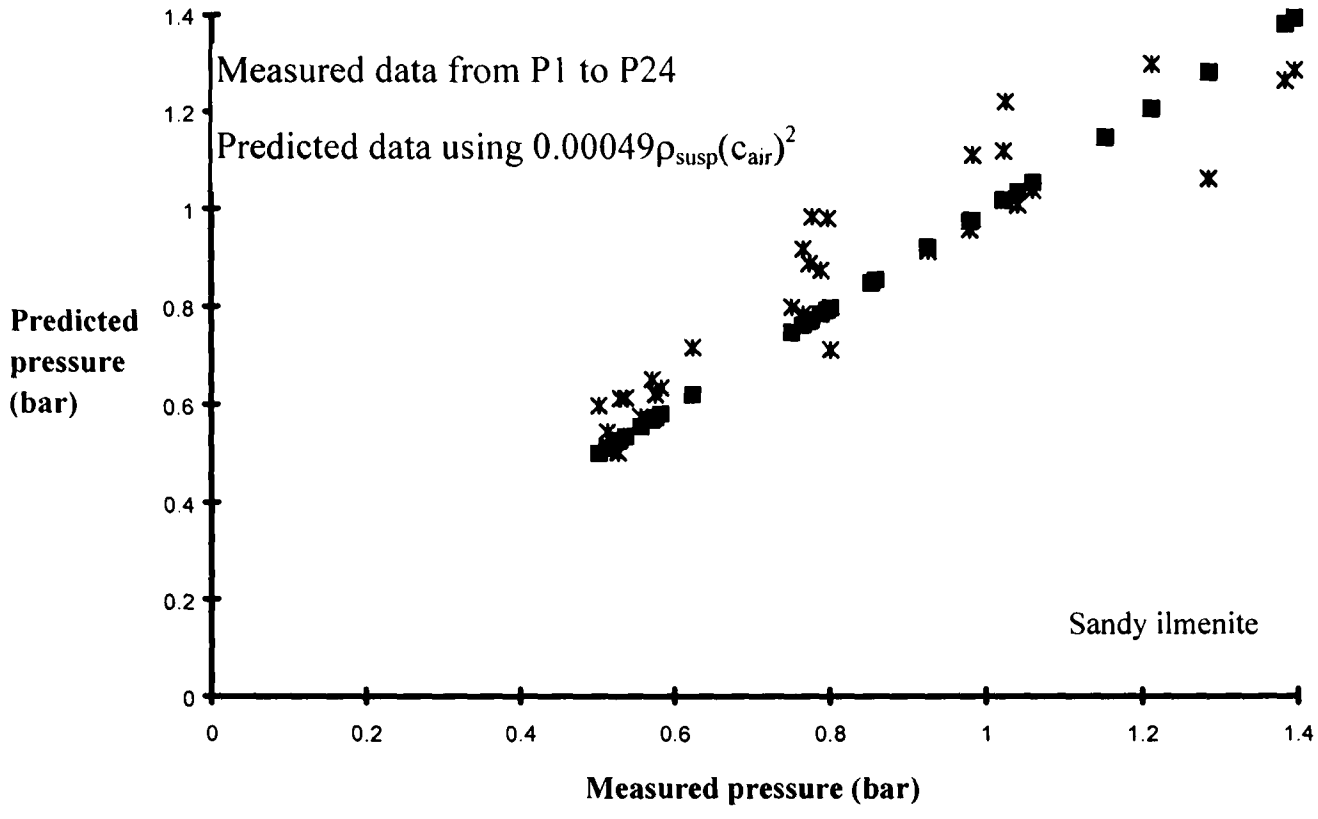

Graph A6.5: Sandy ilmenite- results of predicted and measured losses from pressure transducers 1 to 24.

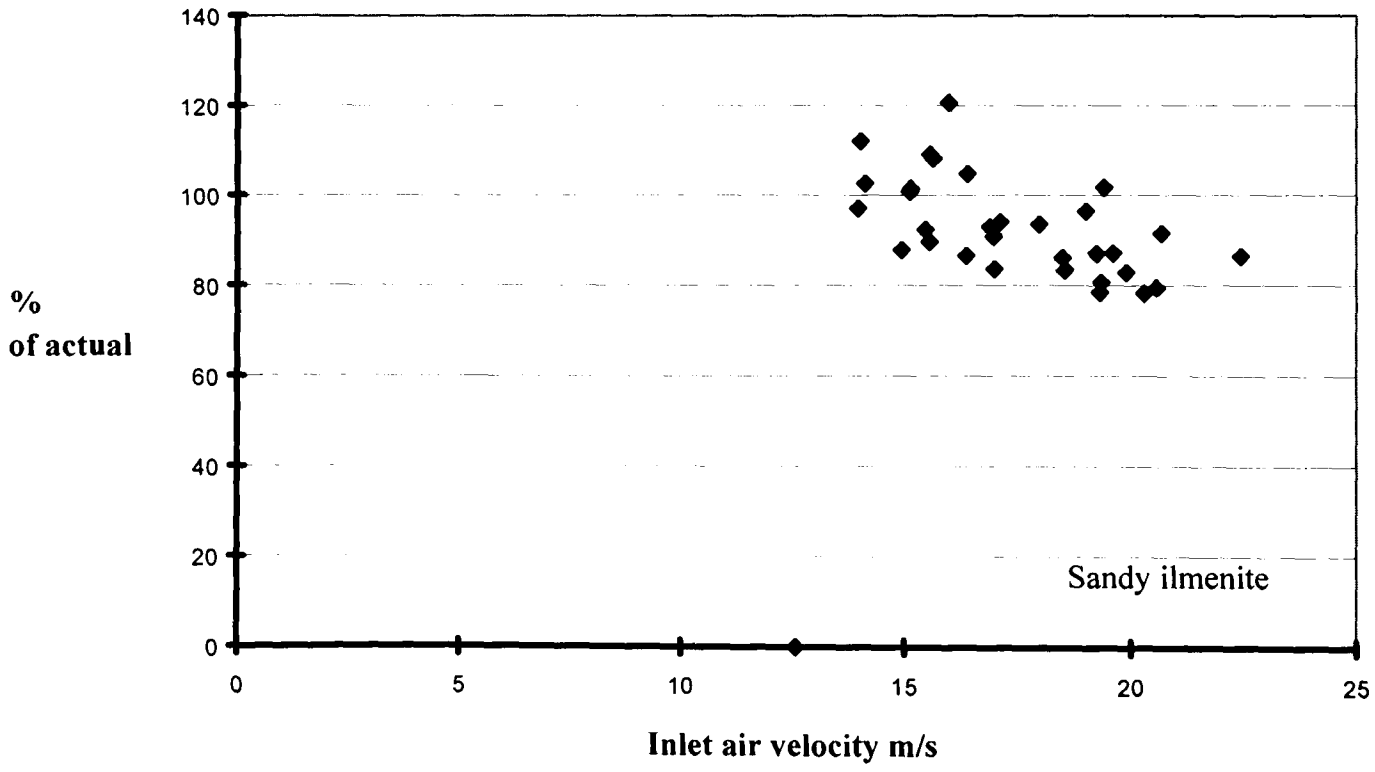

Graph A6.6: Percentage difference between the measured and predicted data for sandy ilmenite.

A6.2.4 Olivine sand graphs

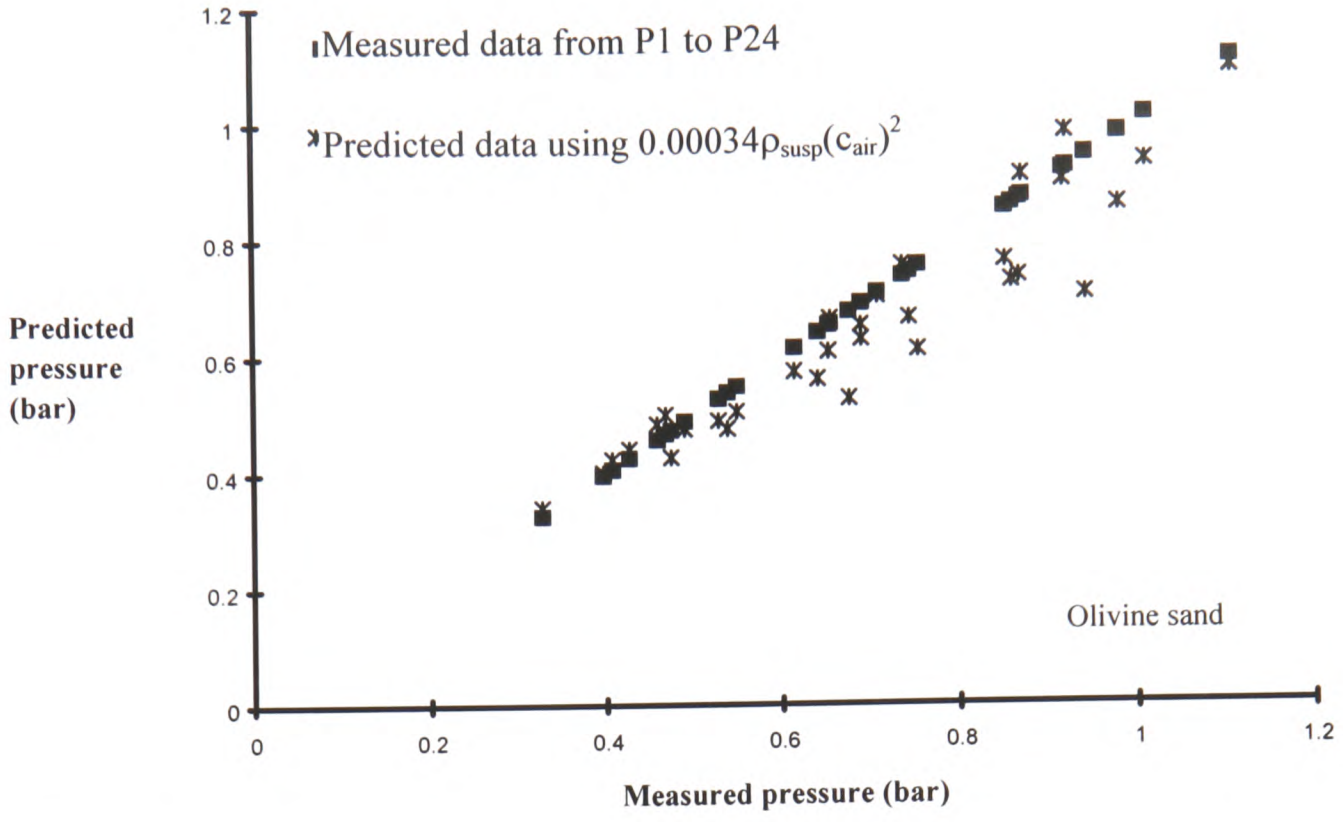

Graph A6.7: Olivine sand - results of predicted and measured losses from pressure transducers 1 to 24.

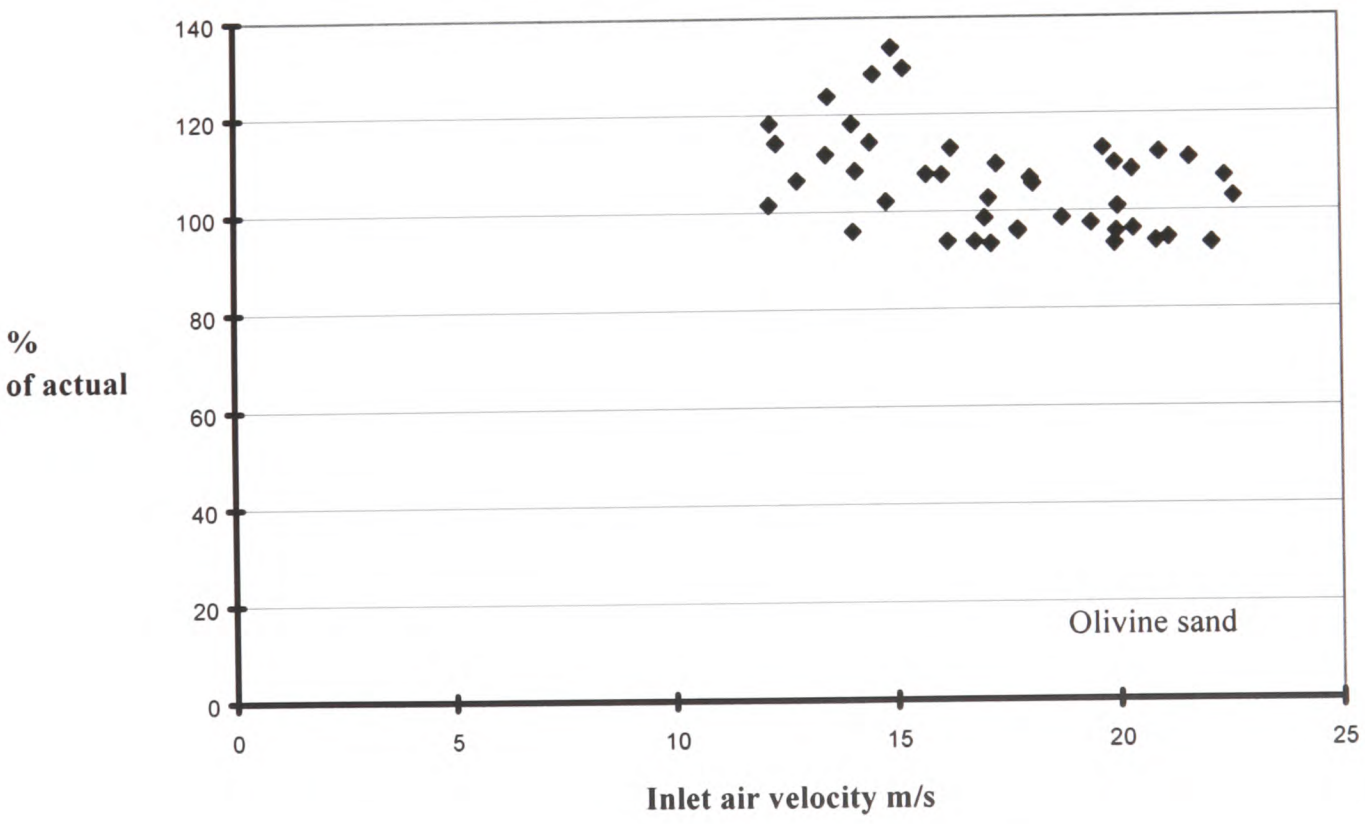

Graph A6.8: Percentage difference between the measured and predicted data for olivine sand.

A6.2.5 Silica flour graphs

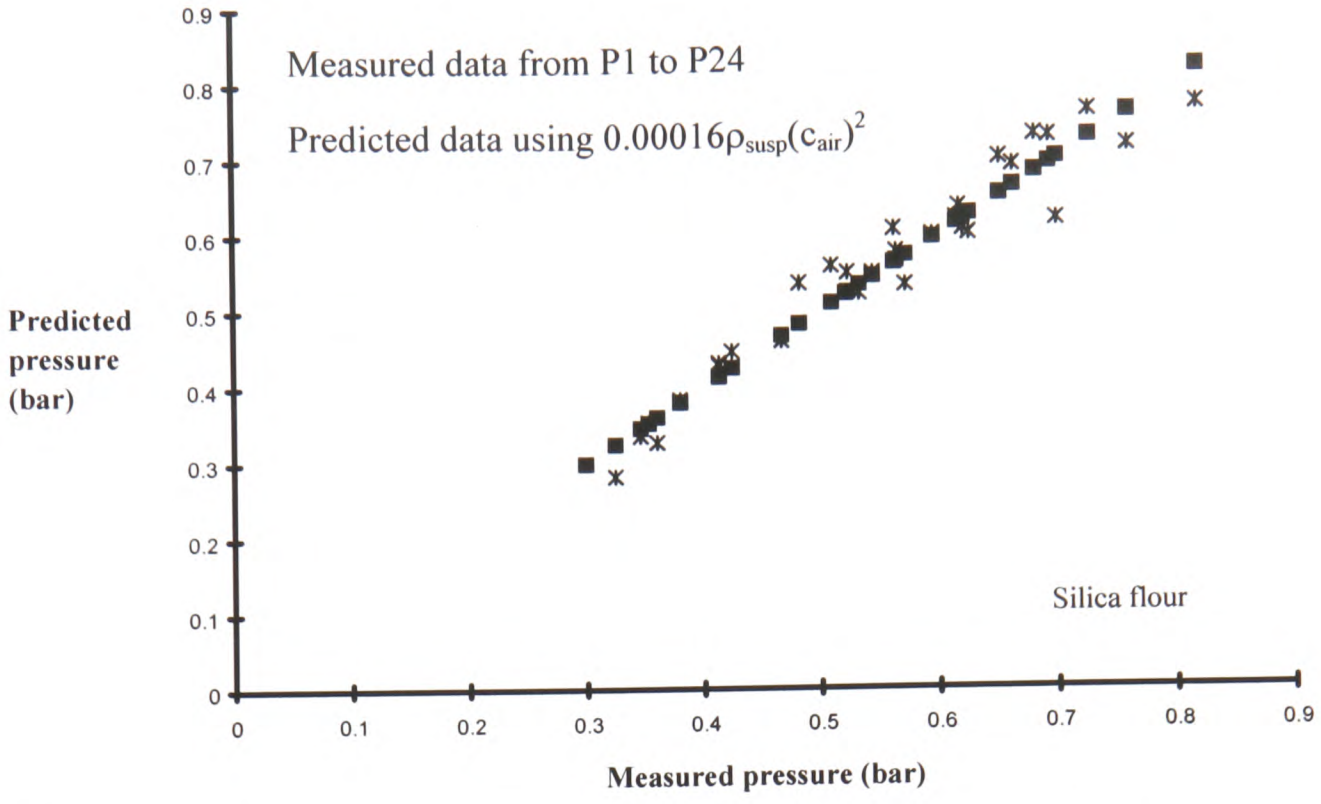

Graph A6.9: Silica flour - results of predicted and measured losses from pressure transducers 1 to 24.

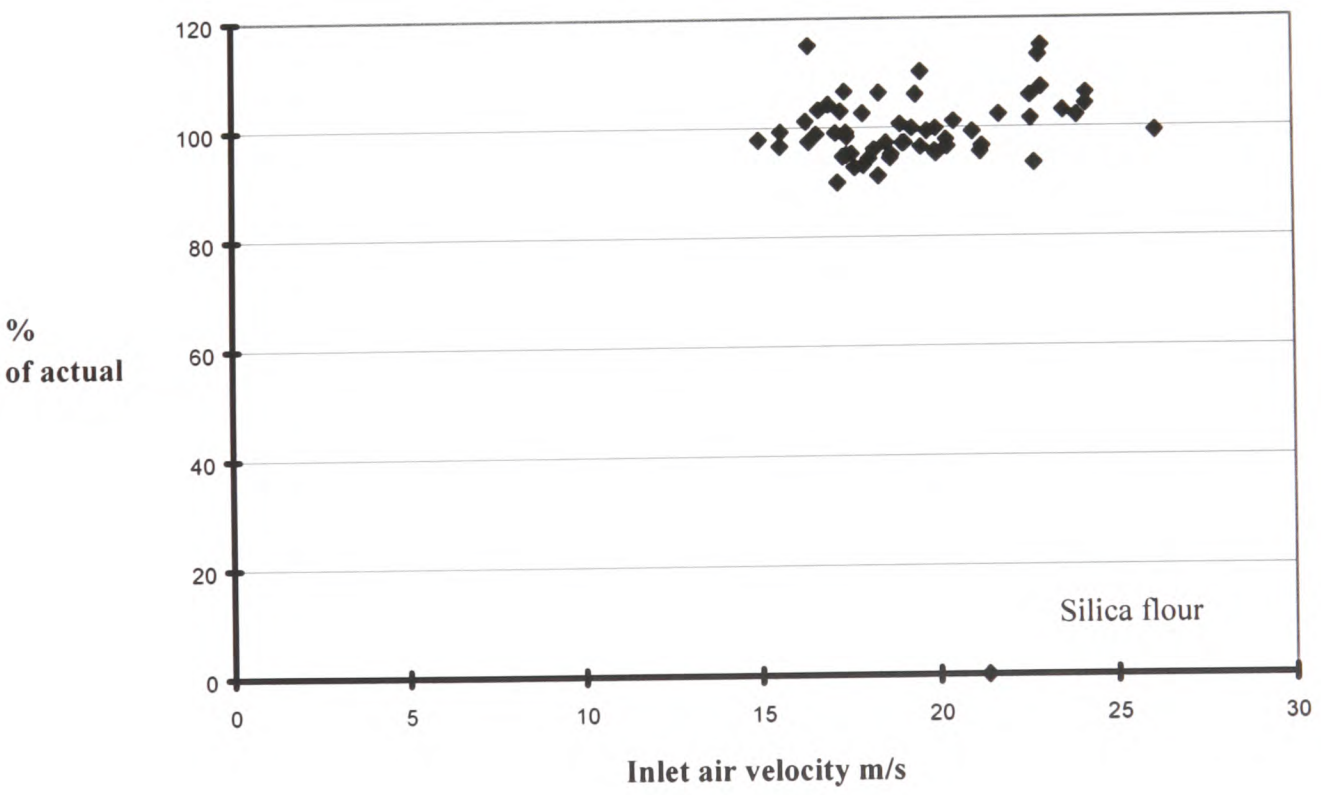

Graph A6.10: Percentage difference between the measured and predicted data for silica flour.

A6.2.6 Golden pea gravel graphs

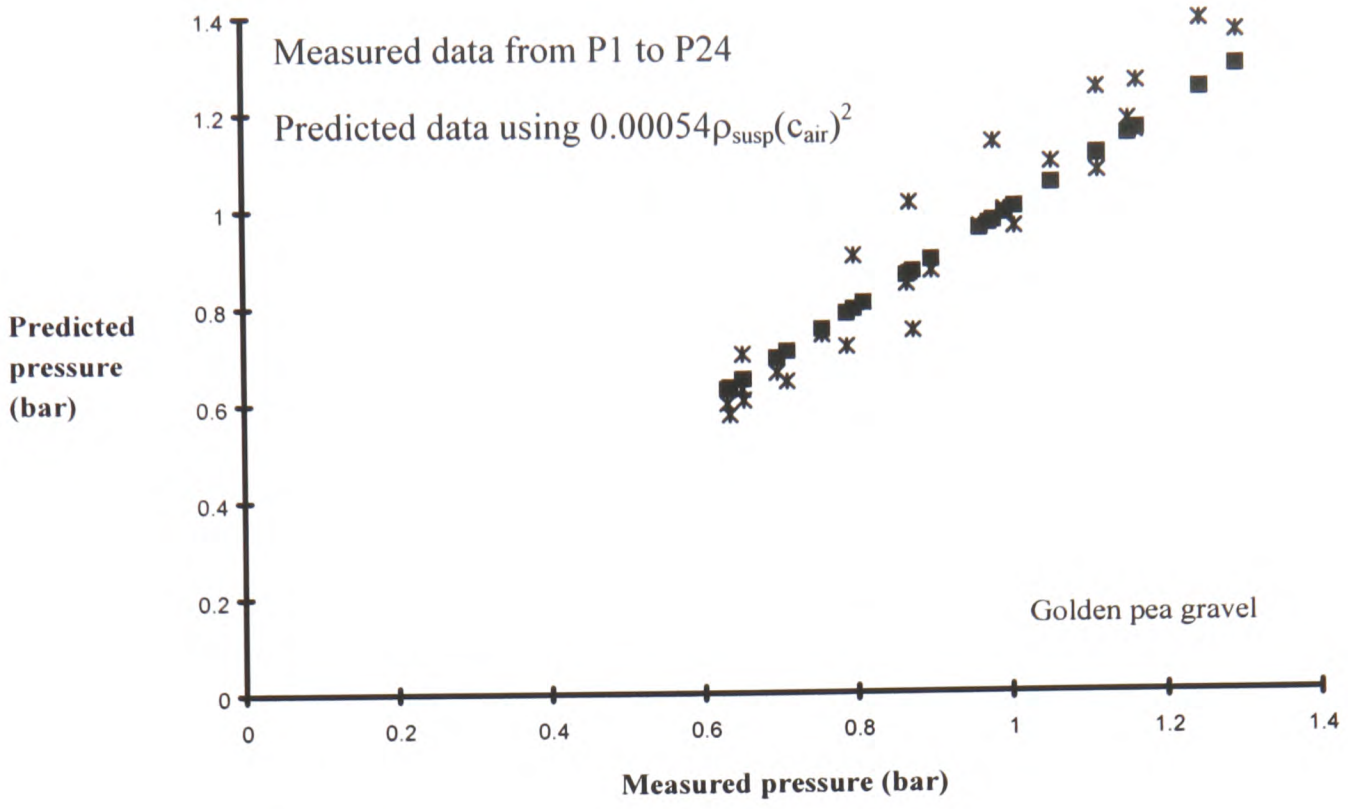

Graph A6.11: Golden pea gravel - results of predicted and measured losses from pressure transducers 1 to 24.

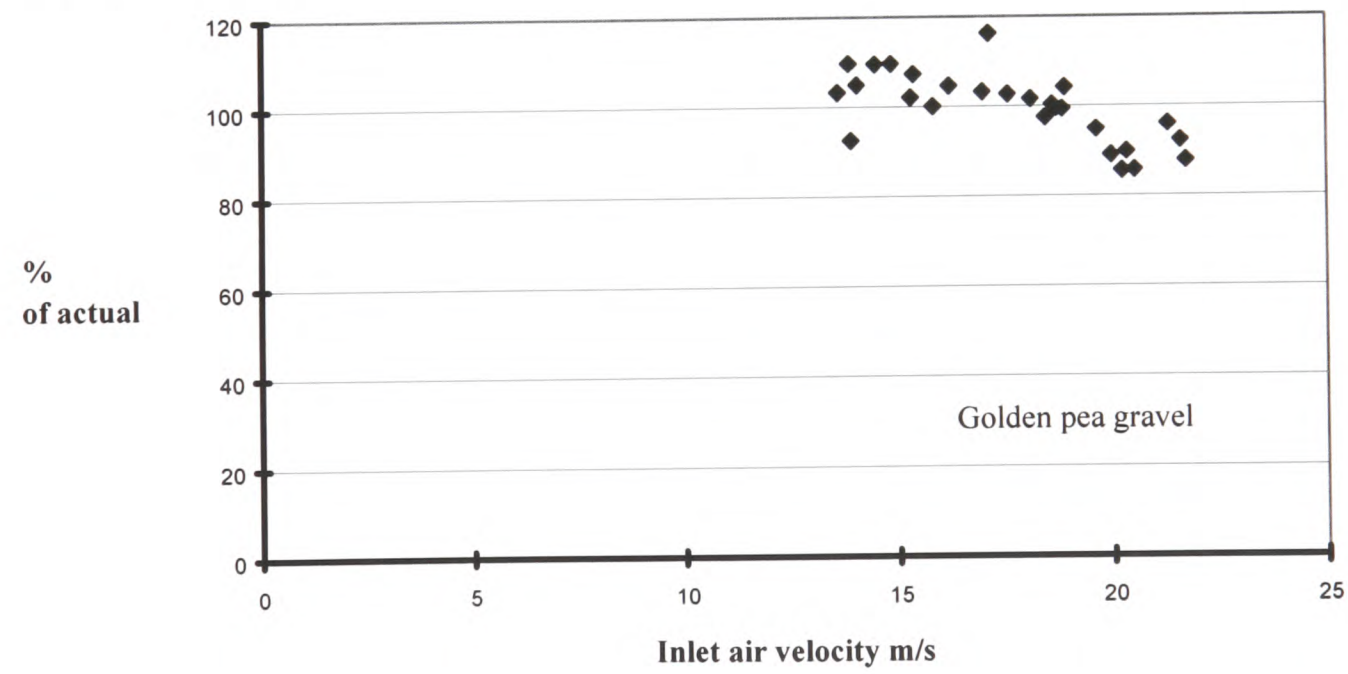

Graph A6.12: Percentage difference between the measured and predicted data for golden pea gravel.

A6.2.7 Granulated sugar graphs

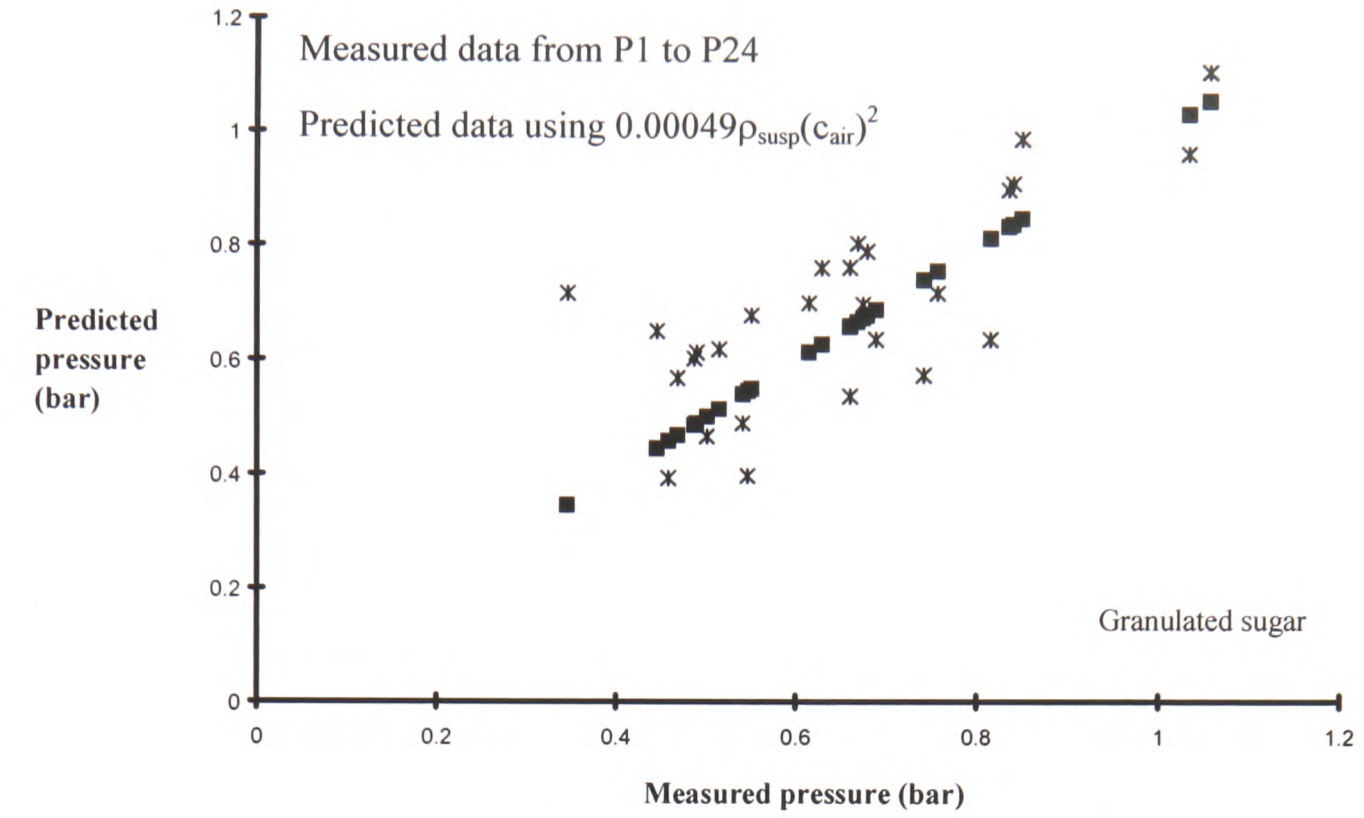

Graph A6.13: Granulated sugar - results of predicted and measured losses from pressure transducers 1 to 24.

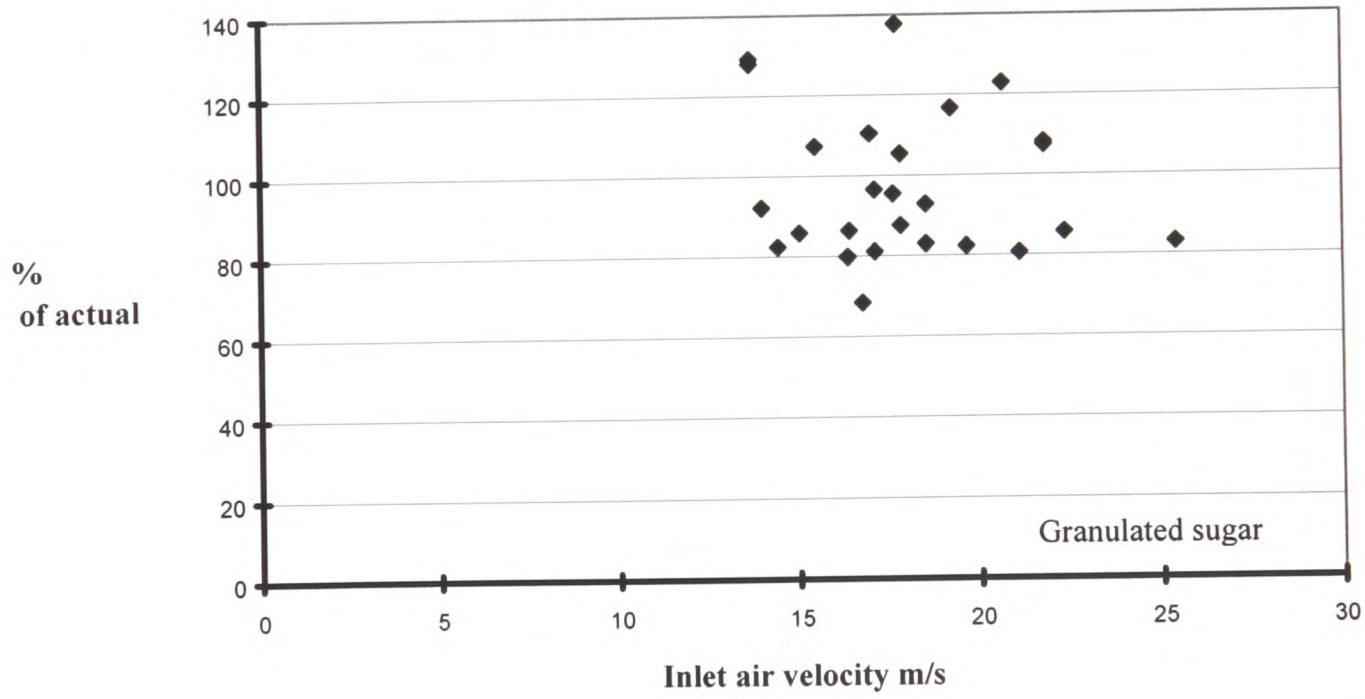

Graph A6.14: Percentage difference between the measured and predicted data for granulated sugar.

A6.2.8 Icing sized sugar graphs

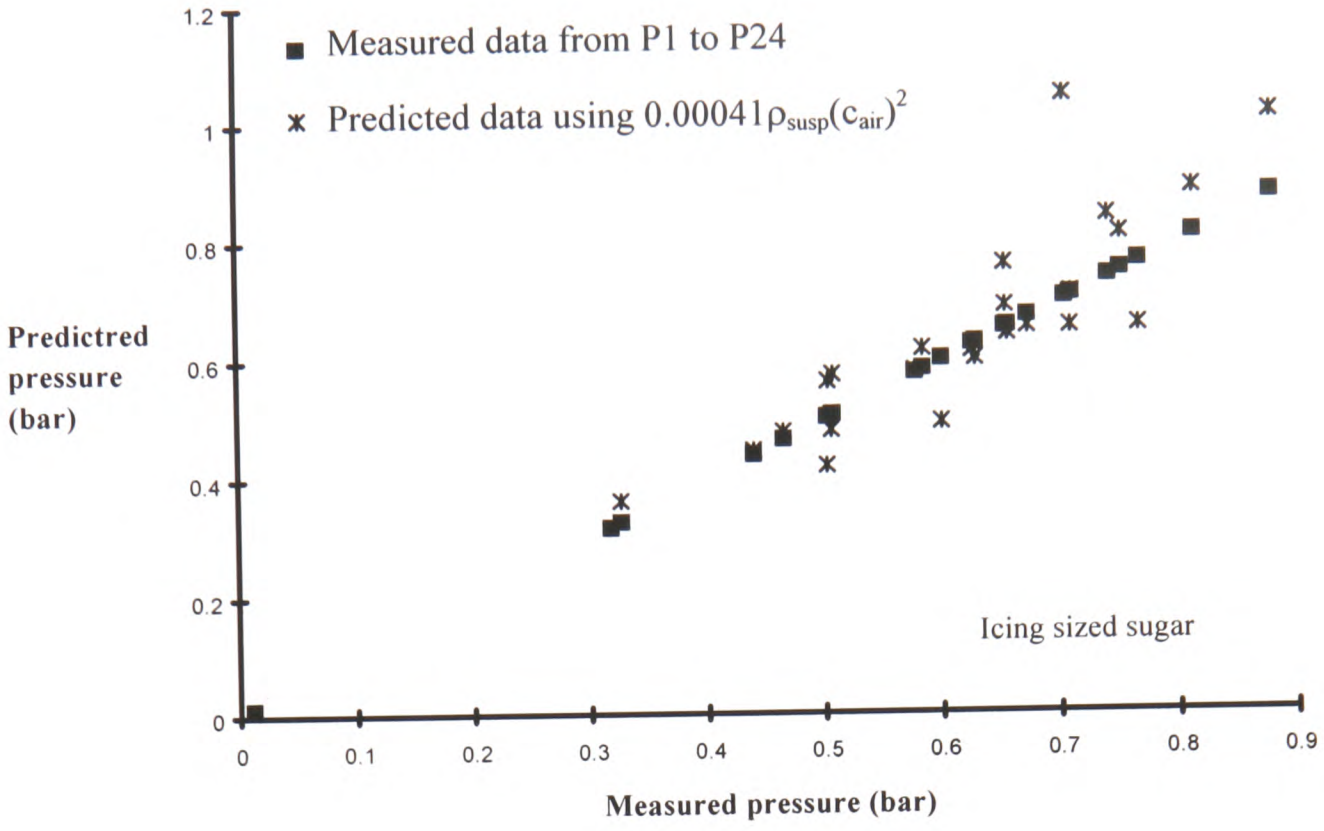

Graph A6.15: Icing sized sugar - results of predicted and measured losses from pressure transducers 1 to 24.

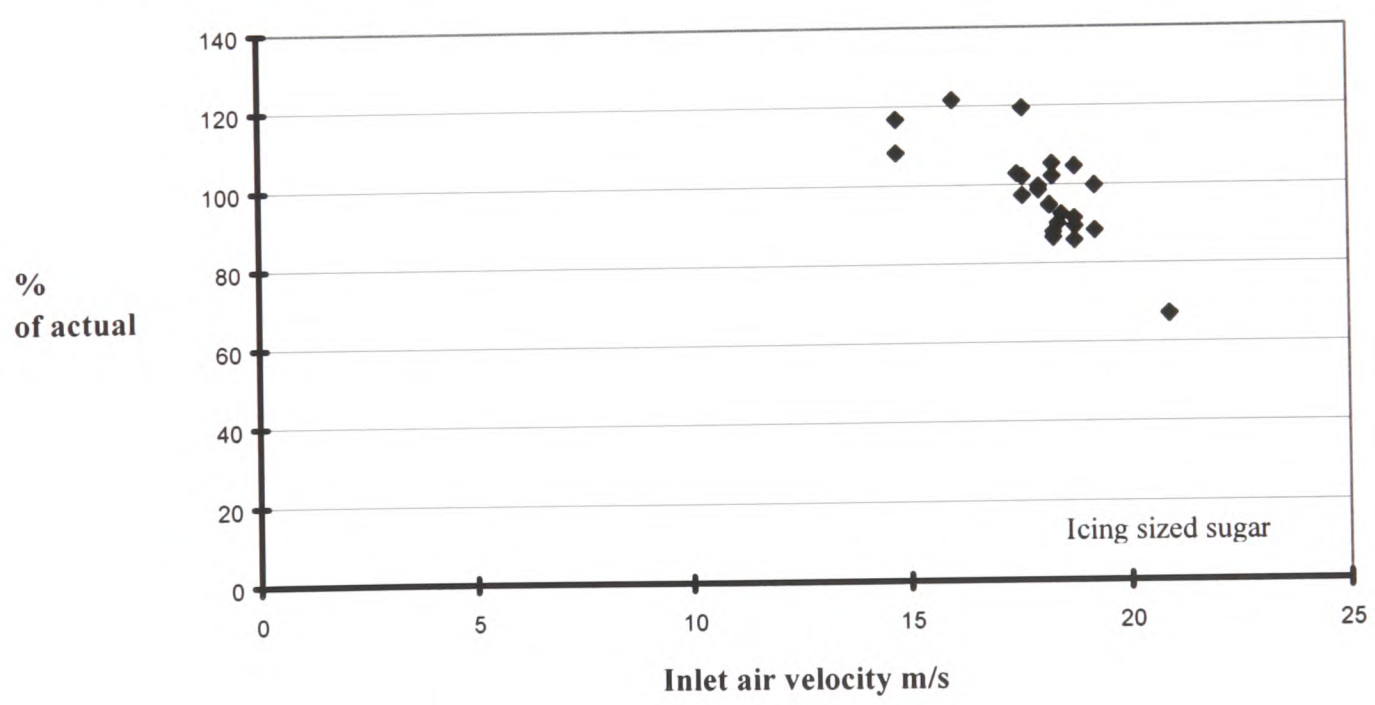

Graph A6.16: Percentage difference between the measured and predicted data for icing sized sugar.

A6.2.9 Boral lytag graphs

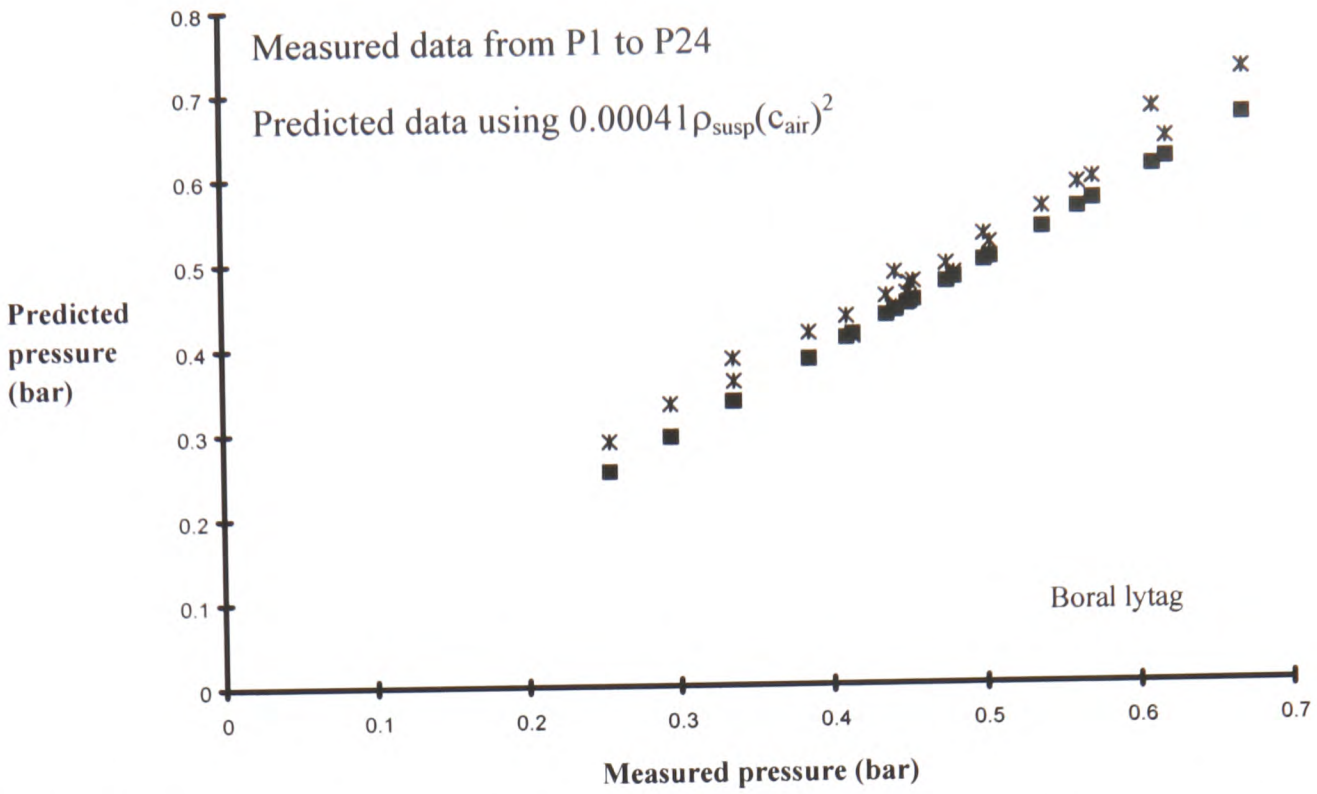

Graph A6.17: Boral lytag - results of predicted and measured losses from pressure transducers 1 to 24.

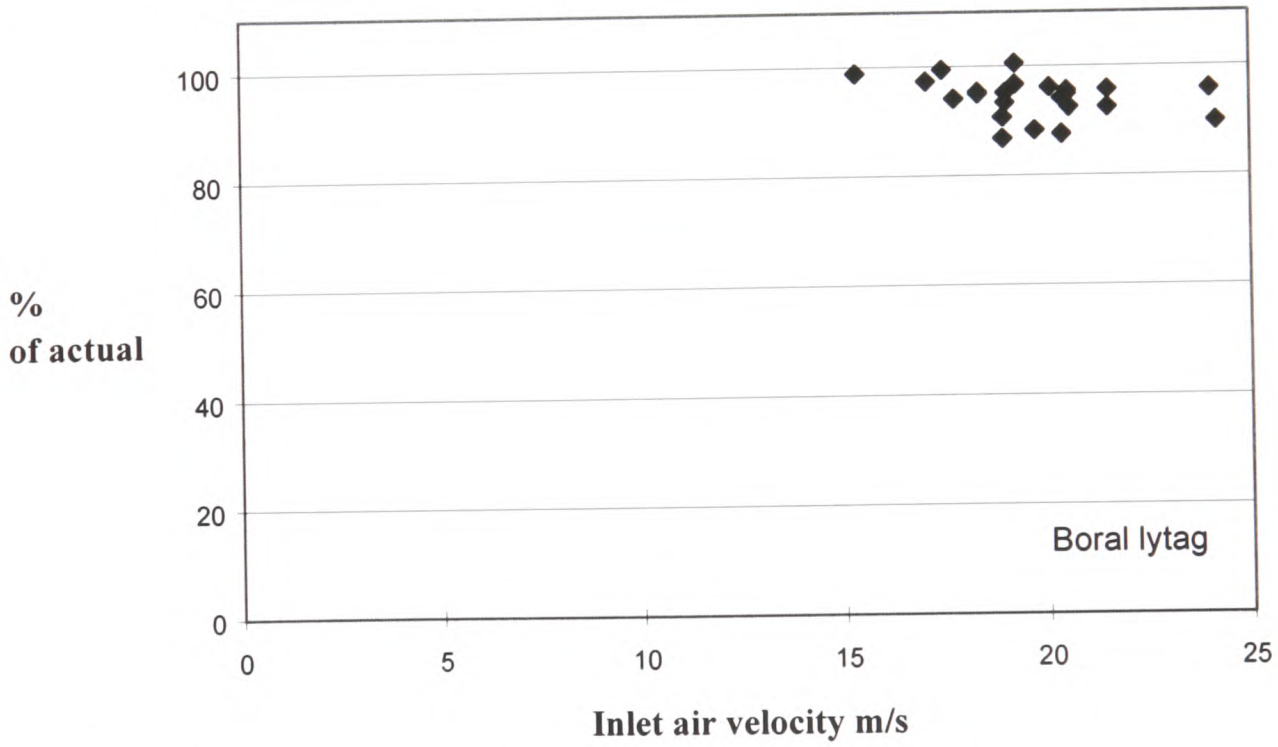

Graph A6.18: Percentage difference between the measured and predicted data for boral lytag.

A6.2.10 Glass beads graphs

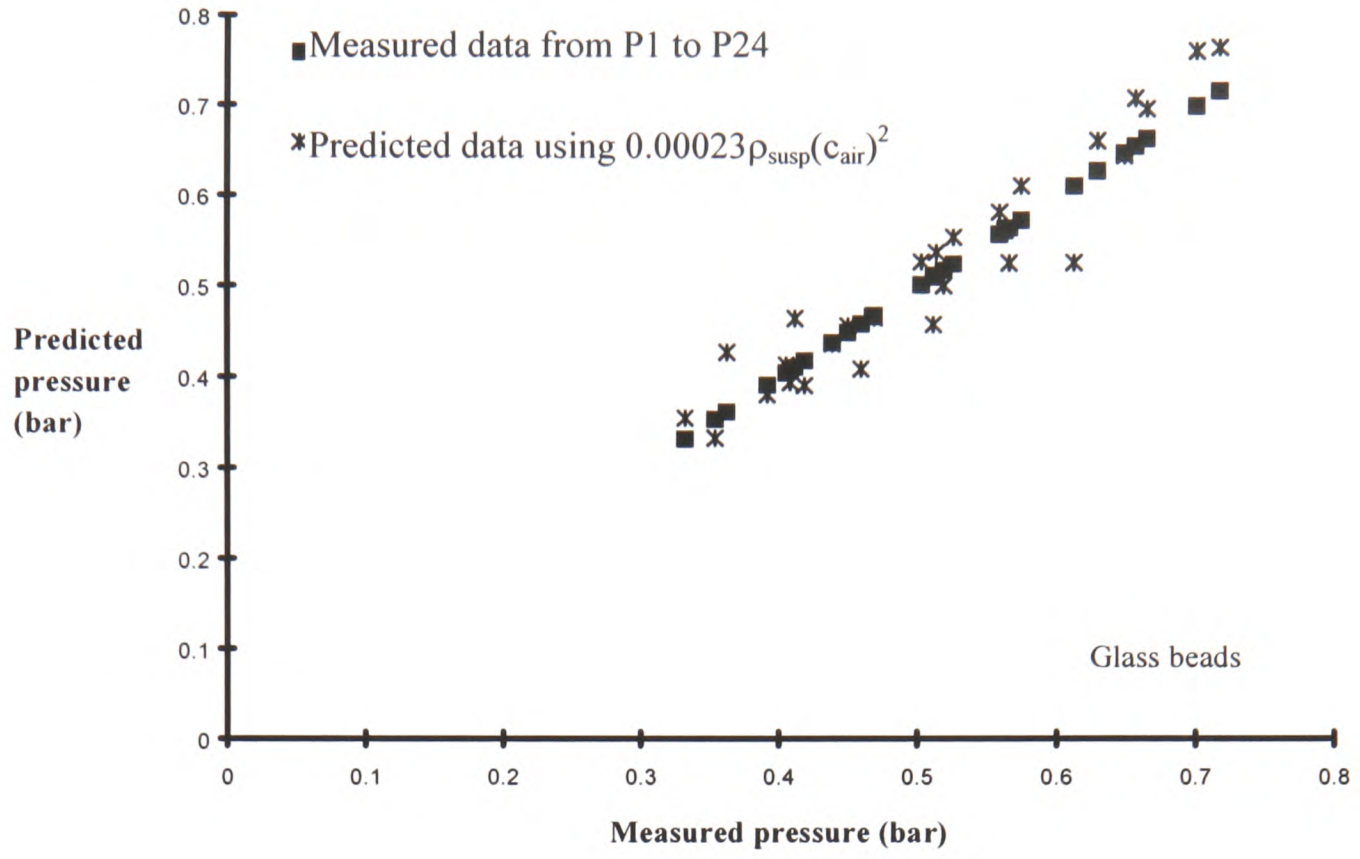

Graph A6.19: Glass beads - results of predicted and measured losses from pressure transducers 1 to 24.

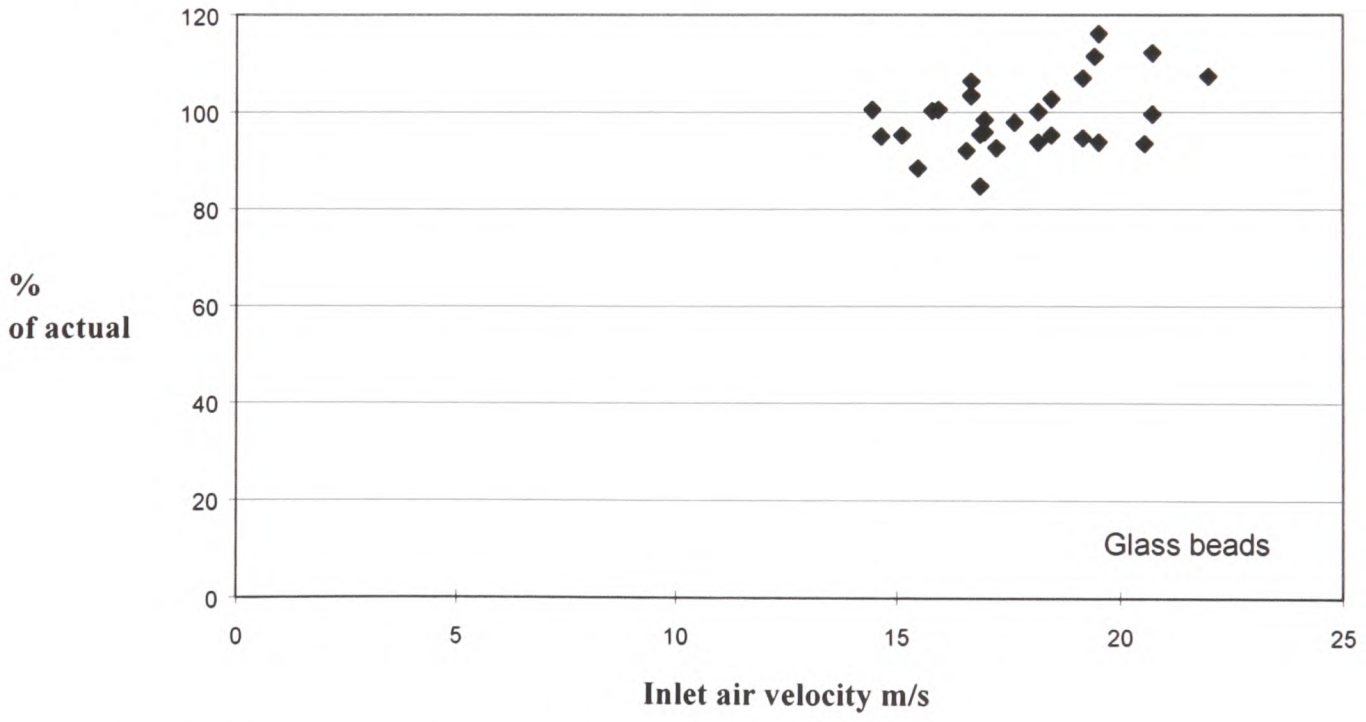

Graph A6.20: Percentage difference between the measured and predicted data for glass beads.

Appendix 7

Photographs of the test materials

A7.1 Photographs of the materials used in the test work programme

All the photographs shown in this section, were taken using a scanning electron microscope.

A7.1.1 Polyethylene pellets

The polyethylene pellets had been used for previous research projects, and were found to remain unchanged after the test work had been carried out using them. For these reasons, only one photograph of the polyethylene pellets is shown below.

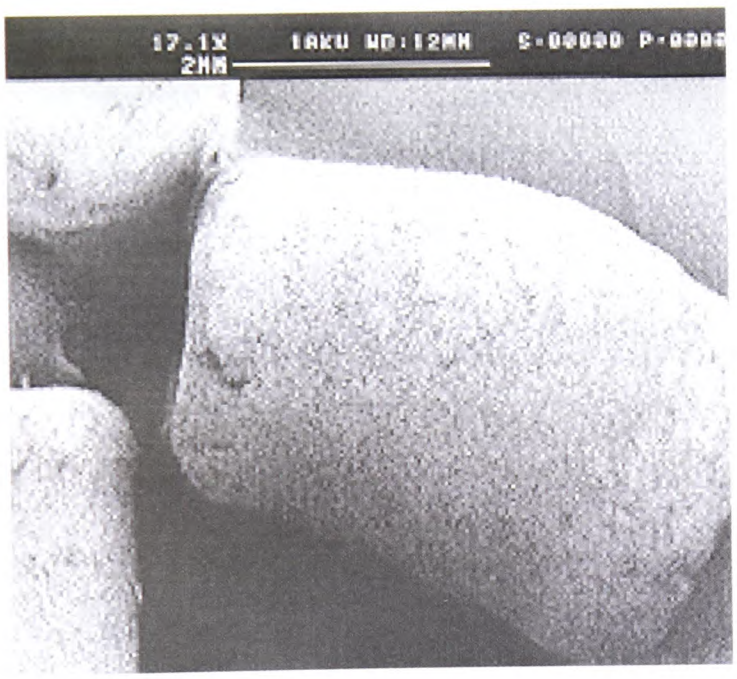

Polyethylene pellets
Median particle size - 3 mm
Particle density 914 kg/m³

Polyethylene pellets pre-test work

Polyethylene pellets - surface area

A7.1.2 Ground ilmenite

The ground ilmenite was obtained from a company that supplied both the batch of sandy ilmenite, and the ground ilmenite. The ground ilmenite is reduced down to the required particle size, by a grinding process. Therefore the sandy and the ground ilmenite have the same particle density and chemical composition.

Particle size range 5-40 μm

Particle density 4600 kg/m³

Unused ground ilmenite

Unused ground ilmenite

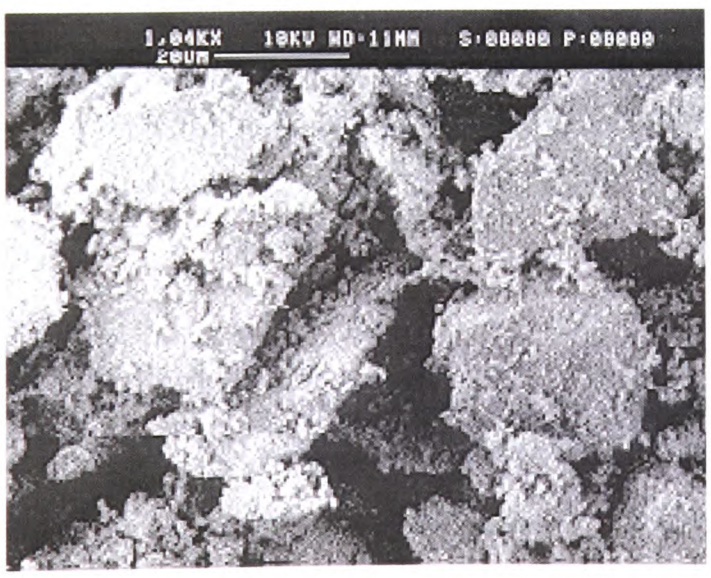

Used ground ilmenite

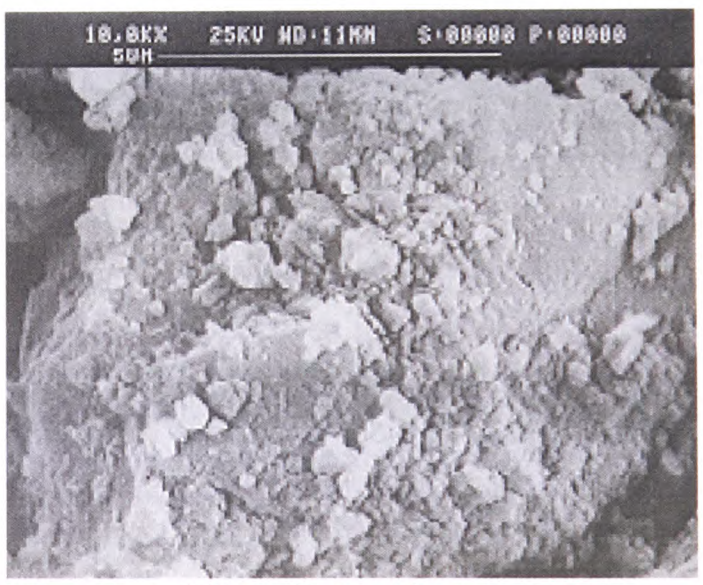

New ground ilmenite - surface area

A7.1.3 Sandy ilmenite

Particle size range 125-180 μm

Particle density 4600 kg/m³

Unused sandy ilmenite

Used sandy ilmenite

Unused sandy ilmenite - single particle

Unused sandy ilmenite - surface area

A7.1.4 Olivine sand

The olivine sand was the first of three materials that were used in the test programme, that were of a similar particle density and chemical composition to two other materials.

Particle size range 200-300 μm

Particle density 3280 kg/m³

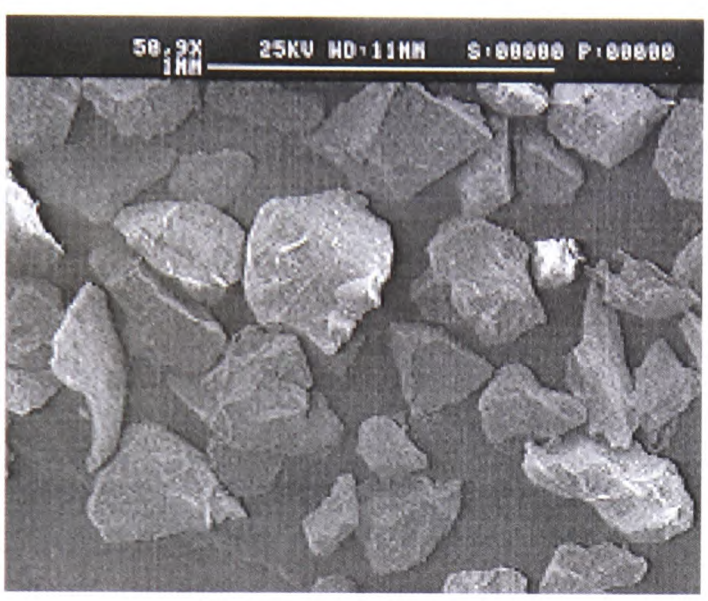

Unused olivine sand

Unused olivine sand - single particle

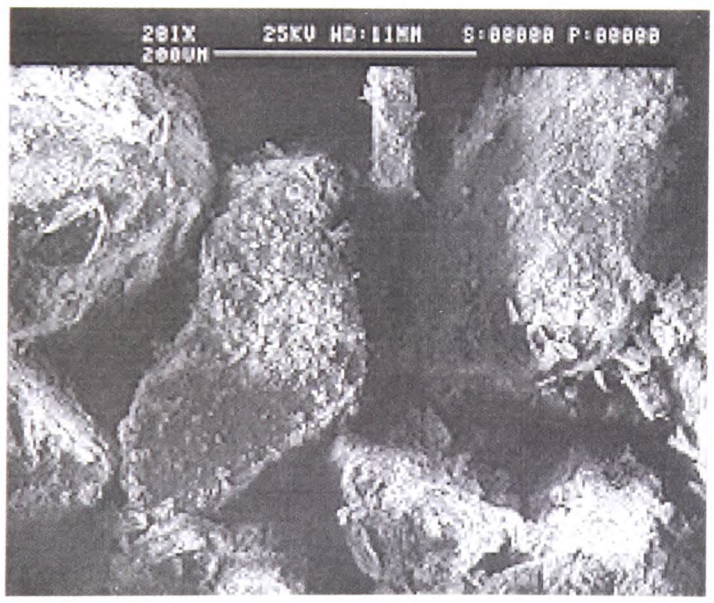

Used olivine sand

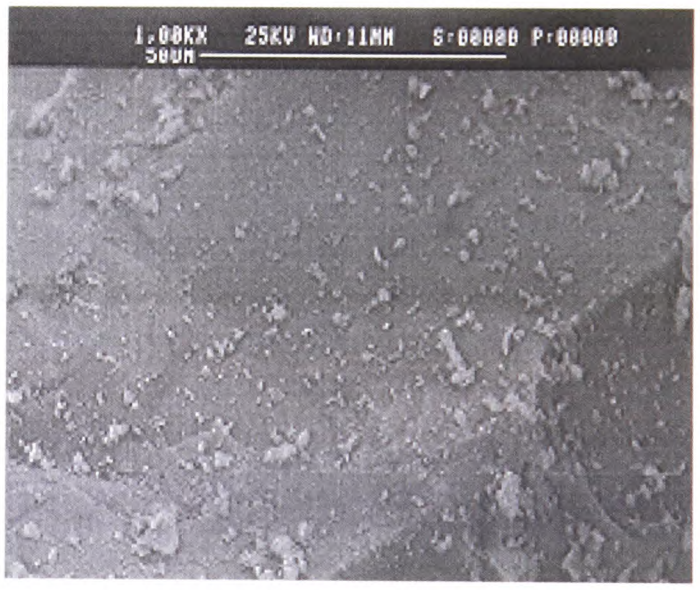

Unused olivine sand - surface area

A7.1.5 Silica flour

Silica flour was the only hazardous material in the test programme, that required the use of masks when handling the product.

Particle size range 0-40μm

Particle density 2700 kg/m³

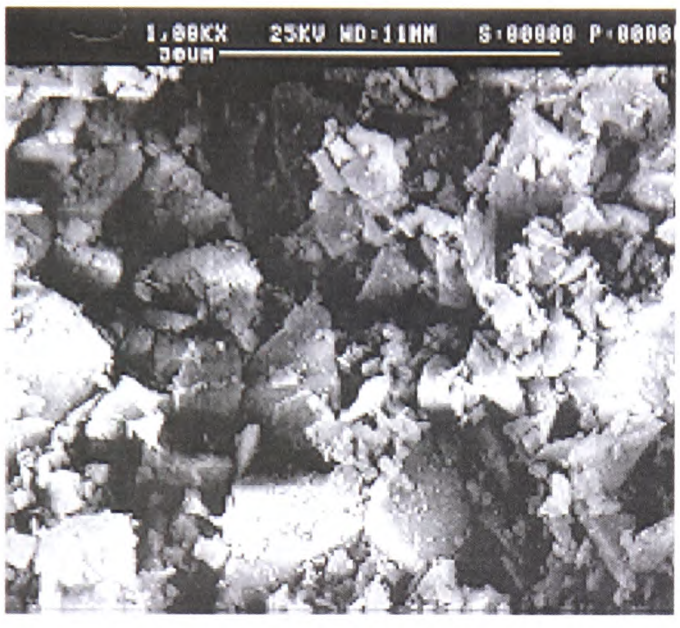

Unused silica flour

Used silica flour

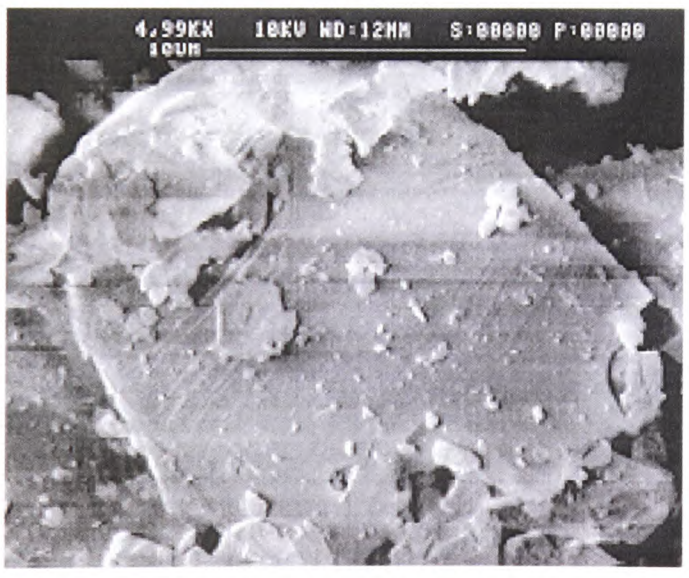

Unused silica flour - surface area

A7.1.6 Golden pea gravel

The size range of the particles when delivered from the supplier, was between 2 and 5 mm. To obtain the particle sizes for the project, one and a half tons was sieved, from which a quarter of the bulk fell into the required range.

Particle size range 2.8-3.5mm

Particle density 2700 kg/m³

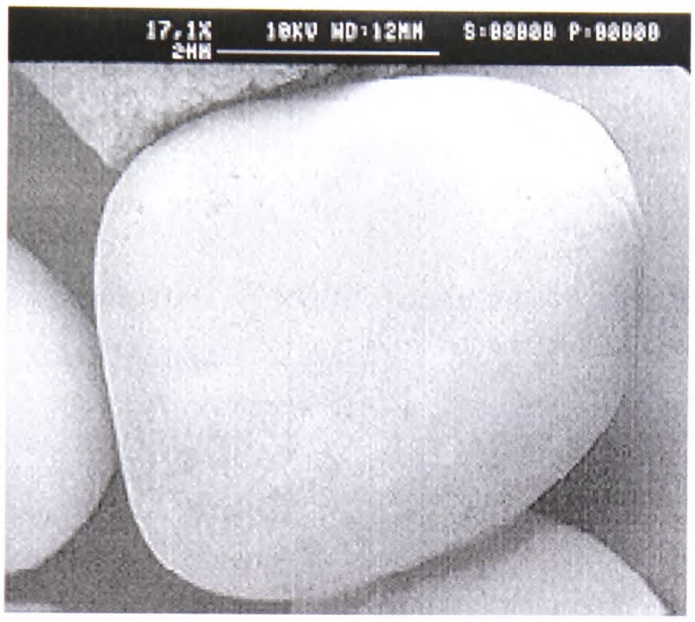

Unused golden pea gravel

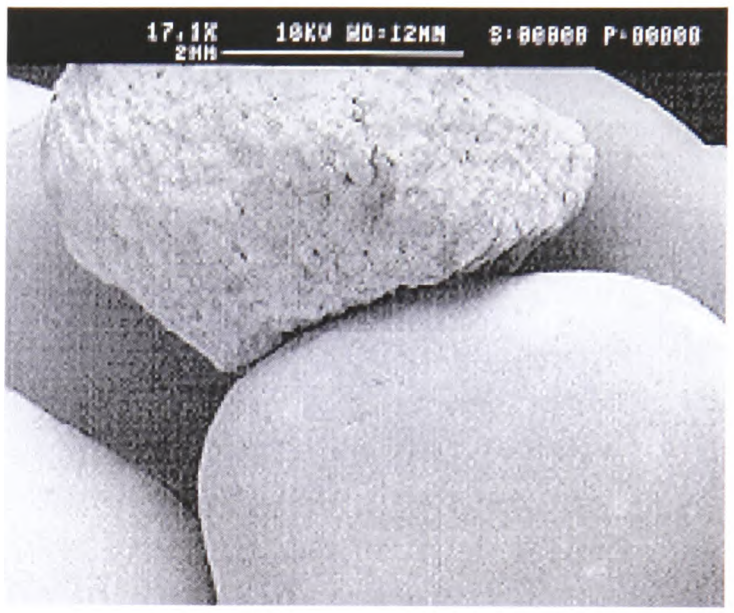

New golden pea gravel

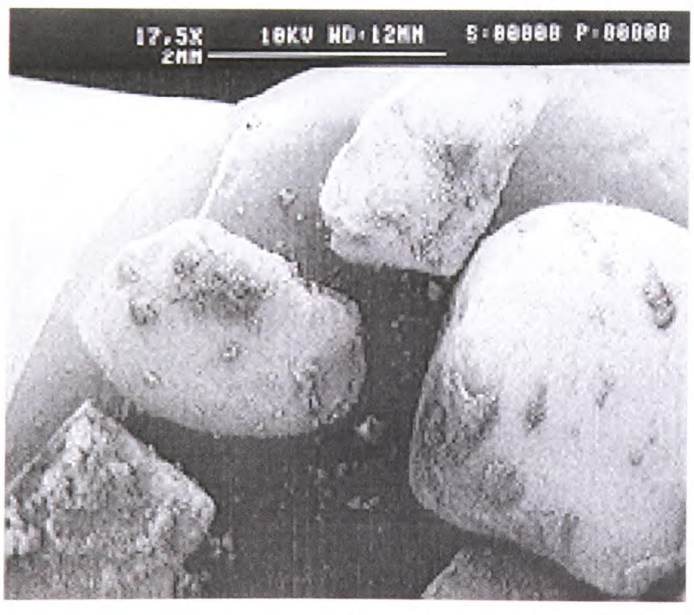

Used golden pea gravel

Unused golden pea gravel - surface area

A7.1.7 Granulated sugar

Particle size range 600µm

Particle density 1600 kg/m³

Unused granulated sugar

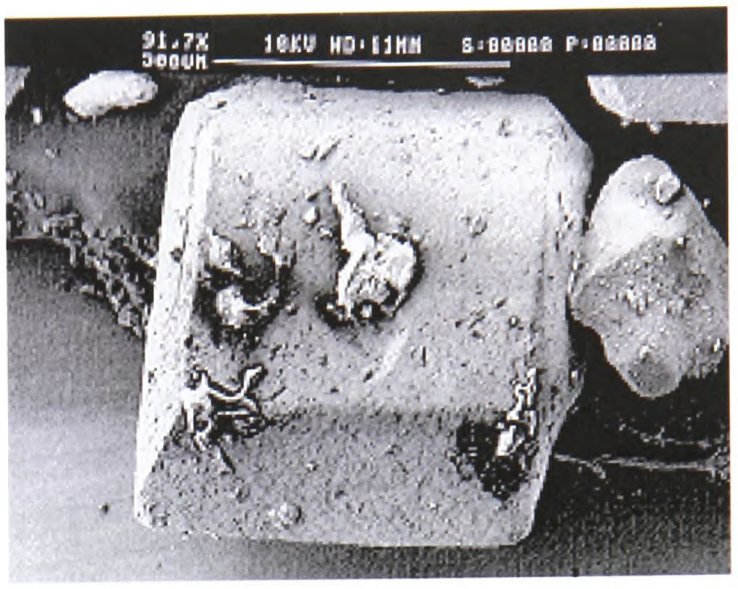

Unused granulated sugar - single particle

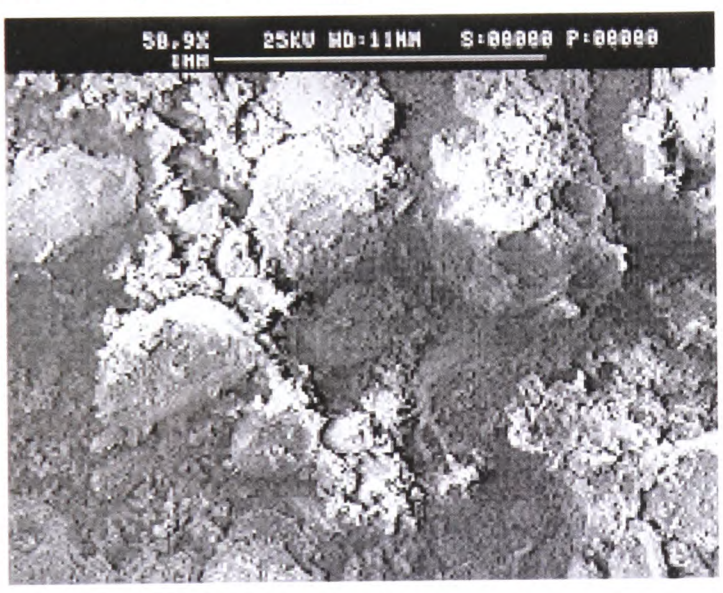

Used granulated sugar

Unused granulated sugar - surface area

A7.1.8 Icing sugar sized material

The granulated sugar was reduced to icing sugar sized particles, by conveying pneumatically around the test rig at high velocities a number a times. In that way, two chemically identical materials, with the same particle density were used in the test programme for comparisons between the particle median sizes.

Particle size range 100 μm

Particle density 1600 kg/m³

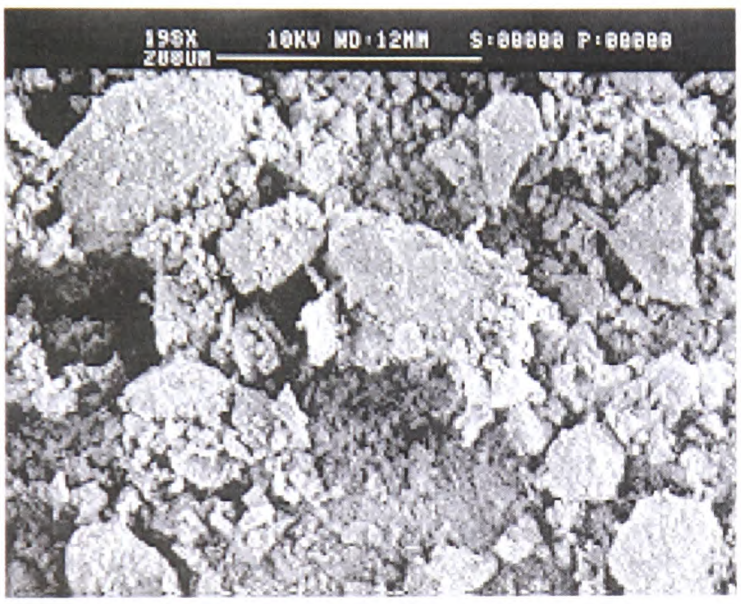

Before test work, icing sized sugar

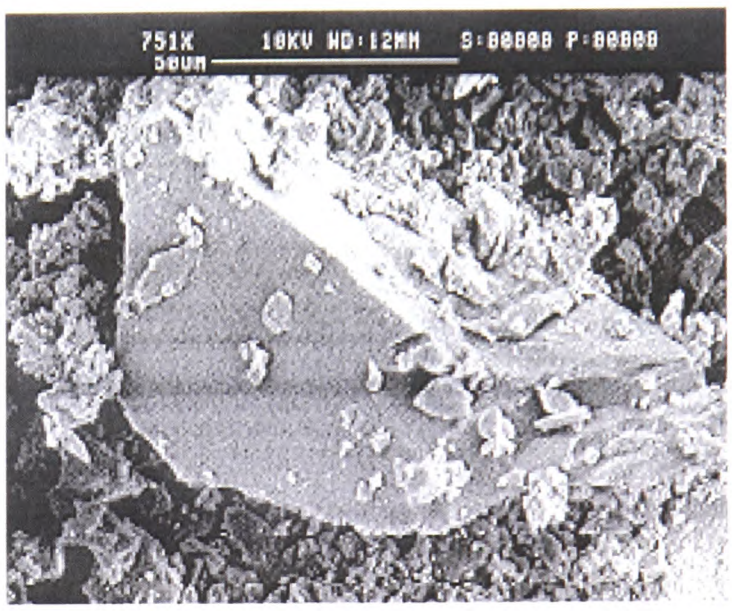

Pre-test work icing sugar - single particle

After test work, icing sugar sized

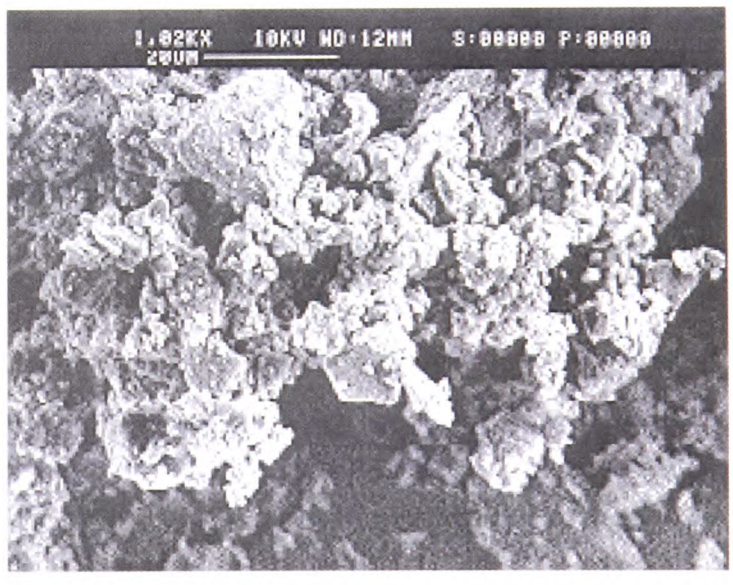

Unused icing sized sugar - surface area

A7.1.9 Boral lytag

The boral lytag had been used for another project, but had not been pneumatically conveyed. Which explains why the material was not classed as 'unused' in the photographs.

Particle size range 4000 µm

Particle density 1560 kg/m³

Pre-test work boral lytag

Used boral lytag

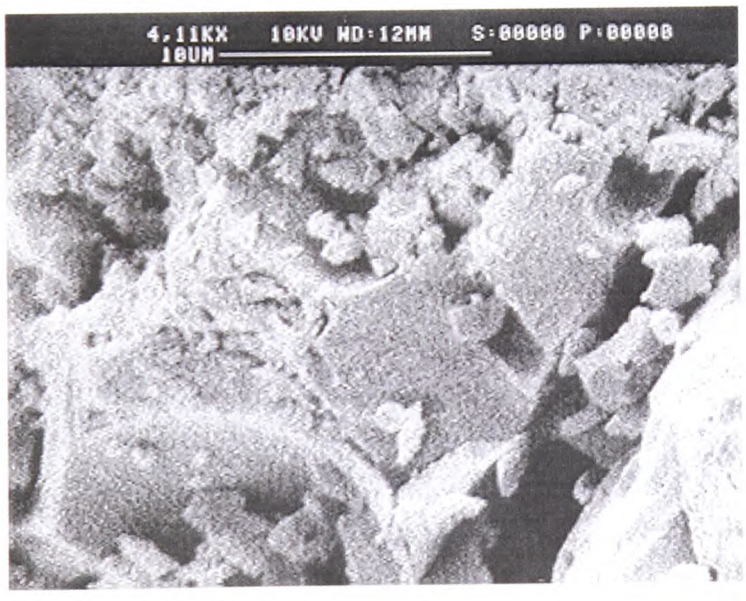

Boral lytag - surface area

A7.1.10 Glass beads

Most of the glass beads were spherical in shape, but the photograph of the unused glass beads shows the variations found in the particle shapes.

Particle size range 400 - 800 μm

Particle density 2500 kg/m³

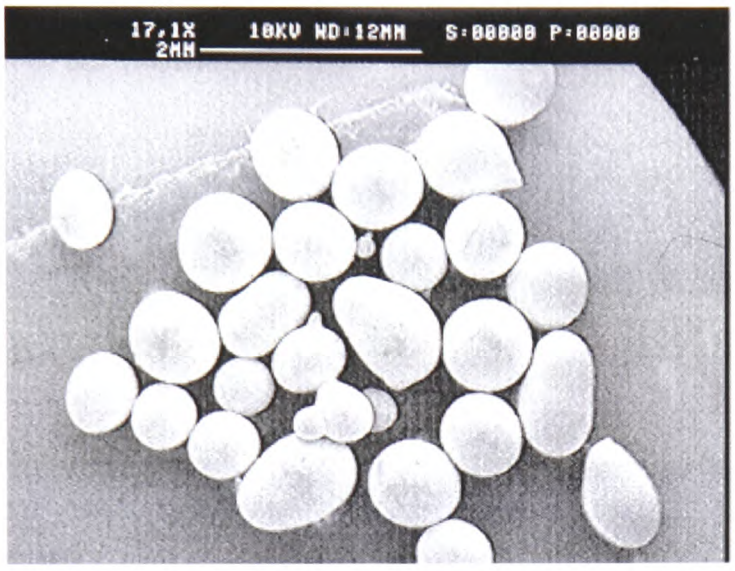

Unused glass beads

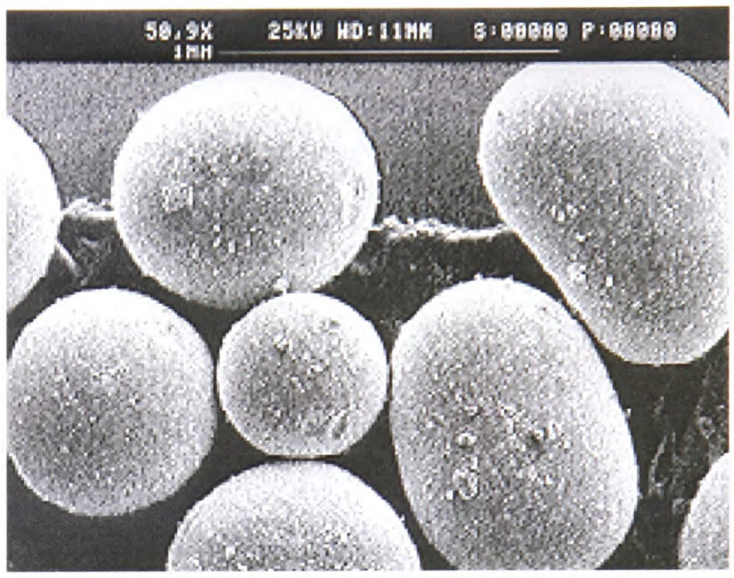

Used glass beads

Unused glass beads - surface area

Used glass beads - surface area

Appendix 8

Copies of papers

During the work on this project, some of the finding were published in a conference proceeding and a journal. Two papers are pending publication, and are included in this section.

The first paper was initially presented at the second international conference on Pneumatic and Hydraulic Conveying Systems, in Davos, Switzerland, June 1999. A revised version has been accepted and awaiting publication in the Powder Technology journal.

The second paper is also due to be published in Powder Technology during 2000.

AN INVESTIGATION INTO THE EFFECT OF PARTICLE SIZE ON STRAIGHT PIPE PRESSURE GRADIENTS IN LEAN PHASE CONVEYING

L.M. Hyder, M.S.A. Bradley, A.R. Reed, and K. Hettiaratchi
The Wolfson Centre for Bulk Solids Handling Technology
School of Engineering
University of Greenwich
Wellington Street
Woolwich
London SE18 6PF
United Kingdom

Summary

This paper presents the results of an investigation into how the median size of the particles affects pressure drop when bulk solids are conveyed pneumatically in suspension flow along a straight horizontal pipeline. It is apparent that pressure drop increases with increasing particle size; the degree of increase tends to be largest towards the smaller particle sizes, diminishing as size increases and also diminishing with increasing transport velocities.

Keywords: Pneumatic conveying, pressure gradient, particle size, horizontal pipeline.

1. Introduction

The work from which the contents of this paper were taken, investigated ways to improve the efficiency and accuracy of pressure loss prediction methods. To do that, a research project critically studied the effect that product particle properties have on the pressure drop per unit length of horizontal pipeline, when particulate materials flow through pneumatic conveying pipelines.

Several different materials were used during pneumatic conveying tests to compare the differences between the particle size and shape properties. The test results from two groups of materials are used in this paper to demonstrate the relationship between particle size and the pressure losses along a pipeline. The groups consisted of materials whose particles have a similar shape and density, but of differing sizes. The materials in the first group were silica flour, olivine sand and golden pea gravel. The second group comprised two forms of the mineral ilmenite. The results show that as the particle size of materials, with similar particle density and chemical composition, increased the pressure losses along horizontal straight pipelines also increased.

2. Objectives

The main objective of the work presented in this paper was to compare materials of similar particle densities, chemical composition and shape. The major differences between all the materials were their particle size ranges, and median particle size. Any measured differences between the test results from the materials, carried out under the same conveying conditions, would be the results of the varying particle sizes. Therefore, the results would determine the effect the particle size has on pressure losses during pneumatic conveying.

Research into the relationship between particle size and pressure losses has been undertaken by others. Mendies et al (ref.1) carried out an investigation using three plastic materials of similar shape and density, but with different particle sizes. They evaluated the solids velocity by measuring the pressure along a horizontal test section in a pilot test plant. This comprised a total of

5 lengths of horizontal pipe measuring 11 metres, using maximum solids loading rations of 9. A graph representing their results, showed that the smaller the particle the higher the solids velocity. Their results indicated that the particle size affects the solids velocity, and consequently, the pressure drop caused by the material. The paper only displayed the pressure drop results of one of the materials tested.

3. Test rig & equipment

The test rig used for the project was part of a previously used test rig (Bradley ref.2) that was modified in some areas. The rig incorporated a 53mm nominal bore pipeline loop, made up of straight sections and bends, 81 metres in length. The majority of the pipeline was in a horizontal orientation. A blow tank was acting as a feeder at the beginning of the conveying line, with a receiving hopper at the end of the line, situated above the blow tank and mounted on load cells. The flow rate of solids was determined by monitoring the gain in weight in the hopper through the load cells, over a known period of time.

The air flow rate was regulated by a bank of choked flow nozzles installed in parallel. The rig was controlled from a mimic panel and the instruments were connected to a data logging system; which also recorded the pressure readings. These readings were then transferred at the end of each test to a computer, for processing.

A diagram showing the layout of the test pipeline is shown in figure 1. The pressure transducers along each straight are separated by two metre intervals. The total length of the test section from the first to the last pressure transducer, is a total of 57 metres.

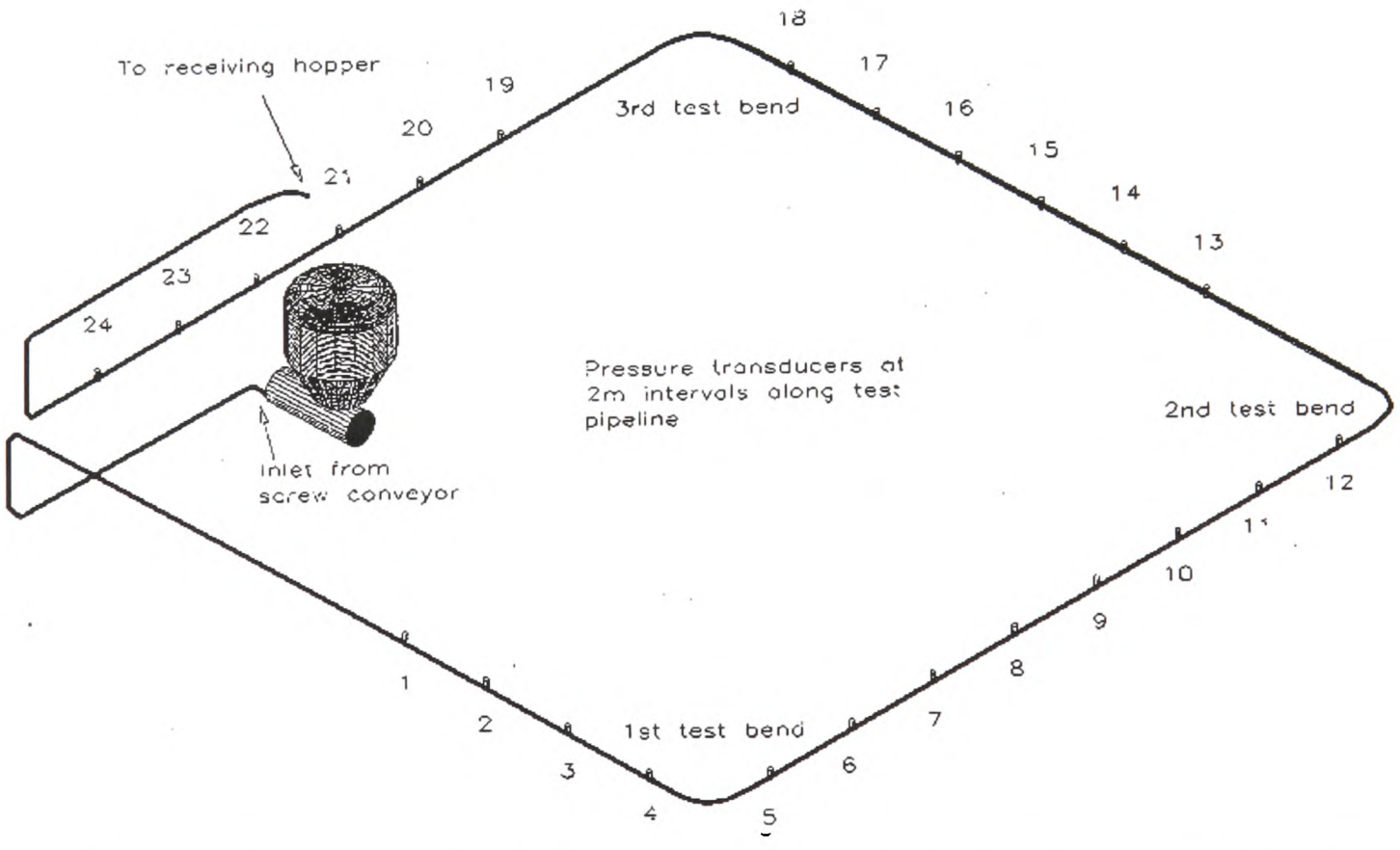

Figure 1. Layout of the test pipeline showing the positions of the pressure transducers and test bends. The receiving hopper has been excluded from the diagram in order to display all the transducers.

4. Test program & materials

Each test run produced raw data scanned from 26 pressure transducers along the test rig, including two that monitored the pressures upstream of the nozzle bank and in the blow tank. In addition, an averaged reading was taken from three load-cell outputs that were positioned beneath a receiving hopper. Fitting a straight line through the readings from the load cells enabled the mass flow rate of material entering the receiving hopper to be determined. During each test run the transducers and load cells were scanned for data every second, over a 150 second time period.

The conveying characteristics were determined by ascertaining the minimum and maximum conveying conditions for each material within the limits of the test rig. The inlet air velocity was reduced for subsequent test runs until the conveying line blocked with material, to determine the minimum conveying air velocity. The suspension density values (kg_{solids}/m^3_{air}) were taken at the midpoint position of the pressure transducers along the straight sections. The conveying conditions for the materials are detailed below.

Material	Inlet air velocity m/s		Min. suspension density kg/m³	Max. suspension density kg/m³	Solids loading ratios
	Min.	Max.			
Silica flour	15	26	6	70	4-22
Olivine sand	12	23	8	85	5-26
Gravel	13	22	14	86	7-25
Ground ilmenite	12	26	5	89	4-31
Sandy ilmenite	12	23	9	55	5-18

The raw data was stored in a data logger and transferred to a computer after each test run was completed. Once stored in the computer, the raw data was then processed and analysed. The analysed data for each material was transferred to a separate database, from which graphs were plotted to compare any differences in results between the materials.

5. Description of test materials

The details of the five test materials are described below.

Material	Particle size range (μm)	Median particle size (μm)	Particle density (kg/m³)
Silica flour	0-40	30	2700
Olivine sand	200-300	270	3280
Golden pea gravel	2000-3500	3000	2700
Ground ilmenite	0-100	30	4600
Sandy ilmenite	60-300	180	4600

The principal points of comparison between the test materials were that they had similar shapes and densities, so that the size difference would be the governing factor on the pressure losses during pneumatic conveying.

6. Results & analysis

The raw data from a test run was first examined on a graph of pressure versus time, to identify the steady state period in which to process the results. Having selected the steady state period, the results for each transducer were averaged and the mass flow rate of solids calculated (Bradley ref.3).

For each straight test section, a least squares best fit line was plotted through the data points, to determine the pressure gradient along each straight section of monitored pipeline. A linear fit was applied to all four straight section gradients, so that a normalised pattern was given to all the pressure gradients (graph 1).

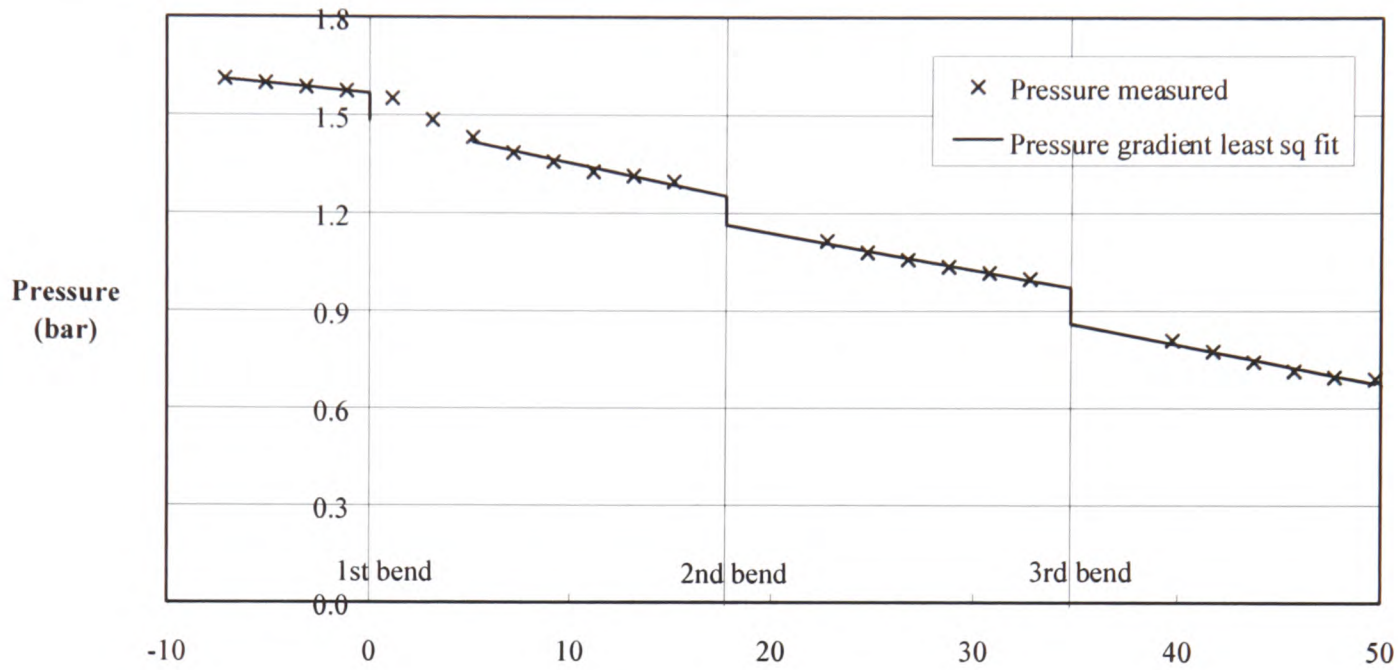

Graph 1: Pressure gradients along straight test sections. The first three transducer readings downstream of the first test bend are ignored due to the re-acceleration length (Bradley & Jones ref. 3 & 4).

The pressure gradients for all four straight sections were stored and transferred to a database when all the test work was completed. From each database, several graphs were drawn for the solids only contribution to the pressure losses (bar/m) against the midpoint suspension density (kg/m^3), from individual air velocity ranges used during the conveying test runs. The solids only contribution to the pressure gradients was derived by deducting the air only pressure gradient value (using a correlation[1]) from the total measured pressure gradient. The graphs were divided into the results from specific air velocity ranges, as shown in graphs 2 to 6.

The individual air velocity ranges were used to reduce the scatter of data so that correlations may be found in the results. A linear line was plotted through the data using the least squares best fit approach. Other mathematical models through the data showed that the linear fit through the data points starting at the origin was as good as the others, so this was chosen because it was the simplest. Plotting the mathematical model through the origin was logical because there can be no solids contribution if no solids are flowing.

[1] The calculation of the air contribution to pressure gradient was undertaken using a pressure loss correlation (in the form of the Fanning equation) which had been determined from air-only tests on the pipeline.

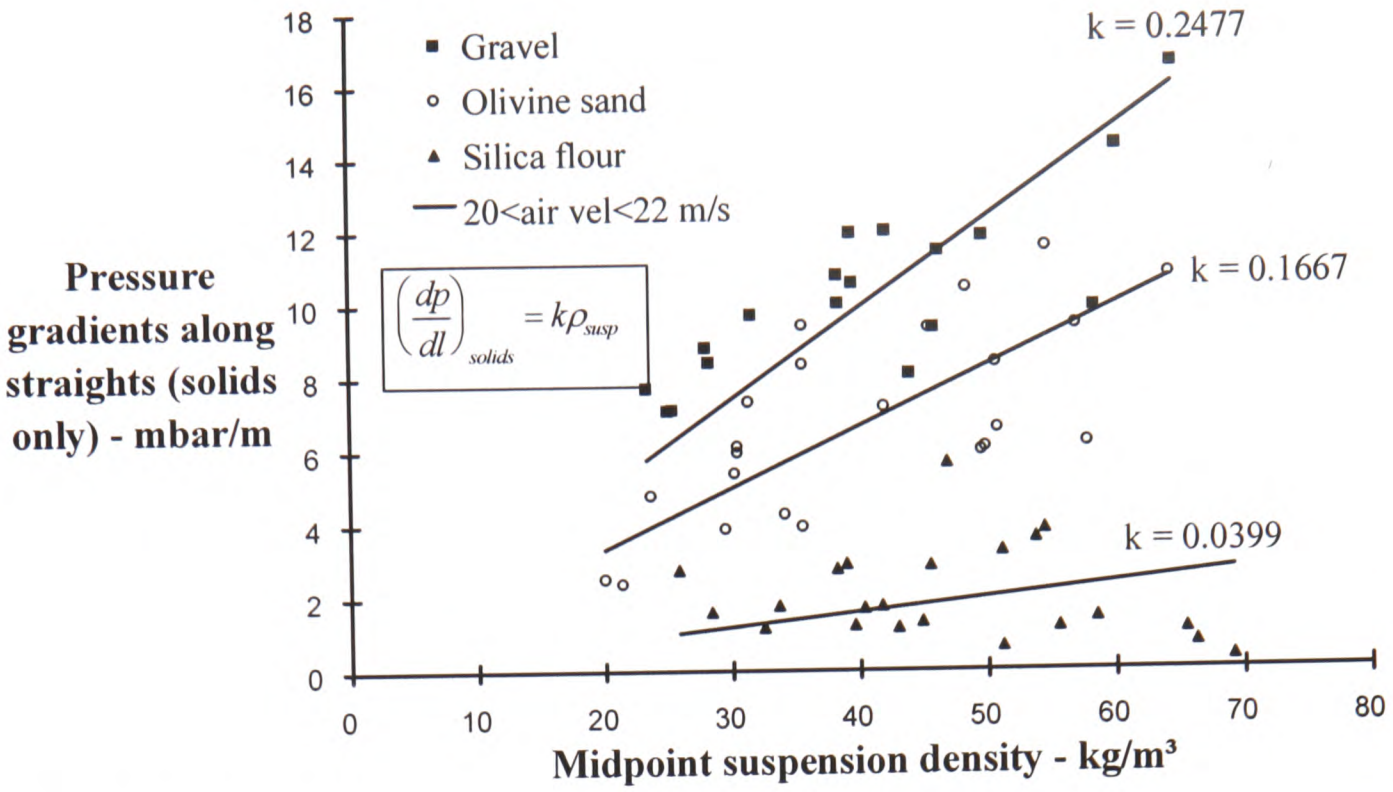

Graph 2a: Pressure gradients along the straight test sections, for the solids contribution to the pressure losses only, versus the midpoint suspension density along the straights. The results plotted for Group 1 were those measured in the air velocity range of greater than 20 m/s, and less than 22 m/s.

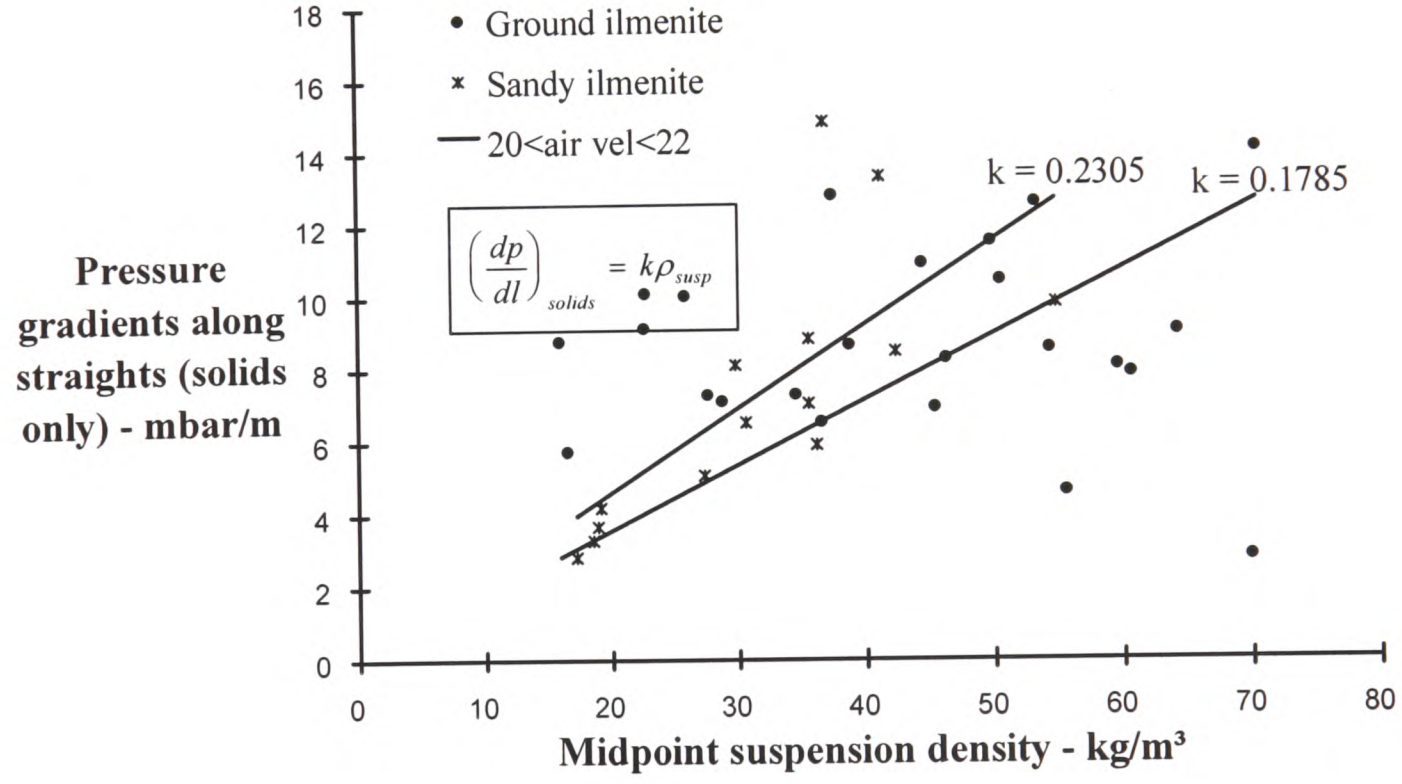

Graph 2b: Pressure gradients along the straight test sections, for the solids contribution to the pressure losses only, versus the midpoint suspension density along the straights. The results plotted for Group 2 were those measured in the air velocity range of greater than 20 m/s, and less than 22 m/s.

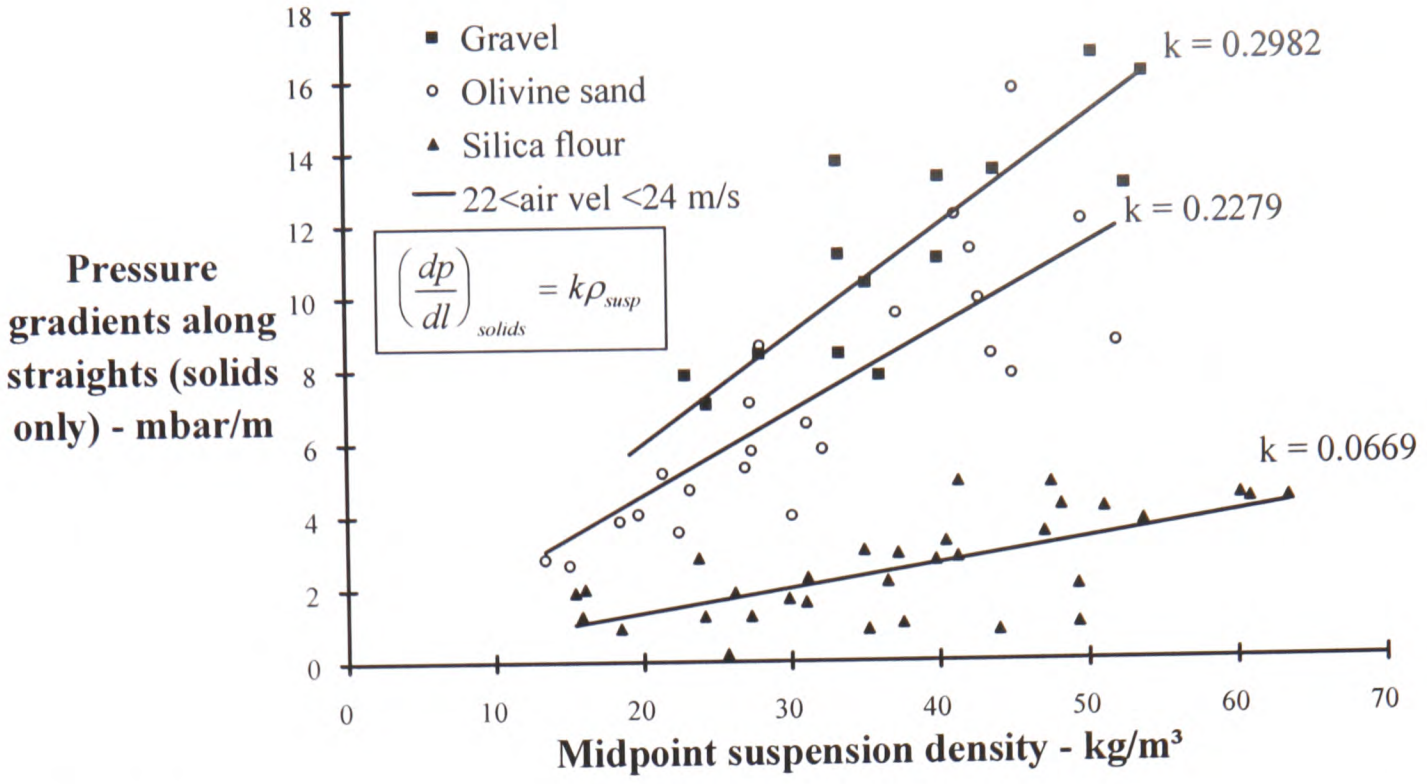

Graph 3a: Similar to Graph 2a, but the results plotted for Group 1 were those measured in the air velocity range of greater than 22 m/s, and less than 24 m/s.

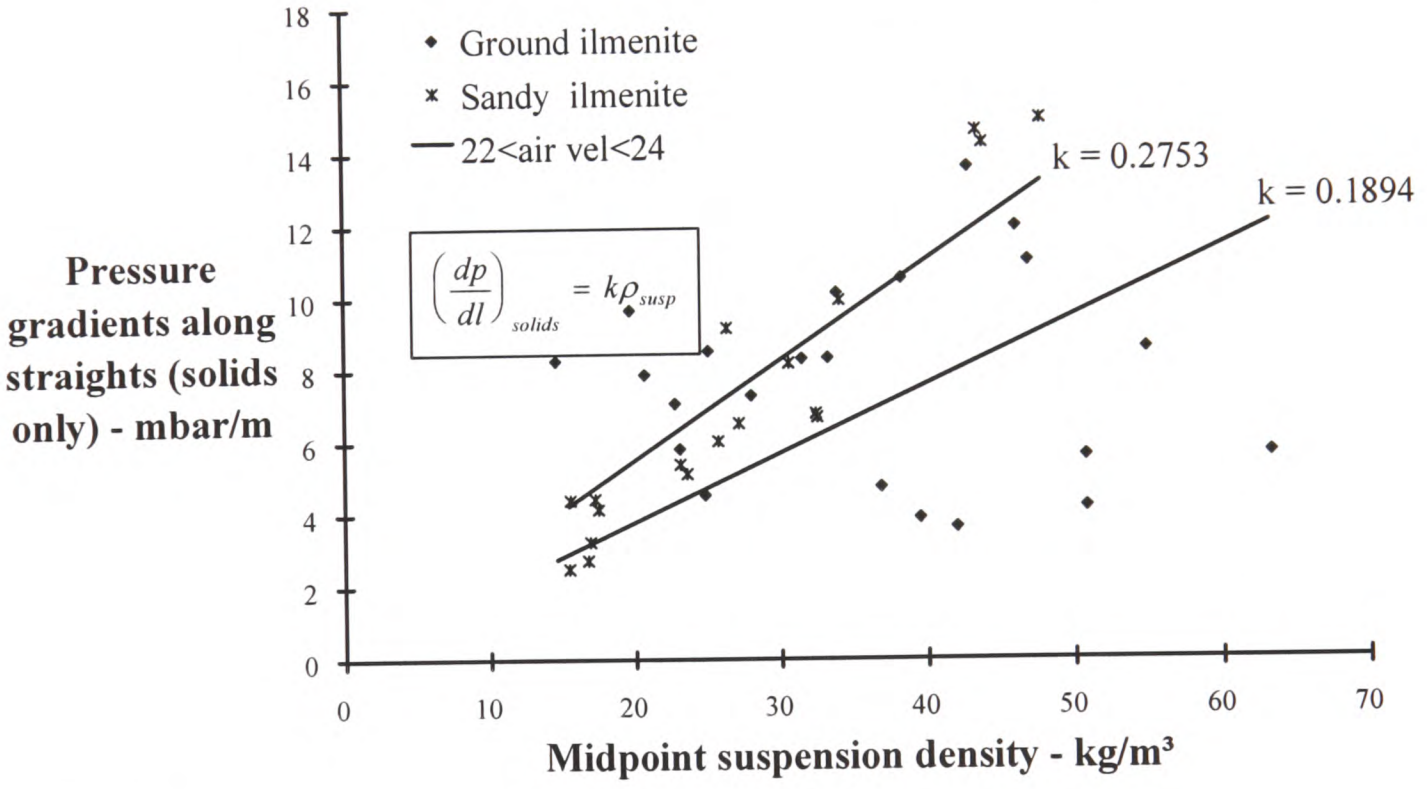

Graph 3b: Similar to Graph 2b, but the results plotted for Group 2 were those measured in the air velocity range of greater than 22 m/s, and less than 24 m/s.

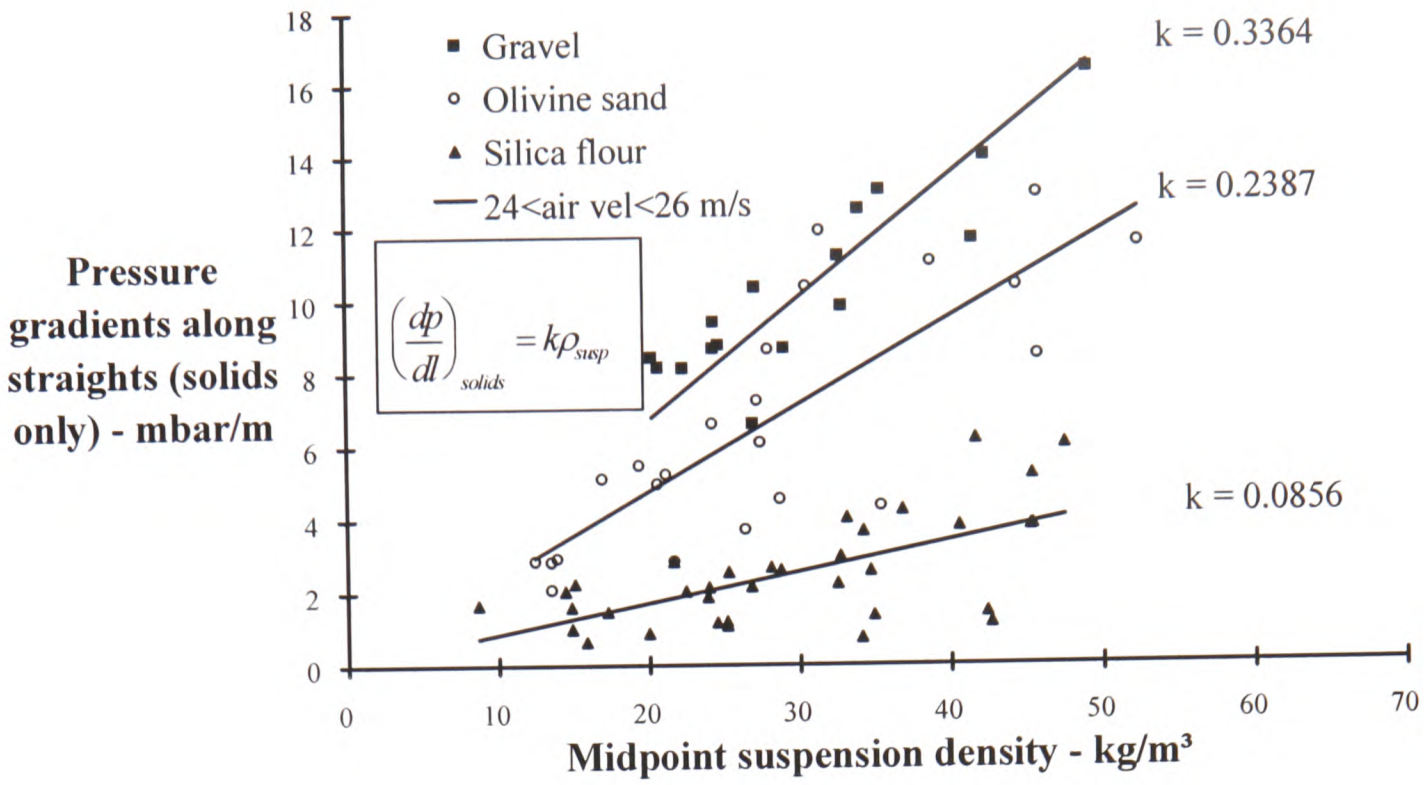

Graph 4a: As the previous graphs, with the results for Group 1 plotted from those measured in the air velocity range of greater than 24 m/s, and less than 26 m/s.

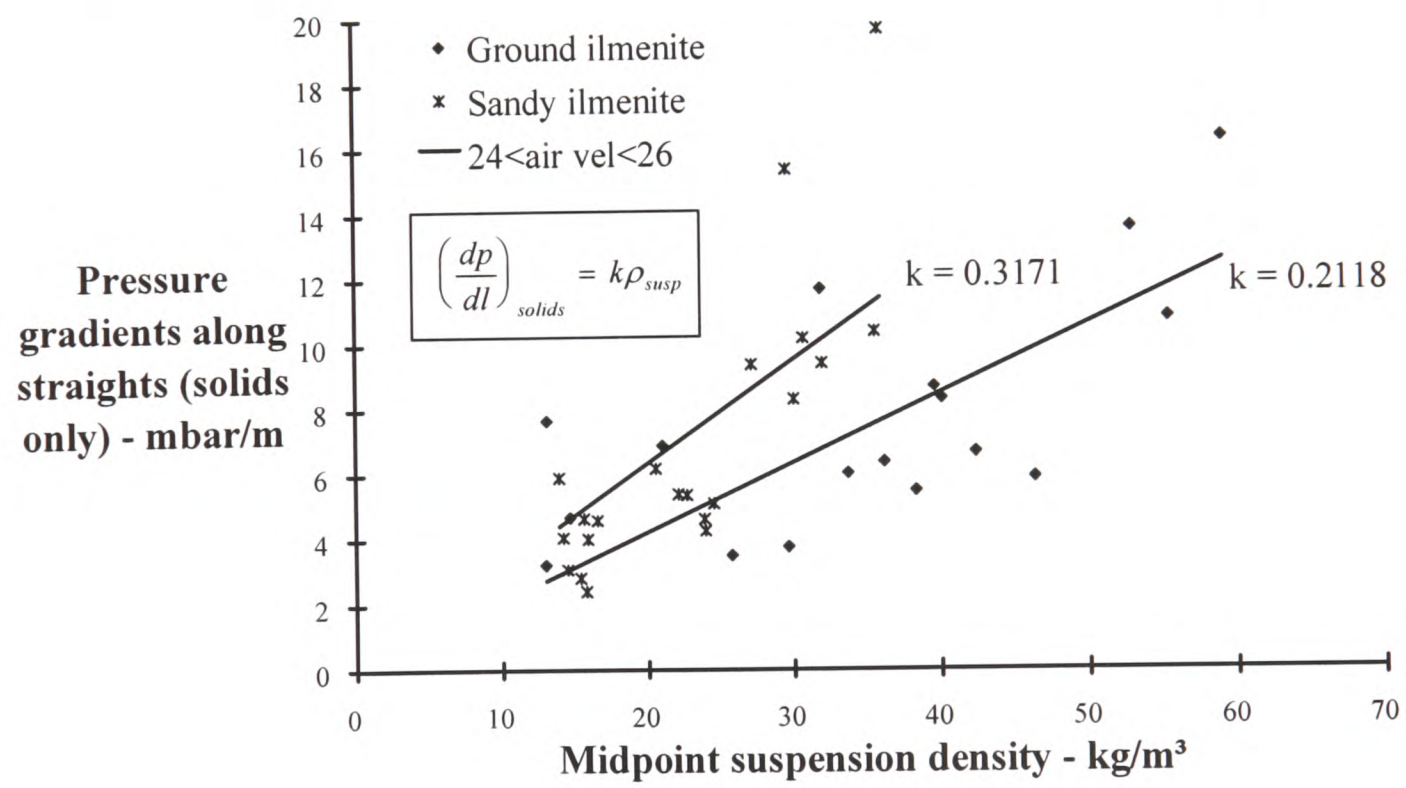

Graph 4b: As the previous graphs, with the results for Group 2 plotted from those measured in the air velocity range of greater than 24 m/s, and less than 26 m/s.

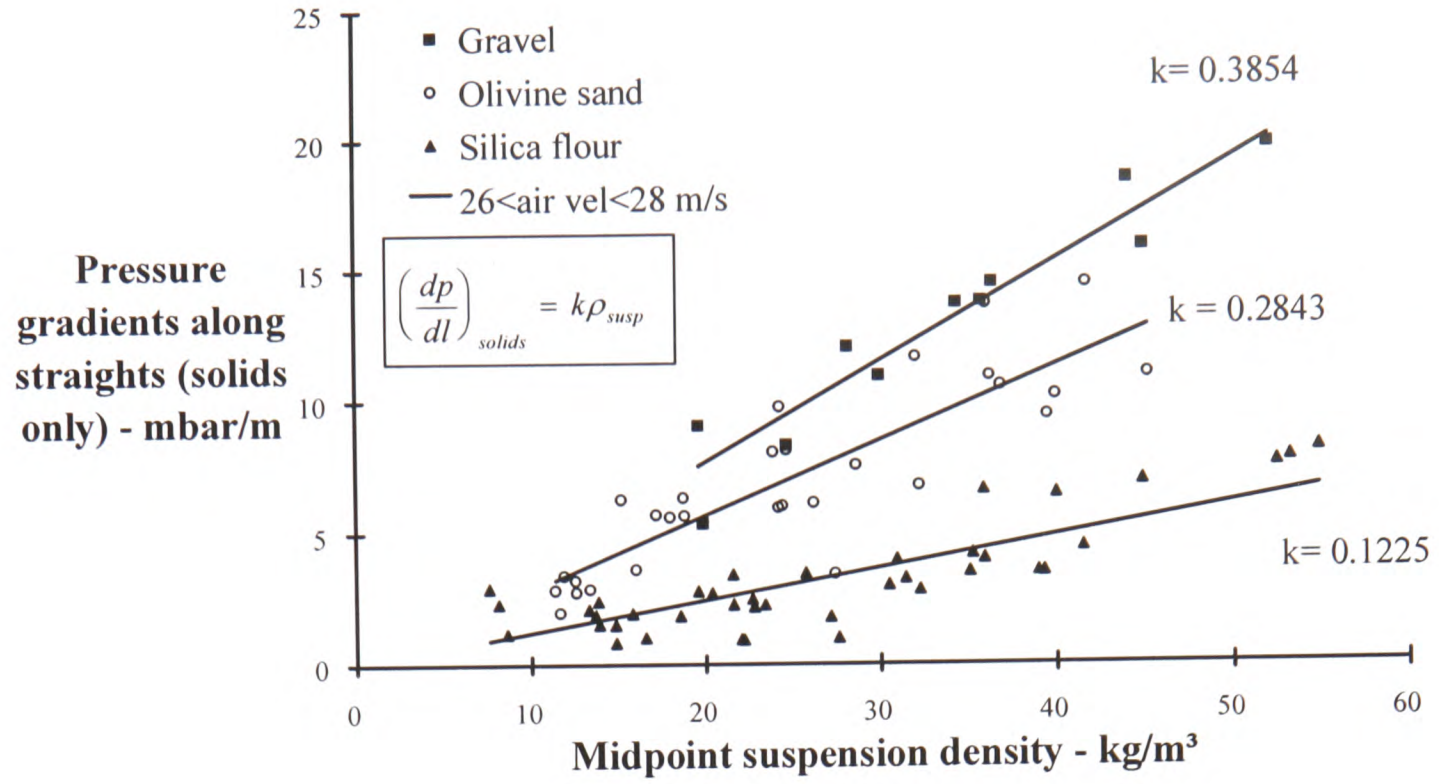

Graph 5a: As before, with the results plotted for Group 1 from those measured in the air velocity range of greater than 26 m/s, and less than 28 m/s.

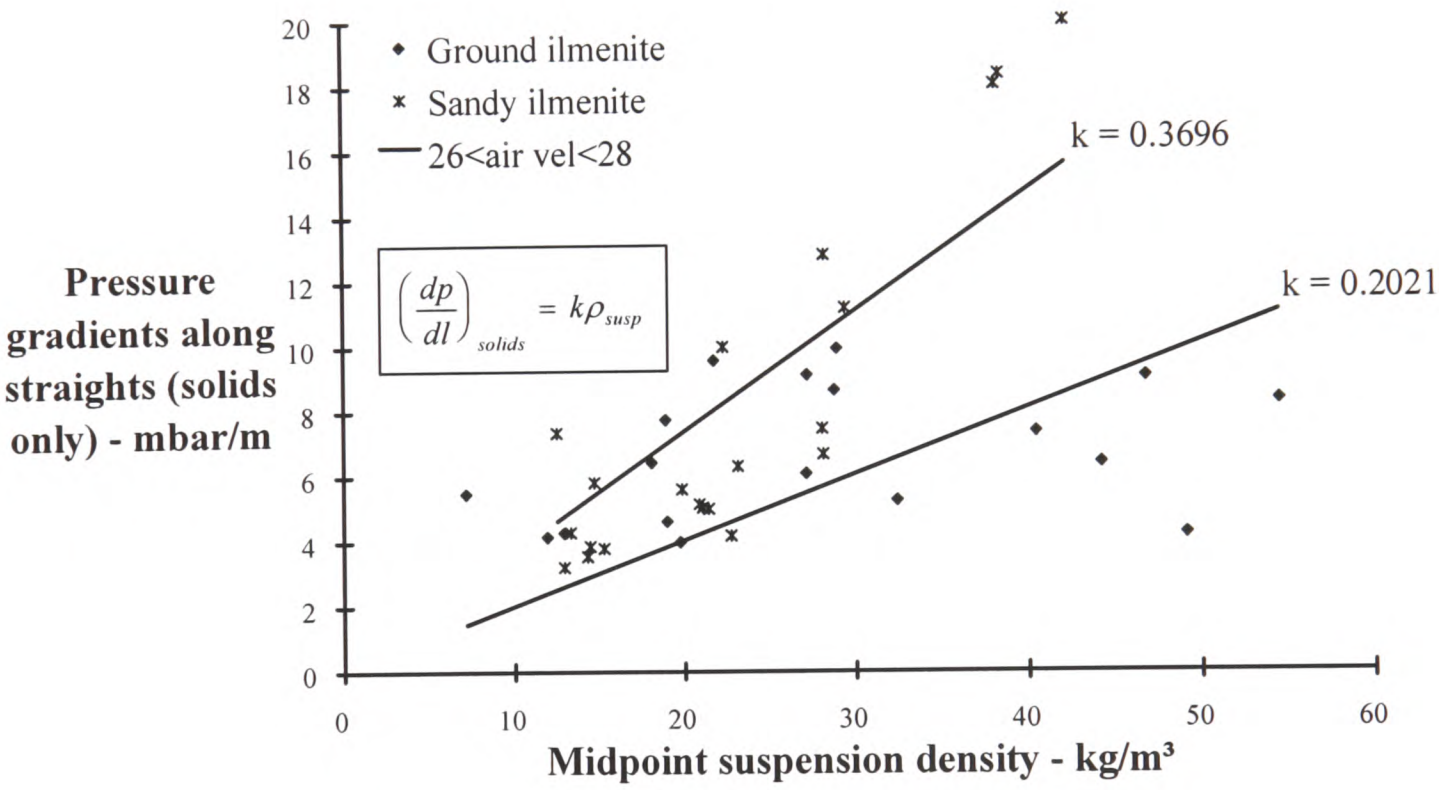

Graph 5b: As before, with the results plotted for Group 2 from those measured in the air velocity range of greater than 26 m/s, and less than 28 m/s.

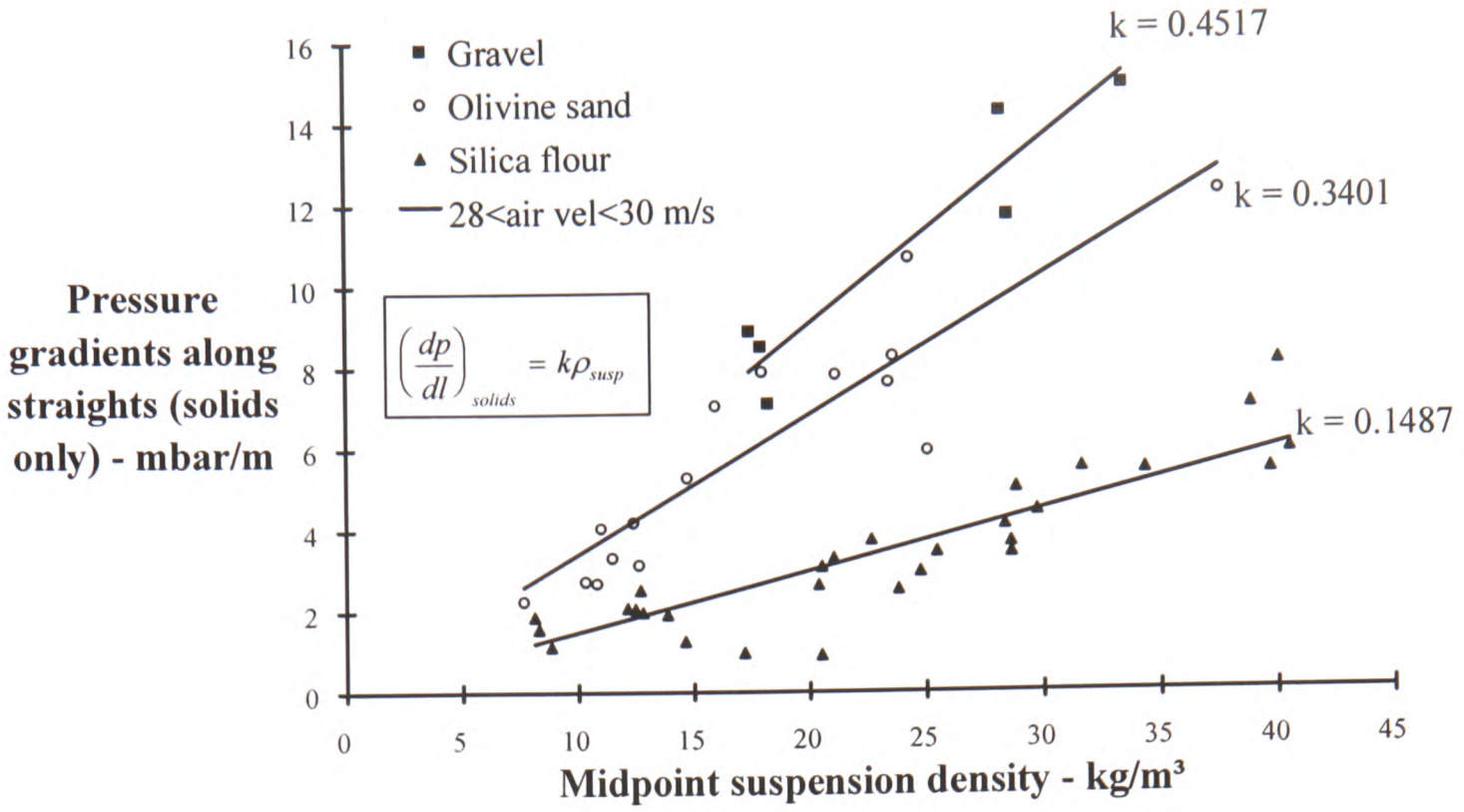

Graph 6a: The last graph for Group 1 with the results plotted from those measured in the air velocity range of greater than 28 m/s, and less than 30 m/s.

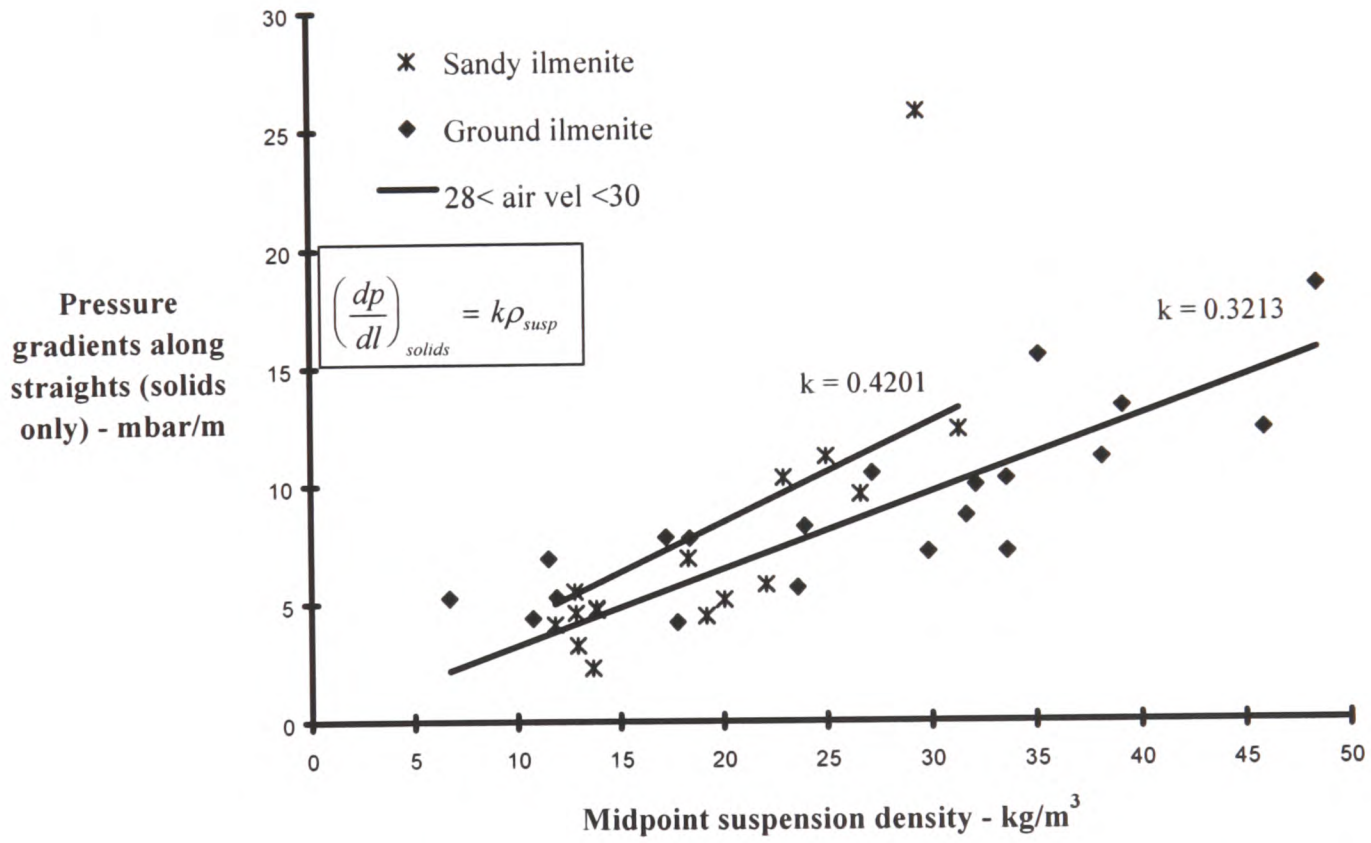

Graph 6b: The last graph for Group 2 with the results plotted from those measured in the air velocity range of greater than 28 m/s, and less than 30 m/s.

The coefficients (k) of the equations from graphs 2 to 6 were plotted on graph 7. This was to show the relationship against the particle sizes of the three test materials that have similar chemical compositions and particle densities. It can be seen that as the particle size increases in the test materials, the pressure losses along the straight sections get larger.

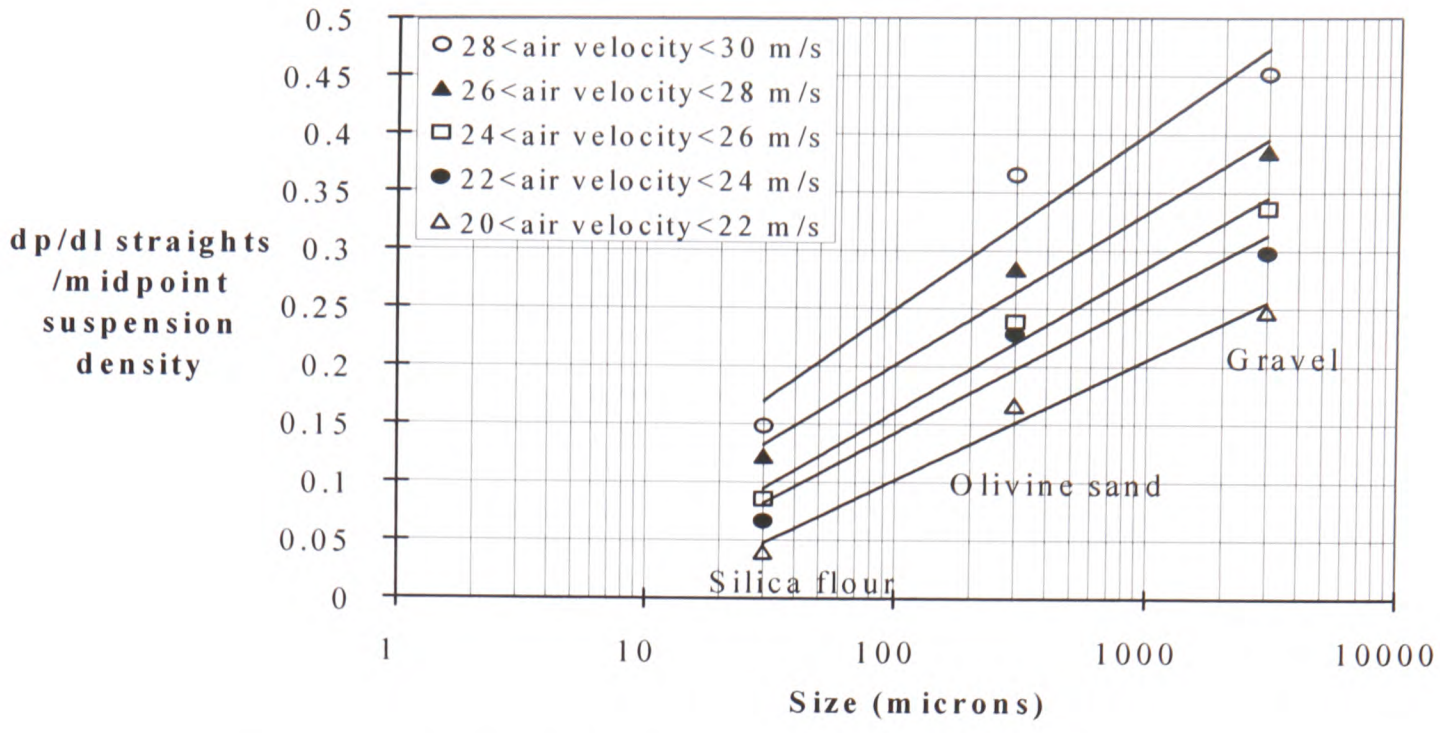

Graph 7a: Results plotting the slope (k) value from each air velocity range graph, against the mass median particle size for each test material in Group 1. The slightly higher pressure drops for the olivine sand may be due to the increased particle density for that material.

The correlation between the particle sizes represented by linear lines, are limited to the particle sizes of the test materials used.

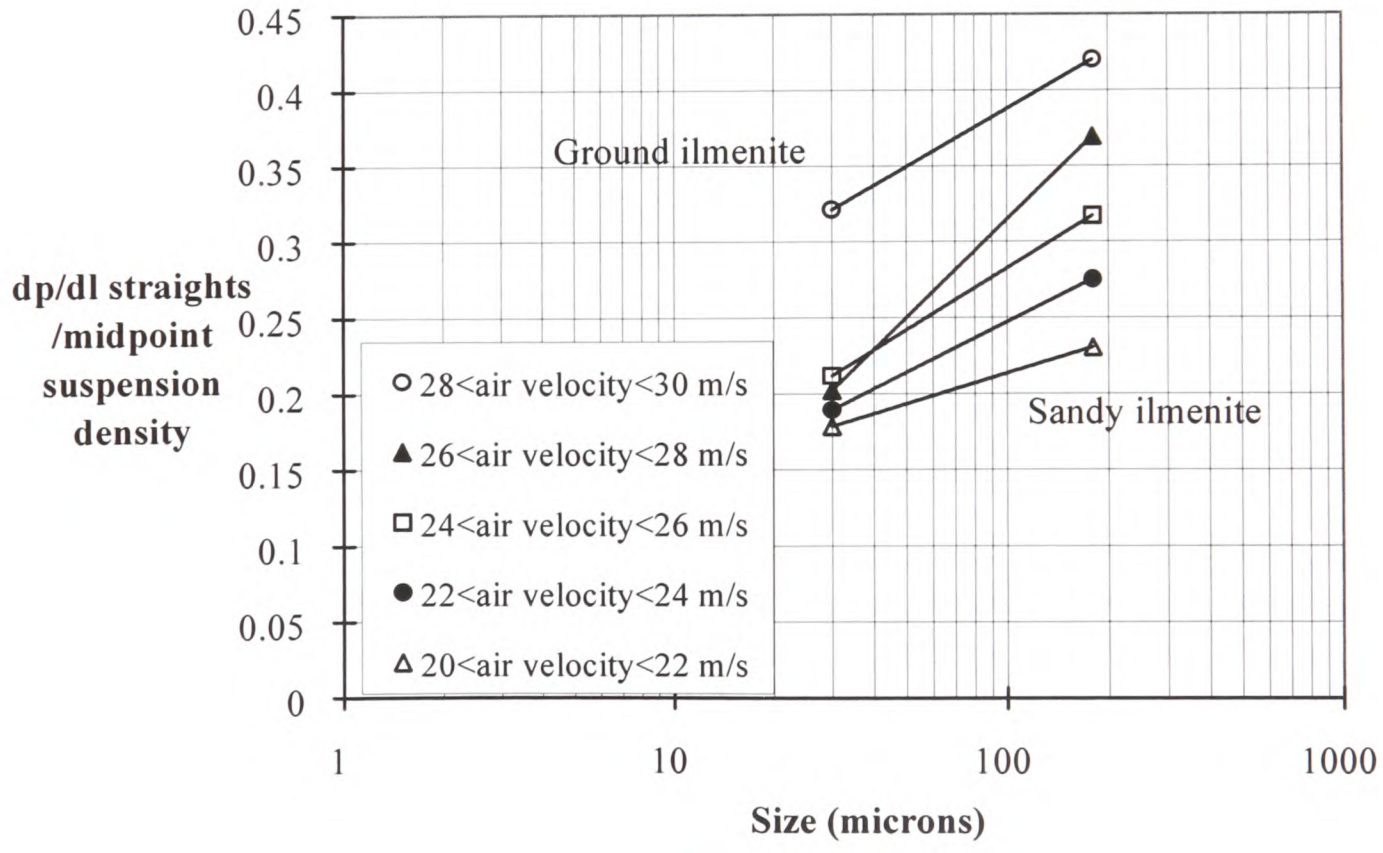

Graph 7b: Results plotting the slope (k) value from each air velocity range graph, against the mass median particle size for each test material in Group 2.

Continuing the analysis of the relationship between pressure drop and particle size, the following model was tested for each of the ranges of mid-air velocity materials from within the same predefined Groups:

$$\text{Ratio}\left(\frac{dp}{dl}\right)_{r_s} = \text{Ratio (Particle Size)}^n$$

E.g. For 20m/s < air velocity <22m/s

$$\frac{k(\text{Silica})}{k(\text{Olivine Sand})} = \left[\frac{\text{Particle Size (Silica)}}{\text{Particle Size (Olivine Sand)}}\right]^n$$

$$\frac{0.0399}{0.1667} = \left[\frac{30\mu m}{270\mu m}\right]^n$$

The values of the exponent, n, were then plotted for the various combinations of materials (within Group 1 and Group 2) at the five mid-air velocity ranges.

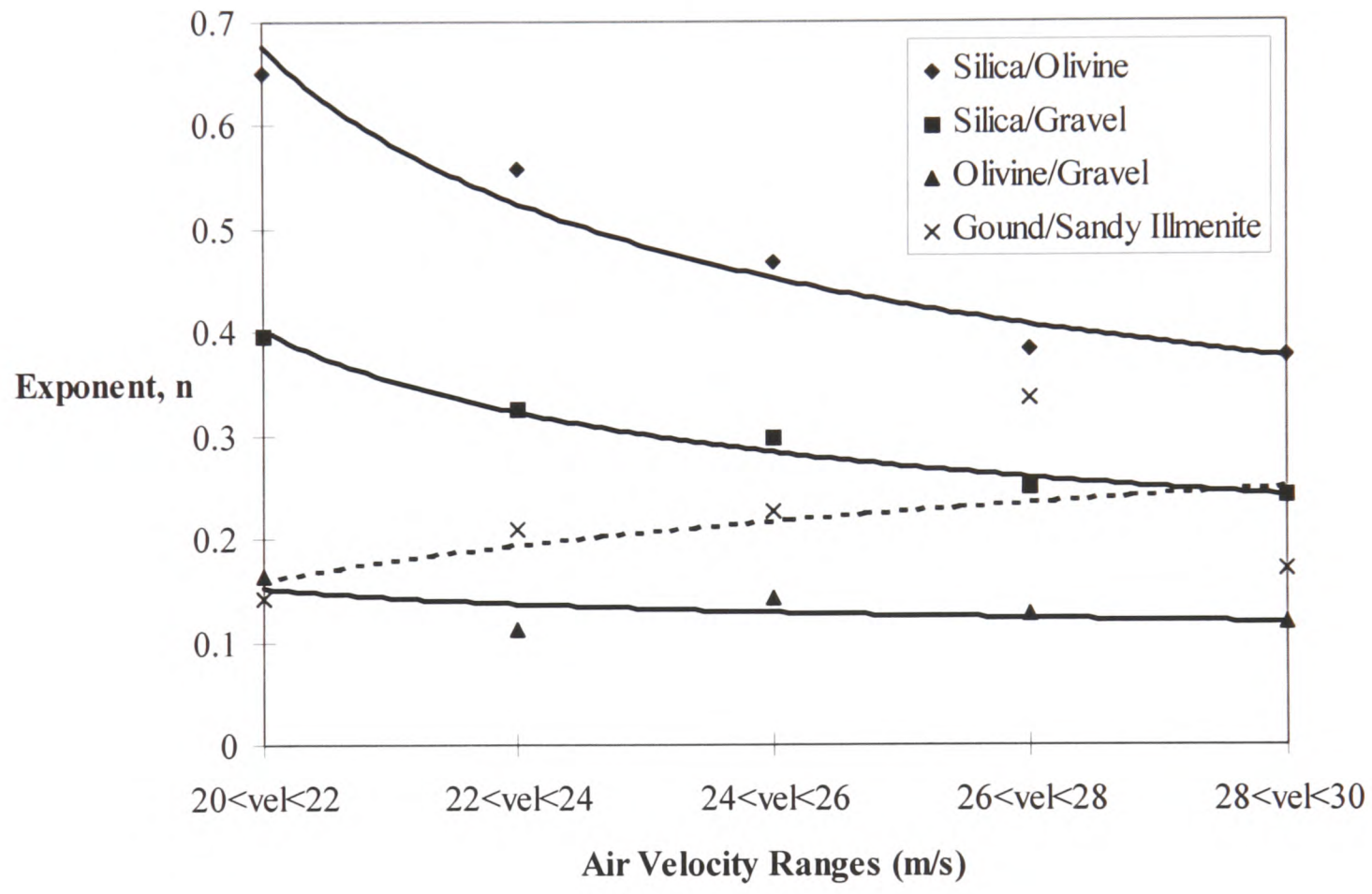

Graph 8: Values of exponent, n, for pairs of materials at various mid-air velocity ranges.

It can be seen that as the conveying air velocity increases the exponent value generally decreases. For the larger particles the value of n ranges between 0.11 and 0.15 while for the smaller particles the values falls between 0.4 and 0.68.

6.1 Comparison of the methods used to characterise the pressure losses

The coefficient k, shown in graphs 2 to 7b, are a function of the gas superficial velocity, and maybe directly related to work found in German literature, e.g. Molerus(1996), Gasterstadt (1924) & Barth (1958). The total pressure loss equations from the German literature, are as follows:-

$$\frac{\Delta p}{L} = \left(\frac{\Delta p}{L}\right)_g + \left(\frac{\Delta p}{L}\right)_s \tag{1}$$

$$= \frac{2}{D} f_{gw} \rho_g U_g^{\,2} + \frac{2}{D} f_{s_w} \mu \rho_g U_g^{\,2} \tag{2}$$

$$\text{where } f_{s_w} = f\left(\mu_1, U_{g1} \ldots\right) \tag{3}$$

$$\text{and } \mu = \frac{\dot{m}_s}{\dot{m}_g} \tag{4}$$

In this work, $\left(\frac{dp}{dl}\right)_{solids} = k\rho_{susp}$ comparing with the second term in (2),

$$\frac{2}{D} f_{s_w} \mu \rho_g U_g^{\,2} = k\rho_{susp} \tag{5}$$

The suspension density, $\rho_s = \mu = \frac{\dot{m}_s}{\dot{v}_g}$

$$\rho_s = \frac{\dot{m}_s}{\dot{v}_g} = \frac{\dot{m}_s}{\dot{m}_g} \rho_g = \mu \rho_g \tag{6}$$

$$\text{Substitute (6) in (5), } = \frac{2}{D} f_{s_w} \rho_s U_g^{\,2} = k\rho_s \text{ or } k = \frac{2}{D} f_{s_w} U_g^{\,2} \tag{7}$$

The objective for the work in this paper concentrated on comparing the effect of the particle sizes on the pressure losses along horizontal pipelines, and no attempt was made to relate the equations for the solids contribution to the pressure gradients in this, to those in the wider literature.

7. Discussion & conclusion

Pressure losses of materials pneumatically conveyed along pipelines vary for each product. The particle characteristics of materials were investigated for their effect on pressure losses. This was carried out in the search for a method that would reduce the amount of large scale test work that is normally required before conveying systems are designed to convey a particulate material.

Measured results from tests carried out on five selected materials has shown that pressure losses along straight pipelines during pneumatic conveying of particulate materials are related to the materials particle size.

Analysing the results of the test work, it is apparent that as the particle size gets larger, the pressure losses along straight sections of pipeline increase. This is shown on graphs 7a and 7b.

The increase in the pressure losses as the size of the particles increases, indicates that more energy is required to convey larger particles for the same conveying conditions. This fact may be due to the higher drag forces on the particles [5, see DIXON].

Separating the data into air velocity ranges was a method used that would allow some correlations between the results to be determined. Plotting a linear line through the data in these graphs, was the most effective method of obtaining values that could be used to compare the differences between the materials. Some materials show more scatter of data than others, and the ground ilmenite results illustrates the less orderly data points. The ground ilmenite was obtained from the same batch of sandy ilmenite, and reduced in size by a grinding process. The process not only reduced the particle sizes, but changed the particle shape, which may have some influence on the reasons for the wider scatter of data points between the two ilmenites.

The details shown in this paper are only a small part of the work carried out by this author, into the investigation of the measured differences in pressure losses between conveying of materials of similar particle characteristics. Further work will be published in due course.

References

1. P.J. MENDIES, J.M. WHEELDON AND J.C. WILLIAMS The velocity of granular material flowing in a pneumatic conveyor Pneumotransport 2, Second International Conference on the Transport of Solids in Pipes, Guildford, Paper DI 1973

2. M.S.A. BRADLEY AND A.R. REED An improved method of predicting pressure drop along pneumatic conveying pipelines, Powder Handling Processing Vol. 2 No. 3 Sept 1990

3. M.S.A. BRADLEY Pressure losses caused by bends in pneumatic conveying pipelines - Effects of bend geometry and fittings Powder Handling Processing Vol. 2 No. 4 Nov 1990

4. M.G. JONES The influence of bulk particulate properties on pneumatic conveying performance - Ph.D thesis Thames Polytechnic 1988

5. G. BUTTERS Plastic Pneumatic Conveying and Bulk Storage, Appl. Sci. Pub., New York, 296pp

ANALYSIS OF COMBINED PARTICLE SIZE AND DENSITY EFFECTS ON HORIZONTAL STRAIGHT PIPE PRESSURE GRADIENTS IN LEAN PHASE CONVEYING

L.M. Hyder, M.S.A. Bradley, R. Farnish, I. Bridle and A.R. Reed
The Wolfson Centre for Bulk Solids Handling Technology
School of Engineering
University of Greenwich
Wellington Street
Woolwich
London SE18 6PF
United Kingdom

Summary

This paper analyses data collected as part of a doctoral thesis (Hyder [1]) which investigated ways to improve the efficiency and accuracy of pressure loss prediction methods. The project concentrated on discerning the effects that product particle properties have on the pressure drop per unit length of horizontal pipeline.

A range of different materials were used during pneumatic conveying tests to try to determine the relationships between various particle properties and the pressure losses along a pipeline. The initial test-work concentrated on a small group of materials whose particle properties varied either in median particle size or particle density. The results of these tests led to the conclusions that increasing either of these particle properties led to an increase in pressure drop plant during lean phase horizontal conveying in the pilot-sized test plant. The initial conclusions were checked with a second group of materials and found to remain true. Trends were identified between the two material groups and further test-work was undertaken with other disparate individual materials to confirm the trends. The overall results were plotted in a style similar to the Geldart Classification Chart. This was to determine whether rough plant pressure drop calculations could be made from this data by plotting the materials position on the generated chart using its known median particle size and particle density.

Keywords: Pneumatic conveying, particle size, particle density, horizontal pipelines, pressure gradients

Introduction

Despite the benefits of pneumatic conveying of solids, the design of such systems has been problematic since they were originally used over a century ago. This is because designers of pneumatic conveying systems need to know an estimated total pressure loss across the proposed system, in order to provide a sufficient, but economical system that will cause as little degradation to the product conveyed as possible, minimise the power consumption, and reduce the amount of wear to the system (Bradley & Reed [2], University of Greenwich [3], Wypych [4].

Previous work on the modelling of pressure drop along straight sections for two phase gas-solids flow, highlighted the fact that little research had previously been undertaken into the measured pressure drop differences between materials of different particle size, shape or density. Of the work that had been carried out in that particular area, the main areas of research have related to the differences in particle size from only a handful of coarse materials (Vogt and White [5], Clark et al [6], Mehta et al [7]).

The examination into the differences in pressure drop caused by the differences in particle characteristics, had not been undertaken before in a comprehensive, systematic way. Careful choice of the test materials allowed the effect of particle characteristics to be seen much more clearly than ever before. The analysis of the test results shows a clear link between these properties and the pressure drop.

The decision to investigate individual particle properties, resulted from the fact that a vast range of materials are pneumatically conveyed along pipelines in industry, but no widely applicable correlation between the particle properties and the pressure losses had previously been identified

Objectives

The main objective of the work presented in this paper was to co-ordinate and correlate data collected for a variety of materials under identical test conditions, with a view to determining whether a simple empirical tool could be engineered to assist in pneumatic conveying pipeline design, by minimising or eliminating the need for test work if particle properties are known

Test rig & equipment

The test rig used for the project was part of a previously used test rig (Bradley [8]) that was modified in some areas. The rig incorporated a 53mm bore pipeline loop, made up of straight sections and bends, 81 metres in length. The majority of the pipeline was in a horizontal orientation, with a number of pressure transducers fitted along the long straight sections. A blow tank was acting as a feeder at the beginning of the conveying line, with a receiving hopper at the end of the line, situated above the blow tank and mounted on load cells. The flow rate of solids was determined by monitoring the gain in weight in the hopper through the load cells, over a known period of time.

The air-flow rate was regulated by a bank of choked flow nozzles installed in parallel. The rig was controlled from a mimic panel and the instruments were connected to a data logging system, which also recorded the pressure readings. These readings were then transferred at the end of each test to a computer, for processing.

A diagram showing the layout of the test pipeline is shown in figure 1. The pressure transducers along each straight are separated by two metre intervals. Each straight lengths of pipe in the test section were 17m in length. This would ensure that the solids following a bend were in a steady state of flow before pipeline pressures were recorded.

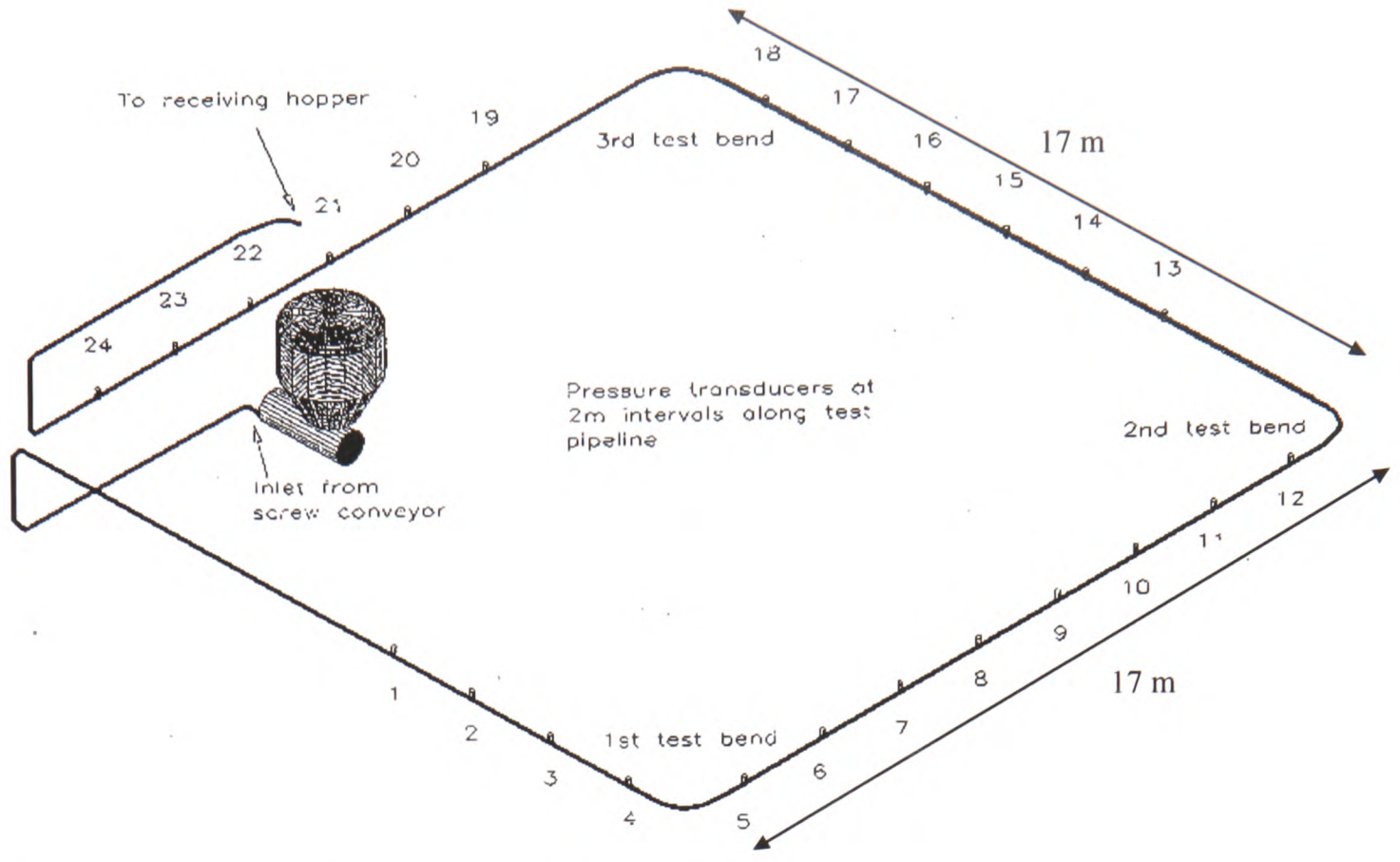

Figure 1. Layout of the test pipeline showing the positions of the pressure transducers and test bends. The receiving hopper has been excluded from the diagram in order to display all the transducers.

Test program & materials

Each test run produced raw data scanned from 24 pressure transducers along the pipeline, plus two that monitored the pressures upstream of the nozzle bank and in the blow tank. In addition, an averaged reading was taken from the outputs of three load-cells that were positioned beneath the receiving hopper. Taking the averaged reading from the load cells enabled the mass flow rate of material entering the receiving hopper to be determined. During each test run the transducers and load cells were scanned for data every second, over a 150-second time period.

The conveying characteristics were determined by ascertaining the minimum and maximum conveying conditions for each material within the limits of the test rig. To determine the minimum conveying air velocity, the inlet air velocity was reduced for several consecutive test runs until the conveying line blocked with material. The suspension density values[2] were taken at the midpoint position of the steady state section of each pressure gradient. The conveying conditions for the test materials are detailed hereafter.

[2] Suspension density is defined as the mass flow rate of solids divided by the actual volume flow rate of air (kg_{solids}/m^3_{air}) at that point in the pipeline. Note it gives a value lower than the actual density of the air-solids mixture in the pipeline, since for the sake of simplicity it ignores the slip velocity of the solids, and the volume occupied by the solids.

Material	Inlet air velocity at start of test loop m/s		Min. suspension density kg/m^3	Max. suspension density kg/m^3
	Min.	Max.		
Silica flour	15	26	6	70
Ground ilmenite	12	26	5	89
Sandy ilmenite	12	23	9	55
Olivine sand	12	23	7	85
Glass beads	14	22	17	67
Polyethylene pellets	10	29	3	33
Golden pea gravel	13	22	13	86
Boral lytag	15	25	7	31

These conditions represent a realistic range of operation of commercial systems. The raw data was stored in a data logger and transferred to a computer after each test run was completed. Once stored in the computer, the raw data was then processed and analysed. The analysed data for each material was transferred to a separate database, from which graphs were plotted to compare any differences in results between the materials.

Description of test materials

The details of all the test materials are described below.

Material	Particle size range (μm)	Median particle size (μm)	Particle density (kg/m^3)
Silica flour	0-100	30	2870
Ground ilmenite	5-110	30	4520
Sandy ilmenite	60-300	165	4520
Olivine sand	70-565	320	3280
Glass beads	600-800	660	2500
Polyethylene pellets	2800-3350	3000	910
Golden pea gravel	2800-4000	3000	2700
Boral lytag	2800-4750	4000	1530

Results & analysis

The raw data from a test run was first examined on a graph of pressure versus time, to identify the steady state period in which to process the results. Having selected the steady state period, the results for each transducer were averaged and the mass flow rate of solids calculated as per Bradley [8].

For each straight test section, the conveying pressure pattern after each bend caused by re-acceleration of the material (Bradley [8] & Jones [9]) was ignored and a least squares best-fit line was plotted through the remaining data points, to determine the pressure gradient along each straight section of monitored pipeline. A linear fit was applied to all four straight section gradients, so that a normalised pattern was given to all the pressure gradients (graph 1).

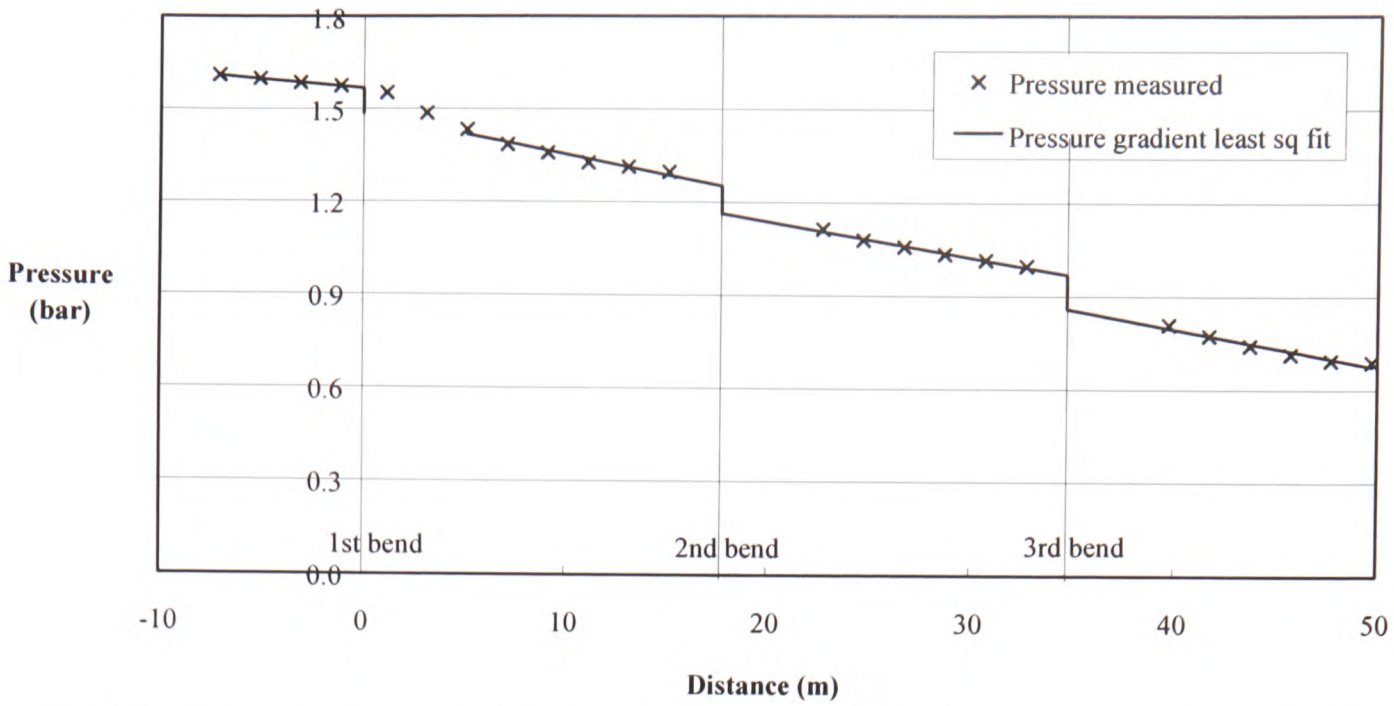

Graph 1. Pressure gradients along straight test sections. Transducer readings in the first 5m downstream of the first test bend are ignored due to the re-acceleration length (Bradley [8] & Jones [9]).

The pressure gradients for all four straight sections were stored and transferred to a database when all the test work was completed. From each database, relating to one material, several graphs were drawn for the solids contribution to the pressure losses (mbar/m) against the midpoint suspension density (kg_{solid}/m_{air}^3), from individual air velocity ranges used during the conveying test runs. The notional solids contribution to the pressure gradients was derived by deducting the air only pressure gradient value (using a correlation[3]) from the total measured pressure gradient. The graphs were divided into the results from specific air velocity ranges, as shown in example graphs 2 and 3. The tests that were carried out concentrated on the air velocity range of 20 - 30m/s, as most industrial lean phase applications fall into this range.

The resultant slope value, a best-fit straight line fitted through the data for each velocity range, was then recorded for each material. The slope values were then plotted against their respective velocity values as shown in graphs 4a and 4b. The results are displayed in two graphs for ease of understanding. All of the graphs produced, indicated a strong relationship between the pressure drop per unit suspension density and the conveying air velocity. The relationship appeared to be of a power law nature; and it was felt that modelling the system using a square-law incorporating a single, multiplying coefficient would yield results for all materials.

$$m = \text{coefficient} \times C^2_{air} \qquad [1]$$

In using a square-law model it allowed dimensional homogeneity to be maintained, which is always desirable in modelling situations. It also correlates with some of the work done by previous modellers, namely Weber [10 & 11] and Keys & Chamber [12].

With each material having specific values for median particle size, particle density and the derived new coefficient, a way was sought to correlate the data. A graph was plotted mapping the median particle size against particle density for each material, with the coefficient as a data label. The results are displayed on graph 5. A combination of extrapolation and interpolation yields graph 6, which attempts to provide coefficient values across a range of materials other than those tested, purely based on the particle characteristic of median size and density.

---

[2]The calculation of the air contribution to pressure gradient was undertaken using a Fanning friction factor which had been determined from air-only tests on the pipeline.

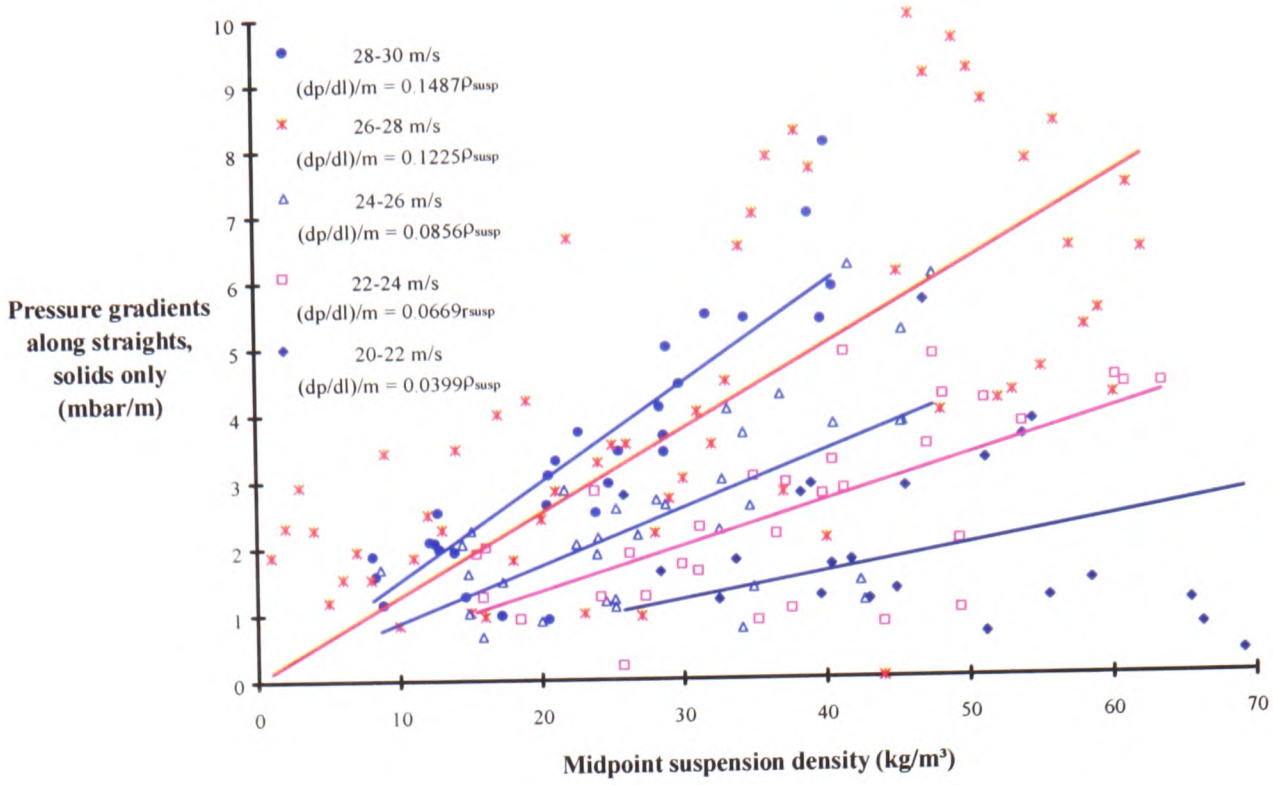

Graph 2: Sample graph for silica flour.

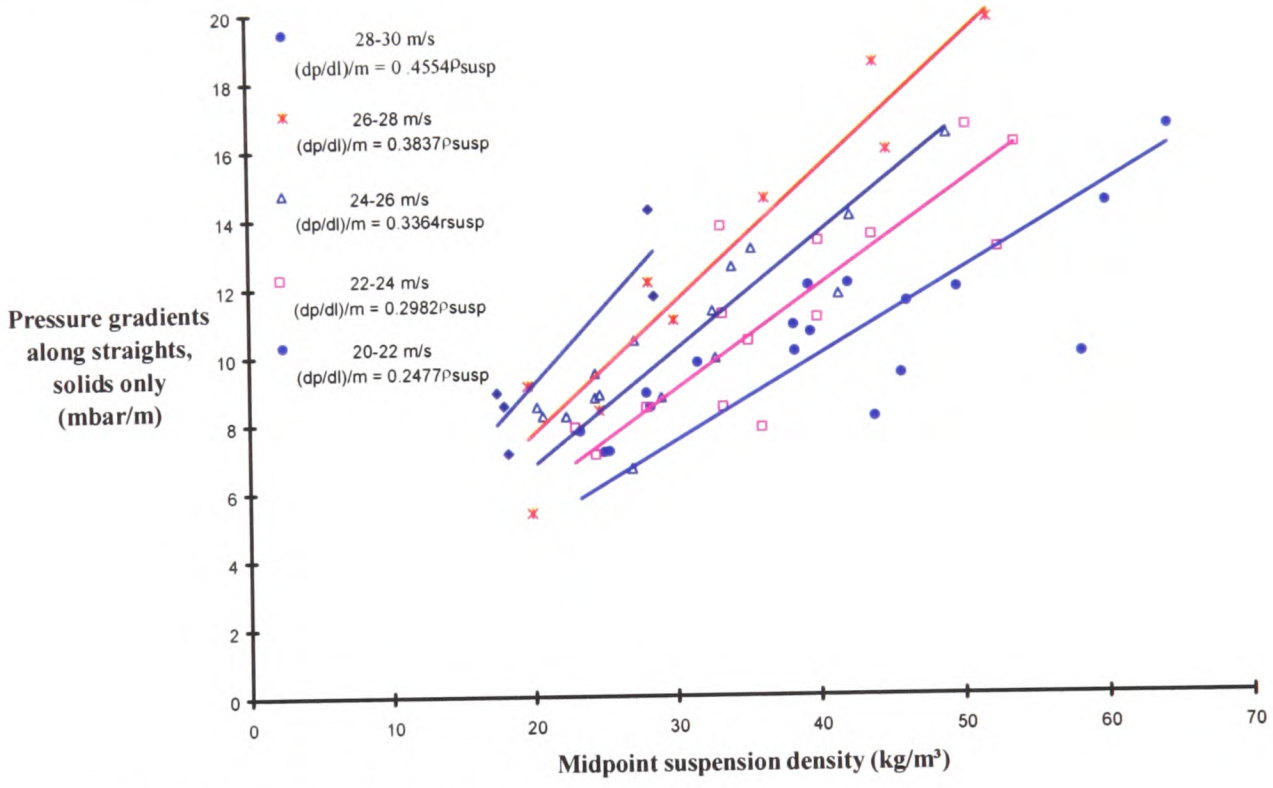

Graph 3: Sample graph for golden pea gravel.

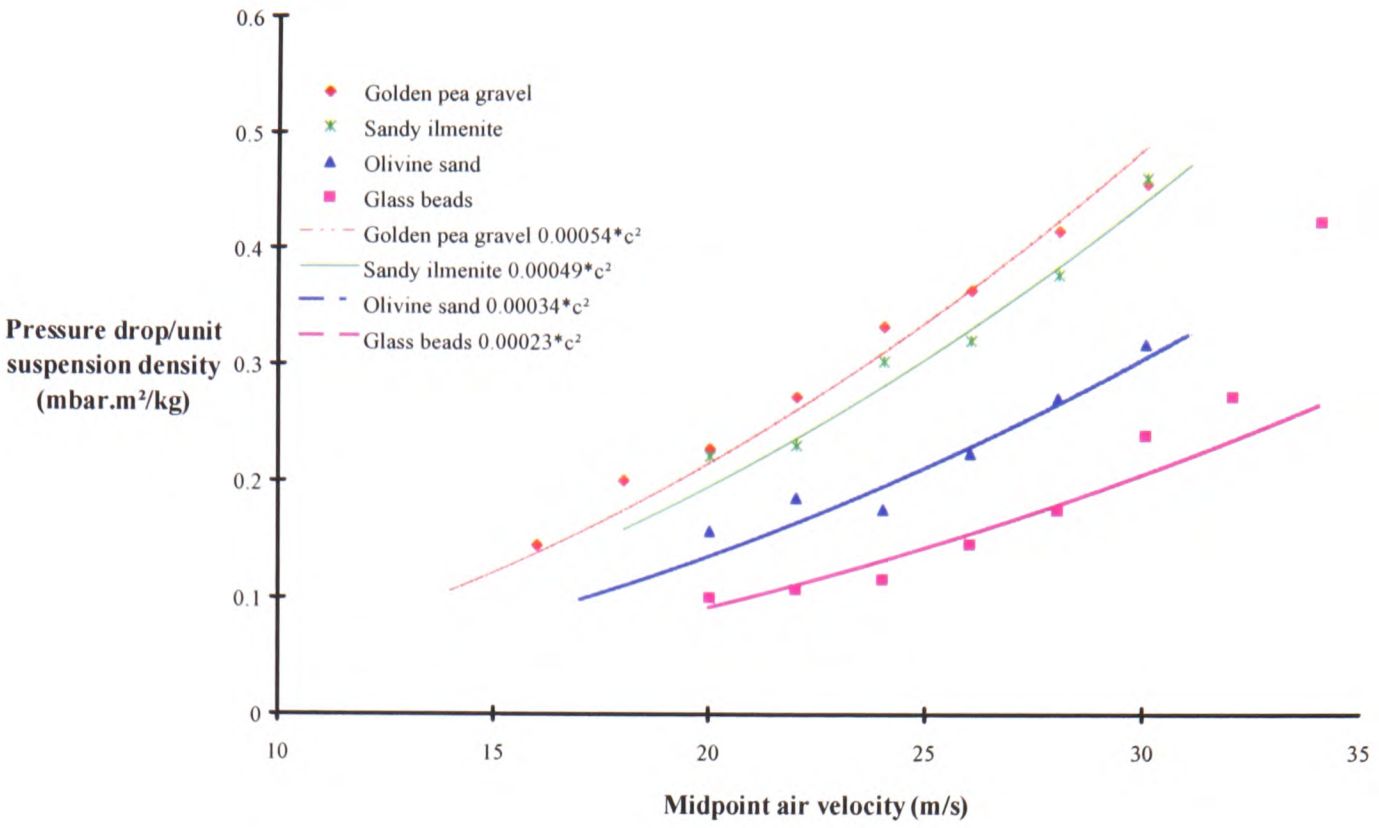

Graph 4a: Plot of pressure drop per unit suspension density against midpoint air velocity, for four of the eight test materials.

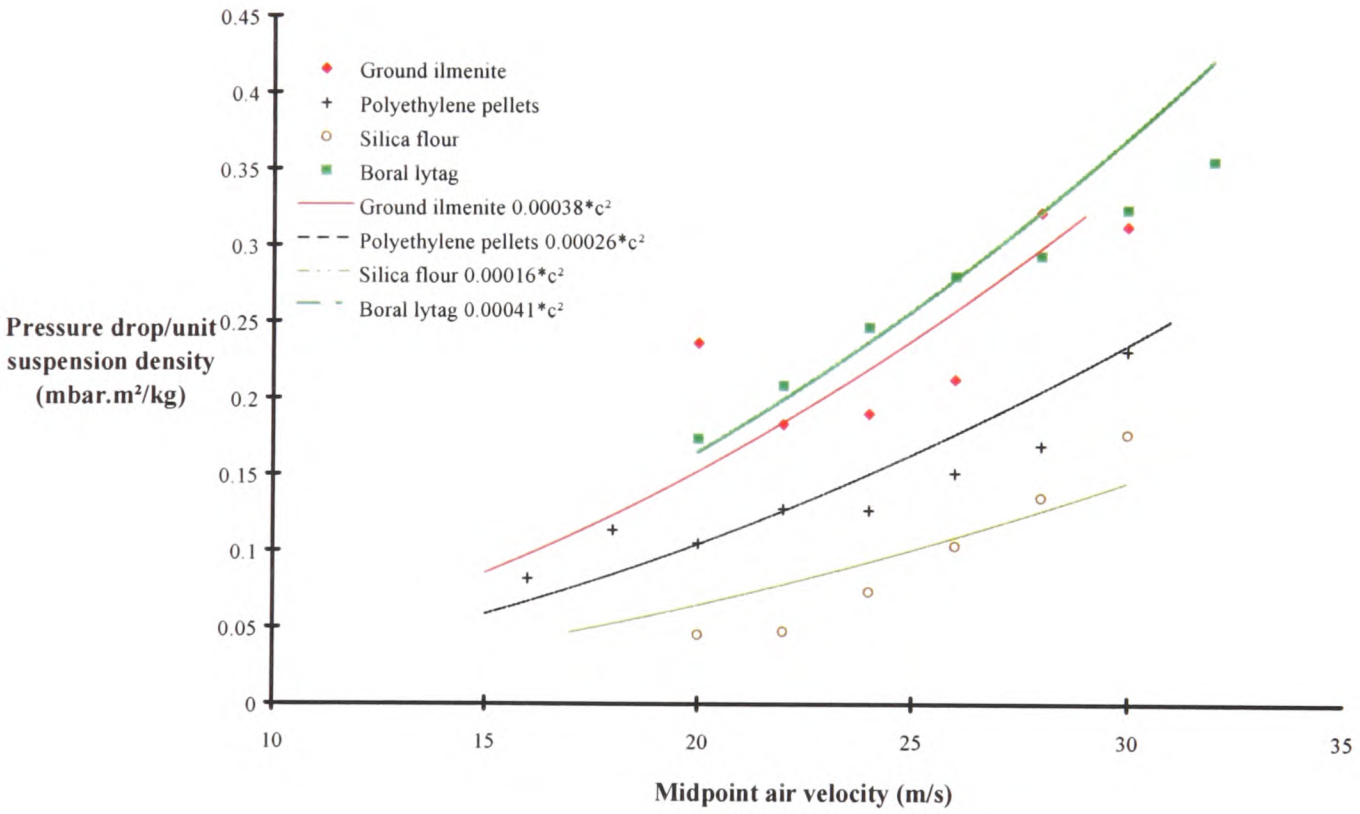

Graph 4b: Plot of pressure drop per unit suspension density against midpoint air velocity, for four of the eight test materials.

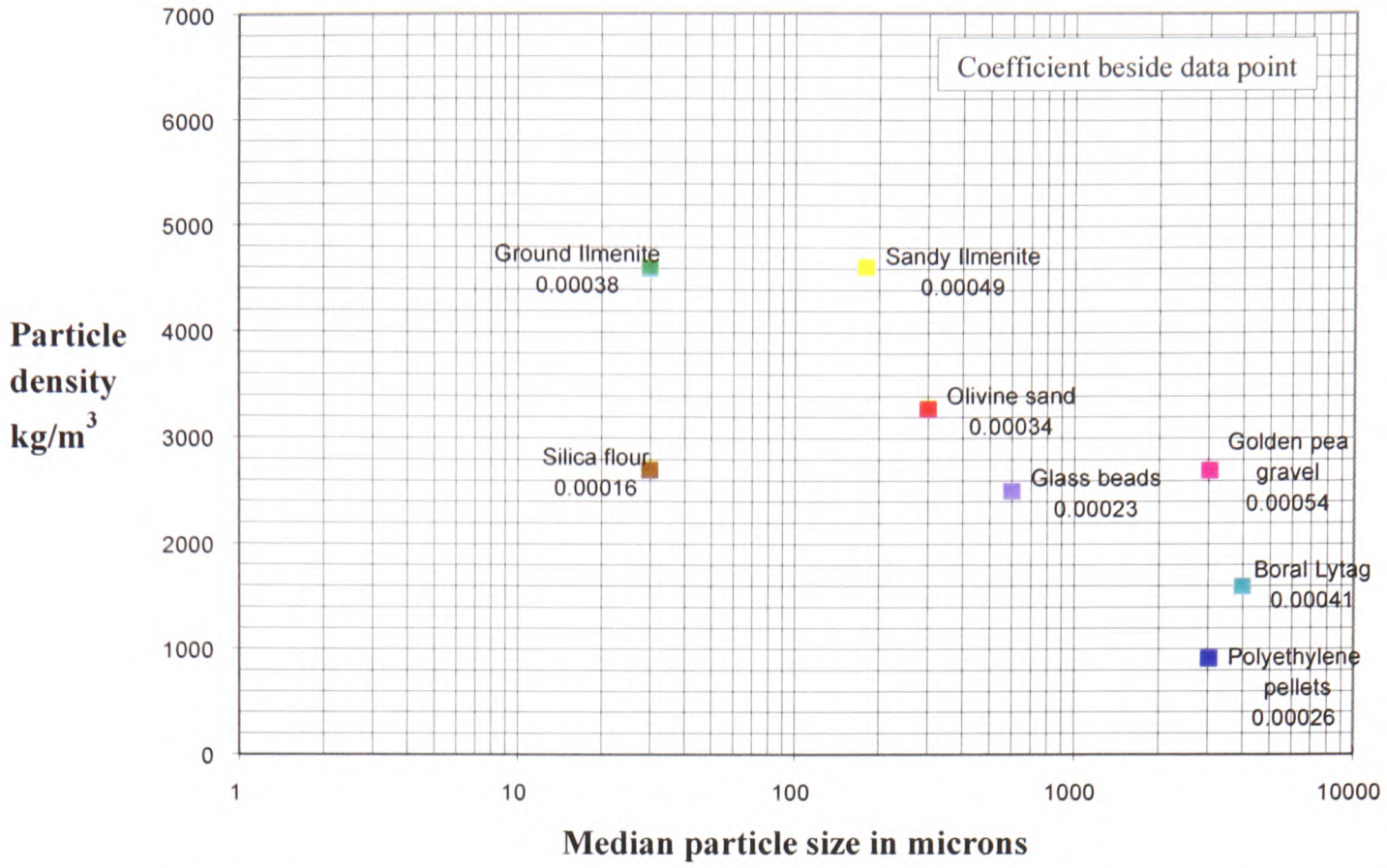

Graph 5: Particle density against median particle size, with data labels adjacent to points indicating respective coefficient values.

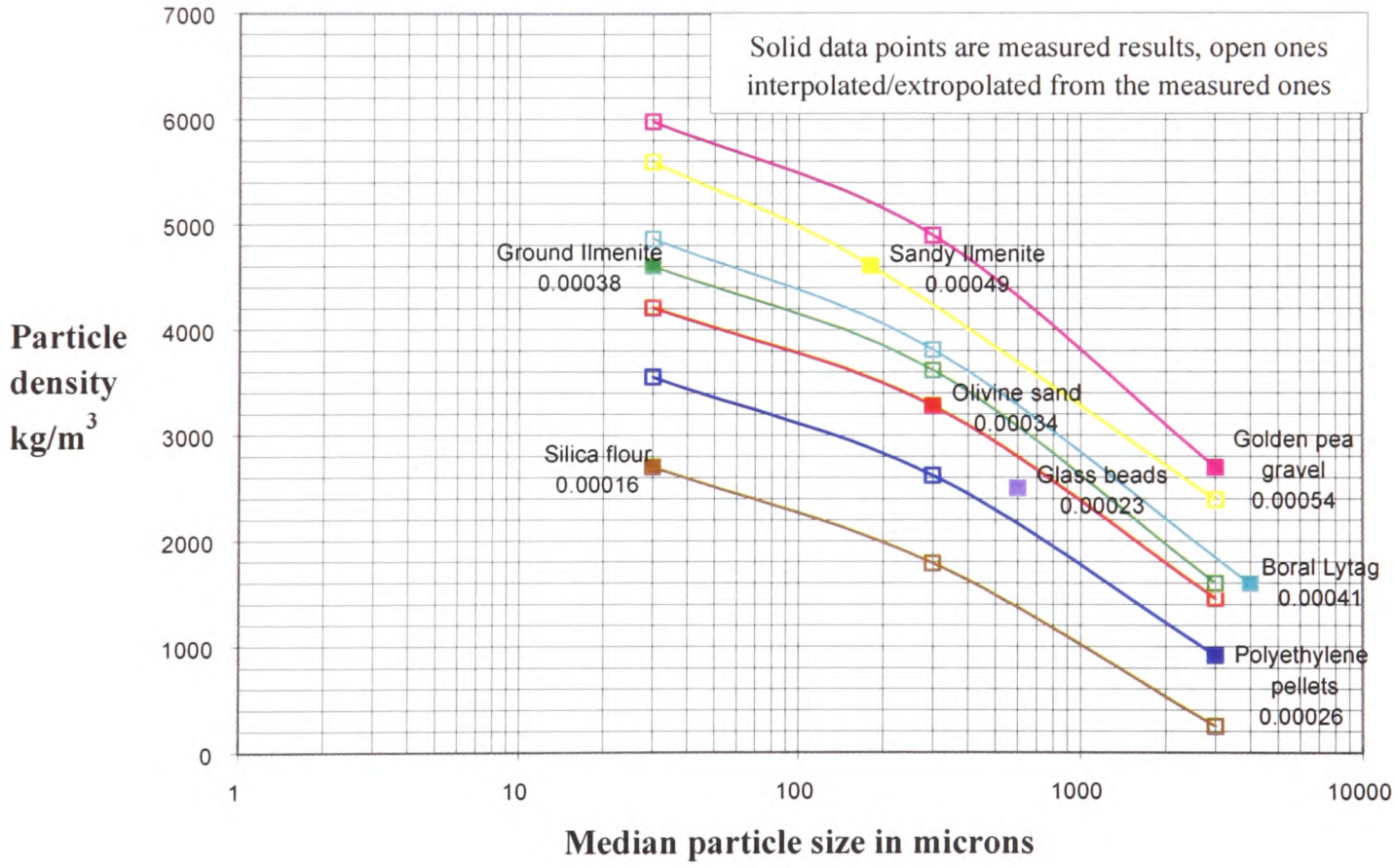

Graph 6: Particle density against median particle size, with interpolated/extrapolated data points added along lines of equal coefficient value.

The concept of solids and air contributions to total pressure gradient

The complex interaction involving the two phases along a pipeline are often represented as a model displayed below,

$$\left(\frac{dp}{dl}\right)_{total} = \left(\frac{dp}{dl}\right)_{air} + \left(\frac{dp}{dl}\right)_{solids}$$

where $\left(\frac{dp}{dl}\right)_{total}$ = pressure gradient observed in pipe.

$\left(\frac{dp}{dl}\right)_{air}$ = pressure gradient when solids are absent, predicted using conventional means e.g. an equation similar to the Darcy or Fanning equation, or an equation produced by tests using air only along the pipeline.

$\left(\frac{dp}{dl}\right)_{solids}$ = Additional pressure gradient, in principle caused by the addition of the solid particles to the air.

Note: The results from the test work in this paper are presented in units of mbar per metre.

The model is purely a concept used as a convenient means of thinking about why the pressure drop increases when solids are introduced, and storing the data.

The pressure losses along straight pipelines due to the 'solids contribution' are commonly used in data analysis because it is considered that the 'air only' pressure contribution to the total pressure losses are small in comparison. Under certain conditions, i.e. very low suspension densities and high air velocities, and in pipes of small size, the air only contribution can become larger and more significant.

Comparison of results with the work of other authors

As the data for each test material was processed, analysed, and its database completed, the data points from which the coefficient (k) for each material was determined, were plotted on a graph together with data from the other test materials. Graph 4a and 4b shows the differences between the materials in terms of the values of k in,

$$\frac{dp}{dl}_{solids} = k\rho_s\left(c_{air}\right)^2$$

For pipes that are horizontal and straight, with flow that is considered to be fully accelerated, the pipe pressure drop can be considered as:-

Data from the work of Keys and Chambers [12], and Weber [10,11] in terms of an air alone friction loss l_f and a particle friction loss m^*l_s, in the pipe loss term, where:

(Keys and Chambers [12]) Pipe loss, $P_L = r_a V^2 L(l_f+m^*l_s)/2D$ [2]

(Weber [11]) $l_f = 1.325/[Ln\{e/3.7D\}+5.74/Re^{0.9}\}]^2$

N.B. e = 0.045 for commercial steel

(Weber [10]) $l_s = 2.1F_s^{0.25}(D/d_i)^{0.1}/(m^{*0.3}F)$

when $d_i < 0.5$mm

(Weber [10]) or $l_s = 0.082F_s^{0.25}(D/d_i)^{0.1}/(m^{*0.3}F^{0.86})$

when $d_i > 0.5$mm

Inputs to above l_s are:
(Weber [11])

$F = V^2/gD$

$F_s = W^2/gd_i$

$W = [4gd_i(r_b-r_a)/(3C_d r_a)]^{0.5}$

Assuming particle sphericity:

$C_d = (24/Re_{di})(1+3Re_{di}/16)$ for $Re_{di} < 1.0$

$C_d = 0.4 + 26/(Re_{di})^{0.8}$ for $1.0 < Re_{di} < 1000$

$C_d = 0.4$ for $Re_{di} > 1000$

Now, considering the total pressure drop and the relationship with the conveying air velocity:

$P_L = r_a V^2 L(l_f+m^*l_s)/2D$

The coefficients arrived at in this paper by the foregoing measurement and graphical methods can now be checked against the theoretical relationships have been defined; as follows:-

Pressure drop per metre/unit suspension density = coefficient . midpoint air velocity^2
- from [1]

Pressure drop per metre = P_L/L - from [2]

Suspension density = $\rho_{susp} = \dfrac{\dot{m}_s}{\dot{V}_a}$

As mass flow rate ratio, m* is defined as: $m^* = \dfrac{\dot{m}_s}{\dot{m}_a} = \dfrac{\rho_s \dot{V}_s}{\rho_a \dot{V}_a}$

Then: $m^* = \dfrac{\dot{m}_s}{\rho_a \dot{V}_a}$

Therefore: $\rho_{susp} = m * \rho_a$

i.e. $(P_L/L)/(r_{susp}) = \text{coefficient} . V^2$

where P_L is from ref 10,11 & 12, and the coefficient is from this paper.

Therefore, for a known material the coefficient can be estimated by the following, if all the properties are known:

$$P_L = \frac{\rho_a V^2 L}{2D}\left(\lambda_f + m * \lambda_s\right) \qquad [3]$$

As the pressure gradient used in the graphical methods are for the solids contribution to the pressure losses only, the air friction term was omitted from the pressure loss equation, to give:

$$P_{solids} = \frac{\rho_a V^2 L}{2D}\left(m * \lambda_s\right)$$

Comparing to the coefficient determined empirically from the data, where the pressure gradient was measure in mbar/m,

$$\frac{dp}{dl}_{solids} = k\rho_s\left(c_{air}\right)^2 \quad \Rightarrow \quad \frac{dp}{dl}_{solids} . \frac{1}{\rho_s\left(c_{air}\right)^2} = k \qquad [4]$$

Where $\left(c_{air}\right)^2 = V^2$ in [2] and [3]

The equivalent coefficient can be obtained from:

$$P_{solids} = \frac{\rho_a V^2 L}{2D}\left(m * \lambda_s\right) \quad \Rightarrow \quad \frac{P_{solids}}{L} . \frac{1}{\rho_a m * V^2} = \frac{\lambda_s}{2D} \qquad [5]$$

As both the left hand terms in [4] and [5] are the same, the right hand terms in both equations must also be the same.
Therefore, the coefficient for the solids contribution to the total pressure losses, determined from the modelling,

$$\text{Coefficient} = \frac{\lambda_s}{2D}$$

Comparison of measured and modelled coefficient

The value of the coefficient for the various materials determined by empirical means and by modelling from refs 10,11 & 12, are shown on table 1 below. To compare the value of the modelling coefficient to the coefficient determined from the test results, data from each test materials database was selected. In order for the comparison to be made for each material, the conveying conditions were as similar to each as possible. The mass flow rate ratio for all the materials were between 14.5 and 15.9. The inlet air velocities ranged from 13.6 to 16.5 m/s^2.

Material	Coefficient value	
	Empirical	Modelling
Silica flour	0.00016	0.00111
Ground ilmenite	0.00038	0.00179
Sandy ilmenite	0.00049	0.00121
Olivine sand	0.00034	0.00102
Glass beads	0.00023	0.000072
Polyethylene pellets	0.00026	0.000101
Golden pea gravel	0.00054	0.000086
Boral lytag	0.00041	0.000068

Table 1: Results of graphical and modelling values for each test material.

Comparing the graphically determined and modelling values of the multiplying coefficient does not indicate a reliable correlation. However, the materials used in the original test work in references 10,11 and 12, on which the modelling equations were based, used fly ash of various sizes and did not venture into the realms of extending the model to other materials.

In addition, the comparison of the results shown on table 1, show that the coefficient from the model of refs 10,11 and 12, used in the modelling, display a reverse trend for the particle sizes. That is, the true coefficient is greatly over predicted for the smaller particles, and under predicted for the larger particles.

It was also found that the model predicted that the coefficient would change with conveying conditions, so to explore this it was necessary to plot some graphs showing the model coefficient against air velocity. Three of the graphs (7, 8 & 9) are shown, for the silica based materials, which vary from each other by their median particle size. It can be seen when comparing the power law curve drawn through the sets of data, that they do not follow a pattern relating to their particle size.

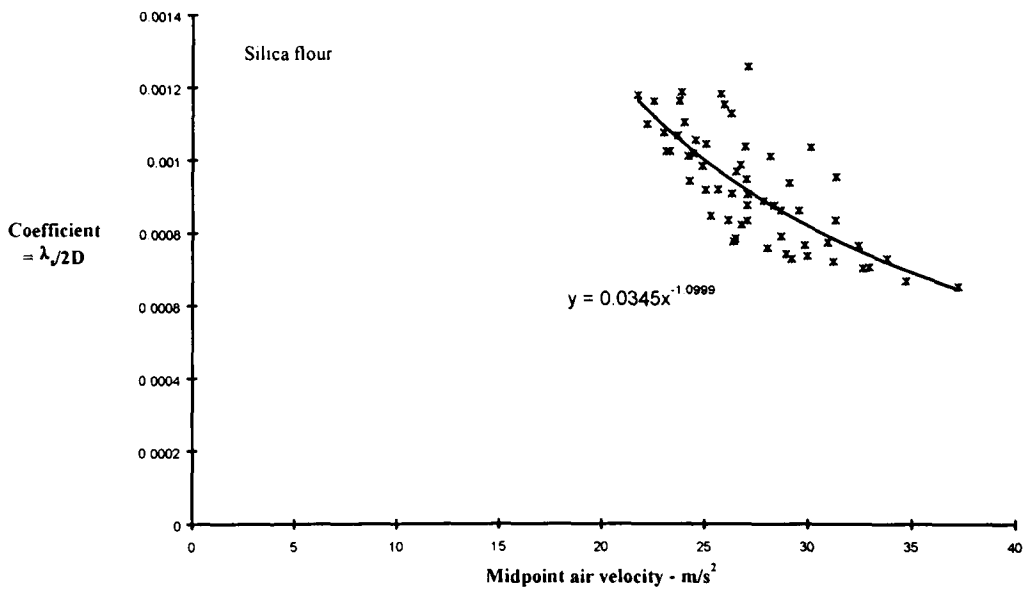

Graph 7: Modelling coefficient using test data conveying conditions for the silica flour, versus midpoint air velocity. Measured coefficient value = 0.00016.

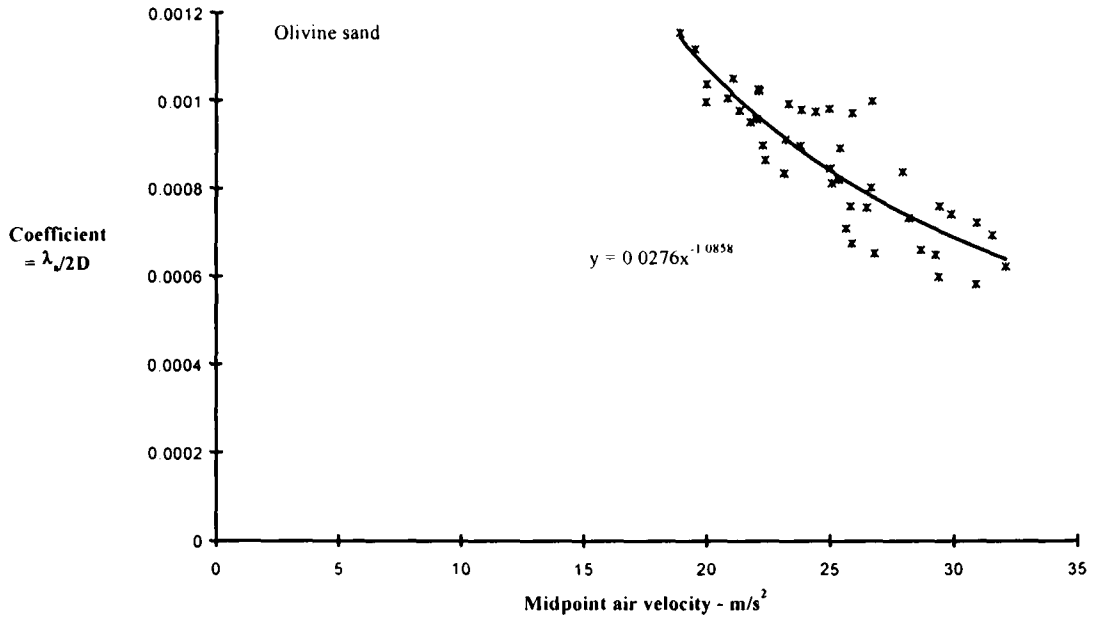

Graph 8: Modelling coefficient using test data conveying conditions for olivine sand, versus midpoint air velocity. Measured coefficient value = 0.00034.

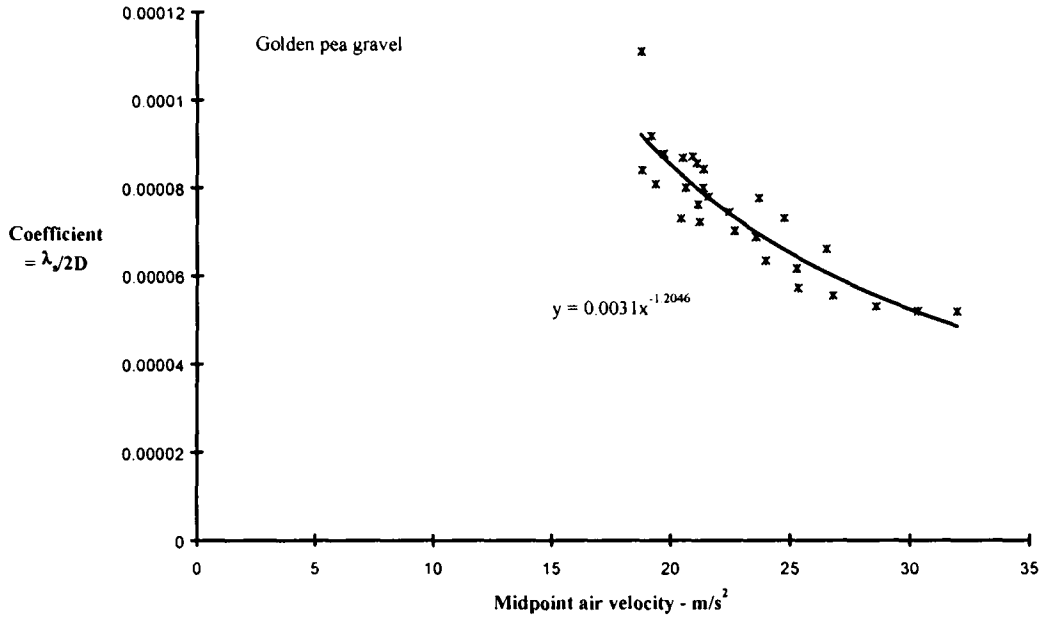

Graph 9: Modelling coefficient using test data conveying conditions for the golden pea gravel, versus midpoint air velocity. Measured coefficient value = 0.00054.

As shown in graphs 7, 8 & 9, the coefficient is not the same for all the conveying conditions. The graphs show that the coefficient predicted by the model varies as the air velocity changes, unlike the coefficients determined empirically. The modelling indicates that a different coefficient should be used as the air velocity changes, whereas from the analysis on the empirically determined data for each material, the conveying conditions for each material were reduced to a single coefficient over the wide range of conditions tested.

Discussion

Pressure losses of materials pneumatically conveyed along pipelines vary from one material to another (for the same flow conditions). To investigate the relationship between the pressure losses and different materials, the particle characteristics of several materials were examined for their effect on the pressure losses. This was carried out in the search for a method that would reduce the amount of large scale test work that is normally required before conveying systems are designed to convey a particulate material.

Measured results from tests carried out on eight carefully selected materials, have shown that pressure losses along straight pipelines during pneumatic conveying of particulate materials, are

related to certain particle properties. A link between the particle density and pressure gradients, and the particle median size and the pressure gradients, has been identified between the materials used in this paper. A graph has been developed plotting particle density versus the particle median size of materials, with lines drawn representing contours of pressure loss coefficient values (graph 6). The graph gives the user a coefficient that can be used in a simple equation, to predict the solids contribution towards the total pressure gradient along straight sections.

The materials used to measure the effects of size, fell into two groups. They were (i) the silica based materials (silica sand, olivine sand and golden pea gravel) (ii) and ground and sandy ilmenites. All materials in each group had a similar chemical composition, but their sizes differed. The results show that as the particle size increases, the pressure losses for the solids contribution to pressure gradient along straight sections also increases. This effect is consistent in both magnitude and direction.

Three groups of materials were also compared to establish the particle density effects, which were similar in particle median size, and all fairly free flowing. They were (i) silica flour and ground ilmenite, (ii) olivine sand and sandy ilmenite, (iii) golden pea gravel, polyethylene pellets and boral lytag. The comparisons between these materials of similar particle median size, but with different particle densities, also show that as the particle density increases, so too do the pressure gradients.

The increase in the pressure losses as either the density of the particles, or the median size of the particles, increases indicates that more energy is required to convey denser, or larger, particles for the same conveying conditions. This fact may well be due to the combination of increased momentum imparted to the particles, for denser materials; and higher drag forces on the larger particles (Dixon [13]).

From the wide distribution of initial data points, shown in graphs 2 and 3, it can be seen that there is significant scatter in the behaviour of any given material from one test run to another, showing the importance of undertaking sufficient number of test runs to find meaningful trends amongst the noise. The degree of uncertainty arising from the scatter gives an indication of the margin of redundant capacity which should be built in to the design of industrial system using such data.

The work using the eight materials in this paper, represent a small number of the varied materials that are pneumatically conveyed in industry. An investigation into what materials are suitable for system design using in graph 6, can only be carried out by testing materials that are both similar to those used in this paper, those that differ only slightly, and some which differ more extremely.

At present, it is recommended that the use of the chart given in graph 6, should be restricted to materials similar to those from which it was developed, i.e. hard, resilient particles (such as mineral or plastics) with monomodal size distribution. The absolute values of the coefficient are likely to alter with materials whose particles do not share those properties, although the trends of increasing coefficient value with increasing particle size and density, are likely to remain.

Conclusion

A correlation has been produced which allows the prediction of the solids contribution to straight pipe pressure gradient in lean phase flow to be predicted, based on a certain range of material particle properties and flow conditions. The prediction is based upon a simple rational equation of familiar form, plus a coefficient whose value has been explored over the selected range of particle properties and flow conditions.

The limitations of the exploration have been materials with a monomodal distribution of hard, resilient and reasonably rounded particles, across a range of median sizes from 20 micron to 4mm

and particle densities from 900 to 4600 kg/m3, under flow conditions between 20 and 30 m/s and suspension densities from 3 to 90 kg/m^3. Within these limits lie a significant proportion of the range of industrial practice.

It is anticipated that where the particle properties and flow conditions lie outside this range, the correlation between coefficient and particle size and density may not hold. It is expected that the qualitative trends are likely to hold for materials whose particles have properties outside the range explored, and that the trends are likely to hold for higher air velocities and higher/lower suspension densities, however they will not be expected to hold for air velocities significantly lower than those tested since the mode of flow in the pipeline alters once saltation begins Jones [9].

The coefficient values determined from the measurements of the flows of the eight materials have been compared with a widely-quoted model of Keys and Chambers [12] based on Weber [10 & 11] and Streeter and Wylie [14], and it is apparent that they deviate by as much as one order of magnitude in either direction. This is believed to be due principally that the model of Keys and Chambers, and Weber was constructed using data from only one material.

Nomenclature

D	Pipe Diameter (m)
d_i	Median Particle Diameter (m)
C_d	Drag Coefficient of Particle
F	Pipeline Froude Number
F_s	Particle Froude Number
g	Gravity Acceleration (m/s^2)
L	Horizontal Pipe Length (m)
$\dot{m}$	Mass Flow Rate (kg / s)
$m^* = \frac{\dot{m}_s}{\dot{m}_a}$	= Mass Flow Rate Ratio
P_a	Acceleration Pressure Loss (N/m^2)
P_p	Predicted Pressure Loss (N/m^2)
P_L	Pipe Friction Pressure Loss (N/m^2)
Re	System Reynolds Number (r V D/m)
Re_{di}	Particle Reynolds Number (r W d_i/m)
V or C	Air Velocity (m/s)
$\dot{V}$	Volume Flow Rate (m^3 / s)
W	Solids Settling Velocity (based on di and r_b) (m/s)
l	Friction Factor
m	Absolute Viscosity of Air (Ns/m)
r	Density (kg/m^3)
r_a	Conveying Air Density (kg/m^3)
r_b	Bulk Product density (kg/m^3)

Subscripts:

a	Air
s	Solids

References

1. L.M. Hyder. The effect of particle size and density on pressure gradients in horizontal pipelines in lean phase conveying, Ph.D Thesis, University of Greenwich, 2000

2. M.S.A. Bradley and A.R. Reed. An improved method of predicting pressure drop along pneumatic conveying pipelines, Powder Handling Processing Vol. 2 No. 3. Sept 1990

3. University of Greenwich - Notes for intensive short course in Pneumatic conveying of bulk materials. 1999

4. P.W Wypych. The ins and outs of pneumatic conveying Int. sump. RELPOWFLO 111, Porsgrunn, Norway. 1999

5. E.G Vogt. and R.R White. Granular solids in gases through pipe, Industrial & Engineering Chemistry Vol. 40, No.9. 1948

6. R.H Clark. D.E. Charles and J.F Richardson. Pneumatic conveying. Part 1. The pressure drop during horizontal conveyance. Trans. Instn. Chem. Engrs Vol. 30. 1952

7. N.C Mehta., J.M Smith. and E.W Comings. Pressure drop in air-solid flow systems Industrial & Engineering Chemistry Vol. 49, No.6. 1957

8. M.S.A. Bradley. Pressure losses caused by bends in pneumatic conveying pipelines - Effects of bend geometry and fittings Powder Handling Processing Vol. 2 No. 4, Nov 1990

9. M.G. Jones. The influence of bulk particulate properties on pneumatic conveying performance - Ph.D thesis Thames Polytechnic. 1988

10 M. Weber. Principles of hydraulic and pneumatic conveying in pipes, Bulk Solids Handling, Vol. 1 No.1, February 1981

11. M. Weber. Correlation analysis in the design of pneumatic transport plant, Bulk Solids Handling, Vol. 2 No.2, June 1982

12. S. Keys and A.J. Chambers. Scaling pneumatic conveying characteristics for pipeline pressure, International Symposium: Reliable Flow of Particulate Solids II, Oslo, Norway. 23-25 August 1993

13. Dixon - see G. Butters. Plastic Pneumatic Conveying and Bulk Storage, Appl. Sci. Pub., New York, 296pp

14. V.L. Streeter and E.B. Wylie. Fluid Mechanics, McGraw-Hill, 562pp, 1981

Appendix 9
References

Code	Authors	Date	Title & Source
A1	Ashenden S.J. Pittman A.N. Burnett A.J. Woodhead S.R.	1995	"Drag reducing flow in Dilute Phase Pneumatic Conveying Systems - is it Significant?" 5th Int. Conf. on Bulk Materials Storage, Handling & Transportation, Australia
A2	Alberti E. Costa F. Finzi L. Pozzetti A. Tavecchio R.	1991	"Advanced design of pneumatic conveying systems-methods and tools" Bulk Solids Handling Vol. 11, No.1
A3	Arnold P.C. Wypych P.W. Reed A.R.	1994	"Advanced in the design of pneumatic transport systems" Powder Handling & Processing Vol.5 No.1
A4	Ashenden S.J.	1989	"An examination of the discharge capabilities of blow tanks as feeders for pneumatic conveying systems" Ph.D. Thesis, Thames Polytechnic
B1	Bradley M.A.S.	1990	"Prediction of pressure losses in pneumatic conveying pipelines" Ph.D. Thesis, Thames Polytechnic
B2	Bell J.M.	1990	"Material characterization and its importance to pneumatic conveying system design" Powder Handling & Processing Vol.2, No.3 pp 213-216

B3	Bates L.	1986	"Interfacing hoppers with screw feeders" Bulk Solids Handling Vol.6 No.1
B4	Burnett A. J.	1996	"The use of laboratory erosion tests for the prediction of wear in pneumatic conveying" Ph.D. Thesis, University of Greenwich
B5	Bonnin J.C. Bouard R.	1990	"Bends in air-cement flow" Pneumatech 4. 4th Conference on Pneumatic Conveying Tech.
C1	Cabrejos F.J. Klinzings G.E.	1992	"Minimum conveying velocity in horizontal pneumatic transport and pickup and saltation mechanisms of solids particles" Int. Conf. Bulk Materials Handling and Transportation: symp. freight pipelines, Wollongong, Australia
C2	Clark R.H. Charles D.E. Richardson J.F.	1952	"Pneumatic conveying. Part 1. The pressure drop during horizontal conveyance" Trans. Instn. Chem. Engrs Vol. 30
C3	C.P.Chen	1978	"Recent results on measurements of solid particles velocity in a two phase turbulent horizontal flow at high loadings" 4th Int. Conference on Pneumatic Transport of Granular Materials
D1	Dhodapkar S.V. Klinzing G.E.	1992	"Pressure fluctuations in pneumatic conveying systems" Int. Conf. Bulk Materials Handling & Transportation: symp. on freight pipelines, Wollongong, Australia

D2	Various	1993	Notes for "Design of hoppers and silos for strength and flow" The Wolfson Centre, University of Greenwich.
E1	Engineering Equipment Users Association	1963	"Pneumatic handling of powdered materials" Pub. Constable & Co. (EEUA handbook No. 15) pp 53-65
G1	Govan A.H. Hewitt G.F. Terry J.W.	1990	"Axial-view measurements of particle motion in a turbulent pipe flow" Part. syst. charact. 7 pp 60-69
G2	Geldart D. Knowlton T.M.	1986	"Gas fluidisation technology" Pub. Wiley, pp 357-359
H1	Haaker G. van Poppelen M.P. Jongejan M.P.	1994	"A method to optimize screw feeder geometry for equable draw down performance" Bulk Solids Handling Vol. 14, No 1.
H2	Hitt R.J.	1985	"An investigation into the low velocity pneumatic conveying of bulk solids" Ph.D. Thesis, Thames Polytechnic
H3		1994	"C.O.S.H.H. safety information sheet on Silica sand" Hepworth Minerals & Chemicals Ltd.
J1	Jones M.G.	1988	"The influence of bulk particulate properties on pneumatic conveying performance" Ph.D. thesis, Thames Polytechnic
J2	Jenike A.W.	1964	"Storage and flow of solids" Utah. Engng. exper. station, Univ. of Utah, Bul.123

K1	Keys S. Chambers A.J.	1993	"Scaling pneumatic conveying characteristics for pipeline pressure" Int. Symp. Reliable flow of Particulate Solids, Oslo, Norway
K2	Kessel S.R.	1986	"The interaction between rotary valves and pneumatic conveying pipelines" Ph.D. Thesis, Thames Polytechnic
L1	Levy A. Mason D.J.	1998	"Numerical investigation of the effect of bend radius on gas solids flow in pneumatic conveying systems" Powder Handling & Processing Vol. 10, No. 3.
L2	Leva M.	1959	"Fluidization" McGraw-Hill,
M1	Mehta N.C. Smith J.M. Comings E.W.	1957	"Pressure drop in air-solid flow systems" Industrial & Engineering Chemistry Vol. 49, No.6
M2	Mendies P.J. Wheeldon J.M. Williams J.C.	1973	"The velocity of granular material flowing in a pneumatic conveyor" Pneumotransport 2, 2nd Int. Conf. Pneumatic Transport of Solids in PIipes
M3	Marcus R.D. Hilbert J.D. Klinzing G.E.	1985	"Flow through bends and acceleration zones in pneumatic conveying systems" Bulk Solids Handling Vol.5, No.4
M4	Mainwaring N.J.	1994	"Characterisation of materials for pneumatic conveying" Powder Handling & Processing Vol.6, No.1

M5	Mainwaring N.J.	1994	"The effect of the physical properties of bulk solid materials on modes of dense phase pneumatic conveying" Ph.D. Thesis, Thames Polytechnic
M6	Morikawa Y. Tsuiji Y. Matsui K. Jittani Y.	1978	"Pressure drops due to pipe bends in air-solids two phase flows: circular and elliptical bends" Int. Journal multiphase flow Vol. 13, No.2
M7	Michaelides E.E. Lai F.C	1987	"Pressure loss through return bends in air-solid flows" Int. Journal multiphase flow Vol. 13, No.2
M8	Mills D.	1992	"Conveying characteristics and scale-up procedures" Short course design and operation of pneumatic conveying systems. Dept Mechanical Eng. University of Wollongong, Australia
M9	Mandelbrot B.B.	1977	"Fractals, form, chance & dimensions" W.H. Freeman, pub. San Francisco, U.S.A.
M10	Molerus O.	1999	"Fluid (mechanics) of steady-state pneumatic conveying s in horizontal pipes" UEF conference, Davos, Switzerland
O1	Ower E. Pankhurst R.C.	1977	"The measurement of air flow" 5th Edition, Pub. Oxford, Pergamon
P1	Pan R. Mi B. Wypych P.W.	1994	"Pneumatic conveying characteristics of fine and granular bulk solids" Kona No.12

P2	Pan R. Mi B. Wypych P.W.	1994	"Design of pneumatic conveying systems for granular bulk solids" Proc. int. con. ATEMH'94, Shanghai, China
P3	Park Y. Zenz F.	1980	"Pressure loss in horizontal to vertical elbow" Pneumotranport 5th Int. Conf. on the Pneumatic Transport of Solids in Pipes
P4	Pan R. Wypych P.W.	1993	"Pressure drop due to solids-air flow in horizontal and vertical pipes" Trans. Mechanical Eng. IEAust. Vol.ME 118, No.1
P5	Pan R. Wypych P.W.	1992	"Scale-up procedures for pneumatic conveying design" Powder Handling & Processing Vol. 4, No. 2
R1	Raheman H. Jindal V.K.	1993	"Stimation of pressure drop in pneumatic conveying of agricultural grains" Powder Handling & Processing Vol. 5, No.3
R2	Raheman H. Jindal V.K.	1994	"Mixture characteristics in pneumatic conveying of agricultural grains" Powder Handling & Processing Vol. 6, No.1
R3	Rose H.E. Duckworth R.A.	1969	"Transport of solid particles in liquids and gases" The Engineer, Mar. 28
R4	Roberts A.W.	1996	"Predicting the volumetric and torque characteristics of screw feeders" Bulk Solids Handling Vol.16, No.2
R5	Richardson J.F. Mcleman M.	1960	"Pneumatic conveying. Part 11. Solids velocities and pressure gradients in a one inch horizontal pipe." Trans. Instn. Chem. Engrs Vol. 38

R6	Rawie A.	1993	"The basic principles of particle size analysis" Malvern Instruments Ltd., Malvern, U.K.
S1	Scott A.M.	1978	"The influence of particle properties on the pressure drop during pneumatic transport of granular materials" Pneumotransport 4, 4th Int. Conf. Pneumatic Transport of Solids in Pipes
S2	Saccani C.	1996	"Solid speed and pressure loss in pneumatic conveying plants: simulation and experimental measurements" Bulk Solids Handling Vol.16, No.2
S3	Soo S.L.	1980	"Design of pneumatic conveying systems" Powder and Bulk Solids Tech. Vol.4, pp 33-43
S4	Selves T.P.	1995	"Analysis & control of splitting ratios of particulate materials at bifurcations in pneumatic conveying pipelines" Ph.D. Thesis, University of Greenwich
S5	Scarlett B.	1976	"Representation of particle size and shape" 4th Int. Congr. Stereology, Gaithesburg, Sept. 1975, U.S. Spec pub. 431, pp 471
S6	Streeter V.L. Wylie E.B	1981	Fluid Mechanics, McGraw-Hill, 562pp
T1	Tsuji Y.	1993	"Discrete particle simulation of gas-solid flows (from dilute to dense flows)" Kona No.11

T2	Tsuji Y.	1982	"Prediction of pressure drop and optimal design of dilute phase pneumatic conveying systems" Pneumatech 1, Int. Conf. on Pneumatic Conveying Technology, Stratford-upon-Avon, U.K.
V1	Vogt E.G. White R.R.	1948	"Granular solids in gases through pipe" Industrial & Engineering Chemistry Vol. 40, No.9
W1	Weber M.	1991	"Friction of the Air and the Air/Solid Mixture in Pneumatic Conveying" Bulk Solids Handling Vol. 11, No.1
W2	Wypych P.W. Kennedy O.C. Arnold P.C.	1990	"Pneumatic conveying of pulverised and crushed R.O.M. coal" 4th Int. Conf. on Pneumatic Conveying Technology, Scotland, U.K.
W3	Wypych P.W.	1999	"The ins and outs of pneumatic conveying" Int. sump. RELPOWFLO 111, Porsgrunn, Norway
W4	Williams O.A.	1983	"Pneumatic system design calculations" Pneumatic and Hydraulic Conveying of Solids Pub. Dekker pp 142-151
W5	Werner D.	1983	"Influence of particle size distribution during pneumatic dense-phase conveying in vertical and horizontal pipes" Bulk Solids Handling Vol. 3, No 2
W6	Wirth K.E. Molerus O.	1982	"Prediction of pressure drop with pneumatic conveying of solids in horizontal pipes" Pneumatech 1, Int. Conf. on Pneumatic Conveying Technology, Stratford-upon-Avon, U.K

W7	Westman M.A. Michaelides E.E. Thomson F.M.	1987	"Pressure losses due to bends in pneumatic conveying" Journal of Pipelines 7, pp 15-20
W8	Weber M.	1982	"Correlation analysis in the design of pneumatic transport plant" Bulk Solids Handling No.2, pp 231-233
W9	Weber M.	1981	"Principles of hydraulic and pneumatic conveying in pipes" Bulk Solids Handling, Vol. 1 No.1.
W10	Woodhead S.R.	1992	"The measurement of particle velocity and suspension density in pneumatic coal injection systems" Ph.D. Thesis, University of Greenwich